Development of 3-Dimensional skin infection models for the evaluation of antimicrobial strategies

Guma A. Yuones Beleid

A thesis submitted in partial fulfilment of the requirements of Sheffield Hallam University for the degree of Doctor of Philosophy
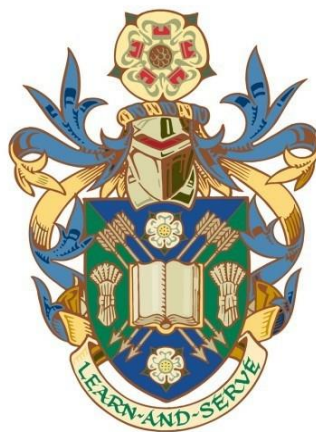
February 2019

Dedication

Praise and thanks to Almighty God for all the indefinite Graces that He conferred on us. I would like to dedicate this thesis to my late father Abdelmalek Beleid who deserves all respect and reverence. My mother has been a source of motivation and strength during moment of despair.

This thesis is also dedicated to my lovely wife and kids who have been a great support and motivation.

Declaration

I hereby declare that:

1. I have not been enrolled for another award of the University, or other academic or professional organisation, whilst undertaking my research degree.

2. None of the material contained in the thesis has been used in any other submission for an academic award.

3. I am aware of and understand the University's policy on plagiarism and certify that this thesis is my own work. The use of all published or other sources of material consulted have been properly and fully acknowledged.

4. The work undertaken towards the thesis has been conducted in accordance with the SHU Principles of Integrity in Research and the SHU Research Ethics Policy.

5. The word count of the thesis is 49,429.

Name	*Guma A. Yuones Beleid*
Date	*February 2019*
Award	*PhD*
Faculty	*Health and wellbeing*
Director(s) of Studies	*Professor Christine Le maitre*

Acknowledgement

I would like to extend my sincerest thanks and gratitude to my supervisors Prof. Christine Le Maitre, Dr. Keith Miller and Dr. Joey Shepherd for their sincere efforts and guidance. Without their assistance this work could not see the light.

I would also like to thank Prof. Thomas Smith for their continued assistance and dedication.

I would also like to thank Dr. Joey Shepherd for her kind help in ultrasound experiment in University of Sheffield.

It is important for all the Facilities to have been offered by BMRC to be acknowledged. I would also go to other staff members of Sheffield Hallam University, particularly microbiology research group and cell biology and regenerative medicine group meeting

Special thanks are also due to Dr. Abdelbasit Gadour, for his sustained support and help and to my intimate friends Dr. Esadawi Abuneeza, Dr. Tarick Nagm, Amin Ehtiwesh, Abdulfatah Dhawga, Ahmed Sassi Belhoul for their valuable advice and intimate relationship.

Thanks are due to the Libyan government, the Ministry of Higher Education and Scientific Research for giving me the opportunity to purse my study for the PhD in medicine.

Presented work and conferences attended

Guma Beleid, Joanna Shepherd, Keith Miller, and Prachi Stafford, The potential of low frequency ultrasound as an antimicrobial therapy for skin wound infections, WBH Winter Doctoral Symposium 2015 at 9th Dec 2015, Sheffield Hallam University, UK.

Guma Beleid, Joanna Shepherd, Keith Miller, and Christine Le Maitre, Development of 3D skin tissue model, BMRC/MERI Winter Poster Event, 12 December 2016, Sheffield Hallam University, UK.

Guma Beleid, Joanna Shepherd, Keith Miller, and Christine Le Maitre, Low Frequency Ultrasound and Medical Grade Manuka Honey as Antimicrobial Therapy for Skin Wound Infections, BMRC/MERI Winter Poster Event, 12 December 2016. Sheffield Hallam University, UK.

Guma Beleid, Joanna Shepherd, Keith Miller, and Christine Le Maitre Development of a 3D skin tissue model, BMRC / MERI Winter Poster Event Friday, 15 December 2017 Sheffield Hallam University, UK.

Guma Beleid, Joanna Shepherd, Keith Miller, and Christine Le Maitre Development of In vitro skin models to investigate the effect of biocidal agents on skin infections, Hallam University Conference, Sheffield Hallam University, UK.

Guma Beleid, Joanna Shepherd, Keith Miller and Christine Le Maitre, Development of a 3D skin tissue model, Tissue and Cell Engineering Society Annual Conference Manchester, 5-7th July 2017 UK

Guma Beleid, Joanna Shepherd, Keith Miller, and Christine Le Maitre, 8th annual BMRC / MERI / Department of Engineering & Maths and Winter Poster Event Friday, 14 December 2018, Sheffield Hallam University, UK.

Guma Beleid, Joanna Shepherd, Keith Miller, and Christine Le Maitre, 3D skin model to investigate biocidal agents for infected burns, The EMBO Workshop Bacterial Persistence and Antimicrobial Therapy, June 10-14, 2018. Ascona, Switzerland.

Guma Beleid, Joanna Shepherd, Keith Miller, and Christine Le Maitre 3D skin model to investigate biocidal agents for infected burns. Tissue and Cell Engineering Society, Annual Conference (TCES) on 2nd - 4th July 2018, Keele, UK

Guma Beleid, Joanna Shepherd, Keith Miller, and Christine Le Maitre. Development of In vitro skin models to investigate the effect of biocidal agents on skin infections - 5th International Conference on Advances in Skin, Wound Care and Tissue Science, October 15-16th, 2018 at Rome, Italy.

Abstract

Wound infection is major health problem, however, there is an urgent need for new anti-microbial strategies to evade the development of antibiotic resistance and local toxicity to skin cells, which hinders wound healing. This is currently hampered by the lack of *in vitro* models of skin infection; this thesis describes the development and validation of a 3D infected skin model for testing new anti-microbial strategies. The effectiveness of two potential anti-microbial strategies for infected wounds, together with effects they exert on mammalian skin cells was determined. Biocides known to have potential anti-microbial activity via free radical formation were investigated alone or in combination with Low Frequency Ultrasound (LFU). To study the biocidal effects, nitrocellulose membranes were used initially to form simple biofilms. A skin model was developed *in vitro* using DED scaffolds, HaCaT cells and commercially available primary fibroblasts. The 3D skin models were burnt, and infected with *S. aureus* or *P. aeruginosa*. Bacterial penetration and migration were determined and effects of biocides investigated. Effects on mammalian cells were determined by measuring skin cell death zones, and immunohistochemistry used to determine phenotype. Biocides reduced bacterial count, with greater effects on planktonic bacteria than on biofilms. Infection caused toxicity to the skin cells in the 3D model, which was greater for *P. aeruginosa* infection than *S. aureus*. Manuka honey was the most effective agent against bacterial infection, while associated with the least toxicity to skin cells.

LFU decreased planktonic bacterial loads. An additive effect was observed when LFU was combined with biocides, enabling lower concentrations of biocides to be used, if combined with US, with less toxic effects on mammalian cells. Together the data presented in this thesis validates a novel 3D skin model which can be utilised to test new anti-microbial strategies in a robust manner *in vitro.*

Contents _Toc20395966

Abbreviations

AHL	Acyl-homoserine-lactone
Ag	Silver
AgNO3	Silver nitrate
ALI	Air liquid interface
AMPs	Antimicrobial proteins
bFGF	Basic fibroblast growth factor
BHI	Brain heart infusion
BIT	Benzisothiazolinone
CFU/ml	Colony for unite/ milter
CK	Cytokeratin
CO_2	Carbon dioxide
CoNS	Coagulase-negative staphylococci
CRISPR	Clustered Regularly Interspaced Short Palindromic Repeats
CMIT	5-chloro-Nmethylisothiazolinone
Cu^{2+}	Cupric ion
DAB	3,3′-diaminobenzidine tetrahydrochloride
DAMPs	Danger associated molecular patterns
DED	de-epidermised dermis
DMEM	Dulbecco's Modified Eagle's medium
DNA	Deoxyribonucleic acid
eDNA	Extracellular DNA
EMRSA-16	Epidemic methicillin-resistant Staphylococcus aureus
EPS	Extra cellular polymeric substance superoxide
Fe2+	Ferrous ion
Fe3+	Ferric ion
FBS	Foetal bovine serum
FGF-7	Fibroblast growth factor 7
GM-CSF	Granulocyte macrophage-colony stimulating factor
H&E	Haemotoxylin and Eosin
HO	Hydroxyl radical
H_2O_2	Hydrogen peroxide
HAIs	Healthcare-associated infections
HEEs	Human epidermal equivalents
HPLC	HIGH PERFORMANCE LIQUID CHROMATOGRAPHY
HSEs	human skin equivalents
IFNs	Interferons
IHC	Immunohistochemistry
IL-1	Interleukin-1
IL-8	Interleukin-8
IMS	industrial methylated spirit
K+	Potassium ion
KGF	keratinocyte growth factor
LPS	Lipopolysaccharides
LBP	Lipopolysaccharide Binding Protein
Mg^{2+}	Magnesium cation
MGEs	Mobile genetic elements
MGO	Methylglyoxal
MIC	Minimum inhibitory concentration
MIT	N-methylisothiazolinone
MOA	Mode of action
MRSA	Methicillin-resistant Staphylococcus aureus
MSCRAMMs	Microbial surface components recognizing adhesive matrix molecules
Na+	Sodium ion
NADH	Nicotinamide adenine dinucleotide
NCCLS	National Committee for Clinical Laboratory Standard
NCIMB	National Collection of Industrial and Marine Bacteria
NEKs	*Normal* Human *Epidermal Keratinocytes*
O2-	Superoxide
O.D	Optical density
K+	Potassium ion
PAMPs	Pathogen-associated molecular patterns

PBP	Penicillin binding proteins
PBS	Phosphate buffered saline
PC	Plysaccharide capsules
PCK	Pancytokeratin
QRDR	Quinolone-resistant-determining regions
QS	Quorum-sensing
RICK	Receptor-interacting protein kinase.
RNA	Ribonucleic acid
ROS	Reactive oxygen species
RS	Reconstructed skin
SEC3	Staphylococcal enterotoxin C3
SEIL	Staphylococcal enterotoxin-like toxin L
TBS	Tris-buffered saline
TCS	Two - component regulatory system
TE	Tissue engineering
TGF-α	transforming growth factor alpha
TSST-1	Toxic shock syndrome toxin 1
TGFs	Transforming growth factors
TNF	Tumour necrosis factor
TNF-α	Tumour necrosis factor-alpha
UV	Ultraviolet
VISA	Vancomycin-Intermediate *S. aureus*
VRSA	Vancomycin Resistant S. aureus
Zn^{2+}	Zinc ion

List of figures

Table list

Chapter 1

General Introduction

1.1- Introduction

Wound infection management is a major medical and financial challenge for healthcare authorities. The cost of ulcer management, for instance, is about £1.4 - 2.1 billion every year in the UK (Bennett *et al.* 2004). The development of this type of infection relies on a number of factors, which include higher longevity, as incidence of burns and infections increase in the elderly. This increased incidence is due to decreased physical activity in the elderly, together with health conditions like diabetes, hypertension and obesity increasing in prevalence in the ageing population. This can result in more complex wounds with prolonged healing, which often leads to the development of slow/non-healing ulcers (Bowler *et al.* 2001). Skin wound infection relates to a range of different pathogens, including bacteria and fungi (O'Dell 1998), which are commonly found in cases of thermal injuries (Church *et al.* 2006) and in patients with chronic wounds (Jeffcoate *et al.* 2003). Recently, there has been growing concern over bacterial infection of wounds, especially in elderly patients or those with diabetes who are more likely to have chronic injuries. Four to ten percent of diabetics suffer from foot ulcers (Singh *et al.* 2005), which can become chronically infected. In addition to this, antibiotic resistance has become an increasing threat to healthcare (Sen *et al.* 2009; Fair *et al.* 2014). Financially, resistant infections cost the healthcare in the US about $20 billion (CDC 2014), and more than 1.6 € billion in the European Union (EMA 2009).

With the improvement of medical treatments, survival of severely burned patients has increased. Furthermore, there has been a considerable rise in hospital acquired infections, which occurs through health workers, patients,

visitors, contaminated medical devices and sub-optimal hospital environment (Mears *et al.* 2009).

To overcome such risks of wound infection and limit the healthcare and economic costs, early diagnosis and appropriate treatment play critical roles in reducing mortality and morbidity. However, wound infection treatment depends heavily on antibiotics; either as topical creams or systemic agents (Howell-Jones *et al.* 2005). The increase in antibiotic resistance and increase in hospital acquired infections (e.g. healthcare acquired methicillin resistant *Staphylococcus aureus*) has resulted in a need to find alternative effective treatments, such as wound irrigation (Valente *et al.* 2003).

These factors lead to increased risk of infection for long term burns patients, who are more prone to infection with both ordinary and antibiotic resistant organisms (Glasser *et al.* 2010), further complicating the condition. Lack of access to new treatments, together with hypersensitivity reaction to antibiotics increases the clinical implications of infections (Glasser *et al.* 2010). Thus, new therapeutic strategies are needed for infected burns of the skin. This thesis discusses the development of model systems which can be utilised to test therapeutic alternatives. These models are utilised to investigate the efficacy of a number of free radical forming biocidal agents and the potential application of ultrasound for infection control.

1.1.1- Morphology of Normal Skin

1.1.2.1- Structure and function of the skin

Skin is the specialised covering of the human body that provides preservation of the body's characteristics (e.g. hydration and temperature) (Romanovsky 2014) and protection against external threats (e.g. pathogens, UV radiation and trauma) (Brohem *et al.* 2011; Belkaid & Segre 2014).

It is the largest organ of the body, forming collectively about 1.8m^2 of highly regulated functional sheet of specialized cells (Gawkrodger *et al.* 2016).

The architecture and dynamics of skin cellularity reflect its functions. It is formed of continuously proliferating and differentiating outer layer of cells, known as the epidermis (outer layer of skin) (Ross *et al.* 1989). The dermis, located between the dermal-epidermal junction and subcutaneous tissue (Figure 1.1), contains blood vessels, lymph vessels, sweet glands and hair follicles (Figure 1.1). The thickness of skin depends on the site of the body (Patton & Thibodeau 2014).

Figure 1.1: Anatomy of skin (Kolarsick *et al.* 2011)

1.1.2.1.1- The epidermis:

The epidermis is the outer layer of the skin that forms a thickness of about 0.1 to 0.2 mm (Sorokin 2010) (Figure 1.2). It is made up of a layer of rapidly proliferating cells (keratinocytes) and is separated from the dermis by a specialist extracellular matrix layer known as the basement membrane (Adra *et al.* 2010; Lee *et al.* 2012) (Figure 1.2).

Figure 1.2: Epidermal layer Anatomy (Salaons 2013).

1.1.2.1.2- The basement membrane:

The basement membrane is a thin lamina of 50-100nm thickness, which is composed of a number of specialist types of extracellular matrix (ECM). The collagen forming the basement membrane is mainly type IV collagen, which is more flexible than the fibrillar type I collagen forming the ECM of the dermis (Paulsson 1992). Other components which make up the basement membrane are the glycoprotein laminin and heparan-sulphate proteoglycans (HSPGs). Laminin is a high molecular weight protein that is found in all basement membranes, whilst heparan sulphate is mainly located in the lamina densa (Timpl *et al*. 1979).

The basement membrane is a transitional zone which separates the dermis and the epidermis, known as the dermal, epidermal junction (DEJ) (Schittny & Yurchenco 1989). With the use of transmission electron microscopy, the DEJ can be seen to be composed of two layers: the lamina densa and the lamina lucida. The two main cellular components of the skin are keratinocytes and dermal fibroblasts. The basement membrane is principally formed by the dermal fibroblasts, although a keratinocyte contribution has been suggested (Varkey *et al.* 2013).

From *in vitro* culture studies, bovine keratinocytes cultured on collagen were unable to form a recognizable basement membrane alone and co-culture with dermal fibroblasts was essential to form a basement membrane (Marinkovich *et al.* 1993).

1.1.2.1.3- Keratinocytes:

Keratinocytes are rapidly proliferating cells of the epidermis, which originate from the basal layer of cells situated on the basement membrane producing daughter keratinocytes that are pushed upwards forming the various layers of the epidermis. The renewal process is continuous in order to maintain the barrier function of all the layers during constant wear and tear which takes place in such exposed and vulnerable part of the body (Pastar *et al.* 2014). The epidermal layers can be described as follows:

1.1.2.1.3.1- Stratum basale:

The basal layer on the basement membrane is known as the stratum basale. Its proliferating keratinocytes gives rise to daughter cells which migrate upwards to form the upper layers. Daughter cells, on their way upwards, differentiate to form the characteristics of each layer until reaching the outermost surface of the skin. There is scientific debate as to whether the basal cells are differentiated cells which further differentiate when proliferating or whether there is a small stem cell population which gives rise to all keratinocytes beginning with the basal cells themselves (Sterry *et al.* 2006; Seyhan 2011).

1.1.2.1.3.2- Stratum spinosum:

The keratinocytes, in this layer become polyhedral with large pale-staining nuclei. Cells in this layer synthesize cytokeratin, a fibrillar protein, whose molecules aggregate together forming tonofibrils and desmosomes to strongly bind adjacent keratinocytes. The cells appear spiny on Haemotoxylin and Eosin

(H & E) staining due to shrinkage of the microfilaments between the newly formed desmosomes giving them their characteristic name (Sterry *et al*. 2006; Seyhan 2011).

1.1.2.3.3- Stratum granulosum:

In this layer, the cells lose their nuclei and their cytoplasm becomes granular due to the abundance of kerato-hyaline granules. These granules are filled with cysteine and histidine-rich proteins to bind together keratin filaments. Thus, adjacent cells become strongly adhered together to perform the preservative and protective function of the skin (Sterry *et al*. 2006; Seyhan 2011).

1.1.2.1.3.4- Stratum lucidum:

The stratum lucidum so named for its clear appearance under the microscope. Formed of dead cells which become clear after they have lost their nuclei, organelles and fill with eleidin, which is an intermediate form of keratin (Sterry *et al*. 2006; Seyhan 2011).

1.1.2.1.3.4- Stratum corneum:

The stratum corneum is the outermost layer of the epidermis, standing for the horny layer (Osseiran *et al*. 2018). The dead cells (corneocytes) become flat with no nuclei or organelles but with mature keratin filaments extending along their cytoplasm, forming together the protective keratin layer, which forms a cornified envelop. In addition, here is an extracellular hydrophobic lipid envelop which together with keratin provides the barrier properties of the skin (Sterry *et al*. 2006; Seyhan 2011). The thickness of the stratum corneum varies with the location of the skin in the body, being thicker in areas subjected to pressure, stress or irritation (Robertson *et al.* 2010; Foss *et al*. 2016). It is also thicker in areas exposed to UV radiation, where increased protective pigmentation is observed (Pearse *et al.* 1987).

1.1.2.2-The dermis:

The dermis is the deep layer of the skin responsible for nourishment and support of the overlying epidermis. Moreover, it forms the preservative and protective part of skin against coarse external factors as stress and trauma. It varies in thickness from 0.3 mm, in the eyelid, to 3.0 mm on the back (Eves *et al*. 2003). It is formed mainly of collagen and elastic fibres, which serve as cushions against stress and strain.

There are about twenty types of collagen, which provide strength and durability to the skin (Compton *et al*. 1998; Kruger *et al*. 2013). Elastic fibres, on the other hand, provide the skin with elasticity and flexibility. The cellular components are formed principally of fibroblasts, which produce the fibrillar part of the dermis as well as producing ECM including glycosaminoglycans. The glycosaminoglycans form a gel-like substance bound together by proteoglycans which are embedded in the fibrillar collagen network and the cellular elements**.** Other cellular components are macrophages and adipocytes.

1.1.3- Classification of wounds

Wounds have been defined as a discontinuity of skin which occurs due to external injury (Saukko & Knight 2015). Wounds usually involve the upper layers, which are the epidermis and dermis, however in severe cases may extend to subcutaneous tissues in deep wounds (Gantwerker & Hom 2012). Wounds can be classified as acute or chronic.

1.1.3.1- Acute wounds

These are wounds which heal with no or minimal scarring within an expected period of time from 4-12 weeks which is determined by its site and its severity (Boateng *et al*. 2008). They may be traumatic or surgical; traumatic wounds occur accidentally in the form of lacerations, cuts or punctures as a result of

injury and usually involve both the skin and subcutaneous supporting tissues (Davis *et al.* 1992; Kumar & Leaper 2005). Since this type of wound is associated with bleeding, this may affect the whole circulation and can lead to circulatory shock; thus, restoration of blood volume is an important priority. Locally, traumatic wounds, especially lacerated ones, should be debrided to remove dead or devitalized tissues so as not to be the seat of infection and to promote the healing process of healthy tissues. Proper dressing and medication significantly reduce the risk of infection and subsequent complications (Demidova-Rice *et al.* 2012). A surgical wound is a deliberate incision into the skin made by a surgeon, usually with a scalpel to get access to the deeper tissues during operations.

1.1.3.2- Chronic wounds

Chronic wounds are characterized by requiring long times to heal (up to 12 weeks) with the possibility of failure to heal or recur (e.g. diabetic and leg ulcers). Chronic wounds require specialized care and treatment to achieve healing (Davis *et al.* 1992; Boateng *et al.* 2008). In chronic wounds, the balance between the formation of ECM molecules (e.g. collagen and chondroitin sulphate) and their degradation is lost, with degradation occurring at a faster rate than formation, leading to the chronicity of the wound (Schönfelder *et al.* 2005). Chronic wounds show incomplete progression through the phases of wound healing (Brownrigg *et al.* 2013; Richmond *et al.* 2013) (See section 1.1.7), with wounds failing to progress beyond the inflammatory phase (Snyder & Sigal 2005).

1.1.3.3- Classification of chronic wounds

Chronic wounds are generally classified into vascular insufficiency ulcers, pressure ulcers, diabetic ulcers and chronic infection ulcers (Nunan *et al.* 2014).

1.1.3.3.1- Vascular insufficiency ulcers:

Insufficiency of blood flow may involve the arterial system or the venous system; both may lead to ulcerations due to different reasons:

1.1.3.3.1.1- Arterial insufficiency ulcers:

Arterial insufficiency occurs mainly due to narrowing of the lumen of arteries with the result of reduction of blood flow to certain parts of the body, together with the overlying skin, a condition called ischemia; hence, the resultant ulcers are sometimes called ischemic ulcers. There are many arterial diseases that produce arterial narrowing, e.g. Burger's disease, atherosclerosis (Thiruvoipati *et al.* 2015) and diabetes.

The diminished blood flow leads to reduced nutrition and oxygenation to the affected tissues leading to necrosis (death) of the tissues and ulceration. Ischaemic ulcers usually take place in the lateral sides of the legs and dorsal surface of the foot and toes. They have a punched-out appearance, grey or whitish dry base and are extremely painful. Signs of ischemia are detectable (e.g. diminished or lost pulse in the affected limb) (Sieggreen & Kline 2004).

1.1.4.3.1.2- Venous insufficiency ulcers:

Venous insufficiency occurs when the drainage of venous blood from the area of skin, is impeded. As in the case of arterial insufficiency, the legs are the most affected parts. The legs are the most affected because the venous blood from the skin drains into superficial veins, which drains into deep veins upto the heart against gravity (O'Meara *et al.* 2014).

There are venous valves between superficial and deep veins and within the deep veins to allow the blood to be drained up to the heart and not in the opposite direction. When the muscles of the leg contract, they pump the blood towards the heart; the venous valves prevent the blood from returning back

(Caggiati, 2013). If these valves become dysfunctional, blood fails to drain properly, instead, blood stagnates and its pressure within the veins increases. Venous hypertension not only impedes venous drainage, but also causes fluid extravasation into the skin and subcutaneous tissues, and deposition of hemosiderin pigments in the skin tissues causing dermatoliposclerosis (Nicholls 2005). With time, the skin becomes unhealthy and ulcerates. The ulcer normally forms in the medial side of the leg, is characteristically shallow, with irregular sloping edges and wet base with exudate (Etufugh *et al.* 2007).

1.1.3.3.2. Diabetic ulcers

Diabetes Mellitus is a common cause of chronic ulcers (Kolluru *et al.* 2012). There are many factors responsible for the development of ulcers in diabetic patients. One of the crucial factors is peripheral neuritis, which usually affects patients with long standing, poorly controlled blood sugar levels. Peripheral neuritis decreases the sensations in the terminal parts of the limbs, especially the lower limbs. Thus, any small injuries in the feet can pass unnoticed and become the site of future ulceration in the presence of other factors.

Secondly, most uncontrolled diabetic patients develop ischemia due to lack of, or resistance to insulin (Kolluru *et al.* 2012). The effect of high blood sugar effect on endothelial cells can lead to endothelial dysfunction which can result in impaired vasodilation and angiogenesis ultimately resulting in ischemia (Bir *et al.* 2009), and slow healing of wounds (Goligorsky 2005).

Thirdly, the high sugar levels in the diabetic tissues encourage infection with bacteria and other microorganisms due to reduce in the response of both T cells and neutrophil function (Peleg *et al.* 2007), also humoral immunity disorder

(Geerlings & Hoepelman 1999). Infection adds to the burden of the immune system to affect wound healing (Reiber 1992; Falanga 2005).

Diabetic ulcers have serious complications which can often lead to amputation, with a 10 to 30 fold higher risk of having amputations in diabetic patients than those without diabetes (Trautner *et al.* 1996; Armstrong *et al.* 1997).

1.1.3.3.3. Pressure ulcers

These are ulcers that develop from prolonged pressure on the skin in certain parts of the body. The parts most commonly affected are those where the skin overlies a bone or a bony prominence, because the skin becomes compressed between the externally applied pressure and the bony part. Since the most common cause of the external pressure is the body weight itself, which is usually the case in immobilized individuals, the most common sites of pressure ulcers are the buttocks (overlying the ischial tuberosities), the heals (overlying the calcaneus) and the shoulder blades (overlying the scapulae) in the recumbent individual. Causes of prolonged recumbency include paralysis; coma or fractures which necessitate immobility (e.g. fracture of vertebrae, pelvis or lower limbs). The continuous pressure on the skin interferes with the cutaneous blood supply leading to ulceration. As such, it can be regarded as a form of arterial ischemic ulcer (Defloor 1999; Reddy *et al.* 2006).

1.1.3.3.4- Chronic infection ulcers:

Repeated infections of a wound decrease its ability to heal properly, and lead to chronic ulcer formation. This is common in diabetic and immunocompromised patients with wounds that have not been treated properly.

1.1.4- Burn injuries

Burn injuries are classed into several degrees of burn, which are determined by the size and depth of the injury which is caused by the intensity and exposure time to the causative factor. There are three burn degrees:

1.1.4.1- First degree burn (Superficial burns):

This type of burn usually occurs after sun exposure, due to UV rays, minor flash injuries or short exposure to a heat source. The burn involves only the epidermis (Hutchinson *et al*. 2007; Saager *et al*. 2010). Usually it affects the uppermost layer (the stratum corneum), which when burnt, leads to increased blood flow giving the skin at this site a pinkish appearance. Although first degree burns are superficial and normally heal without scarring within about a week (Heimbach *et al*. 1992; Sullivan *et al*. 2001; Monstrey *et al*. 2008), they are painful due to the preservation of the nerve endings.

1.1.4.2- Second degree burn (Partial thickness burns):

Second degree burns involve both the epidermis and the dermis, and are very painful, since the nerve endings are exposed. Second degree burns can be further divided according to the depth of the burn into superficial dermal and deep dermal burns.

In superficial dermal burns (superficial partial thickness burns), the deep layers of the dermis are preserved, together with the hair follicles, sweat and sebaceous glands. The skin is erythematous, swollen, painful and blisters form which fill with inflammatory fluid. When the blisters undergo sloughing, the pinkish dermis appears. It classically heals with no or minimal scarring, as the intact dermal layer provides an adequate source of re-epithelialisation in around 14 days (Jackson 1953; Heimbach *et al*. 1992; Monstrey *et al*. 2008).

Deep dermal burns (deep partial thickness burns) involve most of the dermal layer, leaving only a thin viable dermal layer at the base. Generally, it has the pinkish appearance of the residual deep dermis with fewer blisters. It usually heals with scarring due to the induction of fibrous tissue healing rather than re-epithelialization (Sullivan *et al.* 2001; Monstrey *et al.* 2008).

1.1.4.3- Third degree burn (Full thickness burns):

In this class, almost all the depth of the dermis is damaged, and the burn reaches down to the hypodermis, with occasionally scattered minimal dermal tissue at the base. Due to blood capillary damage, the burnt area appears white, very light pink or charred.

However, some capillaries remain viable and regenerate. Thus, a blood supply to the residual tissues is usually maintained, but varies from one site to the other and is generally sluggish (Jackson 1953). To encourage healing, it is essential to maintain viability within residual tissues. The time needed for healing is variable for third degree burns and it can often be unpredictable, and regular reviews are essential to assess response to treatment and healing progress. In many cases, a skin graft is likely to be required. In some cases, there are blisters, but they are generally few and mostly with less fluid or almost dry (Jackson 1953; Sullivan *et al.* 2001; Monstrey *et al.* 2008)**.**

1.1.5- Mechanisms of burn injuries

Burns are classified according to the causative injury, and include scald burns, flame burns, contact burns, chemical burns and electrical burns.

1.1.5.1- Scald burns: These are burn injuries which are caused by hot fluids like water, tea or milk. Burns due to scalds are usually superficial first degree burns but can sometimes reach full thickness third degree burns.

Boiling oils and fats cause serious burns due to their high boiling temperature (Bousfield 2002; Hettiaratchy & Dziewulski 2004; Hettiaratchy *et al.* 2005):

1.1.5.2- Flame burns: These are caused by contact to flames, which can be from a variety of sources (petrol, gas, open fires or electrical fires). They are generally deeper than scald burns. If the burn is caused by a building fire, the condition is often accompanied by inhalation injury due to smoke. Flash burns are a specific type of flame burns where there is a very brief exposure to high voltage electricity (Bousfield 2002; Hettiaratchy & Dziewulski 2004; Hettiaratchy *et al.* 2005):

1.1.5.3- Contact burns: These results from contact to hot objects (e.g. pans, irons). Contact burns can also include friction burns which are caused by the heat of friction, however these are also accompanied by lacerations from the shearing of skin against other surfaces (e.g. the ground in road traffic accidents) (Bousfield 2002; Hettiaratchy & Dziewulski 2004; Hettiaratchy *et al.* 2005):

1.1.5.4- Chemical burns: Chemical burns occur from exposure of the skin to corrosive chemicals (e.g. acids, alkalis, domestic cleaners, bleaches, cement). The resultant burns vary according to the concentration of the chemical and the time of exposure. Strong alkalis tend to cause deeper burns than acids. Because the alkaline effect on our proteins in skin like keratin in a process called denaturing and causes loss in shape and function of cell structure proteins. However, during skin exposure to an acid, the cells die but don't disintegrate, except following contact with hydrofluoric acid which causes damage deep into the skin (Bousfield 2002; Hettiaratchy & Dziewulski 2004; Hettiaratchy *et al.* 2005).

1.1.5.5- Electrical burns: These occur when an electric current pass from an electrical source through the body to the earth.

The resultant damage depends on the voltage and the time of exposure. Domestic 240-volt electricity causes deep burns at the entry and exit sites of the current. The electric current may also interfere with cardiac electricity leading to arrhythmias and may cause stimulation of the body's muscles leading to violent shaking, tears in muscles, tendons or ligaments, falls or other traumatic injuries. 1000-volt electricity which can be obtained from specialist equipment would cause extensive tissue damage both in soft tissues and bones. (Bousfield 2002; Hettiaratchy *et al.* 2004; Hettiaratchy *et al.* 2005).

1.1.6- Wound healing

Infected and chronic wounds either heal slowly or do not heal at all, especially if there is an underlying disease (Prompers *et al.* 2008) or if infected with biofilm forming organisms (Ngo *et al.* 2007; Dowd *et al.* 2008; James *et al.* 2008). Strategies to enhance healing of these wounds vary according to the underlying causes of delayed healing. Of utmost importance is to identify the causative organism and treat the cause with the appropriate antibiotic. In more complicated cases, other measures may be added such as hyperbaric oxygen, electromagnetic therapy, ultrasound, growth factors and bone marrow derived cells. In severe cases, debridement of tissues and even amputations may be needed. Wound healing is the active mechanism by which the body repairs itself following injury. Wound healing is completed via 4 phases: haemostasis; inflammation; proliferation and remodelling.

1.1.6.1- Immediate response (Haemostatic phase):

Following injury, blood vessels are normally severed resulting in bleeding. The first phase is a haemostatic response to prevent excessive blood loss.

Some of the blood accumulates in the site of injury and coagulates forming a blood clot. The blood clot releases cytokines and growth factors to draw

inflammatory cells into the site of injury. The blood clot also serves as a temporary scaffold upon which cells migrate and grow (Guyton 2006).

1.1.6.2- Inflammation phase:

As a consequence of injury, inflammatory cytokines are released at the site of injury. Some of these cytokines, known as chemokines, call for circulating inflammatory cells to come to the site of injury via chemotaxis. The first cells to get to the site are neutrophils. These are followed by monocytes, which differentiate into macrophages after extravasation and settling in the tissues within 24 - 48 hours. The macrophages recognise pathogens in several ways, which include the pattern recognition of the receptors which recognise several of the pathogen-derived chemical molecules (e.g., mannose, lipo-polysaccharides, glucans, and flagellin). They also recognise the pathogen bound complement molecules or the antibodies whose involvement leads to the phagocytosis of the pathogens (Abbas *et al*. 2003; Mosser & Edwards 2008). Additionally, the macrophages release transforming growth factors (TGFs), cytokines including: interleukin-1 (IL-1); interleukin-8 (IL-8); and tumour necrosis factor (TNF)(Kobayashi *et al*. 2003). Although the inflammatory cells serve mainly to defend the body against the injurious agents and activate the body to face the probable upcoming infection after the skin barrier has been violated, they also remove dead and damaged skin cells from the wound region and secrete chemotactic factors and signals for the epithelial cells to move to the site of injury (Kim *et al*. 2008).

1.1.6.3- New tissue formation (Proliferative phase):

Keratinocytes, attracted by cytokines and growth factors, migrate from the wound edges towards the centre of the wound and proliferate to fill the gap, in a process termed re-epithelialization which normally occurs with four weeks in an

uninfected wound (Werner *et al.* 1994). In the dermis, fibroblasts also migrate and proliferate secreting a considerable amount of collagen, the fibroblasts differentiate into contractile myofibrils (Schultz *et al.* 2005). The fibrils contract bringing the edges of the wound together, minimizing the gaps as much as possible.

At the same time, the secreted cytokines and growth factors by fibroblasts and other cells activate the process of angiogenesis by which both blood and lymph vessels invade the wound and supply nourishment and oxygenation to the growing tissues (Bauer *et al.* 2005).

1.1.6.4- Remodelling:

The final process by which the newly formed tissues are restored to the optimum dimensions to regain the continuity which has been breached by the wound is known as remodelling. The process includes a balance between the regeneration of appropriate ECM and structure, whilst degradation of the temporary repair tissue occurs. The balance is achieved and regulated through a network of intercellular communication and signalling pathways. A lot of specialized cells and cytokines are involved and balanced to prevent over-production of tissues with excessive scarring as well as inconvenient contraction of the tissues (Xue & Jackson 2015; Sorg *et al.* 2017).

Although wound healing is a highly organized process, it does not totally regain all the functions of the original skin. First of all, the healed skin lacks all the skin appendages (e.g. hair follicles, sweat and sebaceous glands).

Secondly, the newly formed skin lacks the normal elasticity and other mechanical properties due to the excessive fibrous tissue involved in the healing process (Xue & Jackson 2015). However, foetal skin is capable of healing without the formation of scar tissue, which is attributed to the lower

number of immune cells involved in healing, which raised the hypothesis that excessive inflammatory reaction might restrict the regenerative ability of tissues in adults and activate scar formation (Lorenz *et al*. 1993; Buchanan *et al*. 2009; Walraven *et al*. 2014).

Furthermore, tumours could be arising at sites of chronic wounds or chronic irritation, where it is thought the repair processes during healing in these cases have gone out of control leading to malignant transformation. There are a number of similarities between wounds (specifically healing chronic wounds) and tumours. Both tumorigenesis and wound healing involve angiogenesis, fibrin deposition, proliferation and migration of keratinocytes, conversion of epithelial cells to mesenchymal cells and the differentiation of fibroblasts to myofibroblasts. The intriguing observation was that almost all of these changes are stimulated by similar factors and mitogens. The main difference is that during wound healing these processes are organized and disciplined, whilst in tumours they are out of control (Coussens & Werb, 2002; Schäfer *et al.* 2008; Stuelten *et al*. 2008; Qian & Pollard 2010).

Figur 1.3: Wound healing phases within the skin (Beanes *et al.*, 2003)

1.1.7- Wound infection

Wounds are prone to microbial contamination, from both exogenous and endogenous sources, the seriousness of the wound infection depends on the number, types and virulence of microorganisms involved (Bowler *et al.* 2001; Agostinho *et al.* 2011). Wound infection caused by bacteria embodies a significant concern to healthcare organisations (Wright *et al.* 1990), where approximately 1-2% of the population of developed countries experiences such non-healing or chronic wound inflammation which are often infected by *Pseudomonas aeruginosa* and *Staphylococcus aureus* (Kirketerp-Moller *et al.* 2008).

The common symptoms of wound infection include localised reddening, swelling, heat, pain, and loss of function (Okhiria 2010). Patients with chronic wounds can develop necrotic tissue, wound breakdown and tissue depigmentation (Grey 1998; Stringfellow *et al.* 2000; Baxter 2003).

Infection of skin and mucous membranes by pathogenic organisms takes place when specific conditions related to the pathogenic organisms and the host occur. Pathogenic organisms such as *S. aureus* and *P. aeruginosa* express a number of virulence factors which enable organisms to infect the host (Section 1.1.9) (Tang *et al.* 1996; Williams *et al.* 2000; Sibbald *et al.* 2003; Jensen *et al.* 2007; Cornejo *et al.* 2017). Furthermore, for pathogenic organisms to infect the host, the protective mechanisms of the host (Section 1.1.10) must be compromised. Where the protective skin layer is damaged via wounds such as: abrasions, bruises, lacerations and burns this can facilitate the invasion and spread of the pathogenic organisms (Sinno & Prakash 2013). Even in the absence of such wounds, marked colonisation of the organisms on the skin of the host provides an organismal load that may lead to spontaneous invasion and dissemination of the organism resulting in local and/or remote infections (Kadioglu *et al.* 2008). For the organism to invade the skin or mucous membranes, it must first be attached firmly to them. This attachment is usually achieved through the expression of fimbriae or pili, which possess adhesins at their tips (Choy *et al.* 2007). Adhesins have also been shown to play an important role in both chronic infection and in biofilm formation (Peng *et al.* 2008; Bu *et al.* 2008).

1.1.8- Host defence mechanisms to infection of skin

1.1.8.1- Physical and Immunological skin barriers:

Skin is an essential barrier which prevents the entry of the pathogenic microbes which are present in the surrounding environments. The skin surface has many constitutive properties like a low pH and temperature, the presence of skin commensal microorganisms which compete for space and nutrients, and antimicrobial peptides such as human beta-defensins that can prevent bacterial colonisation. The skin epidermis consists of several keratinocyte layers, including the granular, corneal, spinous and the basal layer. The corneal layer is the main physical skin barrier. This layer is the exit point of many sweat and sebaceous glands, along with hair follicles which extend down through the epidermis. Also, the skin contains many residual immune cells which contribute towards immune responses, including macrophages, epidermal Langerhans cells and dermal dendritic cells, T and B cells, mast cells, plasma cells and natural killer (NK) cells that are present in the dermal layer (Mann *et al.* 2012).

1.1.8.1.1-The normal cells in the dermis include:

Mast cells which contain granules that are packed with histamine among other chemicals; they are released when the cell is upset (Krystel-Whittemore *et al.* 2016). Vascular smooth muscle cells which allow blood vessels to shrink and expand; they are necessary for controlling body temperature (Brozovich *et al.* 2016). Specialised muscle cells such as myoepithelial cells which are present around sweat glands: they contract to expel sweat (Makarenkova *et al.* 2015). Fibroblasts cells which produce and deposit collagen among other elements of the dermis as necessary for growth or for repairing wounds; a resting fibroblast usually has very little cytoplasm that is compared to an active cell; it seems to have a 'naked' nucleus (Darby *et al.* 2014).

Immune cells which are of different types; tissue macrophages (histiocytes) remove and digest foreign or despoiled material (a process known as phagocytosis) (Koh & DiPietro 2011). In the normal dermis, one may see small numbers of lymphocytes. Transient inflammatory cells or leukocytes which are white cells that leave the blood vessels destroying infections, healing wounds, or causing disease. They comprise: Neutrophils (polymorphs) that have segmented nuclei; they are regarded as the first white blood cells that enter the tissues when there is acute inflammation (Leiding, 2017). T and B Lymphocytes that are small inflammatory cells having many subtypes; they appear later but they persevere for a long time in inflammatory skin. They are vital for regulating the immune response. Plasma cells are specific lymphocytes which produce antibody (Alberts 2002).

Eosinophils that have bi-lobed nuclei with pink cytoplasm on H&E stain. Monocytes that shape the macrophages (Bavle 2014)

The skin cells that communicate with each other by discharging great numbers of biologically active cytokines together with chemotactic factors that control their function and movement; they are too small to be seen by light microscopy.

On the other hand, one of the shortcomings of these types of cells is that they are unable to reproduce cellular heterogeneity and skin complexity under inflammatory or basal conditions. Thus, 2D-3D culture systems are proposed; they simulate the differentiation process. In a comparatively short time, one may use a 3D culture system whereby numerous cell lineages keratinocytes, fibroblasts and immune cells will be co-cultured to secure better skin microenvironment reproduction (Li 2011; Colombo 2017).

1.1.8.2- Skin immunity

Skin is the largest organ of the body, which encompasses all other internal organs within, protecting and isolating them from the surrounding environment. Thus, it is considered to be the first line of defence against external challenges (Salmon *et al.* 1994). Infection is one of the main threats to the body. Skin represents a structural and functional barrier that combats infection. Structurally, it provides multiple layers of highly dividing and regenerating cells that reduce microbial attachment and remove pathogenic organisms. Functionally, it forms an essential part of the immune system that detects, interacts and destroys invading microbes (Grice *et al.* 2011; Percival *et al.* 2012; MacLeod *et al.* 2016). Skin cells detect pathogenic organisms through specific molecular patterns on the outer surface of pathogens called pathogen-associated molecular patterns (PAMPs) or danger associated molecular patterns (DAMPs). These patterns are recognized by specialized receptors on the skin cells, Toll-like receptors (TLR) (Grice *et al.* 2011; MacLeod *et al.* 2016). Once pathogens are recognized, skin cells initiate the appropriate immune response through secreting a group of chemokines and cytokines (Grice *et al.* 2011) that play an important role in both responses: the generalised non-specific innate immune response and the specific adaptive immune response (Krishna *et al.* 2012). Cytokines produced by keratinocytes are either pro-inflammatory: e.g. interleukin-1 (IL-1), interleukin-6 (IL-6), T-cell trophic interleukin-7 (IL-7), interleukin-15 (IL-15) and tumour necrosis factor-alpha (TNF-α) or immunomodulatory: e.g. interleukin-10 (IL-10), interleukin-12 (IL-12), interferons (IFNs) and chemkine (IL- 8). The latter group functions as an essential part of the immune process or, alternatively in response to variable stimuli (Gröne 2002).

Other than the main skin cells (keratinocytes), there are immune cells scattered through the epidermis, e.g. Langerhans and antigen-presenting cells. Upon stimulation, they migrate to the local lymph nodes to present foreign antigens to naïve T-cells; thus triggering an adaptive cell mediated immune response (Ilkovitch 2011). It is also suggested that these cells are involved in providing commensal bacteria of the skin with immune tolerance (Chomiczewska *et al*. 2009). Innate immune cells, such as macrophages and mast cells abound in the dermis where they carry out non-specific response to a wide range of pathogens through producing variable inflammatory cytokines and protective enzymes, e.g. proteases (Ilkovitch 2011).

1.1.9- Common infective agents in skin infections

Skin microbiota is open to contamination from the exterior environment; it is an unusual place for the growth of microbes (Bojar *et al*. 2002). The severe conditions of the skin reduce the number of bacteria that can grow there; they become part of the aboriginal micro-flora (Percival *et al*. 2012). The inhabitant commensal micro-flora comprises microorganisms like Staphylococcus, *Propionibacterium*, and *Corynebacterium* and Malassezia yeast strains (Bojar *et al*. 2002; Cogen *et al*. 2008; Dryden, 2009; Holland *et al*. 2009; Holland *et al*. 2008; Percival *et al*. 2012). Additionally, bacterial infections that are Gram positive and Gram negative are the most common ones that cause mortality as a result of thermal injury (Rowan *et al*. 2015). The surface of the burn is a rich environment since it is favourable for microbial colonisation and proliferation. Consequently, the bacteria that rest on the skin or that are connected with skin attachments surviving the thermal offence can inhabit the wound surface within the first two days. Mostly, they are the Gram positive commensal staphylococci like *S. epidermidis* (Church *et al*. 2006). Other species of bacteria such as the

pathogen, *S. aureus*, can also inhabit and cause wound infection within two days after a skin injury; it is visible in the early stages of chronic wounds (Church *et al*. 2006). If the wounds are not properly treated, they will be colonised by other bacteria species such as *P. aeruginosa* and *Escherichia coli* (late colonisers) (Percival *et al.* 2012). A vital factor in burn wound infections is the formation of biofilm by bacteria (e.g. *P. aeruginosa* and *S. aureus*) (Church *et al*. 2006).

1.1.9.1- Nature and distinguishing characteristics of *Staphylococcus aureus*

S. aureus are spherical bacteria that exist in bunches or grape-like clusters. They range from 0.5 to 1.5 µm in diameter. They are non-motile and non-spore forming (i.e. they live as vegetative and reactive forms). But in the absence of oxygen, they can survive depending on anaerobic mechanisms of producing energy; hence they are facultative anaerobes *S. aureus* is a resilient organism capable of surviving in a wide range of environmental conditions, which adds to its durability and pathogenicity.

Structurally, all strains of *Staphylococci* have cell walls, which are bounded by a thick layer of peptidoglycan (e.g. N acetylmuraminic acid and N-acetylglucosamine) (Ghuysen *et al*.1963). *S. aureus* is characterized by having special pentaglycine interbridges that crosslink the glycans. Many strains of *S. aureus* produce polysaccharide capsules (PC), especially pathogenic strains, which have types 5 and 8 PC (Tong *et al*. 1997; Grundling & Schneewind, 2006).

S. aureus produces coagulase, catalase, urease and phosphatase enzymes. These enzymes allow the bacteria to spread and thrive in its environment, whether it is pathogenic or non-pathogenic. The enzymes are also important

during diagnosis, where catalase distinguishes between staphylococci and streptococci, whereas coagulase test differentiates between *S. aureus* and *S. epidermidis*.

1.1.9.1.2- Pathogenicity and Virulence

Although *S. aureus* lives as a commensal organism on the human skin, gastro-intestinal tract and vagina, it becomes more virulent when it gains access to the blood. Its virulence is a consequence of virulence factors.

Firstly, it has the ability to bind proteins e.g. fibrinogen (Bodén *et al*. 1992), fibronectin (Flock *et al*. 1987), collagen (Patti *et al*. 1992), laminin, elastin and thrombospondin (Park *et al*. 1996), allowing it to adhere to basement membranes and endothelial cells, aiding penetration through the skin. This adhesion is via specific surface proteins on its surface that are capable of recognizing certain host molecules to bind to them; these bacterial surface proteins are called microbial surface components recognizing adhesive matrix molecules (MSCRAMMs) (Vazquez *et al*. 2011; Foster *et al*. 2014). One important example of these is Protein A, which binds to immunoglobulin and is considered to be a crucial factor of *S. aureus* virulence (Ghasemian *et al*. 2015). Secondly, *S. aureus* secretes many enzymes that cause host tissue damage and at the same time allow bacteria to invade tissues and spread through them (e.g. protease, lipase, nuclease and staphylokinase) (Recsei, 1986; Smeltzer *et al*. 1993; Said-Salim *et al*. 2003). Furthermore, certain strains of *S. aureus* induce extensive immune reactions leading to shock via excretion of exotoxins such as toxic shock syndrome toxin 1 (TSST-1). Finally, *S. aureus* has to be able to colonise skin and mucous membranes withstanding harsh conditions; hence, it is a potential source of infection with heavy bacterial load once circumstances allow.

1.1.9.1.3- *S. aureus* and resistance to antibiotics

S. aureus developed resistance to penicillin a short period after the discovery of penicillin and its application in the medical field. This is attributed to the genomic plasticity and diversity *S. aureus* possesses (Davies & Davies 2010).

The active antibacterial part of the penicillin molecule is the β-lactam ring. The β-lactam ring binds to penicillin binding proteins (PBP) in the bacterial cell wall inhibiting the synthesis of peptidoglycans cross-links, which are structurally essential. With the normal degradation of these cross-links and the failure of bacterial cells to synthesise new bonds, it occurs as a consequence of peptidoglycan subunit build up in the cytoplasm triggering proGrammed cell death and autolysis. Some strains of *S. aureus* are able to secrete an enzyme, which specifically destroys the β-lactum ring, known as β-lactamase (Lowy 2003). Medical researchers sought to overcome these resistant strains, in 1960, a penicillin derivative was synthesised whose lactam ring was chemically protected from the influence of the bacterial enzyme: Methicillin, which was described as β-lactamase-resistant penicillin (Fairbrother & Taylor 1961). *S. aureus* struggled against the new antibiotic derivative and achieved its second victory within just a few years by evolving new strains also resistant to methicillin; known as methicillin resistant *S. aureus* (MRSA).

A further antibiotic, vancomycin, is capable of combating MRSA. However, strains of *S. aureus* have emerged that are resistant to vancomycin; these are pathogenic, resistant and responsible for considerable mortalities. Two grades of resistance to vancomycin developed: intermediate grade resistance in Vancomycin-Intermediate *S. aureus* (VISA) and high grade resistance in Vancomycin Resistant *S. aureus* (VRSA). Fortunately, VISA and VRSA infections are limited and isolated in hospital settings (Chambers & DeLeo

2009). The cause of VRSA was found to be due to the gene vanA, which is believed to have first developed in resistant enterococci before it was transferred to staphylococci (Chang *et al.* 2003). In contrast, the genetic cause of VISA is still to be fully identified, although certain changes in the phenotype of resistant strains have been observed, e.g. cell wall thickening and increased pigmentation which may provide clues (Renzoni *et al.* 2010).

1.1.9.2- *Staphylococcus epidermidis*

Staphylococcus epidermidis (S. epidermidis), is principally considered as a skin commensal that lives on healthy human skin, is a non-motile Gram positive and coagulase negative bacterium. However, with the medical development that led to the extensive use of devices, it has grown to be pathogen (Otto 2009). Coagulase-negative staphylococci are frequently altogether referred to as CoNS (or CNS). *S. epidermidis* is an important member of this family which is significant clinically (Raad *et al.* 1998; Rogers *et al.* 2009; Otto 2009). Since *S. epidermidis* generally causes infection in immuno-compromised patients or in patients who undergo surgery, it is a recurrent source of nosocomial infections (Otto 2014). In the US, CoNS by themselves cause 31% of all the nosocomial bloodstream infections (BSIs) and 11.4% of total healthcare-associated infections (HAIs) (Wisplinghoff *et al.* 2004; Sievert *et al.* 2013). Medical devices that offer surfaces for the bacteria to adhere to and colonise include intravascular catheters and cardiac pacemakers, joint arthroplasties and implanted heart valves (Simon *et al.* 2005; Parvizi *et al.* 2010).

S. epidermidis infections are resilient for several reasons. They are able to grow in dense accumulations, on both biotic and abiotic surfaces forming biofilms (Otto 2012). The biofilm growth increases the tolerance of the bacteria to antimicrobials compared with planktonic grown cells (Gristina *et al.* 1987; Ceri

et al. 1999). *S. epidermidis* biofilm formation protects against the host immune system (Scherr *et al.* 2014). The polysaccharide adhesion PSA, polysaccharide intracellular adhesion PIA forming a sort of positively charged capsule around *S. epidermidis* as a general mechanism to shield the bacteria from immune system (Cerca 2006, Le2018). Methicillin resistance in isolates of CNS has increased significantly in the recent years, a great percentage of *S. epidermidis* isolated from clinical settings possess methicillin resistance genes which using the *mecA* gene which encodes penicillin binding proteins (PBPs) is *MecA* (Chambers 1997; Diekema *et al.* 2001).

1.1.9.2.1- Virulence factors of *S. epidermidis*
1.1.9.2.1.1- Enzymes and Toxins in *S. epidermidis*

S. epidermidis, is termed as moderately innocuous partly because it lacks the secreted toxins, compared with *S. aureus* secretion, which has a huge large collection of secreted molecules which are toxic to humans, including α-toxin, enterotoxins, and a sequence of leukocidins (Foster 2005). Several reports which describe the irregular incidence of the toxic shock syndrome toxin (TSST) and the enterotoxins in CNS present in *S. epidermidis* (Bautista *et al.* 1988; Marin *et al.* 1992). *S. epidermidis* prosses a pathogenicity island, referred to as SePI, which encompasses staphylococcal enterotoxin-like toxin L (SEIL) and staphylococcal enterotoxin C3 (SEC3) (Madhusoodanan *et al.* 2011). However, the secretion of such toxins by *S. epidermidis* is rare. The acquisition of toxin gene-harboring mobile genetic elements (MGEs), possibly from *S. aureus*, is infrequent. The CRISPR interference mechanism is determined that *S. epidermidis* secretes numerous enzymes that are involved in virulence (Marraffini & Sontheimer 2008). It produces a sequence of secreted proteases that they may contribute to virulence through the processes of host tissue

destruction and the host proteins. It is possible to attribute definitive mechanisms to SepA, that damage the human AMPs (Lai 2007), and to Esp, that destroys fibrinogen and complement factor C5 (Dubin *et al.* 2001).

1.1.9.3- General characteristics of Pseudomonas aeruginosa

P. aeruginosa is a key Gram negative bacterium which is a major cause of wound infections, particularly those in burn patients (Lyczak *et al.* 2000). *P. aeruginosa* forms biofilms rapidly (Harrison-Balestra *et al.* 2003), through the production of quorum sensing molecules (Fuqua 2006), which play an important role in the multistep process of biofilm formation. *P. aeruginosa* also produces an exopolysaccharide alginate which enables it to escape the immune mechanisms of the host (Leid *et al.* 2002).

Infections with *P. aeruginosa* are characterized by greenish blue pus due to the production of the pigment pyocyaneus. *P. aeruginosa* secretes a number of other pigments, e.g. pyoverdine (yellow) and pyorubin (red). These pigments play a role in the pathogenicity of *P. aeruginosa* through inhibiting the host cellular respiratory functions leading to their apoptosis (Allen *et al.* 2005).

P. aeruginosa in laboratory cultures form small rough colonies when isolated from environmental sources as soil or water, whilst those isolated from clinical samples form irregular edged shaped mucoid large colonies, due to the presence of the exopolysaccharide alginate, which has a crucial role in the virulence of these pathogenic forms of *P. aeruginosa* (Mathee *et al.* 1999; Li *et al.* 2005; Pritt *et al.* 2007).

1.1.9.3.1- Pathogenicity and virulence factors of *P. aeruginosa* infections

P. aeruginosa cause serious infections in humans, animals and plants due to its virulence factors, such as strong attachment to the host with pili (Lyczak *et al.* 2000) and the production and secretion of virulence factors including exotoxin A

(Van Delden *et al.* 1998), exoenzyme S (Hamood *et al.* 1996; Woods *et al.* 1997; Jia *et al.* 2006) phospholipase, elastase (Blackwood *et al.* 1983), lipopolysaccharidases and proteases (Woods *et al.* 1997) and the previously mentioned alginate (Potvin *et al.* 2003).

P. aeruginosa has a number of virulence strategies including the secretion of factors such as hyaluronidase and gelatinase enzymes which break down the hosts extracellular matrix, enabling migration of the bacteria (Naglik *et al.* 2003) and exotoxin S which induces apoptosis in host cells (Caldwell *et al.* 2009) (Jia 2006). Both of these *P. aeruginosa* toxins damage host tissue and the host immune response leading to septic shock. LPS of *P. aeruginosa* is composed of the polysaccharide O and core antigens and lipid A composed of fatty acid and phosphate groups bonded to a glucosamine disaccharide (Ernst, Adams *et al.* 2006; Vitkauskiene 2005; Hancock 1983). Elastase is the best proteolytic enzyme secreted by *P. aeruginosa*; it has an extensive range of substrates, such as elastin, collagen, fibronectin and laminen. In addition, molecules of immune and host defence such as fibrin, gastric mucin, transferrin, α-1 proteinase inhibitors, IgG, γ-interferon and components of complement pathway (Engel & Balachandran 2009). The elastase produces when bacteria cells are in the late logarithmic phase (Finnan *et al.* 2004). Some studies have reported that the levels of virulence factors depend on the site of *P. aeruginosa* infection (Runbaugh *et al.* 1999; Hamood *et al.* 1996). For example, toxin A (ExoA or toxA) is a protein performance as a main virulence factor of *P. aeruginosa*, similar in action to that of diphtheria toxin and exoenzyme S release are associated with skin infection. Thus, the production of *P. aeruginosa* of exotoxins in wound infections lead to inhibition of wound healing (Engel & Balachandran 2009). These substances not only destroy the host tissues locally

(Schmidt & Hensel 2004; Hansen-Wester & Hensel 2002). Biofilm formation increases the capability of the organisms to achieve chronic infections (Brady *et al.* 2008).

1.1.9.3.2- *P. aeruginosa* opportunistic and nosocomial infections

P. aeruginosa is the cause of numerous opportunistic and nosocomial infections (Moolenaar *et al.* 2000; Srinivasan *et al.* 2003). Being able to survive with very low nutritional resources, *P. aeruginosa* has been found on medical devices and instruments presenting a common source of infection in hospitals (Srinivasan *et al.* 2003; Kolar *et al.* 2009).

P. aeruginosa causes infection in almost all parts of the human body, including: wounds of the skin (Cooper 2009; Fazli *et al.* 2009), surgical infections (Efem 1988), severe burns (Estahbanati *et al.* 2002), and diabetic ulcer (Dowd *et al.* 2008). *P. aeruginosa* is frequently isolated from individuals with ill health or compromised health conditions, such as opportunistic infections in cystic fibrosis patients (Santucci *et al.* 2003).

1.1.9.3.3- Antimicrobial resistance

P. aeruginosa resists antimicrobial agents through various mechanisms. Some mechanisms are intrinsic to the bacteria, whilst others are acquired from interaction with the surrounding environment. Almost all strains of *P. aeruginosa* (Brinkman *et al.* 2000) have reduced permeability to antibiotic agents, thus reducing the concentration which can reach its target, reducing effectiveness. This decreased permeability has been found due to overexpression of proteins by *P. aeruginosa* on the outer surface of the cells which competes with the lipopolysaccharides (LPS) to bind to rifampicin or gentamicin as the first step of actively passing the antibiotic molecule into the cell (Brodersen *et al.* 2000).

However, low molecular-weight hydrophilic antibiotics such as lactams are not affected because they pass through the aqueous channels formed of outer membrane protein porin proteins (oprD). Porin proteins (oprD) is extremely regulated protein at transcriptional and post-transcriptional levels. Thus, *P. aeruginosa* can develop resistance to lactams by decreasing the expression of OprD proteins (Livermore 2001).

1.1.9.3.3.2- Efflux pumps system:

The efflux pump is an active mechanism by which *P. aeruginosa* selectively drives the antimicrobial molecules back out of the cell. Four types of efflux have been described: mexXY-oprM; mexAB-oprM; mexEF-oprN10 and mexCD-oprJ (Lambert 2002). Most of the antibiotics are susceptible to extrusion by one type efflux systems or more, except the polymyxins (Lambert 2002).

1.1.9.3.3.3- β-lactamase production:

Almost all strains of *P. aeruginosa* have the ability to produce an enzyme which hydrolyses the active ring (beta lactam ring) of penicillins and cephalosporins via the expression of the ampC gene, thus decreasing efficacy (Bradford 2001; Nicasio *et al.* 2008).

1.1.9.3.3.4- Production of extracellular substances:

P. aeruginosa secretes a number of extracellular substances including mucus, capsule and alginate. These aid in the formation of biofilms and reduce antibiotic effectiveness. Alginate and mucins have been shown to hinder the penetration of antibiotics (Hentzer *et al.* 2001).

1.1.9.3.3.5- Mutational changes of target enzymes:

Many antimicrobials act through targeting essential bacterial enzymes to disturb the bacterial metabolism; however, mutations resulting in changes to enzyme structure render them insensitive antimicrobial activity (Moolenaar *et al.* 2000; Martinez & Baquero 2000). For example, *P. aeruginosa* undergoes changes in

the quinolone-resistant-determining regions (QRDR) of gyrA, gyrB, parC and parE leading to changes in the amino acids forming the DNA gyrase, which is the target for quinolone antibiotics, rendering them inactive (Akasaka *et al.* 2001).

1.1.9.3.3.6- Change of metabolic processes:

P. aeruginosa has the ability to change its metabolism from oxygen-dependent (aerobic) into oxygen-nondependent (anaerobic). This advantageous trait of *P. aeruginosa* enables it to escape antimicrobials attacking the aerobic metabolic pathway. Such metabolic change has been observed in patients with cystic fibrosis of the lungs, where originally aerobic *P. aeruginosa* has been able to survive anaerobically when the aerobic pathway is targeted by antibiotics (Hassett *et al.* 2009).

1.1.9.3.3.7 Transfer of genetic materials:

Genetic transfer occurs between *P. aeruginosa* cells, especially those included within biofilms. The change in the genetic make-up of bacterial cells allows them to escape the effect of antibiotics directed towards certain genetic and phenotypic structures (Ghigo 2001). As mentioned already, there are many other factors causing increased resistance of biofilm bacteria relative to their planktonic counterparts.

1.1.10- Biofilm formation

Biofilms are generally defined as the growth of micro-organisms over a surface with the formation of extracellular polymeric substance (Garrett *et al.* 2008). Bacterial biofilms are characterised by a dynamic complex system that exists either on other biological systems (e.g. human skin) or abiotic environments such as plastic surfaces. Biofilm structure is one of the dominant and preferred forms of bacterial existence in nature (Costerton 1999), because it allows protection of bacteria in the face of turbulent environments (e.g. water pipes and

ventilation flues), dehydration, salinity, UV radiation and antibacterial agents. Moreover, biofilm structure facilitates the interaction between bacterial cells in proximity for the benefit of the whole bacterial colony (Hall-Stoodley *et al.* 2004). Once bacteria form biofilms these become less susceptible to biocides and antibiotics than planktonic bacteria (Donlan & Casterton 2002). Accordingly, a bacterial biofilm is a major issue in skin infections, often forming a source of persistent soft tissue infections and infections related to operative devices and prostheses (Cloete 2003).

The resistance of bacterial biofilms to biocides are a result of:

- The protective effect of the extracellular polymeric substance (EPS) matrix, which interferes with the diffusion of antibiotics and other biocidal agents through it and at the same time, allows beneficial supportive interaction between the biofilm cells.

- The resistant nature to antibiotics of biofilm bacteria due to factors such as the slow growth rate and altered metabolic state, together with the high adaptation to the environmental conditions, which are transferred genetically to daughter cells creating subpopulations of highly resistant cells (Cloete 2003; Keren *et al.* 2004).

Many environmental conditions stimulate bacterial cells to form biofilms (Karatan & Watnick 2009). Biofilm formation is a multi-step process, which begins with attachment and terminates with maturation. The process has been the subject of study from many researchers in recent years (Karatan & Watnick 2009).

Cyclic diguanosine monophosphate (ci-di-GMP), a signalling molecule prevalent in most types of bacteria, is a major regulator of biofilm formation, which switches the bacterial growth phase from planktonic to sessile and lastly biofilm

forming bacteria (Van Gestel *et al.* 2015). The association between high intracellular levels of ci-di-GMP and the tendency to sessility has supported the involvement of this molecule in the biofilm process.

The biofilm process often involves two component regulatory systems (TCS). TCS are stimulated at specific receptor sites by environmental factors (e.g. sensor histidine kinase receptors). Then regulatory responses are elicited by response regulators which mediate the expression of multiple genes responsible for EPS and biofilm formation. The conserved GasS-GacA system is one example of a TCS that has been found in *P. aeruginosa* (Karatan & Watnick 2009). Sometimes, the regulatory system is composed of three components, as in Gram negative bacteria: a LuxR receptor homolog, a LuxI synthase homolog and an acyl-homoserine-lactone (AHL) signalling molecules, which works in harmony to form biofilms (Fuqua & Greenberg 2002).

Quorum-sensing (QS) circuits have been shown to play a role in the process of biofilm formation in a wide range of bacterial strains (Karatan & Watnick 2009). QS molecules are small factors which are produced and sensed by bacteria within the EPS of the biofilm. They serve to communicate between bacterial cells, co-ordinate their functions and regulate the responses required to establish the biofilm architecture. They are thus called auto-inducers and are effective when their concentration in the EPS exceeds a certain threshold.

Biofilm forming bacteria have been the subject of many studies to elucidate the process of biofilm formation, beginning from attachment and ending in maturation. Biofilm formation is a five-stage process that starts with attachment and proceeds to the biofilm maturation and then to the bacterial cell detachment (Figure 1.4) (Otto 2008; Otto 2012).

Bacterial adhesion (attachment) to a surface-material is the principal step in the attachment process; it is typically a nonspecific process depending on the forces operating between the surface of the bacterial cell and the surface material, like the hydrophobic interactions between bacteria and polyethylene plastic (Jacquin *et al*. 2019). In the case of inserting an indwelling medical device or an implant into the body, it is rapidly covered with host matrix proteins serving as bacteria receptors (Veerachamy *et al.* 2014). The most significant factor in the preliminary attachment is typically adhesion to these proteins. Microbial surface components can bind adhesive matrix molecules: they are able to link to host matrix proteins such as vitronectin, fibronectin, collagen and fibrinogen (Patti *et al*. 1994; Bowden *et al*. 2008). Additionally, some proteins directly mediate adherence to both the matrix proteins and the surface material (Heilmann *et al*. 1997). Thus, being able to connect directly to the mammalian cell surface polymers and to host matrix proteins is one of the most significant of the microorganism, and is particularly important in device-related infection (Otto 2013). Biofilm structuring is the next vital step in the maturation process. Biofilm structuring depends on the disruptive processes that lead to the mushroom-like structure formation and the complex structures such as the fluid filled channels for exchanging metabolic waste products and nutrients (Sanford *et al*. 1996). The detachment of the bacteria clusters or the single cells from the biofilm is the final step in the life cycle of the biofilm. This process depends on parts of the matrix that are detached from the remaining of the biofilm; for example, through enzymatic activity or mechanical forces that break down the molecules of the matrix (Rollet *et al*. 2009).

Figure 1.4: A model of biofilm formation and development on an abiotic surface: The five main stages of biofilm development: (1) Initial attachment; (2) reversible attachment (3) aggregated cells change to a non-motile state and become irreversibly attached (4) colonies develop into mature biofilms where the bacteria are fixed in an exopolysaccharide matrix; (5) final stage is biofilm forming, it may disrupt and disperse cells into the external environment (Riedel and Eberl 2007).

1.11.1- Effect of biofilms on wound healing

Biofilms have been observed in wounds with chronic infection (Ngo *et al.* 2007). Although the human immune mechanisms endeavours to clear invading bacteria and limit spread into tissues, biofilm formation remains a challenge to both the body and external treatment mechanisms (Guyton 2006).

S. aureus in biofilms has been demonstrated to be less sensitive to antimicrobials than its planktonic counterparts (Davis *et al.* 2008). The multispecies nature of biofilm forming bacteria presents a virulent microbial load (Ngo *et al.* 2007; Malic *et al.* 2009), that is often associated with complications (Bjarnsholt *et al.* 2008; Rhoads *et al.* 2008).

Two of the mechanisms involved in the resistance of biofilm organisms are prevention of phagocytosis (Leid *et al.* 2005; Günther *et al.* 2009) and opsonisation of bacteria owing to the protective action of EPS within the biofilm.

Spontaneous healing of wounds infected with biofilms is unlikely due to the high bacterial production of toxins, which interferes with the healing processes and physical impediments.

The presence of high levels of antigens has grave consequences on wound healing (Cerca *et al.* 2006). Some studies have observed that QS molecules (QSMs), produced by Gram negative bacteria, such as *P. aeruginosa* in biofilms, inhibit keratinocyte migration, hence preventing wound healing (Whiteley *et al.* 2001; Hofmann *et al.* 2005).

Moreover, the resistant bacteria showed cross-resistance to other unrelated antipseudomonal agents (Mulet *et al.* 2009). As such, mutant strains develop in the context of treating chronic wound infections (Hofmann *et al.* 2005). Thus, it is of great importance for medical practice and care to eradicate biofilms in managing chronic wounds, (section; 1.1.12).

1.1.12- Skin wound infections therapy

1.1.12.1- Wound cleansing and debridement

For wounds to heal both foreign bodies and devitalised tissues should be removed, as they interfere with the healing processes and provide suitable media for infection (Grey & Segre 2006; Stadelmann *et al.* 1998; Ng *et al.* 1997; Leaper 2002). Cleansing is the term used for removal of foreign materials and debridement is that used for removal of devitalised tissues. Cleansing is mechanical, chemical or biological, which can be performed using water (Riyat and Quinton, 1997), saline or antiseptic solutions (Ferguson *et al.* 2004; Anglen 2001).

Moore and Cowman, 2008, demonstrated a saline spray with aloe vera, silver chloride and decyl glucoside was superior to saline alone in healing of pressure ulcers.

1. 1.12.2- Autolytic debridement

Autolytic debridement, which is caused by the patient's own enzymes, removes eschar and slough from the wound. This natural phenomenon needs moist environments to occur (Hofman 2007; König *et al.* 2005).

1.1.12.3- Maggot (larval) Debridement

The green bottle fly larvae debride dead tissues in wounds by feeding on them (Chan *et al.* 2007; Church *et al.* 2002). The larvae also decrease the bioburden of wounds by secreting bactericidal metabolic products (Steenvoorde & Oskam ,2006; Armstrong *et al.* 2005; Church *et al.* 2002). Moreover, it is not effective when the causative agent of wound infection is *P. aeruginosa*, since the organism is lethal to the larvae (Andersen *et al.* 2010).

1.1.12.4- Enzymatic debridement

Enzymatic debridement utilises enzymes such as collagenase, streptokinase, and fibrinolysin to digest the protein components of sloughs or eschars of wounds (Marazzi *et al.* 2006). Enzymatic debridement is selective according to the specific action of the enzyme used. For instance, collagenase degrades only the collagen components of wound sloughs (Marazzi *et al.* 2006; Moore & Jensen 2004).

1.1.12.5- Surgical debridement

Surgical debridement is mechanical removal of most of the necrotic tissues, usually in operating theatres under anaesthesia. It is fast, effective and can prevent further complications such as amputation if slower methods of debridement are used and fail, especially in vulnerable patients, e.g. diabetics (Werner *et al.* 2008; Wang *et al.* 2008; Armstrong *et al.* 2002; Faglia 2006).

1.1.12.6- Topical Oxygen Therapy

Oxygen is delivered to a wound in the form of supersaturated oxygen (Davis *et al.* 2007; Gottrup 2004). It provides cells with energy that is utilized in protein production and angiogenesis, which are necessary for wound healing (Davis *et al.* 2007; Gottrup 2004).

1.1.12.7- Hyperbaric oxygen therapy

This form of oxygen therapy is needed where oxygenation is lacking, e.g. in devitalized chronic wounds especially in diabetic patients (Kalani *et al.* 2002). It provides oxygen tension required by the tissues to support wound healing (Flanagan *et al.* 2009; Roeckl-Wiedmann *et al.* 2005).

1.1.12.8- Negative pressure wound therapy (NPWT) via vacuum-assisted closure

Negative pressure wound therapy (NPWT), also known as vacuum-assisted wound closure. Using sub-atmospheric pressure to the superficial area of wounds and management of various acute and chronic wound treatment (Capobianco *et al.* 2009). This therapy helps wound closure and healing (Armstrong *et al.* 2007; Steenvoorde & Oskam 2006). but is currently lacking clinical evidence (Novak *et al.* 2014; Panayi *et al.* 2017).

1.1.12.9- Antiseptics/ topical applications

These are mainly used to reduce the microbial load of wounds, but they can achieve total clearance of microbes in some instances. Accordingly, they are primarily used as prophylactic measures to prevent or decrease the risk of wound infection (White *et al.* 2001). One drawback of their use is the occasional development of resistant strains (Cheng *et al.* 2008).

1.1.12.9.1- Povidone iodine

Povidone iodine is either used alone or combined with other antimicrobials to maximize and widen its effect (Ferguson *et al.* 2003; Sherlock 1984). There is controversy regarding the efficacy of iodine in decreasing the bioburden of wounds with conflicting results (Giacometti *et al.* 2002). Cooper (2007), confirmed in his review that poviodone iodine is an effective, broad-spectrum agent with no recorded organismal resistance. It has also been shown that it is less toxic than most antimicrobials (Muller *et al.* 2008). This suggests it may be one of the best topical antimicrobial preparations for management of wounds.

1.1.12.9.2- Silver dressings

Silver compounds have been demonstrated to be successful in treating wounds (Parsons *et al.* 2005), in both *in vitro* and *in vivo* studies (Ip *et al.* 2006; Church *et al.* 2006). Of these compounds, the most known agents are silver sulphadiazine and silver impregnated activated charcoal. Silver compounds carry out their antimicrobial effect through depriving the organisms of vital ions. This has been demonstrated by X-ray microanalysis (Hobot *et al.* 2008). Silver has been showen to require higher concentartion to kill bilfilm organisms than planktonic organisms (Knight *et al.* 2009; Bjarnsholt *et al.* 2007), regardless of whether the biofilm is formed of single or mixed bacterial strains. Effectiveness of silver dressings is related to the rate of silver release, which should be taken into consideration to choose the appropriate dressing type.

1.1.12.9.3- Combined dressings

Combinations of antimicrobials in dressings increase their efficacy due to their synergistic effects on microbes. Examples of these are 1% silver-zinc allantoinate cream (Margraf & Covey 1977) and Povidone iodine and alcohol (Mertz *et al.* 1984). Although, these are more effective than single

antimicrobials, these combinations may fail due to the heavy microbial burden (Mertz *et al.* 1984) or the presence of biofilms (Percival *et al.* 2004).

1.1.12.9.4- Surgical intervention

Surgical interventions may be resorted to in cases of non-healing wounds or if there is high risk to organs or life. They vary from removal of dead tissue, with skin replacement, to amputation of a toe, foot or the whole limb.

1.1.13- Possible new alternative skin wound infection treatment

To date, treatment of skin wound infections has heavily relied on the use of antibiotics as either topical creams or administered systemically (Howell-Jones *et al*. 2005). However, the increase in antibiotic resistance have encouraged researchers to find solutions for managing both wound infections in general and antibiotic resistance. Recent studies have shown that ultrasound can be used in conjunction with antibiotics to treat infection (Yua *et al*. 2011; Ensing, *et al*. 2006; Carmen *et al*. 2004; Redisk *et al*. 1998; Williams & Pitt 1997; Redisk *et al*. 2000). This method relies on the basis that ultrasound causes an increase in membrane permeability allowing large molecules such as antibiotics to enter the infected cells (Runyan 2006) which increases efficacy of antibiotic delivery and aids wound healing (Alumia 2013; Lewin *et al.* 2013). Ultrasound is a potential alternative method which could be used either alone or in combination with other approaches.

Ultrasound is defined as mechanical waves, which penetrate different materials, such as fluids and soft tissues. The main mechanism of therapeutic action of ultrasound as it can stimulate cell activity, and enhances the movement and vibration of cellular fluids near the surface of cell (Ward 2015). Acoustic cavitation caused by ultrasound, in which tiny bubbles form in surrounding liquids and rapidly collapse with a huge increase in local pressure and shear

stresses is one mechanism by which ultrasound may have antibacterial properties and form of free radical (Erriu *et al*. 2014; Scherba *et al.* 1991). In one study using ultrasound alone, Joyce *et al.* (2003) investigated the effect of power ultrasound at different powers and frequency (20, 38,512 and 850 kHz) on Bacillus subtilis. They found that low frequency ultrasound (20 and 38 kHz) can reduce viable numbers of cultured Bacillus subtilis, while high frequency (512 kHz and 850 kHz) effectively disperses clumps of bacteria.

Therefore, it would be beneficial to investigate the use of antibiotic-independent, lower frequency ultrasound in reducing the bacterial load of infected skin wounds (Chapter 6).

1.1.14- Aim and objectives

Many of the current agents used to treat wound infections, also result in toxicity to mammalian cells and the extent to this and their effects on wound healing is not fully understood. Novel anti-microbial strategies are needed which avoid the limitations of antibiotic resistance and local toxicity to skin cells which delay wound healing. Thus, this thesis aimed to investigate the effects of different types of anti-microbial strategies which generate active free radicals to reduce bacterial load in infected wounds. Using tissue engineered skin as an infected-wound model, the effects of antimicrobial strategies were determined on the bacterial load and the skin cells.

To achieve this, this thesis will discuss a number of objectives:

1- Investigate the effects of different types of anti-microbial strategies which generate active free radicals or reactive oxygen species (Chapter 2, section 2.1.2.1.3.2, Equation 2.1) in common skin infecting organisms in planktonic and biofilm culture.

2- Establish an *in vitro* tissue engineered skin model using easily accessible and well characterised cell lines: HaCaT and fibroblasts.

3- Evaluate the use of a tissue engineered 3D skin as a model for infected wounds and burns.

4- Determine the effect of biocidal agents on the viability of bacteria on 3D skin wounds and burns.

5- Determine the effect of biocidal agents and infective agents on keratinocyte and fibroblast viability and phenotype.

6- Investigate the effect of low frequency ultrasound (LFU) on bacteria and skin cells.

Chapter 2

Effects of biocides on planktonic and biofilm bacteria

2.1- Introduction

Biocides are chemical compounds containing one or more active substances which kill or inhibit microorganisms (McDonnell & Russell 1999). However, biocides have non-specific target activity and generally can inhibit any organism present rather than showing selectivity to specific types of bacteria (Maillard 2002)

Biocidal agents have been applied for centuries. Agents such as oils and balsams were used as early as 2400 B.C during mummification of the dead. In addition, the use of copper and silver containers for storage of drinkable water, were utilised for centuries to reduce bacterial load within water. Moreover, natural compounds such as salt and spices have been used for the preservation of foods, and treating of skin wounds using vinegar and honey (Maillard 2002; Russell 2003).

There are a wide range of biocidal agents in common use both during preservatives and in the medical area as antiseptics and disinfectants (Hugo 1991; Russell, 2003). Biocidal agents have the ability to inhibit or destroy infectious microorganisms. However, these are different from biocides, with the key difference being mode of action.

An antimicrobial can be defined as a low concentration of medicines exerts an action exhibits selective toxicity towards against microbial pathogens. Typically, the antimicrobial agents have one specific target site within the microorganism with an essential function (Saga & Yamaguchi 2009). For example, β-lactams and glycopeptides which inhibit peptidoglycan layers synthesis in the cell wall, whilst, tetracyclines, chloramphenicol and (macrolide antibiotics) prevent protein synthesis (Riesbeck *et al.* 1990), and sulphonamides disrupt folic acid

synthesis. However, biocidal agents have multiple and unspecific target sites in the microorganisms affecting cytoplasmic membranes, proteins, DNA, RNA and other cytosolic components (Russell 2003).

Antimicrobial therapy is applied *in vivo* and is often targeted to the locus of infection, the concentrations utilised are sometimes near the minimum inhibitory concentration (MIC), decreasing bacterial load and enabling the immune system to eliminate the pathogen. Biocides are often applied at concentrations much higher than the MIC and the minimal bactericidal concentration (MBC). Biocidal agents are commonly used as decontaminants on surfaces, and are utilised for short time periods, whereas antimicrobial therapies are applied to the patient directly for days to weeks (Maillard 2002).

2.1.1- Application of biocidal agents

During the twentieth century several biocidal compounds became common in clinical use. Today, biocides play an important role in controlling infectious diseases and in the prevention of healthcare-associated infections (Maillard 2005). However, with the increase in antimicrobial resistance worldwide leading to increased mortality and morbidity as a result of infections, the importance of infection control and the role of preventative biocides in health care are paramount. Biocides are used in many aspects of the environment such as treatment of water; disinfection during clinical practice; industrial food stuffs; cosmetics and pharmaceutical products.

2.1.2- Mode of action of oxidising biocidal agents

Biocides are broad-spectrum (Figure 2.1) and can be used in various settings with multiple and unspecific target sites within microorganisms, targeting the cytoplasmic membrane, proteins, DNA, RNA and other cytosolic components. Oxidising biocidal agents are low molecular weight compounds, and thus have

the ability to pass through bacterial cell membranes and attack internal targets or cause disruption of bacterial cell walls and membranes causing cell death (Figure 2.1). There are wide ranges of oxidising biocides available; this thesis focuses on four potential biocidal agents: silver nitrate, hydrogen peroxide, isothiazolone and medical grade manuka honey (Figure 2.1).
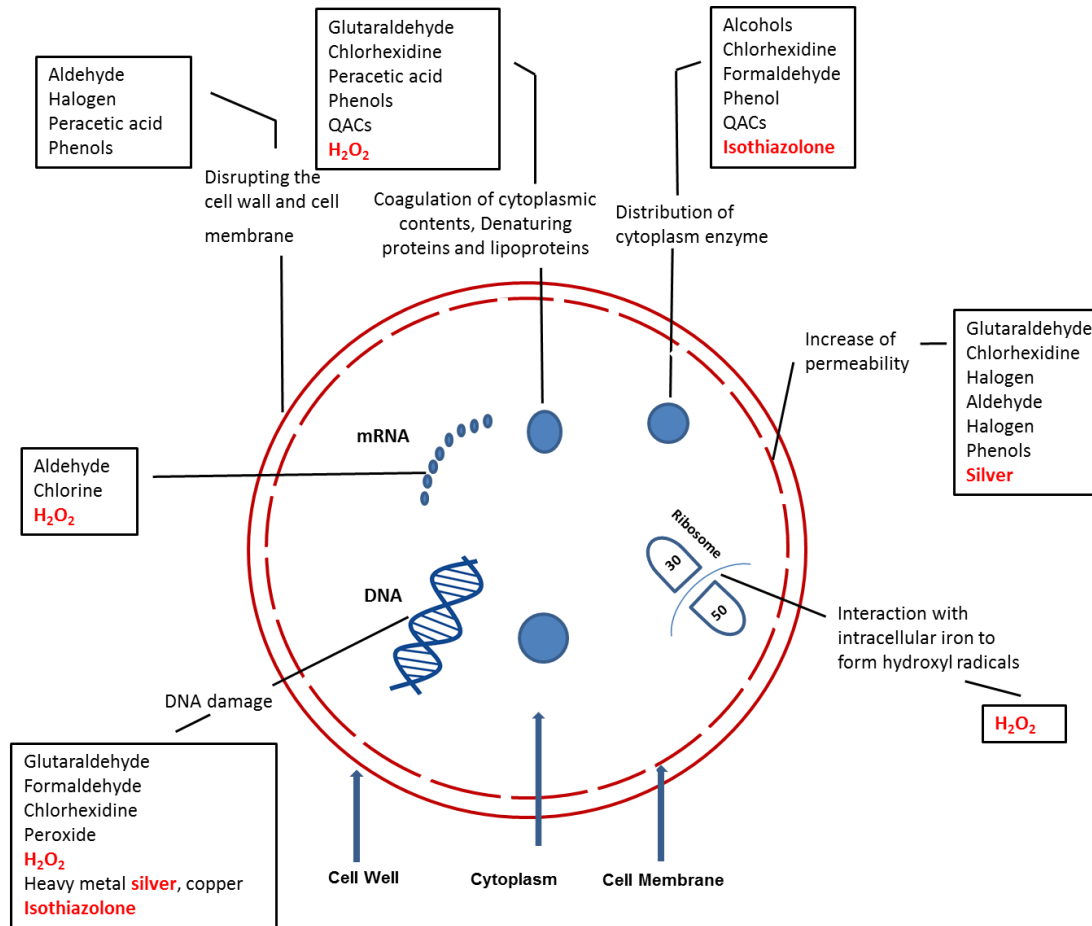
Figure 2.1: Mechanism of different types of biocides and target site action. Four potential oxidizing biocidal agents used in this project: silver nitrate, hydrogen peroxide, isothiazolone (shown in red).

2.1.2.1- Silver nitrate

Silver (Ag) is a natural heavy metal with a specific gravity of more than 5 (Silver 2003) (Duxbury *et al.* 1986). It is a transition metal according to its electron configuration (McNaught & McNaught 1997), when ionised (Ag+), is a weak acid (Gadd 1992). The antibacterial activity of silver was discovered thousands of years ago (Rai *et al.* 2009). There is evidence of Silver nitrate (AgNO$_3$) utilisation for medical conditions during Roman periods in 69 B.C (Klasen 2000). In the 14th century, AgNO$_3$ was used as a prophylaxis against wound infection by local application and in the following century (Alexander 2009). In the 19th century, silver compounds were discovered to have antibacterial activity, especially against *S. aureus* and *Bacillus anthracis* (Schneider 1984*).*

The success of silver in infection prophylaxis persisted until the early 20th century. For instance, the efficacy of Silver-containing dressings in preventing infections in burns and wounds was established (Castellano *et al.* 2007; Chopra 2007). Silver was also used in the treatment of eye infections, e.g. streptococcal sepsis, which were treated with silver suspensions (Roe 1915; Sanderson-Wells 1918). There was a drop in the use of silver as an antibacterial agent after the discovery of antibiotics (Chopra 2007; Davies *et al.* 2013). Neverthless, in the 1960's, AgNO$_3$ represented a cheaper more effective alternative than antibiotics in the prevention of infections of burns (Moyer *et al.* 1965).

A 0.5% concentration of AgNO$_3$, was found to inhibit the growth of *Streptococcus pyogenes* and *P. aeruginosa*, the most common organisms to colonise burns, without affecting the successful application and acceptance of a subsequent skin graft (Moyer *et al.* 1965).

2.1.2.1.1- Current applications of antibacterial silver

$AgNO_3$ continues to be the standard prophylaxis for ophthalmia neonatorum in some developing countries (Mullick *et al.* 2005). Although silver-containing dressings were originally used in burns, their use has expanded to include almost all types of wounds, e.g. acute, chronic, pressure ulcers, diabetic and neuropathic ulcers, especially heavily infected ones (Edwards-Jones 2009). (Silver *et al.* 2006; Atiyeh *et al.* 2007).

Another important medical use of silver is its incorporation into medical devices which are implanted in the body to prevent colonisation of bacteria on these devices with subsequent complications (Weber & Rutala 2001). The antibacterial effect of silver was utilised in non-medical products as well, e.g. clothing, deodorants, kitchen appliances, children's toys and water purifiers (Luoma 2008).

The use of silver as an antibacterial agent has markedly increased during the last decade (Chambers *et al.* 2007). In 2004, the expenditure of the NHS on silver dressings was £858,000, which rose to £25 million in 2010 (National Prescribing Centre 2010). One concern related to the increasing exploitation of antibacterial silver is the development of bacterial silver resistance, thus impinging upon its efficient use in combating infection (Chopra 2007).

2.1.2.1.2-Toxicity of silver

Heavy metals, e.g. mercury, arsenic and lead, are known to be toxic at low concentrations (Ibrahim *et al.* 2006); nevertheless, silver is well tolerated when applied to wounds with only minimal adverse effects like skin irritation (Weber & Rutala 2001). Silver-containing implanted medical devices (e.g. catheters and endotracheal tubes) were not associated with any toxicity to patients and high-risk patient populations are rare (Veenstra *et al.* 1999).

The effect of anti-sub-cytotoxic Ag^+ concentrations is that it enhances the human keratinocytes proliferation that might be linked to a modest increase in intracellular ROS levels (Duan *et al.* 2018).

Silver toxicity to skin cells based wound dressings which need to be managed by a wound nurse who can determine at which point the dressing becomes more harmful than helpful. On the other hand, repeated systemic introduction of silver, either orally or by injection, may confer some risk through deposition in liver, lungs, spleen, brain and skin. Silver deposition in skin and mucous membranes causes argyria, a condition characterized by bluish grey discolouration of tissues with life threatening consequences. Fortunately, this resolves upon stoppage of silver treatment (Lansdown 2007).

The only organ that seems to be adversely affected by silver deposition is the brain and the nervous system giving rise to conditions like myoclonic status epilepticus, seizures and peripheral neuropathy (Vik *et al.* 1985; OHBO *et al.* 1996; Mirsattari *et al.* 2004). In view of the above, there is no sound reason to stop using silver as a local antibacterial agent for skin infections (Lansdown 2007).

2.1.2.1.3- Antibacterial mode of action of silver

Ag^+ binds to several anions, including sulphur (Grier 1968). Since sulphur is abundant in biological systems, it has been suggested that Ag^+ performs its antibacterial activity through binding to vital bacterial sulphur-containing nucleophiles (Nies 1999). Some of these targets have been discovered and will be discussed below.

2.1.2.1.3.1. DNA

It has been suggested that silver compounds perform their antibacterial activity through binding to the DNA of bacterial cells (Rosenkranz & Carr 1972). Fox,

1969, determined the sites involved in this binding to be the nitrogen atoms sharing in the hydrogen bonds between the two DNA strands, specifically N1 of adenine and guanine and N3 of cytosine and thymine; thus, deforming the DNA enough to interfere with its replication.

Later, it was confirmed, through Fourier transform infrared spectroscopy that Ag+ can bind to DNA *in vitro*; but contrary to Fox's hypothesis, the binding takes place through N7 of guanine and adenine (Arakawa *et al.* 2001)*. In vivo*, this binding leads to condensation of the bacterial DNA as seen by the transmission electron microscopy and also by X-ray microanalysis, which interferes with its subsequent replication. It is not known for sure whether the DNA condensation is directly related to silver binding or is secondary to other damage caused by Ag+ (Feng *et al.* 2000).

2.1.2.1.3.2. Protein
Silver is known to bind to amino acids; and indeed is utilised to stain proteins in polyacrylamide gels (Clement & Jarrett 1994). Ag^+ binds to sulphur residues or nitrogen-containing side chains of amino acids (e.g. arginine, histidine, lysine and methionine) (Jover *et al.* 2008). As a consequence of this binding, the tertiary structure of proteins is disrupted with inhibition of its function (e.g. enzymes lose their catalytic functions).

Although *in vitro* studies have specified the enzymes that can be inhibited by Ag+ (e.g. succinate and NADH dehydrogenases, NADH quinone reductase and phosphoribosyl 1-pryrophosphatase), this is not a guarantee that the same action would occur *in vivo* or that the enzymatic inhibition is the cause of the antibacterial MOA of Ag+ (Martin 1963; Bragg *&* Rainnie 1974; Semeykina *et al.* 1990; Xu & Imlay 2012). However, it is well established that Ag+ can inhibit

dehydratase enzymes of *E. coli in vivo* and that these enzymes may well be considered targets for antibacterial agents (Xu & Imlay 2012).

It has been found that binding of Ag^+ to dehydratases results in the release of Fe^{2+} as a consequence of the reaction of Ag^+ with the 4Fe-S clusters within the enzymes (Xu & Imlay 2012). It has been proposed that the release of Fe^{2+}, rather than the enzymatic inhibition per se, that leads to bacterial cell death, as Fe2+ produces toxic reactive oxygen species (ROS) through the Fenton reaction (Xu & Imlay 2012)(Equation 2.1).

$$Fe^{2+} + H_2O_2 \rightarrow Fe^{3+} + OH\bullet + OH^-$$

Equation 2.1: The Fenton reaction (Benatti *et al.* 2006)

2.1.2.1.3.3- Cell membrane

The cell membrane was found to be one of the main targets of Ag^+, with 80% of Ag+ in antimicrobial silver preparations binding to the cell membrane, with the remaining 20% bound to nucleic acids, as evidenced by radiolabelled Ag+ (110AgSu) applied to *P. aeruginosa* for 1 h, (Rosenkranz & Carr 1972). Further studies using TEM showed the effect of AgSu on *S. aureus* (detachment of the cell membrane from the cell wall) and on *P. aeurginosa* (distortion of cell membranes) (Coward *et al.* 1973).

Whether detachment or distortion of cell membranes is the mechanisms responsible for the antibacterial MOA of Ag^+ remains unclear. Ag^+ was found to cause fast dissipation of the proton motive force at the cell membrane in *E. coli* and *Vibrio cholerae* (Dibrov *et al.* 2002; Holt & Bard 2005), which denotes that the function, in addition to the structure, is disturbed by Ag+. Lok *et al*, 2006, confirmed this concept by observing that exposure of *E. coli* cells to Ag^+ led to rapid and substantial leakage of K^+ and ATP out through their cell membranes.

Moreover, Ag^+ was found to interfere with the oxidative phosphorylation pathway stalling the electron transfer at complex I (NADH dehydrogenase), suggesting inhibition of this complex (Holt & Bard 2005).

As a consequence of electron transfer stalling, reactive oxygen species (ROS) may be released with further damage (Holt & Bard 2005).

2.1.2.1.3.4. Generation of reactive oxygen species

During metabolic oxidation reactions, molecular oxygen is reduced to either hydroxyl radical (HO), hydrogen peroxide (H_2O_2) or superoxide (O^{2-}), which are collectively known as ROS (Imlay 2013). O_{2-} and H_2O_2, are short-lived with minimal toxic effects but they can interact with iron-sulphur clusters in various enzymes releasing free iron (Fe^{2+}), which, in turn, may react with H_2O_2 producing OH through the Fenton reaction (Imlay 2013).

OH, contrary to O^{2-} and H_2O_2, has high oxidating potential that may damage DNA, proteins or cell membranes and eventually may lead to cell death (Kohanski *et al.* 2007). The toxic potentials of ROS are guarded against by specific scavenging enzymes (e.g. catalses and superoxide dismutase scavenging H_2O_2 and O^{2-} respectively). It has been suggested that Ag+ would create favourable conditions for O^{2-} generation through binding In the cytoplasm to thiol-containing enzymes (e.g. NADH and succinate dehydrogenase) (Texter *et al.* 2007), the target of silver nitrate in the cytoplasm by binding to the Thiol groups and causing inactivation of enzymes and proteins. The main interaction of Silver with the 30S ribosomal subunit, led to disorders of activity and activity of cellular enzyme (Yamanaka *et al.* 2005). Silver may also act directly on DNA, producing many changes condensation and degeneration of DNA strands and cell death (Klueh *et al* 2000; Warriner *et al.* 2005).

2.1.2.2- Isothiazoline

Isothiazoline compounds, such as N-methylisothiazolinone (MIT), 5-chloro-N-methylisothiazolinone (CMIT) and benzisothiazolinone (BIT), are characterized by antibacterial activities (Nicoletti *et al.* 1993).

These antibacterial activities affect a wide range of bacteria and work in a wide range of temperatures and pH values, making isothiazolone a favourable bacteriostatic agent (Russell *et al.* 2004), comparable and even superior to formaldehyde. The available suspensions of isothiazolone are water soluble and tend to undergo chemical degradation to non-toxic compounds. Furthermore, they are compatible with a wide scale of products. These characteristics have also made isothazoline preparations commercially successful in a wide range of industrial purposes (Nicoletti *et al.* 1993). Preservative preparations are one of the common uses of isothiazolones in industry. However, due to its irritative nature, isothiazolone preservative solutions are restricted in use.

Chloromethylisothiazolinones, which are included in personal care products for example, are not intended to come into contact with mucous membranes. Another example of the industrial restricted use is Benzisothiazolinone, which is not legalised to be used in personal care products in Japan (Ministry of Health, Labor and Welfare 2005) and Europe (European Union 1976); this is used in household products, paints, adhesives and industrial emulsions.

As preservatives against bacteria, isothiazolones are assumed to chemically react with thiol containing cytoplasmic and membrane bound bacterial enzymes (Denyer 1995). This mechanism of action is supported by the finding that the activity of isothiazolones is markedly antagonised by competitive materials containing thiol within their structure. Isothiazolone antibacterial action is

automatically intensified by the character that the interaction of isothiazolone with bacterial enzymes leads to the oxidation and the production of more ring-opened forms of biocides and more isothiazolone dimers that add to the antibacterial action (Collier *et al.* 1991). In addition, some preparations like chloro-methyl-isothiazolinone affect and damage of DNA (Russell & Chopra 1990).

2.1.2.3- Hydrogen peroxide

2.1.2.3.1- Nature and characteristics

Hydrogen peroxide is a colourless acid that is slightly more viscous than water (Housecroft *et al.* 2010). Due to its antimicrobial properties it was mainly used as a disinfecting and sterilizing agent for surfaces and instruments. Thanks to its relative safety, its use extended to wide scale use as a food preservative and even as a local treatment to combat bacterial infections (e.g. in wound infections).

2.1.2.3.1.2- Historical background

Hydrogen peroxide was first discovered in 1818 by the French chemist Thenard (Thénard 1818), but it was the British doctor, Richardson who first suggested its use as a disinfectant in 1858 when he observed its ability to get rid of foul odours, based on the belief, which was not far away from the truth, that foul odours were related to offensive disease-producing micro-organisms. Thus, hydrogen peroxide was commercially used as a disinfectant for the first time under the name of Sanitas (Block 2001).

2.1.2.3.1.3- Hydrogen peroxide existence in the biological systems

Hydrogen peroxide is naturally produced in many organisms as an intermediate product during cellular oxidation processes. When oxygen carries out its function of oxidising cellular substrates to produce energy, it becomes reduced

forming several compounds. The ultimate end product of these compounds is water, but it is formed in steps passing through intermediate potentially harmful compounds including hydrogen peroxide.

For that reason, organisms evolved ways to safeguard their structures against it.

One of the solutions was to evolve enzymes capable of degrading hydrogen peroxide, like catalase, peroxidase and superoxide dismutase (Winterbourn 2013). These enzymes are the main cause of resistance to externally applied hydrogen peroxide.

2.1.2.3.1.4- Range of activity

Hydrogen peroxide is active against a wide range of micro-organisms: bacteria, protozoa, prions, viruses, yeast and fungi. Concerning its action on bacteria, it is highly effective against vegetative bacteria, but it also hinders the growth of a wide range of anaerobic bacteria and bacterial spores (Baldry *et al.* 1983). With greater activity on Gram negative than Gram positive bacteria (Dorobantu *et al.* 2015), this is thought to be due to the difference in cell walls. The concentration of hydrogen peroxide preparations varies according to the application. As a skin antiseptic or in wound treatment, it is used in a concentration of 3-6% v/v in water. In dental disinfection, it is applied in a concentration of 0.4-1% v/v. Whilst at a concentrations of 7.5% v/v, it is used as disinfectant, where it is able to inactivate all micro-organisms except large spores (SCENIHR (Scientific Committee on Emerging and Newly Identified Health Risks) 2009).

2.1.2.3.2- Mechanism of action

Hydrogen peroxide, after entering the bacterial cell, reacts with bacterial intracellular iron or trace elements according to the Fenton reaction. The reaction results in the production of free oxygen radicles (e.g. hydroxyl ions),

which have a high potential of oxidising vital structures in the cell destroying them. This oxidative damage is the consequence of breaking vital molecular bonds. For example, it causes DNA and RNA damage (Henle & Linn 1997), deformities in the backbone of vital proteins (Dean *et al*. 1997) and also directly damages the cell membrane and membranous organelles like mitochondria and the cytoplasmic reticulum (Brandi *et al*. 1991; Peterson *et al*. 1995; Baatout *et al*. 2006). Colobert, in 1962, confirmed the pivotal role of iron, or other metal ions for the antibacterial action of hydrogen peroxide, by demonstrating that in the absence of such metal ions, no bactericidal activity would be observed. He conducted his experiments on *E. coli* using ethylene diaminetetracetic acid as a chelating agent to remove free ions from the media (Colobert *et al*. 1962).

2.1.2.3.3-Advantages of hydrogen peroxide

One of the advantages of H_2O_2 is the wide spectrum of micro-organisms it combats. Thus, when used for disinfection or sterilisation in the appropriate concentrations, the disinfected place or instrument is ensured to be reducing of living micro-organisms. It has been used successfully in USSR and the US for sterilisation of spacecraft and was reported to be practical in this field (Wardle *et al.* 1975). Another advantage is its safety within a considerable range of concentrations; it is naturally degraded into water and oxygen. For this reason, hydrogen peroxide is used as a food and water preservative (Yoshpe-Purer *et al.* 1968; Naguib & Hussin 1972).

2.1.2.3.4- Microbial Resistance to hydrogen peroxide

As it has been pointed out above, some micro-organisms possess enzymes that are capable of degrading hydrogen peroxide into water and oxygen (e.g. catalase, superoxide dismutase and peroxidase), which is the main cause of resistance to hydrogen peroxide. Almost all aerobic bacteria and some

facultative anaerobes possess catalase enzymes (Baureder *et al.* 2012). Thus, they are potentially resistant to the action of H_2O_2 if subjected to it in moderate concentrations.

Fortunately, the concentrations of H_2O_2 in-use in the various antimicrobial activities referred to above are considerably higher than that which can be overcome by the organismal natural resistance (Rutala *et al.* 1999). Accordingly, limited tolerance has developed against hydrogen peroxide in spite of the agent having been used for a long time. Another cause of bacterial resistance against H_2O_2 is the formation of biofilms.

2.1.2.3.5- Hydrogen peroxide action on biofilms

H_2O_2 has been shown to have lower activity on biofilm bacteria when compared with planktonic cultures (Exner *et al.* 1987; Vincent *et al.* 1989). This reduced activity was related to decreased penetration and diffusion of H_2O_2 through the extracellular polymeric substance (EPS) of the biofilm, a finding that was confirmed by the observation that bacteria near the outer surface of the biofilm were affected to a greater extent compared to those in deeper layers.

Accordingly, the production of oxygen from a biofilm culture treated with H_2O_2 is an indicator of breakdown of H_2O_2 by resistant catalase-producing bacteria. Further laboratory confirmation of the role of catalase in resistance was the finding that when a catalase inhibitor such as 3-amino-l, 2, 4- triazole was added to the culture, no oxygen was released (Gee *et al.* 1970; Paul *et al.* 1973).

However, compared to other disinfectants, H_2O_2 is still more active in combating biofilms. For instance, it has been shown that contact lens storage solutions using H_2O_2 were accompanied with significantly lower incidence of

contamination with biofilms than in cases where other disinfectants were used (Wilson *et al*. 1990).

2.1.2.4- Honey

2.1.2.4.1- Honey and medical history

Honey is produced by bees from nectar of flowers they feed on. The main components of honey are sugars including fructose and glucose which contribute about 40% and 30% of the total mass respectively (White & Doner 1980) with smaller amounts of sucrose (1% to 12%) and maltose (about 9%). Water and enzymes (diastase, invertase, glucose oxidase and catalase) form the rest of the content (Kamal *et al*. 2002). In addition, honeys contain phenols, which influence its antimicrobial activity, and minerals, such as Mg^{2+}, K^+, Na^+, Zn^{2+} and Cu^{2+} (Farooq Khan & Maqbool 2008), antimicrobial peptides dependent upon the pollen source (Danihlík *et al.* 2018). In order to use honey as a medicine, it should be stored below 20 ^oC to preserve its active constituents for long storage periods, it is recommended to store honey below 4^oC to avoid the accumulation of hydroxy-methyl-fur aldehyde (HMF) (Rybak-Chmielewska *et al.* 1995).

2.1.2.4.2- Physico-chemical properties of honey

These depend on the constituents of honey. Natural honey contains minor substrates such as carbohydrates and water. But the major components are proteins, minerals, phytochemicals and antioxidants, as well as other physico-chemicals including H_2O_2, acids, enzymes and antimicrobial peptides (Abdulkhaliq *et al.* 2017).

2.1.2.3.2.1- pH of honey
Honey is naturally acidic, with pH ranges between 2.19 to 4.5 (White & Doner 1980; Ghazali 2009). Honey's acidity prevents most microrganisms from

growing in it. The presence of caffeic and ferulic acid in honey adds to its antimicrobial effect (Wahdan 1998).

2.1.2.3.2.2- Osmolality of honey

Honey has high osmolality 532 ± 38 mOsm/L (Crailsheim 1985), being a saturated mixture of monosaccharides in a low water content. Although the high osmolality of honey is essential for its antimicrobial effect, it is not the only mechanism. Diluted honey still preserves its antimicrobial effect when compared with concentrated sugar solutions (French *et al.* 2005).

With honey constituents, rather than the osmolality alone, are providing the antimicrobial activity (French *et al.* 2005; Molan 2006).

2.1.2.3.2.3- Hydrogen peroxide activity of Honey

H_2O_2 is the product of the enzymatic breakdown of glucose by glucose oxidase (White *et al.* 1963), exerting an antimicrobial activity, without causing toxicity to the patient's tissues, due to its slow release (Molan 2006). Its release is regulated by a negative feedback mechanism; the H_2O_2 increases the acidity, which in turn decreases the activity of glucose oxidase enzyme responsible for its release. Another regulating factor is the breakdown of H_2O_2 itself by the catalase enzyme contained in honey as well as discussed above. Mammalian tissues are further protected, by iron contained in honey, which reacts and neutralises free oxygen radicals released as side products of H_2O_2. Some honeys fail to generate peroxides; thus, their antimicrobial action are related to other honey constituents, especially phytochemical ones (Mavric *et al.* 2008; Adams *et al.* 2008; Atrott *et al.* 2009).

2.1.2.3.2.4- Phytochemical components of honey

Phytochemical components of honey can also generate antimicrobial affects (Molan 2006; Mboto *et al.* 2009), especially in non-peroxide honey, e.g. Manuka honey. Methylglyoxal (MGO) is one of these compounds (Atrott *et al.* 2009;

Mavric *et al.* 2008; Adams *et al.* 2008). MGO ranges from 189 to 835 mg/kg in Manuka honey with antibacterial activity of 12.4 to 30.9 % phenol concentration equivalent.

MGO has been found to be 1000 times higher in manuka honeys than conventional honeys (Mavric *et al.* 2008). Manuka honey (30% w/v) has also been shown to have more antimicrobial effect than ordinary honeys, which are only show anti-bacterial effects 80% w/v. Adams and colleagues (2008) confirmed the non-peroxide activity of 49 manuka honeys.

The antimicrobial activity was found to be attributed to methylglyoxal through HPLC analysis. Methylglyoxal is produced by the action of honey enzymes on dihydroxyacetone (Adams *et al.* 2008; Kwakman *et al.* 2010).

2.1.2.4.2.5- Antioxidant properties of honey

Free oxygen radicals are harmful active substances that react with tissues leading to their damage. They are produced by some pathogenic organisms, such as *P. aeruginosa*, involved in wound infection. Antioxidants neutralize oxygen free radicals, thus, protecting tissues from their lethal effects. Honey has also been shown to have antioxidant properties (Henriques *et al.* 2006; Oddo *et al.* 2008). It has also been shown that the antioxidant content of honey diminishes with time, especially after six months, regardless of the storage conditions (Jiménez *et al.* 1994); hence, fresh honey is more beneficial than stored, as the level of antioxidants is higher. The antioxidant activity of honey varies according to the phenolic content (Gheldof *et al.* 2002), floral content and source of honey (El-Hady *et al.* 2007).

2.1.3- Bacterial Biocide Resistance

Bacterial resistance to preservatives and disinfectants is both a growing economic and health problem that causes serious concern (Chapman 2003). Reduced bacterial sensitivity to many biocidal compounds has been extensively

reviewed, together with the mechanisms of resistance (Chapman 2003; Tumah 2009). However, there is scientific controversy regarding the appropriateness of the term biocide resistant as compared to the commonly used term of antibiotic resistant (Russell 2003). It was suggested that the term reduced susceptibility is more acceptable in this domain (Beumer *et al.* 2000). Contrary to the MIC breakpoint of antibiotics defined by the National Committee for Clinical Laboratory Standard (NCCLS), the MIC breakpoint of preservatives and disinfectants are variable according to the case.

This difference is due to the fact that antibiotics target specific sites, whereas biocides act on various targets (Chapman 1998). Bacterial resistance to biocides can be divided into two categories. The first is intrinsic resistance due to the inherent property of an organism and the second is acquired resistance due to mutation or through acquiring a plasmid or transposon (McDonnell & Russell 1999).

The most described mechanism of intrinsic bacterial resistance is cell membrane impermeability to biocides, which prevents their penetration or uptake (e.g. Gram-negative bacteria). Other intrinsic mechanisms are the efflux system, which actively pumps biocides out of the cytoplasm (e.g. mex pump in *P. aeruginosa*) and the enzymatic biodegradation of the biocidal compound (e.g. pseudomonas inactivation of phenols and aldhydes). The resistance acquired by mutation or acquisition of resistant genes is of particular importance in cases of cross resistance and co-resistance (Chapman 2003).

While cross-resistance is a description of the bacterial resistance being extended (i.e. resistance to a certain biocide would make the bacterial strain resistant to other biocides sharing the same target, uptake or metabolic routes),

co-resistance describes the resistance conferred by certain gene cassettes or gene arrangements, which act against a set of biological agents. As a consequence, both cross-resistance and co-resistance lead to the provision of bacteria with insusceptibility to more than one biocidal agent (Chapman 2003).

An important mechanism of bacterial resistance to antimicrobials is the formation of biofilms. Biofilms form when bacteria come into contact with surfaces, which provokes an interaction leading to the formation of a sessile form of bacterial communities embedded in a slime-like matrix formed of extracellular polymeric substances (EPS) (Stoodley *et al.* 2002) (Section 1.1.12).

2.1.4- Aims and objectives

The aim of this chapter was to investigate the effects of different types of anti-microbial strategies which generate active free radicals to reduce bacterial load in planktonic and biofilms culture. To achieve this chapter will discuss a number of objectives:

1- The effects of different types of biocides including (silver nitrate Isothiazolone, H_2O_2 and medical grade manuka honey) which generate active free radicals or reactive oxygen species to inhibit four strains of bacteria; *Staphylococcus aureus* SH1000, *Pseudomonas aeruginosa* NCIMB 2895, *Staphylococcus epidermidis* and Methicillin-resistant *Staphylococcus aureus* (MRSA) as planktonic and biofilms culture which are important in infections following burns.

2- Determine the effect of biocidal agents and infective agents on keratinocyte and fibroblast monolayer viability and phenotype.

2.2- Materials and Methods

2.2.1- Bacterial strains

Bacterial strains representing both Gram classifications which are important infective agents in skin infections in burns patients were selected. Including the Gram-positive strains *S. aureus* (SH1000) was isolated by Simon Foster group in Sheffled Hallam university, a *S. epidermidis* clinical isolate from Northern general hospital (Sheffield, Microbiology department) and Methicillin-resistant *Staphylococcus aureus* (EMRSA-16) and the Gram-negative bacteria *Pseudomonas aeruginosa* (NCIMB 8295) strain. These are the most common bacteria that are found in both acute and chronic skin wound infections and produce an extensive range of virulence factors (Sukumaran & Senanayake, 2016). It is therefore important to provide adequate antimicrobial coverage for these infections.

2.2.1.1 Recovery of frozen bacteria

One mL of Brain heart infusion (BHI) broth (VWR, UK) was added to frozen vials of bacteria (*S. aureus, S. epidermidis,* MRSA *and P. aeruginosa*)*,* vortexed and then 0.5 mL of the bacterial suspension used to inoculate a BHI agar plate which was then incubated in a non-shaking incubator at 37°C for 24 hours. Frequent reversion to the seed culture from the frozen stocks was used to keep the genotype as unaltered as possible.

2.2.1.2- Broth cultures

In all experiments requiring a broth culture, a single colony of the required bacteria strain from a BHI plate was used to inoculate 10 mL of BHI broth. This was then incubated in a shaking incubator for 24 hours at 37°C.

2.2.1.3- Viable Counts

Viable counts were used to determine the concentration of viable bacteria in a suspension. All the bacterial cultures were grown overnight in BHI broth and serially diluted (down to 1×10^{-6}) in a microtiter plate. Aliquots (100 µl) were taken from all tubes and ten microliter drops were plated out for each dilution according to the Miles & Misra method in triplicate on BHI agar (Miles & Misra, 1938). Numbers of CFU/mL in the original cultures were then calculated. Measuring the optical density (O.D) defined is an indirect way to determine the number of cells present in the bacterial broth. In addition, serial dilution was also used to determine bacteria CFU/ml. The correlation between OD600 and cell number for each bacterial species was established by means of a standard curve.

2.2.1.4 Standardisation of cultures

All bacteria strains were grown overnight in BHI broth and suspended in 10 mL of BHI broth. Serial 1 in 10 dilutions were performed and optical density readings were taken on a spectrophotometer (Biosciences, UK) at 600 nm. Each individual dilution was further serially diluted and plated out using the Miles & Misra method. All experiments were repeated in triplicate. This data was then used to create a calibration graph by plotting the optical density against CFU/mL which was used for future reference.

2.2.3- Biocides

The biocides used were hydrogen peroxide, sliver nitrate, 2- methyl- 4- isothiazolone, (Sigma, Dorset, U.K.) and 100% medical grade Manuka honey (Advancis Medical, UK) as antimicrobial agents. Fresh stocks were prepared for each use due to instability of reagents.

2.2.3.1- Minimum inhibitory concentration (MIC) testing

The MIC of biocidal agents values were determined by using microdilution as described previously (Forbes *et al.* 2013). Briefly, overnight bacteria were adjusted to optical density 0.8 and diluted 1:100 in BHI to produce a bacterial inoculum for susceptibility testing, MICs were determined using doubling dilutions of biocide to give an indication of the susceptibility of the organism to a specific biocide. 1.2% w/v alginate extracted from seaweed (Sigma, Poole, UK) in 0.15 M NaCl was used to apply biocides to biofilms and thus was used here alone as a control to ensure no toxicity was seen to bacterial cultures. All of bacteria strains in the project were grown overnight in BHI broth. The microtitre plate was then incubated for 24 hours at 37°C in plate reader (CLARIOstar, Offenburg, Germany). The MIC was the lowest concentration of biocide where bacterial growth was inhibited.

2.2.4- Bacterial biofilm preparation on nitrocellulose membrane

Sterile nitrocellulose membranes of 1cm^2 (Thermo Scientific) were used to create biofilms. The protocol described by Merritt *et al.*, (2005) was applied. Approximately one colony of each bacterial strain was incubated in 10 mL BHI in a shaking incubator at 37^{0}C for 24 hours. The nitrocellulose membranes were then added to the culture for 24 hours to allow bacterial adherence to the surface.

Membranes were washed by phosphate buffered saline (PBS) to remove any planktonic bacteria, then transferred using sterile forceps to the surface of agar media 24 hours; forming a biofilm on the nitrocellulose membrane. Biofilms were treated with 62.5µg/ml silver nitrate, 62.5 µg/ml Isothiazolone, 0.046 v/v hydrogen peroxide resuspended in 1.2% w/v alginate/0.15M NaCl, and neat medical grade manuka honey was applied directly on the forming bioifilm,

together with untreated and 1.2% w/v alginate controls and incubated at 37^0C for 24 hours in triplicate.

2.2.4.2- Viable bacterial biofilm count

Following 24 hours of incubation of nitrocellulose membrane in bacterial broth, three membranes were removed from the media and washed in sterile phosphate buffer in order to remove all planktonic cells. These were then transferred into separate tubes containing 10 ml of sterile PBS and were then transferred to a sonicating bath for one minute on/ one minute off for five cycles to release all viable cells. The tubes were finally vortexed for 30 seconds to homogenise the suspension and $1x10^{-1}$ to $1x10^{-6}$ serial dilutions were generated to obtain colony forming unit count (CFU/ml). Filters soaked in phosphate buffer without bacteria were used as negative controls.

2.2.6- Statistics

All experiments were performed independently at least three times. Effects of biocidal agents on biofilms are demonstrated with scatter plots to demonstrate all data points together with the median. Statistical significance of the experimental results (significance level of $P{\leq}0.05$) was calculated by using Stats Direct (StatsDirect Ltd, UK). Data did not follow a normal distribution, thus, non-parametric Kruskal-Wallis and a Connover Ingman post hoc test were applied to investigate significant differences from untreated and alginate treated controls.

2.3- Results

2.3.1- Standard curve of optical density versus cell number for each bacterial stain

In this project two methods were utilised to determine bacterial counts: optical density (O.D.) with Miles and Misra enumerations and counting numbers in bacterial chambers to determine the original cell density by CFU/cm^3. The correlation between OD_{600} and cell number for each bacterial species was established by a standard curve, which showed correlations between the OD_{600} of bacteria and number of bacteria ($R^2 > 0.95$ for all) (Figure 2.2, 2.3, 2.4, 2.5).
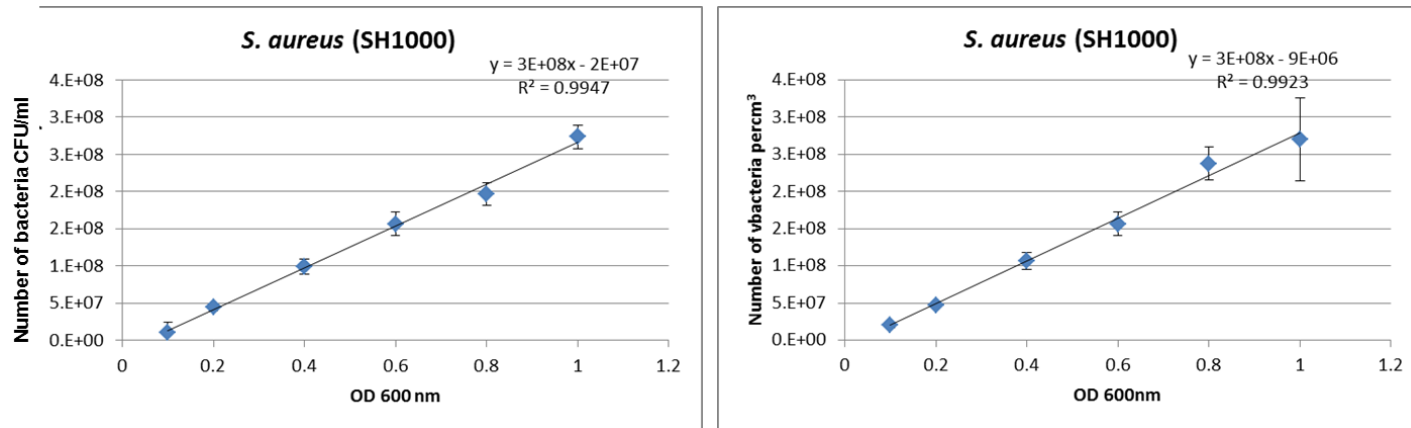
Figure 2.2: Standard curve of optical density (OD) versus bacterial cell number. The correlation between OD600nm and bacterial cell number for *S. aureus* was established by means of a standard curve for both a; (log CFU/mL) and b; counting chamber of bacteria.
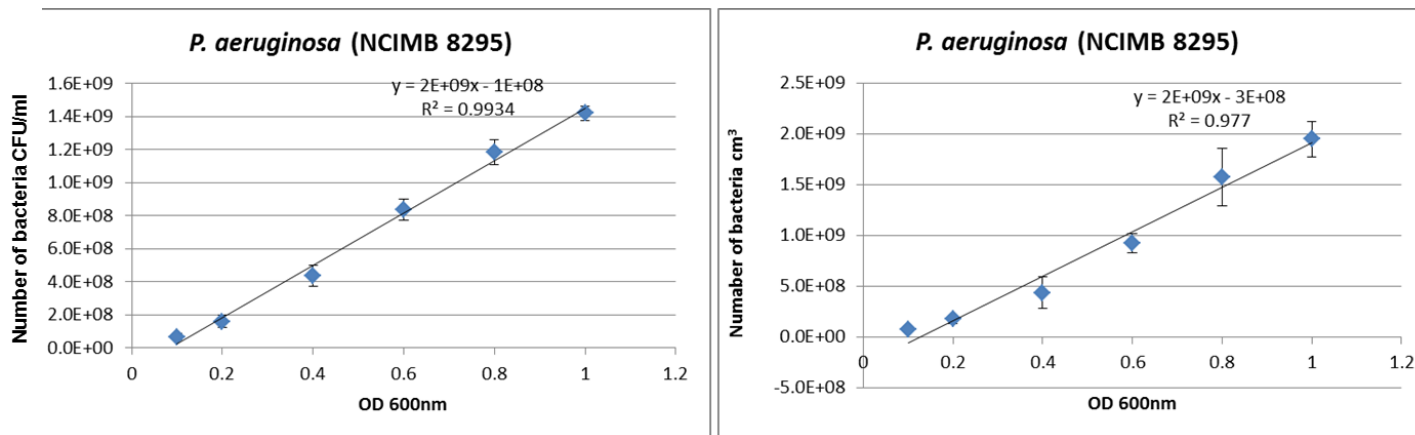
Figure 2.3: Standard curve of optical density (OD) versus bacterial cell number. The correlation between OD600nm and bacterial cell number for *P. aeruginosa* was established by means of a standard curve for both a; (log CFU/mL) and b; counting chamber of bacteria.
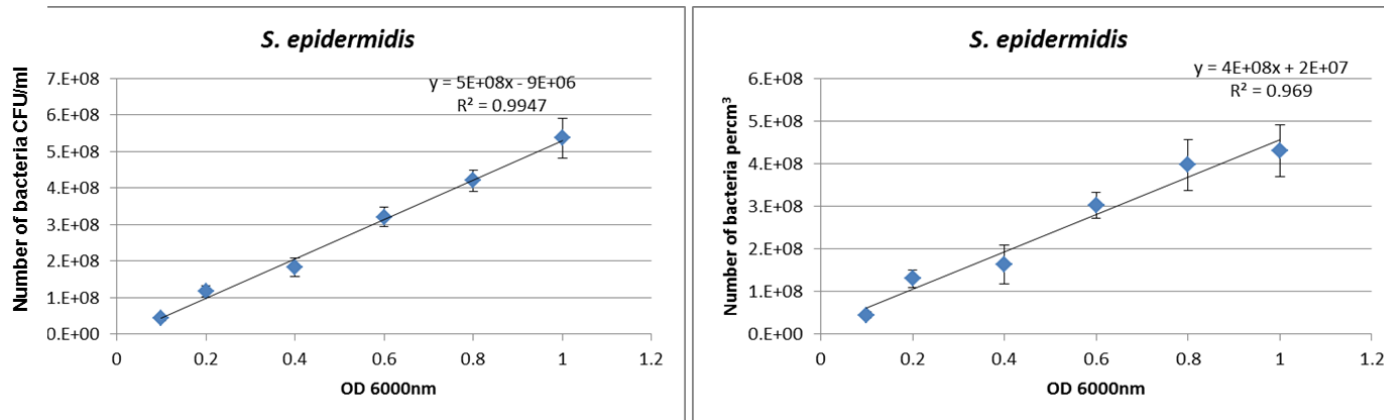
Figure 2.4: Standard curve of optical density (OD) versus bacterial cell number. The correlation between OD600nm and bacterial cell number for *S. epidermidis* was established by means of a standard curve for both a; (log CFU/mL) and b; counting chamber of bacteria.
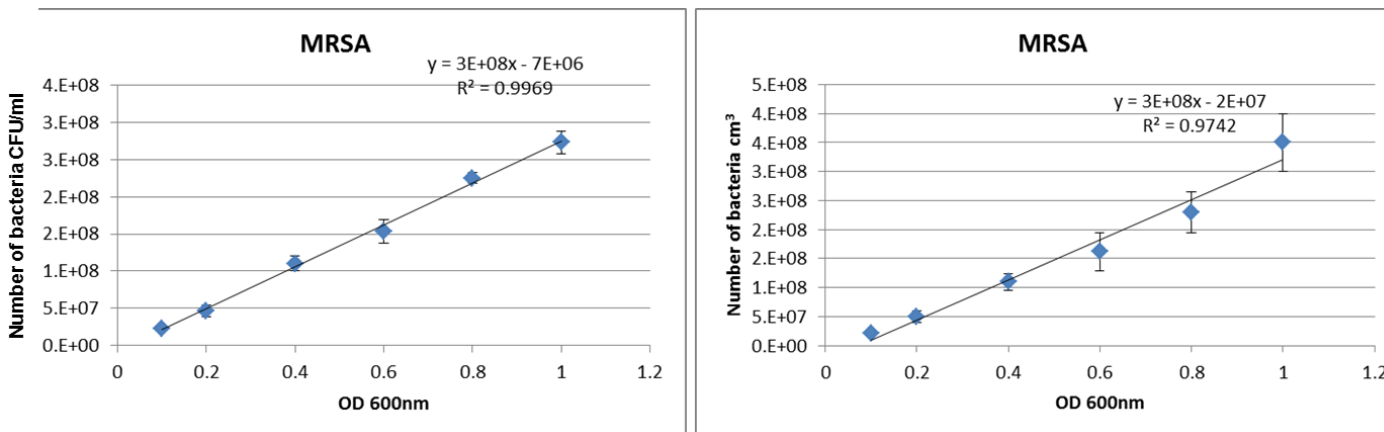
Figure 2.5: Standard curve of optical density (OD) versus bacterial cell number. The correlation between OD600nm and bacterial cell number for MRSA was established by means of a standard curve for both a; (log CFU/mL) and b; counting chamber of bacteria

2.3.2- Minimum inhibitory concentration (MIC) of silver nitrate against *P. aeruginosa* (NCIMB 8295), *S. aureus* (SH1000), a *S. epidermidis* clinical isolate and MRSA (EMRSA-16)

The susceptibility of *S. aureus, P. aeruginosa, S. epidermidis* and MRSA were determined by measuring the MIC of biocides (Table 2.1). There was evident bacterial growth in both the control and the alginate treated cultures following two hours of incubation, denoting that bacteria were viable, no significant effect was seen following treatment with alginate demonstrating alginate did not affect normal bacterial growth (Figure 2.7, 2.8 and 2.9). Serial dilutions of silver nitrate and 2- Methyl-4-isothiazoline-3-one of 250 µg/ml,125 µg/ml, 62.5 µg/ml and 31.25 µg/ml were used to identify the MIC of bacteria after 24 hours (Table 2.1). At the concentration of 62.5 µg/ml, no bacteria growth was observed. The results obtained from the plate reader showed that following treatment with 31.25 µg/ml the bacterial was observed following 8-10 hours of incubation for the all bacterial strains while in case of the of hydrogen peroxide MIC was $\geq$ 0.046%v/v (Table 2.1)

Table 2.1: The MICs of biocides and bacteria strains

Biocide Bacteria	Silver nitrate	2- Methyl -4- isothiazoline -3-one	Hydrogen Peroxide
S. aureus	62.5 µg/ml	62.5 µg/ml	0.046 v/v
P. aeruginosa	62.5 µg/ml	62.5 µg/ml	0.046 v/v
S.epidermidis	62.5 µg/ml	62.5 µg/ml	0.046 v/v
MRSA	62.5 µg/ml	62.5 µg/ml	0.046 v/v

2.3.3- Effect of biocides on the bacterial biofilms

Four biocidal agents, Manuka honey, silver nitrate, 2- Methyl -4- isothiazoline - 3-one and Hydrogen peroxide were tested against biofilms of *S. aureus, P. aeruginosa, S. epidermidis* and MRSA biofilms *in vitro* using the nitrocelluose biofilm method.

2.3.3.1- Effect of Manuka honey on the bacterial biofilm

Bacterial biofilm models (*S. aureus, P. aeruginosa, S. epidermidis* and MRSA) were produced on a nitrocellulose substrate and were exposed to Manuka honey. The effect of honey was measured after 24 hours of application using viable counts. Manuka honey significantly reduced the bacterial count in all models compared with control groups ($P = 0.0008$, $P = 0.0001$, $P < 0.0001$ and $P = 0.0003$) for *S.aureus, P.aeruginosa, S.epidermidis* and MRSA respectively (Figure 2.6). The biocidal efficacy was more pronounced in *P. aeruginosa, S. epidermidis,* and MRSA than in *S. aureus* (Figure 2.6, a). The reduction in *S. epidermidis* and *P. aeruginosa* were 2 to 2.23 $\log_{10}$ reduction in CFU/ml. Whereas in *S. aureus* and MRSA, only 1.87 and1.69 $\log_{10}$ reduction CFU/ml (Figure 2.6).
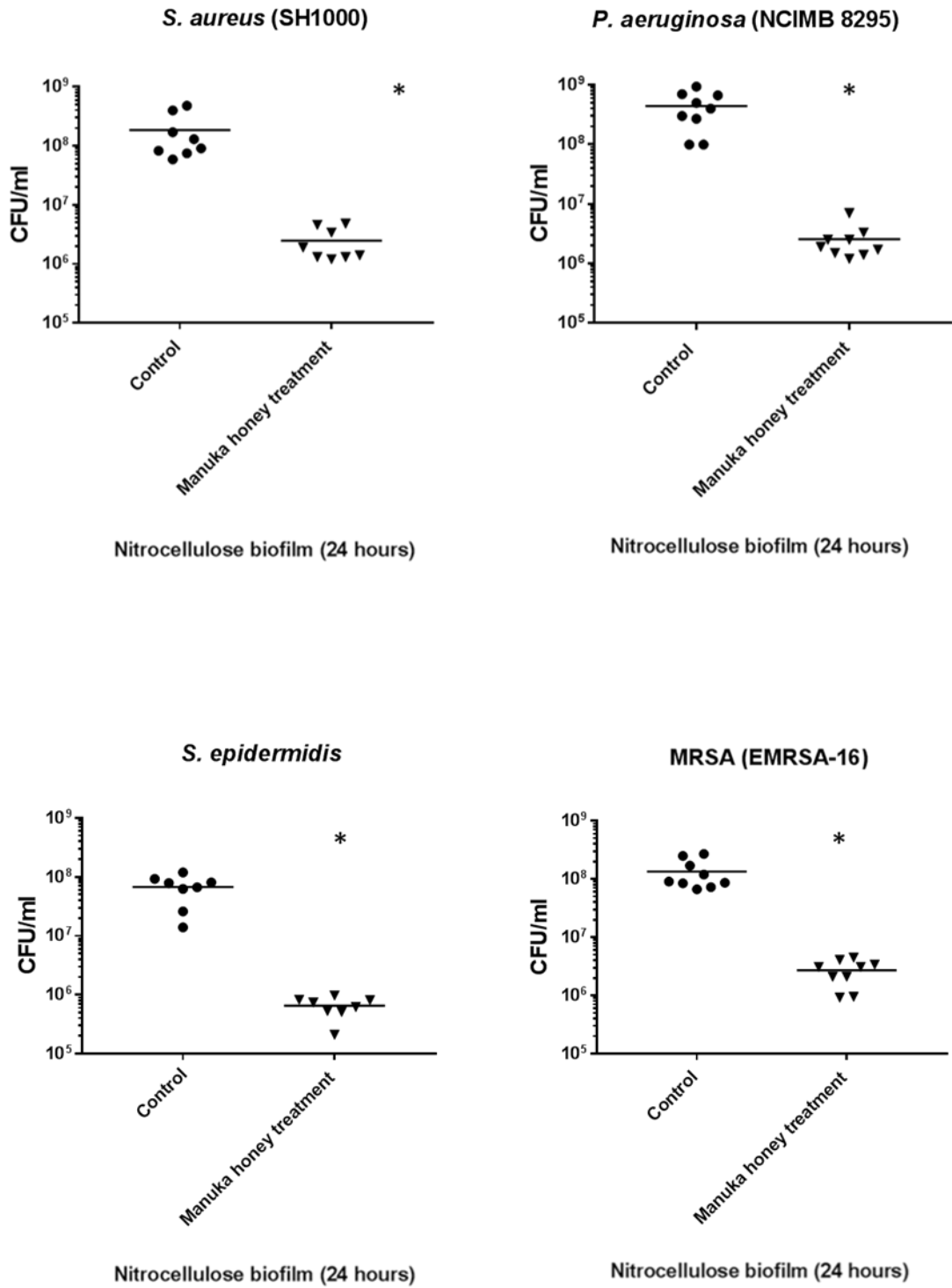
Figure 2.6: Effect of Manuka honey on *a; S. aureus b; P. aeruginosa c; S. epidermidis d;* MRSA infected 3D nitrocellulose models. The Manuka honey biocide effect was compared between controls and nitrocellulose biofilm biocidal treated samples. * = P<0.05

2.3.3.2- Effect of silver nitrate on the bacterial biofilm

From the previous experiments on planktonic bacteria, the planktonic MIC of silver nitrate for all bacteria investigated (*S. aureus, P. aeruginosa, S. epidermidis* and MRSA) was 62.5µg/ml. Thus, this dose was applied to bacterial biofilms grown on 3D nitrocellulose to investigate whether the biofilm mode of growth would affect the efficacy of the biocidal agent.

The effect of silver nitrate on the four bacterial strains (*S. aureus, P. aeruginosa, S. epidermidis* and MRSA), together with treatment of bacteria with alginate alone as a control was examined (note alginate utilised to enable delivery of biocidal agents to biofilms). No significant difference in the CFU/ml between the control and alginate groups was observed indicating that alginate had no adverse effect on bacterial growth ($P > 0.05$) (Figure 2.7).

Silver nitrate significantly reduced the bacterial count in all the models compared with the bacterial control and alginate groups $P < 0.05$. The biocidal efficacy was more pronounced in *P. aeruginosa* than in the other three examined strains (Figure 2.7), with a 1.76 $\log_{10}$ fold reduction in *P. aeruginosa* CFU/ml, whereas in *S. aureus, S. epidermidis* and MRSA the decreases were 1.38, 1.47 and 1.6 $\log_{10}$ reduction in CFU/ml, respectively (Figure 2.7).
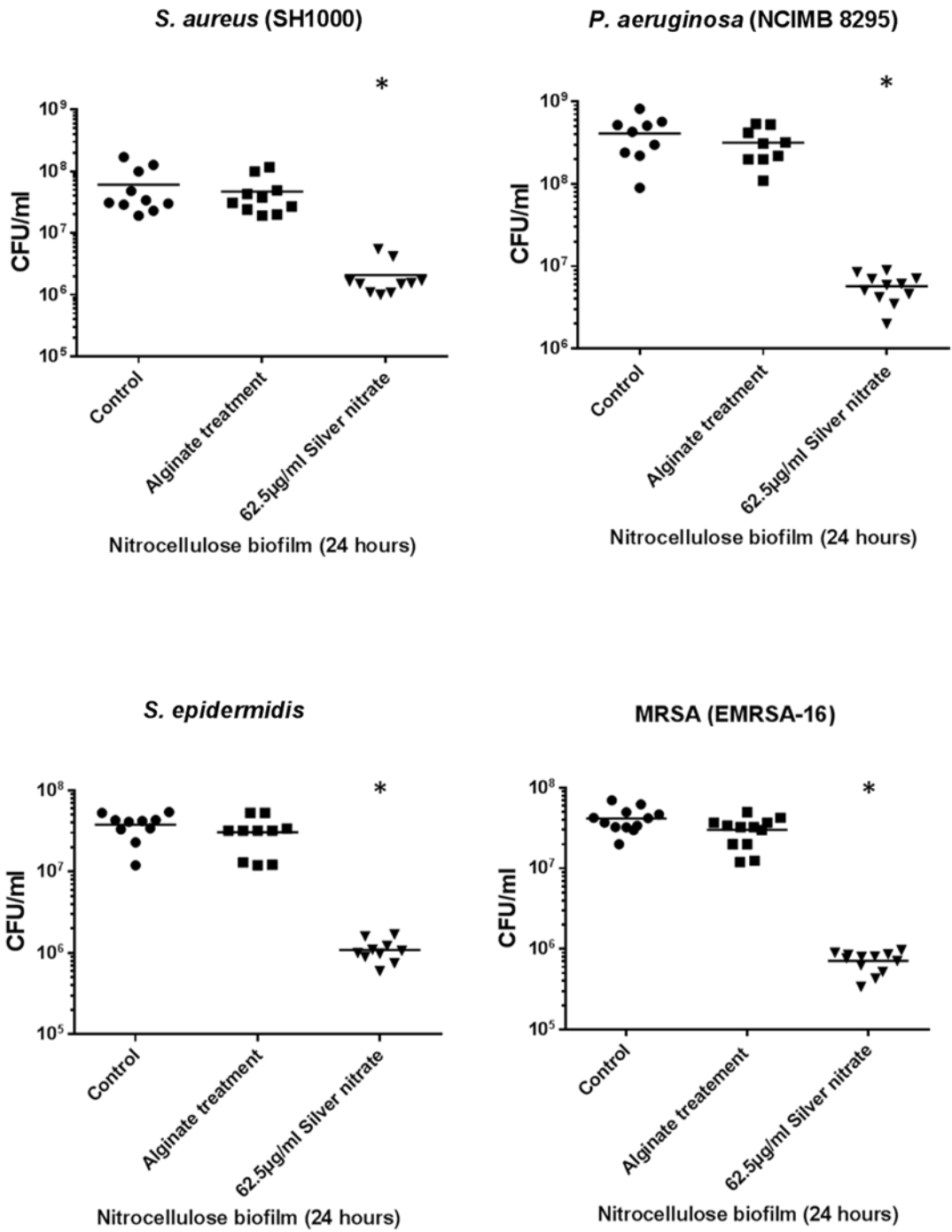
Figure 2.7: Effect of Silver nitrate on *a; S. aureus b; P. aeruginosa c; S. epidermidis d;* MRSA infected 3D nitrocellulose models. The Silver nitrate biocide effect was compared between controls and nitrocellulose biofilm biocidal treated samples. * = P<0.05

2.3.3.3- Effect of 2- Methyl -4- isothiazoline -3- one on the bacterial biofilm

The planktonic MIC of 2- Methyl-4-isothiazoline-3-one for all bacteria investigated (*S. aureus, P. aeruginosa, S. epidermidis* and MRSA) was 62.5μg/ml, thus this concentration was applied to biofilms grown on nitrocellulose to investigate whether the biofilm structure would affect the efficacy of the biocidal agent.

2- Methyl - 4- isothiazoline -3- one significantly decreased CFU/ml bacteria recovered from biofilms of all the four tested bacterial species (*S. aureus, P. aeruginosa, S. epidermidis* and MRSA) ($P < 0.0001$) (Figure 2.8). *S. epidermidis* and *P. aeruginosa* were the most sensitive strains with 2.5 and 2 $\log_{10}$ reduction of CFU/ml compared to 1.4 and 1.6 $\log_{10}$ reduction of CFU/ml of *S. aureus* and MRSA respectively (Figure 2.8).
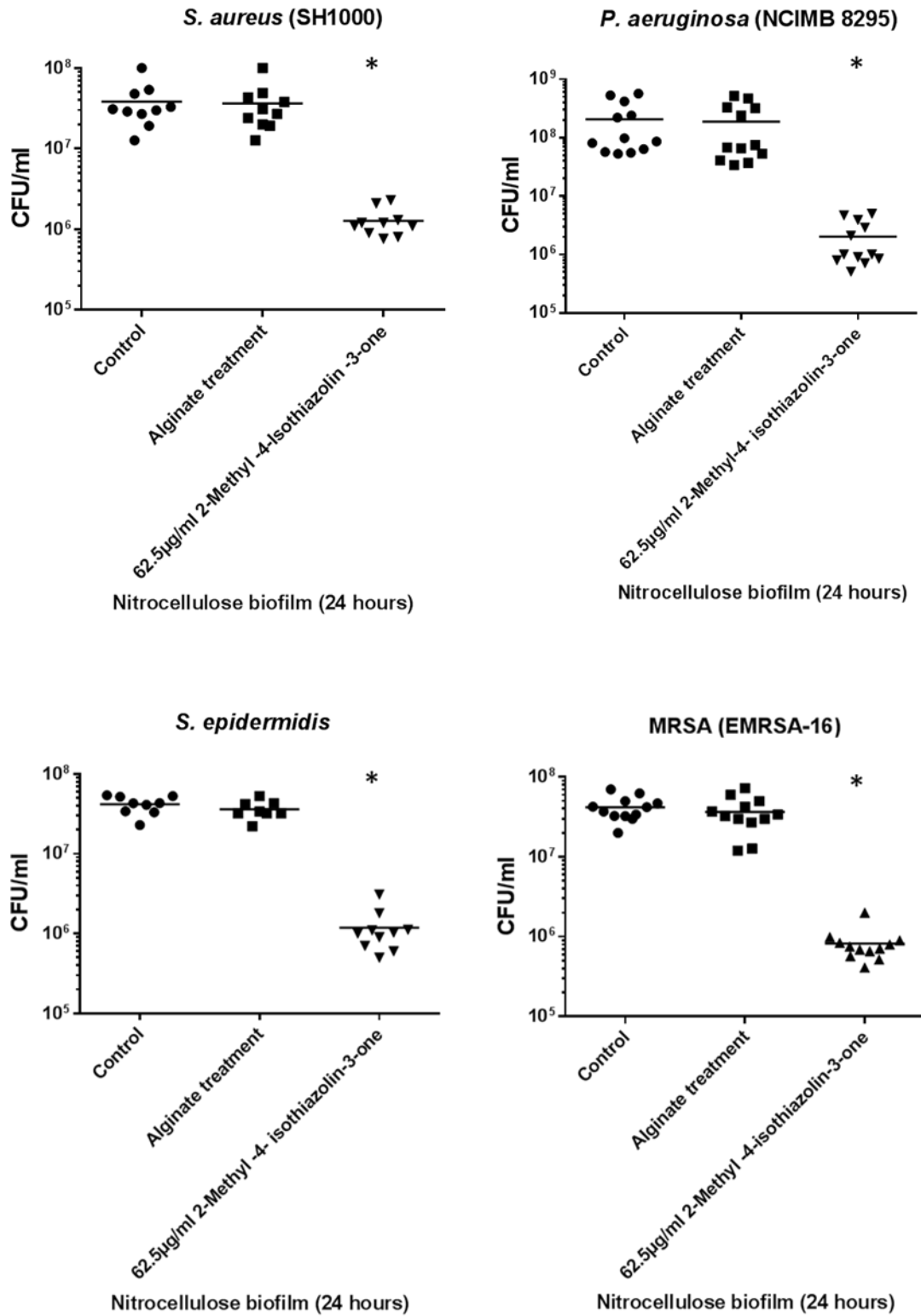
Figure 2.8: Effect of 2- Methyl -4- isothiazoline -3- one on a; *S. aureus* b; *P. aeruginosa* c; *S. epidermidis* d; MRSA infected 3D nitrocellulose models. The 2- Methyl -4- isothiazoline -3- one biocide effect was compared between controls and nitrocellulose biofilm biocide treated samples. * = P<0.005

2.3.3.4- Effect of Hydrogen peroxide on the bacterial biofilm

The planktonic MIC of Hydrogen peroxide for all bacteria (*S. aureus, P. aeruginosa, S. epidermidis and* MRSA) was 0.046 % v/v. thus this concentration was applied to biofilms grown on nitrocellulose to investigate whether the biofilm structure would affect the efficacy of the biocidal agent.

Hydrogen peroxide was shown to be an effective biocidal agent against *S.aureus, P.aeruginosa, S.epidermidis* and MRSA on bacterial cells cultured as a biofilm on nitrocellulose membranes. Hydorgen peroxide resulted in 1.88 $\log^{10}$ fold significant decrease in *P.aeruginosa* CFU/ml compared to control and alginate treated group P < 0.0001 (Figure 2.9). *S.aureus, S.epidermidis* and MRSA also showed significant reduction with 1.7, 1.6 and 1.48 $\log_{10}$ reduction in CFU/ml (P < 0.0001). *P.aeruginosa* was shown to be the most senstive stain of the four investigated (Figure 2.9).
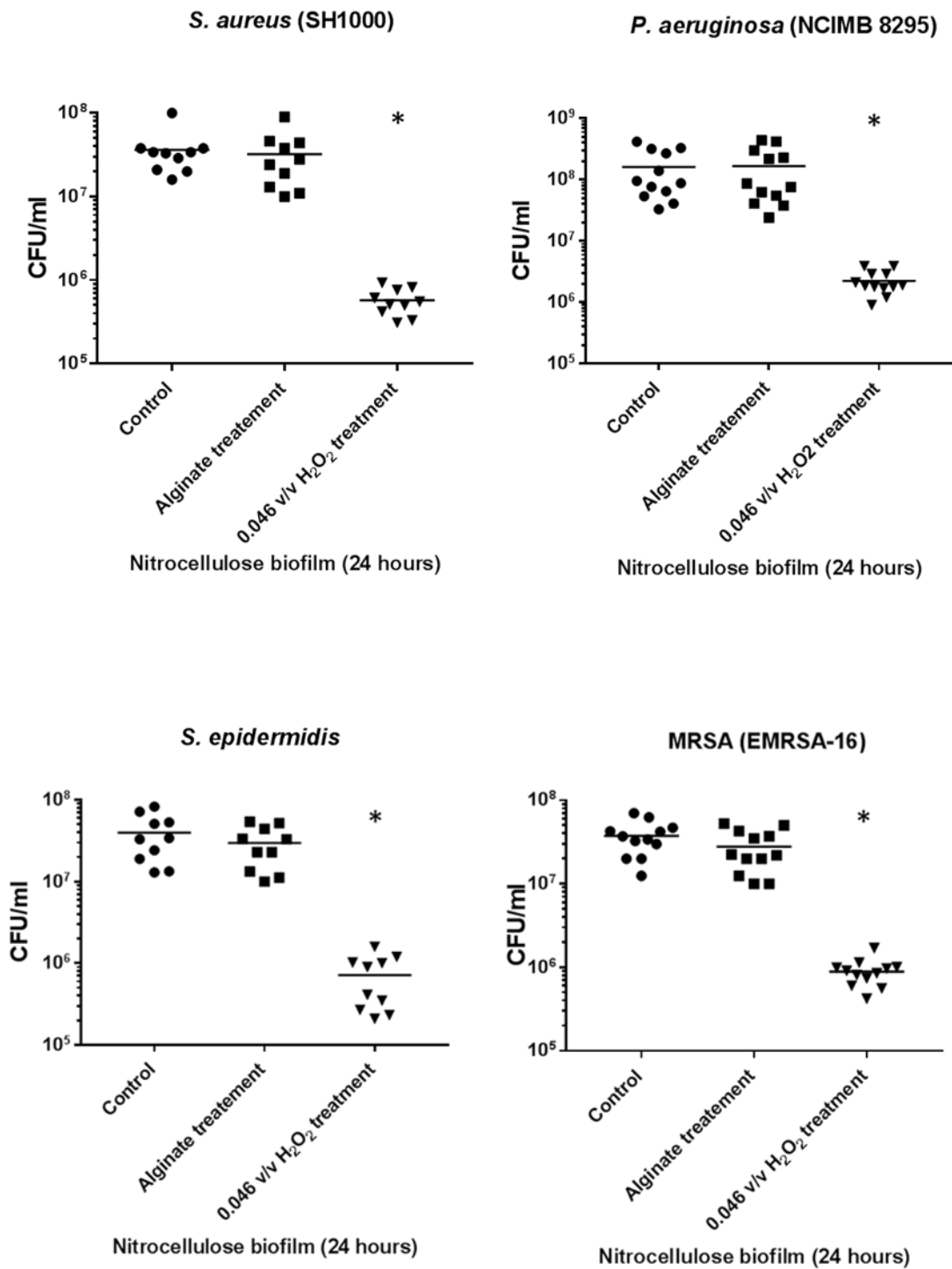
Figure 2.9: Effect of Hydrogen peroxide on *a; S. aureus b; P. aeruginosa c; S. epidermidis d;* MRSA infected 3D nitrocellulose models. The Hydrogen peroxide biocide effect was compared between controls and nitrocellulose biofilm biocidal treated samples. * = P<0.05

2.4- Discussion

This study utilised a selection of Gram positive and negative bacteria which are representative of infective organisms for burn wounds (*S. aureus*, *P. aeruginosa, S. epidermidis* and MRSA (Sukumaran & Senanayake, 2016, Gauglitz *et al.* 2017)). A number of potential biocidal agents which are thought to work via free radical formation were investigated, including: silver nitrate; isothiazolone; hydrogen peroxide; and medical grade Manuka honey. The effects of the biocidal agents were determined on bacterial growth in planktonic cultures and biofilms formed on nitrocellulose membranes.

2.4.1- Biocidal effects on planktonic and biofilm cultures

2.4.1.1 Biocidal effects of Silver nitrate in planktonic culture

The unspecific antimicrobial actions of silver are produced by the high reactivity of silver ions with cellular component. MIC concentration of silver nitrate on bacterial growth was determined in the current study within planktonic growth, with an MIC of 62.5µg/ml against all bacteria investigated. This was slightly higher than that found in previous studies where MIC has been found to in the range of 5 – 40 µg/mL (Randall *et al.* 2012; Zheng *et al.* 2017; Burrell 2003; Ug *et al.* 2003). Similarly, all the bacteria investigated in this thesis were sensitive to $AgNO_3$. The differences between specific MICs reported may be due to the culture media utilised (Hamilton-Miller & Shah, 1996; Sondi & Salopek-Sondi 2004; Ruparelia *et al.* 2008; Randall *et al.* 2012), but more likely due to the detection method. This project utilised a plate reader which is a sensitive technique and thus may have detected bacteria at lower levels than other methodologies.

2.4.1.2- Biocidal effects of Silver nitrate within biofilms

Exposure of *S. aureus*, *P. aeruginosa, S. epidermidis* and MRSA significantly reduced CFU/ml bacteria within biofilms formed on nitrocellulose membrane following exposure to the planktonic MIC of silver nitrate, although viable bacteria remained on biofilms demonstrating lower efficacy of treatment in biofilms compared to planktonic culture. Sharma *et al*., (2015) reported that the MIC of silver in ≤ 25 µg/mL planktonic bacteria had no effect on the biofilm of *P. aeruginosa* (MTCC) also demonstrating loss of efficacy (Sharma *et al.* 2015). In addition, Sutterlin *et al.,* 2012 found that the MIC values for the silver nitrate determined were 16–32 mg/l for *S. aureus* strains. Whilst the biocides were not as effective on biofilms as compared to planktonic bacteria, silver nitrate at 62.5µg/mL inhibited of *P. aeruginosa* approximately 100 fold (2 $\log_{10}$ fold) with biofilm (Sutterlin *et al.* 2012).

2.4.2- Isothiazolone

Isothazolines are water soluble and undergo chemical degradation to toxic compounds. Furthermore, they are compatible with a wide range of products. These characteristics have also made isothazoline preparations commercially successful in a wide range of industrial purposes (Nicoletti *et al.* 1993b). Preservative preparations are one of the common uses of isothiazolone in industry. However, due to its irritative nature, isothiazolone preservative solutions are restricted in use (Lundov *et al.* 2012; Bregnbak *et al.* 2013). 2-Methyl-4-isothiazoline-3-one (MIT) was used in this study as an antimicrobial agent. The application of MIT as an individual treatment as a potential antimicrobial biocide for use in mammalian infections is a novel application. Following treatment of biofilms on nitrocellulose membranes with MIT at the planktonic MIC, *S. epidermidis* and *P. aeruginosa* were shown to be the most

sensitive strains, although CFU/ml for *S. aureus* and MRSA were also significantly reduced. Interestingly isothiazolone has not been previously used as a potential treatment for bacterial infection in any medical purpose, but rather in environmental sanitation and cosmetic purposes (Garcia-Hidalgo *et al.* 2017),

2.4.3- Hydrogen peroxide

Hydrogen peroxide is broadly used for decontamination of microorganisms in a variety of settings (Ríos-Castillo *et al.* 2017). Bacterial biofilms *of S. aureus*, *Pseudomonas aeruginosa, S. epidermidis* and MRSA were exposed to planktonic MIC levels of hydrogen peroxide. The viable bacteria counts were significantly reduced.

Painter et al., (2015) revealed that *S. aureus* SH1000 exposure to H_2O_2 at sub-lethal concentrations (400 µM) resulted in a positive inhibition. No bacterial growth was noticed in the entire CFU counts with respect to the existence of 1 mM H_2O_2.The result is a prolonged hold-up phase that continued until the reduction of the H_2O_2 concentration to ≤ 400 µM, when the H_2O_2 concentration was reduced (Painter *et al.* 2015). In contrast, Elkins *et al.*, (1999) reported that 3-5% v/v H_2O_2 eradicated biofilms generated by clinical *S. epidermidis* isolates (Elkins *et al.* 1999). This concentration is considerably higher than the one used in the present research.

Tote *et al.*, (2010) observed that the hydrogen peroxide concentration required to inhibit *S. aureus* (ATCC 6538) biofilms was 2.5% v/v, which affected 50% of the bacterial sustainability; whereas a lower concentration of hydrogen peroxide 1.7% was found to be the MIC for *P. aeruginosa* (ATCC 700928). The destruction of biofilm matrix was observed around 3.2% (Tote *et al.* 2010).

The use of hydrogen peroxide as a disinfectant resulted in a reduction in the residual contamination of MRSA in hospital rooms. Moreover, it reduced the number of patient's hospital infections. (Mitchell *et al*. 2014).

2.4.4- Manuka honey

Interestingly hydrogen peroxide is generated as a free radical from Manuka honey which could lead to its biocidal effects; however, Manuka honey also has a number of other potential mechanisms including acidic pH, osmolality, hydrogen peroxide, phytochemical and antioxidants properties. Activon medical Manuka Honey induced a significance reduction in all the bacteria biofilms investigated here. The MIC of natural (wild) Manuka Honey has previously been reported as 12.5-25 % (Grecka *et al*. 2018; George *et al*. 2011; Grecka 2018). Fidaleo *et al*., (2011) noted that inhibition of bacteria increased with increasing concentration of Italian honeys of different floral origin from 12.5 % w/v and 17.5% w/v. The Gram negative *P. aeruginosa* ATCC1045 was more sensitive than *S. epidermidis* and *S. aureus* (Fidaleo *et al*. 2011) which agreed with the current study.

Almasaudi (2017) investigated the effect of five types of Manuka honey on *S. aureus*, affecting both the methicillin resistant bacteria and the sensitive *S. aureus* at the highest concentration of honey (20% w/v). In contrast to previous studies using wild Manuka honey, our study, using the medical grade Manuka honey, displayed low bactericidal activity against the biofilm (Almasaudi *et al*. 2017).

2.4.5-The effect of biocidal agents on the biofilms v/s planktonic cultures

Bacteria and EPS are essential for the development of biofilms, and thus to enable targeting of bacterial biofilms targeting both components will provide greater efficacy.

Biofilms generally are more resistant to killing by an extensive range of antimicrobial agents. Four biocides were included in this study. MICs were determined for these biocides against planktonic bacteria.

The *P. aeruginosa* and *staphylococci* biofilms showed similar sensitivity to biocidal agents. Manuka honey was the most effective biocide on biofilms in all types of bacteria.

2.4.6- Conclusions

This study demonstrated that biocidal agents (silver nitrate, isothiazolone, hydrogen peroxide and medical grade Manuka honey) decreased planktonic and biofilm viability and could be useful agents for the treatment of infections. However planktonic bacteria are known to respond differently to biofilms and as the biofilm models here were simple nitrocellulose models, these results may not relate to clinical results. The biofilms utilised here were formed on nitrocellulose membranes, this is a good initial model to screen biocidal agents but may fail to mimic biofilm formation on skin. Thus, it is essential to determine efficacy of biocidal agents for skin infections the effects of the biocidal agents on biofilms formed in contact with skin cells. Further the effects of these biocidal agents on the native skin cells must be determined to identify potential side effects and local toxicity.

Chapter 3

Development of an *in vitro* 3D skin model

3.1- Introduction

Skin is a major barrier to infection, however, when damaged; infection can become a major problem (Pereira *et al.* 2013; Frykberg *&* banks 2015; Wang *et al.* 2018). Current skin infection treatments include wound cleansing and debridement (Madhok *et al.* 2013), Maggot debridement (Gottrup & Jorgensen 2011), topical hyperbaric oxygen therapy (Kaufman *et al.* 2018), negative pressure (Cole 2016), and topical or systemic antibiotics (Howell-Jones *et al.* 2005). However, these treatments have a number of disadvantages such as pain linked to debridement (Bechert & Abraham 2009), and antibiotic resistance (Johnson *et al.* 2013). *In vivo* animal skin models have been used (e.g. murine and guinea pig) to experimentally inflict wounds and test various treatment modalities but this was at the expense of animal suffering and the high risk of causing toxicity, especially when applying high treatment doses, as in maximization testing (Magnusson 1969). Furthermore, the use of experimental animals is costly and there are differences between human and animal skin immunity that would inaccurately predict the real human response to the tested treatments (Mestas & Hughes, 2004; Geer *et al.* 2004). In accordance with 3Rs principle (Russell *et al.* 1959), there is an urgent need to develop alternate skin models, which characterise human skin physiology.

In response to these challenges, *in vitro* skin models have been developed, to enable testing of new therapeutic agents and approaches (Geer *et al.* 2002). The development of full thickness skin models is essential to investigate the topical administration of drugs and skin diseases.

For a successful *in vitro* 3D skin model various factors need to be considered such as the sources of necessary cell types (keratinocytes and fibroblasts) (Rheinwatd & Green, 1975); the ECM substrate; and the culture environment, including the presence of growth factors. Keratinocytes are the main cell type in the epidermis of the skin; whilst fibroblasts support the keratinocytes via paracrine signalling, such as production of Interleukin 1(IL-1) α and β; keratinocyte growth factor/ fibroblast growth factor 7 (KGF/FGF-7) and transforming growth factor α (TGF α) (Dlugosz *et al.* 1994, Werner & Smola 2001, Maas-Szabowski, Stark *et al.* 2000). The basal membrane between the epidermis and dermis comprises collagen type IV, collagen type VII, laminin, heparin sulphate and fibronectin. The combination of extracellular matrix (ECM) components and paracrine signals control keratinocyte proliferation and phenotype (Marinkovich *et al.* 1993; Fleischmajer *et al.* 1998)

The first skin models were developed ~80 years ago, utilising trypsin powder containing elastase to separate the epidermis from the dermal layer (Medawar 1941). Since then, numerous studies have been conducted to tissue engineer skin models *in vitro*, such as the use of human keratinocytes in *in vitro* tissue engineered skin models (Rheinwatd *et al.* 1975; Xie *et al.* 2010; MacNeil 2007; Deshpande & Ralston *et al.* 2013). 3D tissue models have been extensively used, with a number of systems investigated to date. The majority of these skin models utilise scaffolds as dermal equivalents which can be cellular or acellular (Shevchenko *et al.* 2010). These organotypic cultures utilise dermal scaffolds such as de-epidermised dermis (DED), collagen matrices, fibrin gel, fibroblast derived matrices and lyophilised collagen and glycosaminoglycan matrices (Table 3.1).

Table 3.1: *In vitro* 3D skin models

Authors /years	Cells used	Scaffold	Medial/ GFS	Result
Maas-Szabowski *et al.* 2003	HaCaT cells, Primary human fibroblasts and keratinocytes	a collagen type I gel	DMEM, supplemented with 10% FCS and TGF-α for HaCaT. Greens medium for Normal human keratinocytes (NHK)	TGF-a-treated cultures demonstrated that the improvement of survival of HaCaT cells was the main function of TGF-a in the development of epidermal tissue; thus, it is has contributed significantly to increasing the number of cell layers.
Harrison *et al.* 2006	Primary human fibroblasts and keratinocytes	De-epidermised dermis (DED)	Greens medium (DMEM/Ham's F-12 (3:1), 1% UG, 50 mg/mL gentamycin, 1 mM hydrocortisone, mM isoproterenol, 0.1 mM insulin, and 2 ng/mL KGF)	This *in vitro* model of human skin considered definite cross-linking paths as potential pharmacologic targets for inhibiting graft contracture *in vivo*.
Carlson *et al.* 2008	Primary human fibroblasts and keratinocytes	Human skin equivalents (HSEs)as a collagen matrix	Green's media	Illustrating that the model reacts to the topical use of skin sensitizer as demonstrated by the up-regulation of CD86 and HLA-DR on the mDCs.
Shepherd *et al.* 2009	Primary fibroblasts and keratinocytes	De-epidermised dermis (DED)	Green's media	New models of complex human skin infection were applied to examine the microbial invasion of normal skin epithelium, connective tissue and basement membrane; as a model, it is used to study approaches to decrease bacterial load in skin wounds.
Canton *et al.* 2010	Primary human fibroblasts and keratinocytes	Collagen matrix and EPISKIN1	Green's media	3D tissue contrived co-culture models for the *in vitro* testing of annoying chemical
Bellas *et al.* 2012	Normal human keratinocytes (NHK)	Using silk and collagen biomaterials	DMEM/F12, 10%, 1% PSF + 2day 500uMIBMX, 5uM Rosiglitasone ect.	comprehending some essential factors required to design a steady functional model of full-

Authors /years	Cells used	Scaffold	Medial/ GFS	Result
Deshpande *et al*. 2013	Thickness skin. Primary keratinocytes (NHK) and fibroblast	Euroskin (DED)	Green's media	Displayed the creation of a well-connected epithelium together with several features of normal skin while a basement membrane is present. Nonetheless, physiological levels of calcium are required for the stratified epithelium formation while a basement membrane is absent.
Chau *et al*. 2013	HaCaT, HEKn-CaY or HEKn and human foreskin fibroblast	commercially available microfibre made of wet spun PES/viscose rayon microfibre material containing a butadiene copolymer,	Green's medium.	Combining Y-27632 Rock Inhibitor with Low Calcium raises the Proliferative Capacity, Lifespan of Primary Human Keratinocytes and Expansion Potential whereas, it retains Their Capability to Distinguish into Stratified Epidermis in a 3D Skin Model
Reijnders *et al.* 2015	human TERT-immortalized keratinocytes and fibroblasts	Human skin equivalents (HSEs)	Green's medium.	TERT-HSE can re-epithelialize and discharge wound-healing mediators that are inflammatory.
Jung *et al.*, 2016	HaCat cells and fibroblast	Human Skin Equivalent Model	DMEM High glucose conentration + 10% FBS	The device can rebuild the epidermal morphology, comprising the cornified layer, that resembles its formation *in vivo*
Groeber et al, 2016	Primary human fibroblasts and keratinocytes	Declearized segment of a pocrine jejenum	Keratinocytes 2 medium	in cell barrier formation endothelial cells lined the walls of the vessles
Smits *et al.* 2017	Two immortalized keratinocyte cell lines (N/TERT1, N/TERT2G)	human epidermal equivalents (HEEs)	Green's medium.	They effectively produced N/TERT-HEEs along with psoriasis or atopic dermatitis features and Stratum corneum penetrability.

3D tissue skin models can be utilized in academic and industrial research laboratories (Ahn *et al.* 2009; Pacak *et al.* 2011). A number of different kinds of human skin equivalents have been investigated to date, including: human epidermal equivalents (HEEs) model is de-epidermized dermis (DED) skin development and human keratinocyte cultures demonstrated that air exposure; human skin equivalents (HSEs) as full thickness 3D skin models are bioengineered substitutes composed of primary human skin cells (keratinocytes, fibroblasts and/or stem cells) and components of ECM (mainly collagen) such as *in vitro* reconstructed skin (RS), commercially available 3D tissue models include: EpiSkin; Skin Ethic RHE; EpiDerm and EST1000 models (Ponec *et al.* 2002; Netzaff *et al.* 2005; Macfarlane *et al.* 2009). These systems have been utilised to investigate the genotoxicity potential of topically applied compounds and for screening chronic and acute skin irritation (Macfarlane *et al.* 2009). EST1000 and EpiDerm were approved for skin irritation and skin corrosion studies (Cannon *et al.* 1994; Fentem *et al.* 2001). However, these skin models comprise only keratinocytes, lacking dermal components, fibroblasts and immune cells (Gibbs *et al.* 2013; Desprez *et al.* 2015). To meet these challenges, a number of research groups have improved *in vitro* skin models to test new therapeutic approaches and agents.

In 1983, Pruniéras used human isolated keratinocytes cultured on a de-epidermised dermis (DED) (Prunieras *et al.* 1983). Human dermis was treated to remove cellular content, producing acellular DED. Fibroblasts and keratinocytes were then seeded onto DED and exposed to air liquid interface (ALI) for 14 days demonstrating formation of skin like structures such as rete ridges and differentiated epidermal layers (MacNeil 2007).

Efforts have been exerted over the past decade to develop 3D skin models utilising acellular DED. The substitute DED can be attained from human cadaveric skin (MacNeil 2007; Shepherd *et al.* 2009; Shepherd *et al.* 2011) which can be accessed via skin banks or obtained as excess skin from surgeries including breast reduction and abdominoplasties (MacNeil 2007; Shepherd *et al.* 2009; Shepherd *et al.* 2011). A number of studies have investigated improvements for these 3D skin models using DED; for example, Kanta (2015) seeded fibroblasts in collagen matrixes which were then overlaid by DED and seeded with keratinocytes (Kanta 2015). However, with collagen matrices, a number of limitations are present, for example, collagen gels shrink following seeding with fibroblasts in a cell number dependant manner, which subsequently affects scaffold stiffness (Rnjak *et al.* 2011).

In 2007, MacNeil utilised DED to culture primary keratinocytes, which were proposed to be applicable to tissue-engineered skin for both clinical use (such as to replace partial thickness skin in burns patients) and academic laboratory research (MacNeil 2007). However, the use of DED directly from cadaveric donors has the drawback of variable thicknesses and risk of infection to the user. In utilising DED human skin as a scaffold, primary human keratinocytes and fibroblasts are seeded onto the DED and cultured at the ALI. The culture media is supplemented with growth factors including epidermal growth factor together with fetal bovine serum, and insulin (MacNeil 2007). Deshpande, (2013) overcame donor related drawbacks by sourcing DED directly from cadaveric skin by using Euroskin (a skin bank which enables selection of skin thickness) (Deshpande *et al.* 2013). However, the same risks of donor variability and risk of infection (e.g. HIV and hepatitis) were present due to the use of primary cells from donor biopsies.

Furthermore, the use of primary cells is not accessible to all laboratories as it requires access to clinical samples and ethical permission for extraction. Primary cells are also limited in their replication potential which limits the number of models which can be prepared from each patient sample.

To avoid the disadvantages of using human primary cells, cell lines of immortalised keratinocytes have been investigated for the development of 3D skin models (Reijnders *et al.* 2015; Smits *et al.* 2017). Boelsma *et al,* 1999 investigated the use of HaCaT cells, a non-tumorigenic human keratinocytes line on three types of scaffold: DED; collagen gel matrices; and filter inserts (Boelsma *et al.* 1999). The HaCaT cells grown at an ALI undergo incomplete epidermal differentiation, i.e. the terminal steps of differentiation such as development of a stratum granulosum and stratum corneum did not take place. The type of substrate and culture conditions did not seem to play a crucial role in this terminal differentiation process. No significant difference was observed in terms of epidermal differentiation when the cultures on collagen gels were kept submerged for one or seven days. Similar outcomes were observed when natural substrates like DED or filter inserts were used to grow HaCat cells (Boelsma *et al.* 1999).

However, the 3D architecture showed pronounced improvement when a higher proportion of fibroblasts were involved in the substrate. Without growth factors, the epidermal layer development was delayed. Basal and suprabasal keratinocyte cells were present (Boelsma *et al.* 1999). However, there was an impaired capacity of HaCaT to synthesize lipids that were important for barrier formation, and tissue structure was disordered (Boelsma *et al.* 1999). Maas-Szabowski, (2003) was able to achieve a structured, differentiated, functional and ordered epidermis in HaCaT cell lines grown in collagen type I when

cultured in the presence of transforming growth factor alpha (TGFα). Where TGFα improved proliferation and differentiation lead to the formation of multiple layers of epithelium following two to three weeks of ALI (Maas-Szabowski *et al.* 2003). However, this model lacked a dermis and only utilised keratinocyte like cells, and thus was not fully representative of human skin.

In 2016 Jung, developed *in vitro* 3D skin models which co-stimulated HaCaT cells by mechanical stress and air liquid exposure. Mechanical stress induced differentiation of the keratinocytes and air exposure induced stratification of epidermal layers (Jung *et al.* 2016).

Recently, an advancement of 3D printing technology referred as bioprinting was exploited to make cell loaded scaffolds to produce constructs which are more matching with the native tissue. A fascinating field that offers new opportunities for creating skin models is 3D bioprinting (Cubo *et al.* 2016). The disadvantages are only applicable for viscous liquids, poor functionality for vertical structures, low cell densities and High cost, thermal damage due to nanosecond/femtosecond laser irritation (Hopp *et al.* 2012) lack of printing multi-cells, and damage to cells during photo curing

The current study investigates the development and characterisation of an *in vitro* tissue engineered skin model using immortalised HaCaT and commercially available primary fibroblast cells layered on a Euro skin bank DED scaffold. Such a model would be easily transferable across laboratories for high throughput testing of novel therapies for the skin.

3.2 - Materials and Methods

3.2.1- Cell Culture

The keratinocyte cell line (HaCaT) (Cat Number; T0020001) was supplied by AddexBio (San Diego, USA) and Normal Human Dermal Fibroblasts (NHDF- C 39315) were supplied by PromoCell (Heidelberg, Germany). HaCaT cells were grown in Dulbecco's modified Eagle's medium (DMEM) (Biosera Ltd, Ringmer, UK) supplemented with 10% v/v foetal bovine serum (FBS) (VWR, UK); penicillin (100 U/mL); and streptomycin (0.1 mg/mL). HaCaT cells were used between passages 20 and 35. NHDF cells were grown in fibroblast medium (PromoCell, Germany) which contains recombinant human basic fibroblast growth factor (bFGF) (1ng/µl), recombinant human insulin (1ng/µl) with 10% v/v foetal bovine serum (FBS) and penicillin-streptomycin (100 U/Ml - 0.1 mg/mL). Cells were incubated at 37 °C for 24 h with 5% CO_2. Fibroblasts from passage 3 to 8 were used for the experiments. All cells were routinely checked for mycoplasma and were mycoplasma free throughout the study.

To prepare cells for the skin model, cells were detached using Trypsin-EDTA (0.05% v/v), (Gibco®. Grand Island, New York). The detached cells were centrifuged at 400g for 10 minutes. Cells were counted using Countess™ automated cell counter (Invitrogen).

3.2.2- Three-Dimensional Tissue Engineered model

The protocol for creating TE skin was adapted from MacNeil *et al.,* (2011) as follows: dermal scaffolds (de-epidermised dermis, DED) for the construction of the TE skin were created by de-cellularising human donated skin obtained from Euro-skin (Beverwijk, Netherlands).

De-cellularised human skin was washed by placement into PBS which was changed daily, up to 5 days at 37 ⁰C incubation, and then the DED was

removed and placed into 1M NaCl overnight at 37 °C or until there was visible separation of the dermis from epidermis. The dermis was then gently separated from the epidermis using sterile blunt forceps. DED was stored in DMEM supplemented with 10% v/v foetal bovine serum (FBS); penicillin (100 U/mL) and streptomycin (0.1 mg/mL) at 4 °C for 48 hours. DED was cut with a cork borer (VWR UK) into a circle of approximately 18 mm diameter and kept moist in DMEM media. A 0.4µm pore size cell strainer (Thermo, Fisher Scientific, Loughborough, UK) was placed inside each well of a 6-well tissue culture plate (ThinCertTM Greiner). Each tissue segment was gently placed into the cell strainer with the reticular surface uppermost and pressed down with sterile forceps, and excess media was removed. Each DED sample was seeded with fibroblasts and keratinocytes in 500 µl of culture media (Table 3.2 for cell densities investigated). Three different media substrates were used to optimise 3D tissue skin models: a) commercial keratinocyte media (PromoCell, Heidelberg, Germany); b) DMEM media supplemented with 10% v/v FBS; and c) DMEM media supplemented with 10% v/v FBS and 2ng/ml of transforming growth factor alpha (TGF-α). The wells were filled with media to feed the skin from underneath. Following 48h, 500 µl of media covering the DED was removed, and the media bathing the tissue from underneath replaced with 1.5 ml fresh media, forming an ALI. Following this, the culture media in the wells were changed every 2-3 days with freshly prepared 2ng/ml TGFα and the 3D cultures were removed for analysis following 4, 7, 14, and 21days in culture at ALI. All experiments were performed in triplicate and repeated as three independent experiments.

Table 3.2: 3D skin models cell densities investigated

Models and cells density	Model 1	Model 2	Model 3	Model 4	Model 5
Density of HaCaT Cells	$3X10^5$	$6X10^5$	$9X10^5$	$6X10^5$	$9X10^5$
Density of Fibroblast Cells	$1x10^5$	$1x10^5$	$1x10^5$	$2x10^5$	$3x10^5$

3.2.3- Histology of 3D skin models

Following culture for 4, 7, 14 and 21 days, triplicate skin models were removed from culture and fixed in 10% v/v formalin for 36-48 h at 4ºC. The skin was then processed to wax overnight using a Leica TP1020 processor from Leica microsystems (Milton Keynes UK). Four micron sections were then prepared using a Leica microsystems SM 2400 (Leica, Milton Keynes UK) with Leica low profile microtome blades, type 819 (Leica, Milton Keynes UK) and mounted onto X-traTM Adhesive slides, (Leica, Milton Keynes UK).

3.2.3.1- Haematoxylin and Eosin (H & E)

Skin sections were dewaxed and stained with H&E to investigate morphology. Sections were deparaffinised in Xylene substitute (sub-x) (Leica, Milton Keynes UK) for 3x5 minutes followed by 100% v/v, 70% v/v and 50% v/v industrial methylated spirit (IMS) for 5 minutes each. Slides were then submerged into Harris haematoxylin (Leica Microsystems, Milton Keynes UK) for 5 minutes and washed in running tap water for 5 minutes. Sections were stained with eosin for 2 minutes followed by dehydration using graded IMS (Fisher, Loughborough UK) 30% v/v, 70% v/v, 100% v/v. Following clearing in sub-X (Leica Microsystems, Milton Keynes UK) (3 x 5 min), sections were mounted in DPX (Leica Microsystems, Milton Keynes UK).

3.2.3.2- Masson's trichrome stain

Following dewaxing and rehydration, Masson's trichrome stain (Bio OPtica, Milano, Italy) was performed according to manufactures instructions to stain collagens within the skin models. Following staining, sections were washed in distilled water for 5 minutes, dehydrated in IMS (Fisher, Loughborough UK), cleared in sub-X and mounted with DPX (Leica Microsystems, Milton Keynes UK).

3.2.4- Immunohistochemistry

Anti-Caspase-3, anti-collagen IV, anti-S100A4, anti- Cytokeratin 10 anti-Cytokeratin 14 and anti-Pancytokeratin (PCK-26), were selected for immunohistochemistry (IHC) to assess variability and differentiation capacity of 3D skin models (Table 3.3). Sections were prepared as described for histological analysis; IHC was performed as previously described (Le Maitre, *et al.,* 2005). Briefly, 4 μm thick paraffin sections were dewaxed in xylene and rehydrated in IMS and endogenous peroxidase-blocked using hydrogen peroxide (Sigma, Aldrich Poole UK). 3D tissue slides were subjected to antigen retrieval methods (Table 3.2).

Following washes in tris-buffered saline (TBS; 20 mM tris, 150 mM sodium chloride, pH 7.5) nonspecific binding sites were blocked for 90 min at room temperature with 25% w/v serum (Abcam, Cambridge, UK) in 1% w/v bovine serum albumin in TBS. Primary antibody was added to sections and incubated overnight at 4°C (Table 3.3). Negative controls in which mouse or rabbit IgGs (Abcam Cambridge UK) were used in place of the primary antibody at the same protein concentration were applied (Table 3.3). Following washing in TBS, tissue sections were incubated with 1:500 biotinylated secondary antibody (Table 3.3).

Avidin biotin complex was used to detect secondary antibody during 30 min incubation (Vector Laboratories, Peterborough, UK). After washing in TBS, 0.08% v/v hydrogen peroxide in 0.65 mg/mL 3,3′-diaminobenzidine tetrahydrochloride (DAB) (Sigma Aldrich, Poole UK) in TBS was added for 20 min incubation. Mayer's Haematoxylin (Leica Microsystems, Milton Keynes UK) was used as counterstain, dehydrated in IMS (Fisher, Loughborough UK) (3 × 5 min), cleared in SubX (Leica Microsystems, Milton Keynes UK) (3 × 5 min) and mounted in Pertex (Leica Microsystems, Milton Keynes UK). Sections were analysed using an Olympus BX 51 Microscope and images captured by camera (name camera) and capture pro OEM v8.0 software (Media Cybernetics, Buckinghamshire, UK).

Table 3.3: Target antibodies marker used in IHC and antigen retrieval methods.

Antigen retrieval methods are three types (a)- non retrieval (b)- heat antigen retrieval, (0.05 M Tris Buffer, pH 9.5 pre-heated to 60 °C, (2x5 min) 40% and 20% microwave irradiation) (C)- enzyme antigen retrieval (20 mM Tris, 150mM sodium chloride, 46.8mM Calcium chloride dihydrate pH 7.5 and 0.01% w/v α-chymotrypsin bovine pancreas at 37 °C for 30 min).

Target antibody	Clonality	Optimal dilution	Antigen retrieval	Secondary antibody	Serum block	Cat No.
Caspase-3	Rabbit polyclonal	1:400	Enzyme	Goat anti-rabbit	Goat	ab4051
Ani-collagen IV	Rabbit polyclonal	1:400	None	Goat anti-rabbit	Goat	ab6586
S100A4	Rabbit polyclonal	1:100	Enzyme	Goat anti-rabbit	Goat	ab41532
Cytokeratin 10	Mouse monoclonal	1:400	None	Rabbit anti mouse	Rabbit	ab9026
Cytokeratin 14	Mouse monoclonal	1:100	None	Rabbit anti mouse	Rabbit	ab7800
Pan cytokeratin (PCK-26)	Rabbit polyclonal	1:400	Heat	Goat anti-rabbit	Goat	ab6401

3.3- Results

3.3.1- Effect of culture media composition on 3D skin model development

To establish an *in vitro* 3D culture system to represent human skin, HaCaT cells and primary fibroblasts were seeded on a DED scaffold. Differentiation of HaCaT was achieved by culturing the 3D skin model at an ALI for up to 21days.

HaCaT cells underwent noticeable changes in the epidermal morphology when exposed to ALI during culture (Figure 3.1). When decellularized tissue of dermis alone (DED) was cultured in the absence of HaCaT or fibroblasts, no evidence of cellular material was observed, indicating successful deceullurisation (Figure 3.1a). A thin layer of cells were observed, when HaCaT cells and fibroblasts were cultured in Keratinocyte medium, with only small increases in cell layers seen with time in culture (Figure 3.1b). Culture of HaCaT cells and fibroblasts in TGFα-free DMEM demonstrated a thin layer of cells on the surface of the DED, although increased cells were seen with increasing time in culture minimal differentiation was evident (Figure 3.1c). In contrast, TGFα was added to DMEM, the epidermal cell layer showed thicker cell layers and evidence of differentiation with increasing time in culture, evident with changes in cellular morphology (Figure 3.1d).
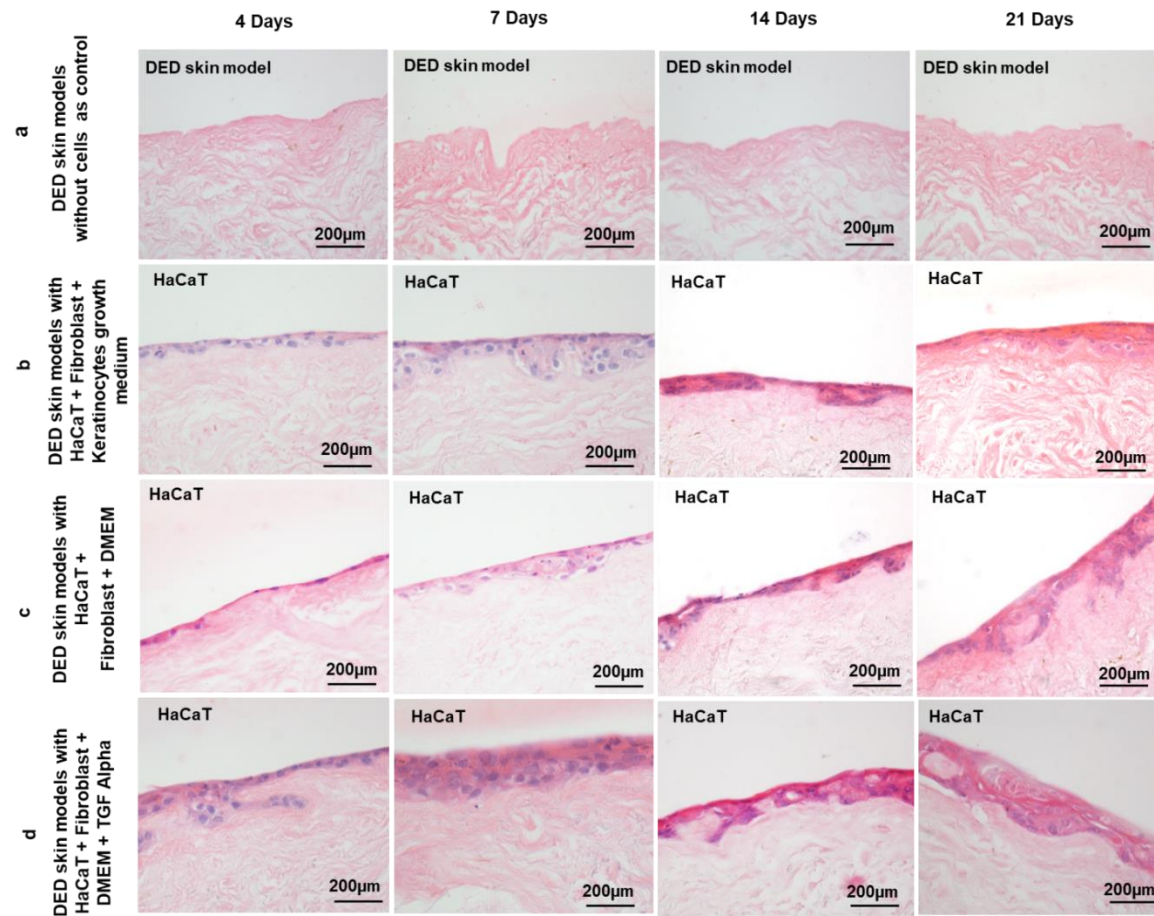
Figure 3.1: H&E stained 3D skin models. a: decellular tissue controls; b: DED, HaCaT cells and fibroblasts in keratinocyte medium 2; c: DED, HaCaT cells and fibroblasts cultured in DMEM media without TGFα; d: DED, HaCaT cells and fibroblasts in DMEM media with TGFα (d). Scale Bar = 200μm.

Skin models were stained with Masson's trichrome stain. The epidermal layers showed red to dark purple by the Weigert's hematoxylin component of the stain, DED dermal layers appeared blue indicating presence of collagen fibres (Figure 3.2). In addition, caspase 3 immunohistochemistry was deployed to investigate the presence of apoptosis. Since caspase 3 is a major executioner of apoptosis, positive caspase activity in stained cells is an indicator that the cells have undergone apoptosis. Very low numbers of HaCaT cells showed immunopositive staining for caspase 3 (Figure 3.2c), compared with caspase 3 immunostained lymph nodes as a positive control (Figure 3.2b) suggesting excellent viability of HaCaT cells and fibroblasts. Since models cultured with DMEM in TGF-α demonstrated the thickest layers of cells and potential evidence of differentiation these were selected for further optimisation.
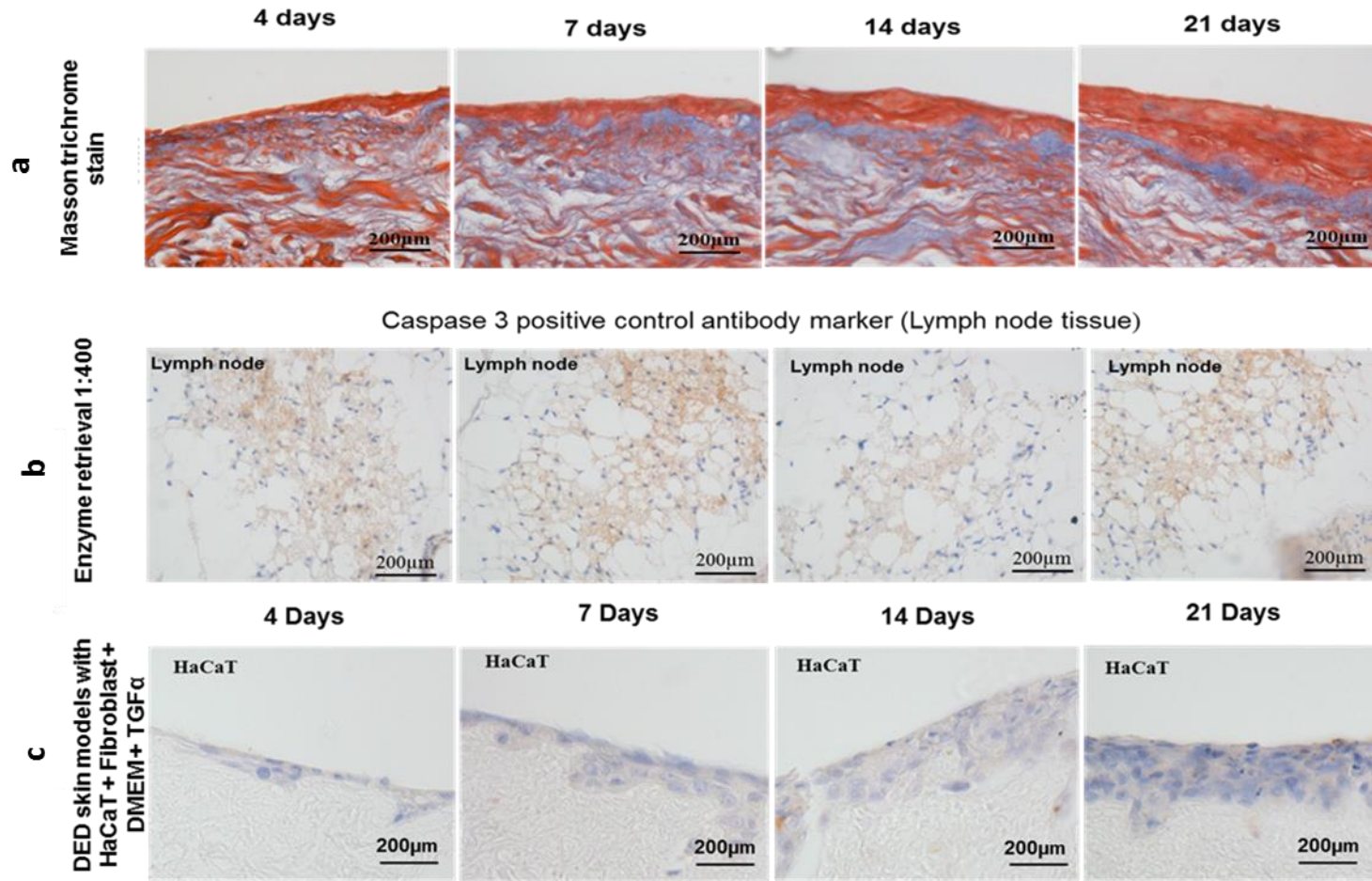
Figure 3.2: a: Masson trichrome stained 3D skin models with HaCaT cells and fibroblasts cultured in DMEM media with TGFα (collagen is shown in blue).b: Caspase 3 immunopositive staining by enzyme retrieval positive control tissue (lymph node). c: Apoptosis was measured using a Caspase 3 antibody marker. 3D skin models with HaCaT cells and fibroblasts cultured in DMEM media with TGFα stained using caspase 3 immunohistochemistry. Scale bar = 200µm

3.3.2- Effect of cell seeding density on 3D skin model formation

Cell seeding of HaCaT cells and fibroblasts in the ratio of $3x10^5$ and $1x10^5$ respectively, resulted in successful proliferation, differentiation and reasonable skin depth layer at 21 days (Figure 3.3). Caspase 3 immunostaining demonstrated low levels of apoptosis (Figure 3). Thus, seeding experiments with variable ratios of HaCaT cells ($3 x10^5$, $6 x10^5$ and $9 x10^5$) and fibroblasts ($1x10^5$, $2x10^5$ and $3x10^5$) were performed in order to reach the optimal seeding density to achieve the optimal thickness of the epidermal layers of skin models.

H & E stained models demonstrated formation of multi-layered HaCaT cells and fibroblasts in all cell densities investigated (Figure 3.3).The denser the seeding ratio was, the thicker the epidermal layer became (Figure 3.4 & 3.5). The optimal thickness of epidermal layers was achieved with the seeding ratios of $2x10^5$ fibroblast & $6x10^5$ HaCaT, demonstrated by being on average 64μm thicker than all other cell densities (Figure 3.5). This ratio also resulted in multilayers of keratinocytes in the epidermal layer, which was clearly shown in tissue sections stained with H&E and Caspase 3 antibody (Figure 3.4).

With Masson trichrome stain, the epidermal layer appeared red to dark purple, whilst the dermal layer stained blue indicating the presence of collagen fibres (Figure 3.3). Only a thin layer of keratinocytes were obtained from low density HaCaT and fibroblasts. The best results were obtained with ratios of ($2x10^5$ fibroblast & $6x10^5$ HaCaT) and ($3x10^5$ fibroblast & $9x10^5$ HaCaT), as was determined from H&E staining (figure 3.3). Caspase 3 immunohistochemistry showed limited staining, indicating low levels of cell death with the skin models (Figure 3.3).
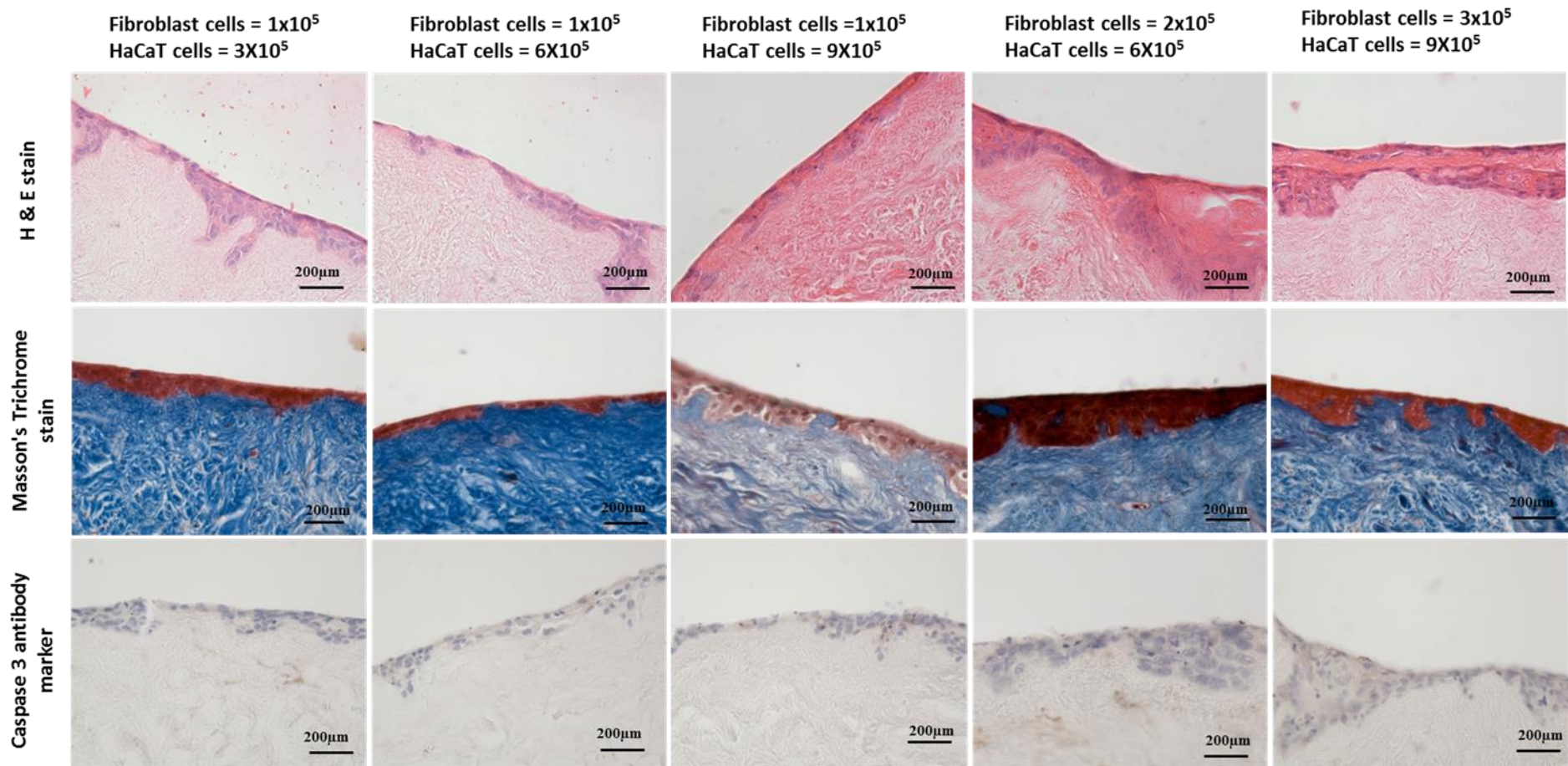
Figure 3.3: 3D skin models with different densities of HaCaT and fibroblast cells. Stained for H & E, Masson Trichrome and immunohistochemistry caspase 3.
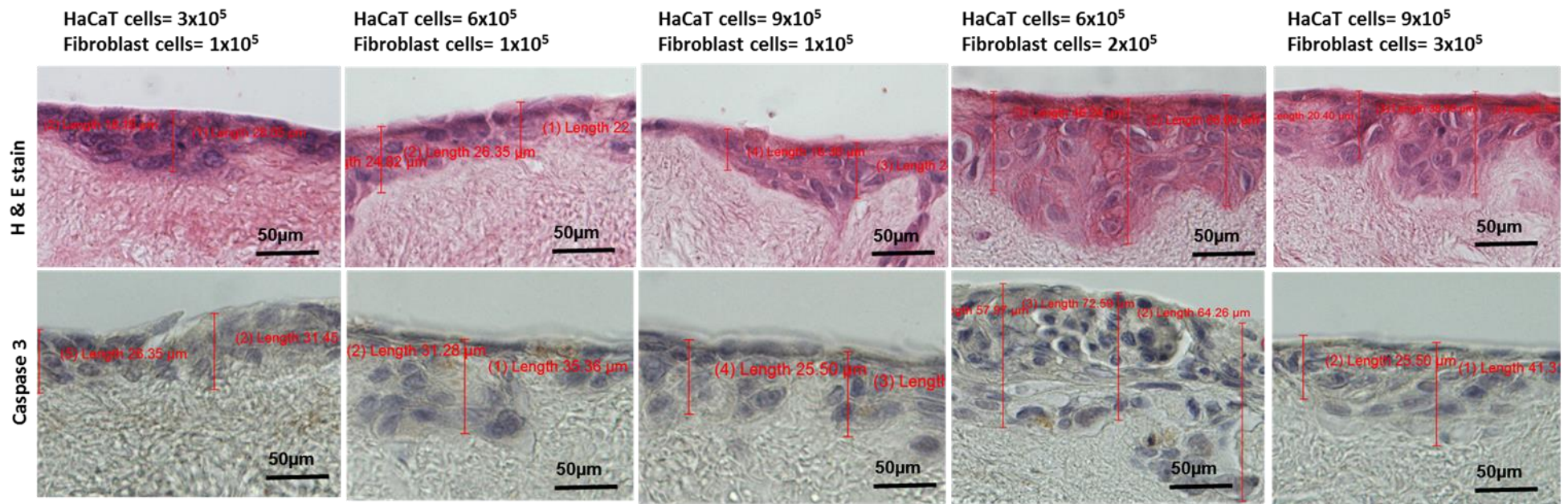
Figure 3.4: 3D skin epidermal layer thickness. Optimal condition seen in 2×10^5 fibroblasts with 6×10^5 HaCaT cells
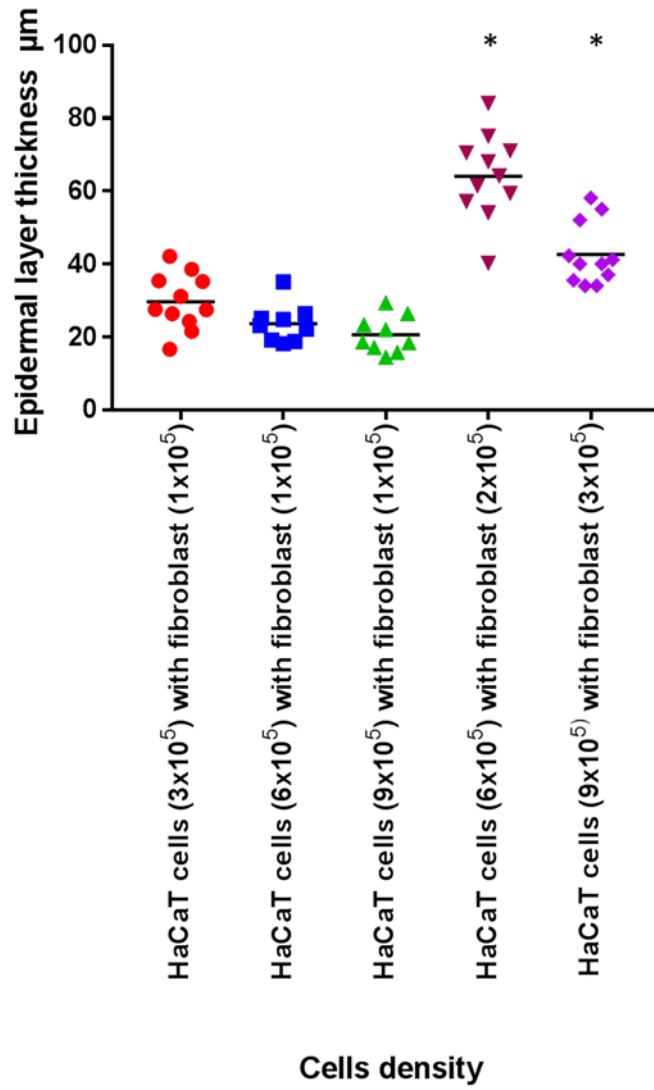
Figure 3.5: 3D skin epidermal layer thickness. Different density of Keratinocyte and fibroblast seen, optimal density is $2x10^5$ fibroblasts with $6x10^5$ HaCaT cells

The human epidermis is comprised of distinct differentiated layers and a characteristic polarised pattern of keratinocyte growth, with actively proliferating cells situated at the dermal-epidermal junction. The expression of various keratinocyte differentiation markers in *in vivo* skin (from the same donor) were analysed using immunohistochemistry (Figure 3.6). Caspase 3 immunostaining demonstrated low levels of apoptosis (Figure 3.6a). Pancytokeratin immunopostive staining was observed across the entire epidermis. Cells remaining formed cornified envelopes (Figure 3.6b). The presence of cytokeratin 14 appeared to be more strongly detected around the basal keratinocytes in native skin (Figure 3.6c). In human skin tissue, a gradual decrease in the expression of keratin 14 immunopositivity was observed from the suprabasal cell layers towards the stratum corneum. The expression of cytokeratin 10 was investigated as a marker of terminally differentiated keratinocytes in the epidermis (Freedberg *et al.*, 2001) and collagen type IV observed in the basement membrane, the expression was notably clear between the epidermal and dermal junction (Figure 3.6d). There was a more uniform distribution and slightly diminished expression of S100A4 immunopositivity among the epidermal layer (Figure 3.6e).
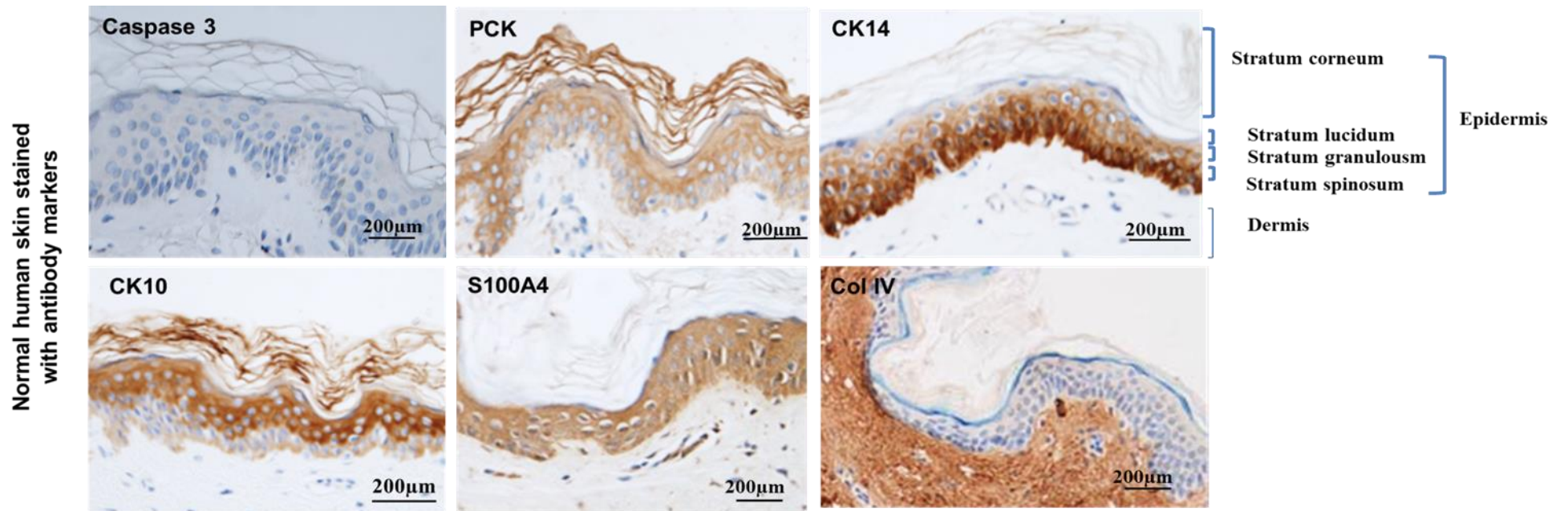
Figure 3.6: Normal human skin was stained by a. caspase 3; b. PCK; c.CK14; d.CK10; and e. S100A4. Scale bar = 200μm

Following culture of 3D skin models *in vitro* at ALI for 7, 14 and 21 days, they were investigated using immunohistochemical analysis to determine the cellular phenotype and differentiation status using protein markers (collagen type IV, Pancytokeratin, Cytokeratin 10, Cytokeratin 14 and S100A4). Varying ratios of HaCaT cells and fibroblasts were used to build skin models with the aim of defining the ideal ratio capable of achieving appropriate differentiation, and localisation of proteins as well as optimal epidermal thickness.

Collagen type IV was abundant in all skin models whatever the ratio was, as was the main component of the DED which cells were seeded onto (Figure 3.7). Low density HaCaT and fibroblast models, showed partial immunopositivity for collagen type IV between the dermal and epidermal layers by day 7 and 14 of culture (Figure 3.7). In high density models (2×10^5 fibroblasts and 6×10^5 HaCaT cells), the collagen type IV expression was observed in the basement membrane at the epidermal-dermal junction following 21 days (Figure 3.7).

There was also evidence for organised expression of type IV collagen. Furthermore, the upper layer of stratum corneum was observed in high density models (2×10^5 fibroblasts and 6×10^5 HaCaT cells) (Figure 3.7).
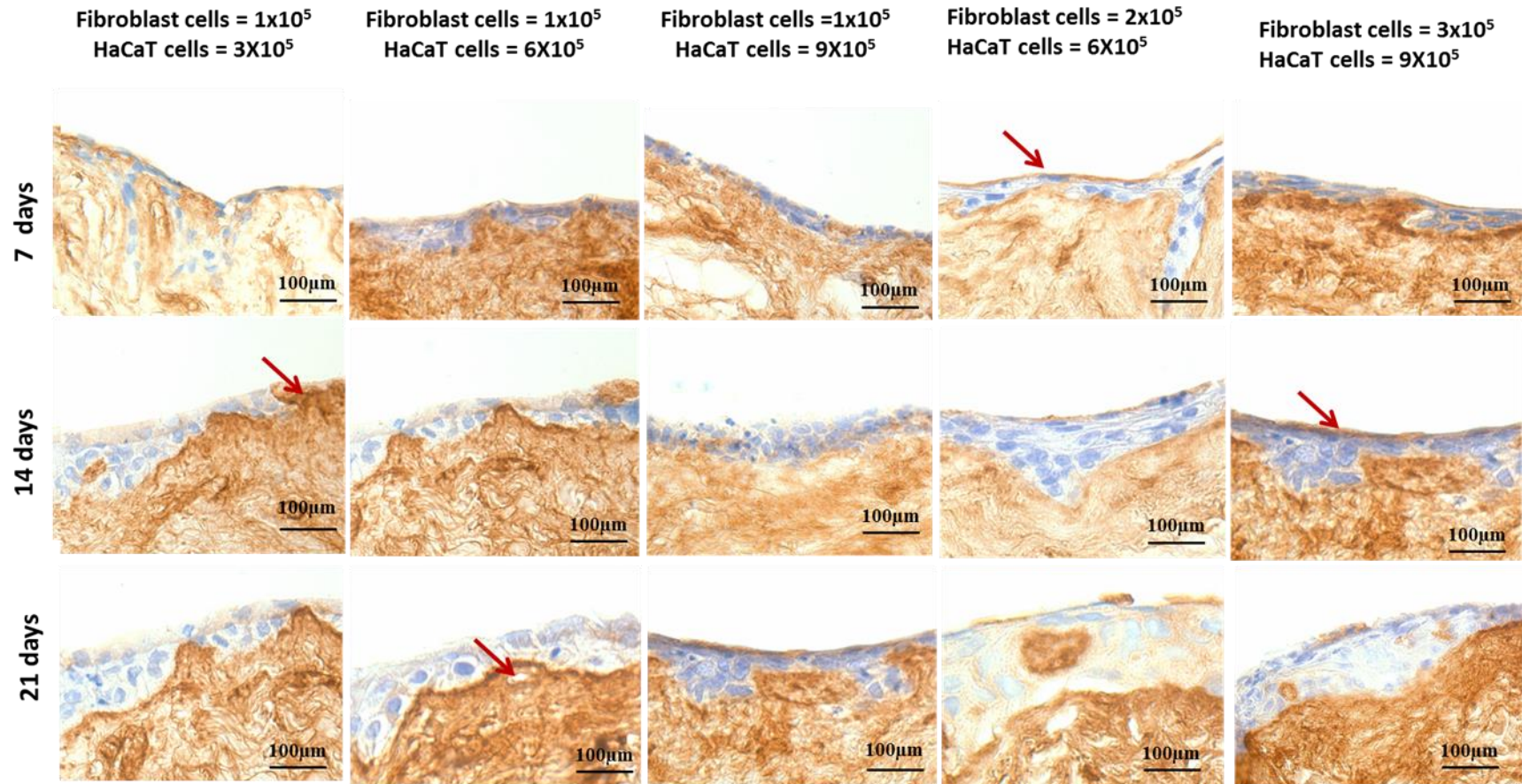
Figure 3.7: 3D skin models with different densities of HaCaT and fibroblast cells, following culture for 7, 14, 21 days at air liquid interface (ALI). Immunohistochemistry for collagen IV, Optimal condition was seen in $2x10^5$ fibroblasts with $6x10^5$ HaCaT cells. Scale bar = 100μm

Immunopositive staining for Pan cytokeratin (PCK), was observed following 7-14 days. The thickness of the PCK expressing layer increased with increasing time in culture to reach its highest at day 21 (Figure 3.8). In the optimal cell density of $2x10^5$ fibroblasts and $6x10^5$ HaCaT cells, normalised epithelial tissue morphology was achieved following 21 days (Figure 3.8).

At that time, cytokeratin 14 immunopositivity was observed in the basal layers indicating the formation of stratum basale resembling that of normal human skin (Hill *et al.* 2015) (Figure 3.9).However, in early time points (7 and 14 days) and in low density HaCaT and fibroblast cultures, the growing basal layer was not sufficient to support fully the cytokeratin 14 expression seen in normal skin (Figure 3.9).

Cytokeratin 10 was shown to be expressed in the terminally differentiated keratinocytes among the basal and suprabasal layers of the epidermis in higher density HaCaT and fibroblast cultures following 21 days in culture, denoting the presence of well differentiated keratinocytes. No CK10 expression was observed in the epidermal layers in low cell density cultures at 7 and 14 days, (Figure 3.10).
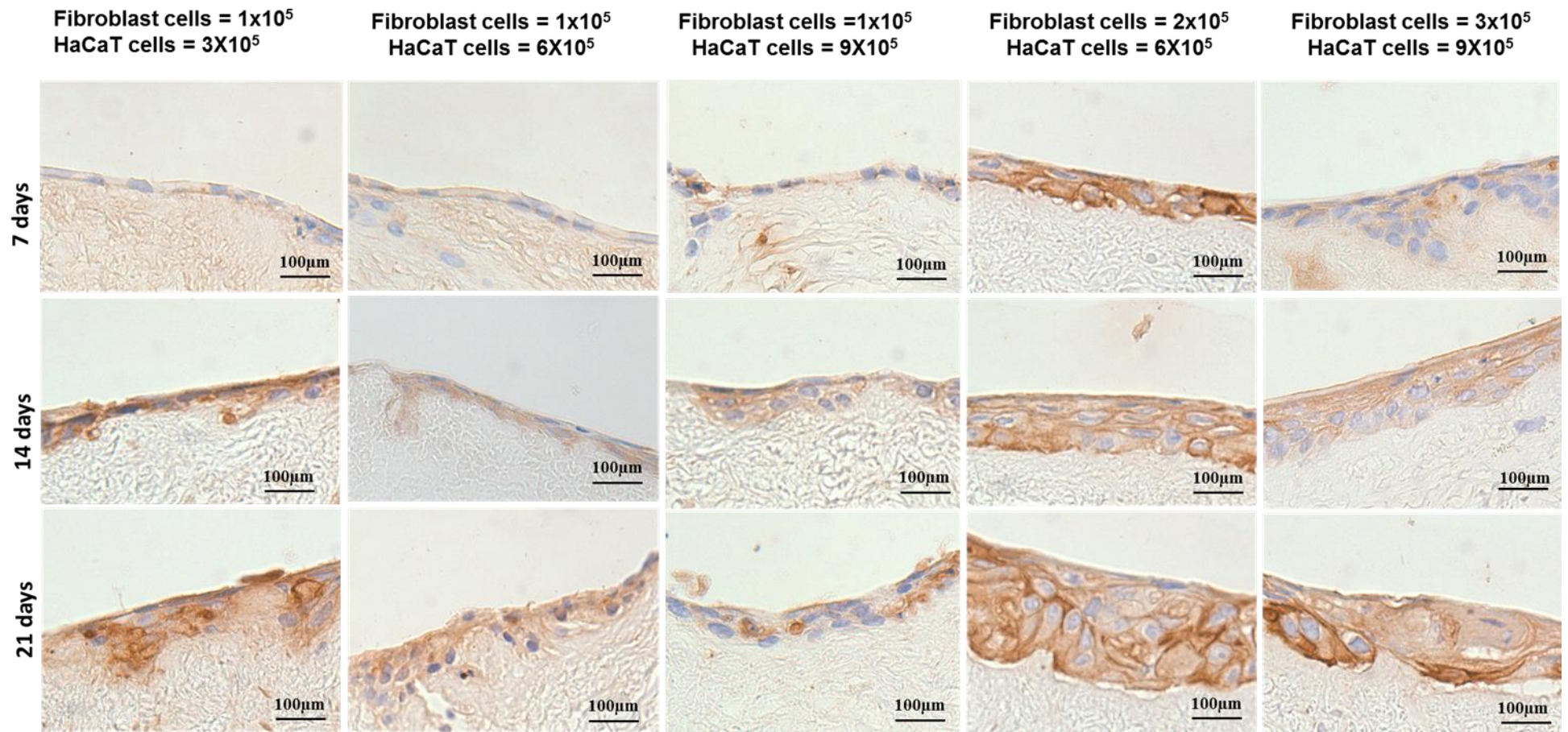
Figure 3.8: 3D skin models with different densities of HaCaT and fibroblast cells, also different time point 7, 14, 21 days Air liquid interphase (ALI). Immunohistochemistry for Pan Cytokeratin (PCK), optimal condition seen in $2x10^5$ fibroblasts with $6x10^5$ HaCaT cells, Scale bar = 100μm.
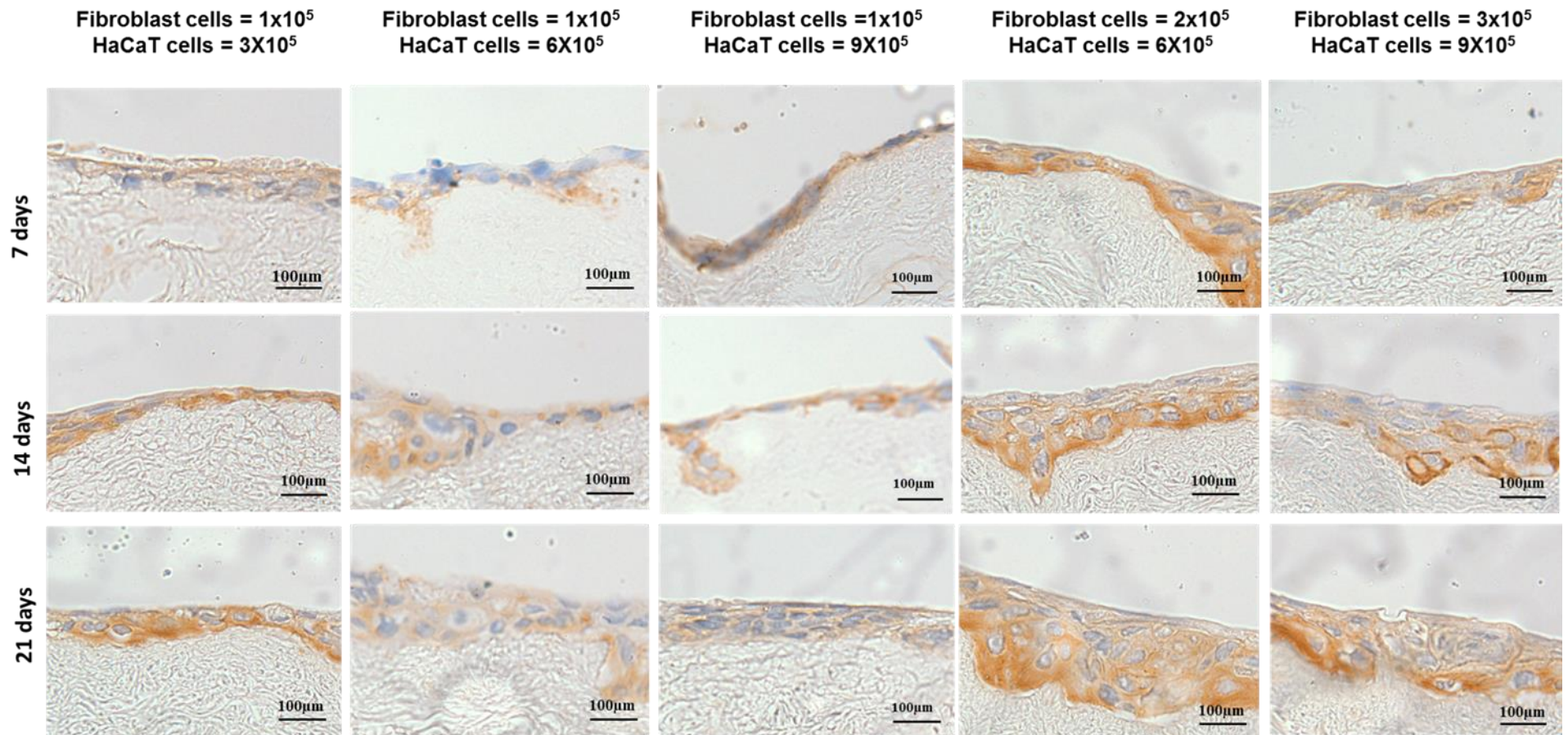
Figure 3.9: 3D skin models with different densities of HaCaT and fibroblast cells, also different time point 7, 14, 21 days Air liquid interface (ALI). Immunohistochemistry for Cytokeratin 14 (CK14), optimal condition seen in 2x105 fibroblasts with 6x105 HaCaT cells, Scale bar = 100μm.
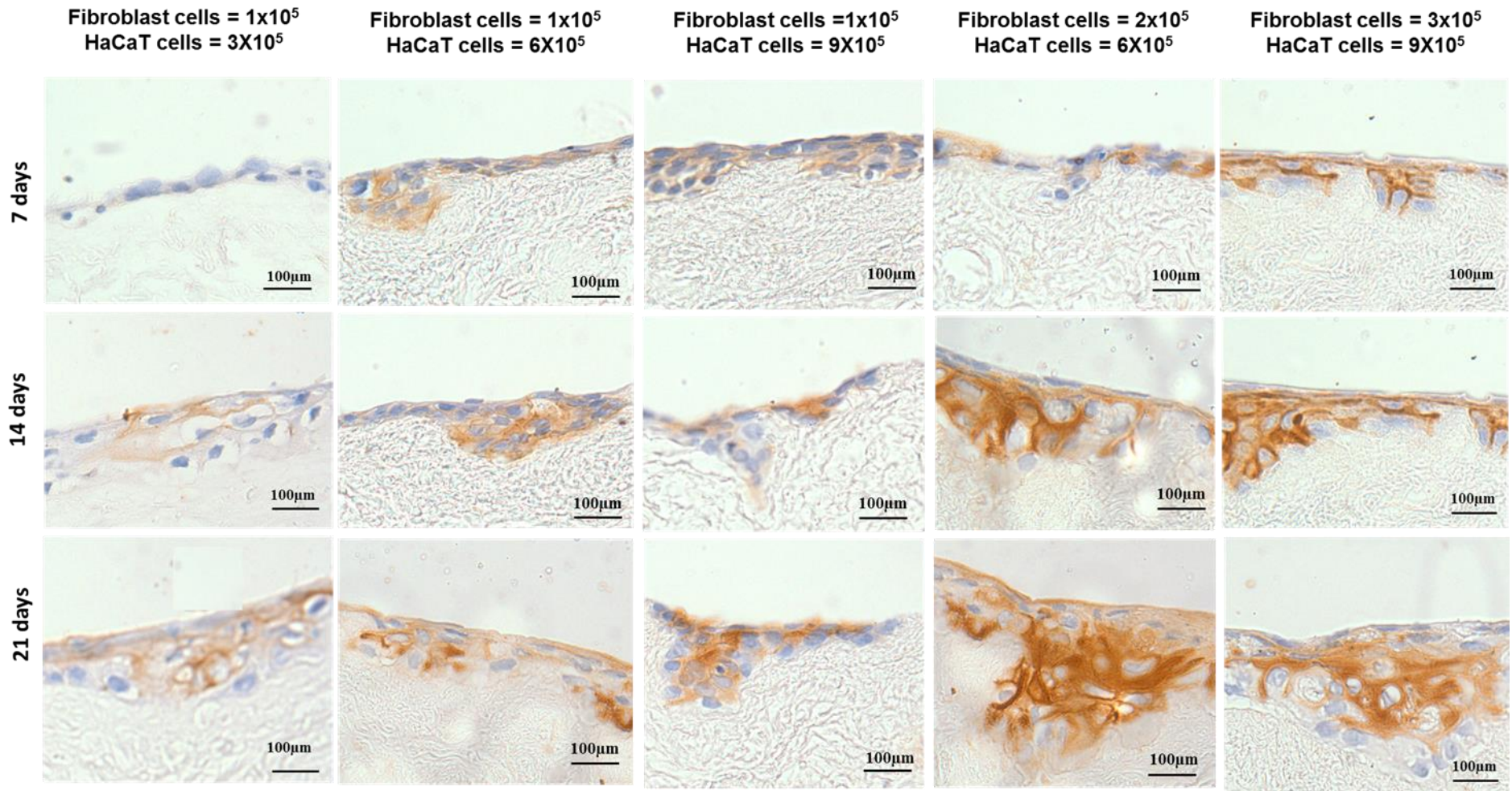
Figure 3.10: 3D skin models with different densities of HaCaT and fibroblast cells, also different time point 7, 14, 21 days Air liquid interface (ALI). Immunohistochemistry for Cytokeratin 10 (CK10), optimal condition seen in 2×10^5 fibroblasts with 6×10^5 HaCaT cells Scale bar = 100μm

Fibroblasts were detected immunohistochemically by S100A4 antibody. During the growth of the skin model, the fibroblasts were seen to proliferate through the dermal layer (Figure 3.11). S100A4 immunopositivity was shown to be expressed along a wider thickness of dermis and epidermis in the optimal ratio ($2x10^5$ fibroblasts with $6x10^5$ HaCaT) cells after 21 days, demonstrating a potential increase in fibroblasts through the layers of the model. Expression levels of S100A4 were not clearly detected with low density cultures, or in those cultured for 14 days or less (Figure 3.11).
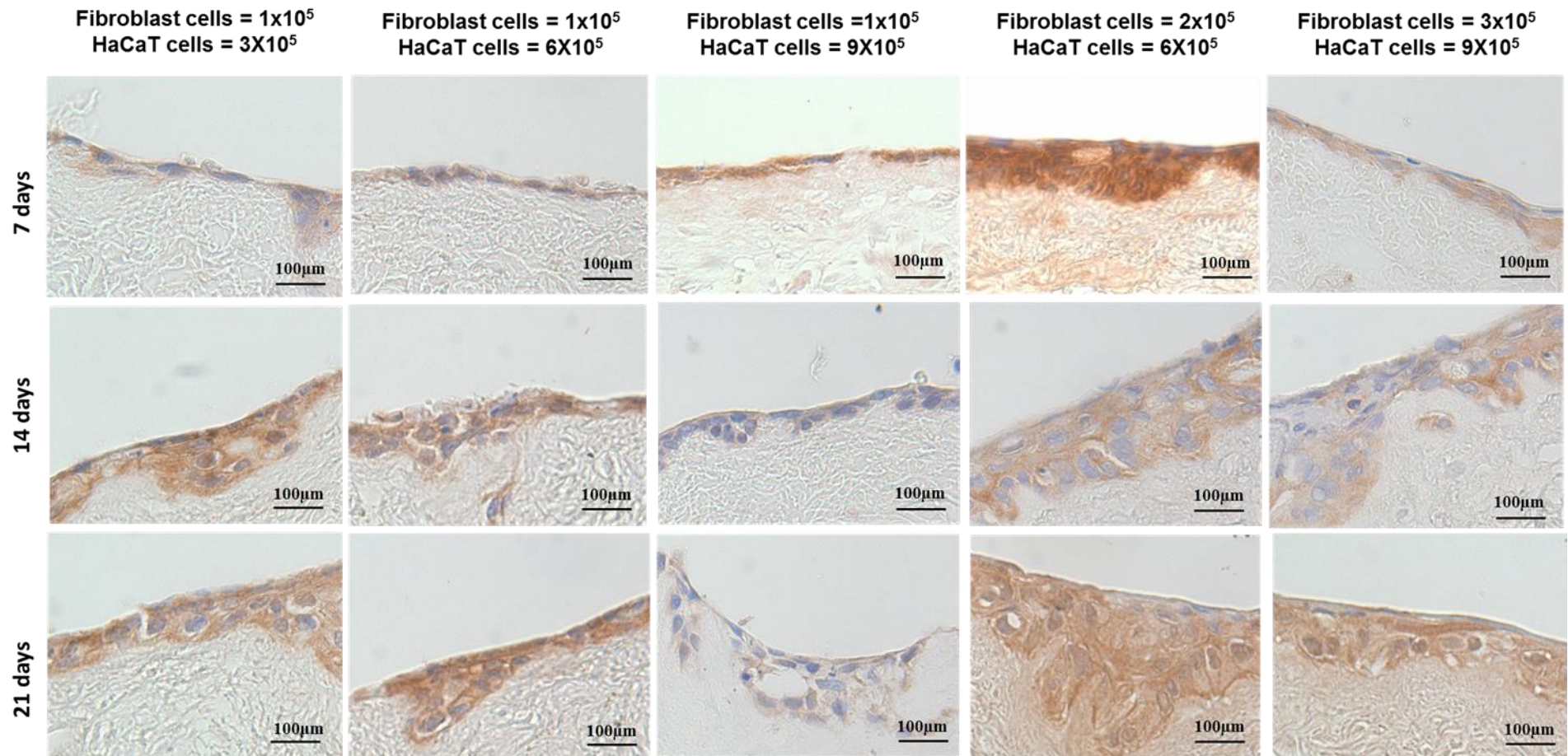
Figure 3.11: 3D skin models with different densities of HaCaT and fibroblast cells, also different time point 7, 14, 21 days Air liquid interface (ALI). Immunohistochemistry for S100A4, Optimal condition were seen in 2x105 fibroblasts with 6x105 HaCaT cells. Scale bar = 100µm.

3.4- Discussion

The generation of the various types of tissue-engineered skin constructs capable of modelling the morphology and organisation of the human epidermis, has previously been documented (Prunieras *et al.*, 1983; Ponec *et al.*, 1997; Bernerd *et al.*, 2012).

Currently, there is still an urgent need for the development of simple *in vitro* 3D human skin models for human skin burns, skin infection and treatment, although there are different *in vitro* 3D models that are frequently used. However, some of the studies focused on the use of primary human cells and the lack of dermal skin, because these use materials such as collagen matrices as a scaffold for reconstructing 3D skin at an air-liquid interface with dermal keratinocytes and fibroblasts (Carlson *et al.* 2008; Chen 2014). Prunieras *et al.*, (1983), Regnier *et al.*, (1981) and Shepherd (2009) reported that exposing cultured primary keratinocytes to ALI develops cell recognition and leads to the differentiation of a stratified epithelium, consisting of all epidermal layers. However, the immortalized human keratinocyte line HaCaT is extensively utilized as a representative of primary keratinocytes due to its similar function and phenotype to primary human keratinocytes. According to Breitkreutz *et al.* (1998), Micallef *et al.* (2009) and Jung *et al.* (2016), such kinds of culture conditions, involved complicated alterations in cellular responses, specific supplement culture medium for keratinocyte growth and differentiation such as growth factors and calcium level. In addition, the paracrine interaction between the two cells at the (ALI). Further research was carried out to improve the cells growth prior seed it onto DED scaffold skin culture conditions.

Many studies report that culturing of keratinocytes prior to seeding them onto the DED or using other scaffolds. Culturing of keratinocytes on a layer of Fibroblast feeder cells, usually irradiated 3T3 cells which provide signals to the keratinocytes so they differentiate properly when seeded onto DED. (Rheinwald *et al.* 1975; Carlson *et al.*, 2018; Chen 2014; Prunieras *et al.*, 1983; Regnier *et al.*, 1981 and Shepherd *et al.* 2009). Thus, optimal HaCaT cell growth is required to the fibroblast feeder cells (Schoop *et al.* 1999; Mass-Szabowski *et al.* 2000).

The present work demonstrates that the ratio 3:1 of HaCaT cells with fibroblasts in the 3D skin models was optimal. It was found out that HaCaT with fibroblast failed to reach full thickes and it was unable to produce a defined epidermal layer. However, the ratio 3:1 of HaCaT cells with fibroblasts resdponding to is to the TGFα on DED. The results showed the enhancing effect of TGFα on the proliferation and differenation of epidermal layer. However, the morphological features (H & E stain, Masson's trichrome) of the epidermal layer thickness found out that the thickness of the epidermal layer was thinner in this case to form a confluent upper surface interface.

Importantly, the transforming growth factor α (TGF-α) production, a known keratinocyte autocrine factor such as growth factors, strongly reduced differenentiaton protein expression in HaCaT epithelial compared to that of normal human keratinocytes cells NEKs (Smits *et al.* 2017, Mass-szabowski *et al.* 2003). Previously, HaCaT cell keratinocytes were used to build a full thickness skin model, in which fibroblasts seeded into DED, derived from cadaver skin, collagen matrices and inert filters without TGFα were utilized (Boelsma *et al.* 1999). However, the use of the HaCaT cells in the full thickness skin model was a less successful epidermal differentiation than NHKs.

On the other hand, Maas-Szabowski *et al* (2003) used HaCaT cells with collagen type I gel as a scaffold cultured in DMEM with 2ng/ml TGFα. It was reported that TGFα supplement induced HaCaT cell line to form structured epidermal tissue in line with the current model.

The current study presents the first model that demonstrates the combination of Euro- skin tissue as a source of DED scaffold, HaCaT cells and culture media containing TGF-a produced a well differentiated epidermal layer with many hallmarks of normal human skin. This was dependent on HaCaT to fibroblast ratios, with a 3:1 ratio. Maas-Szabowski *et al.*, (2000), Schoop *et al.,* (1999) and Maas Szabowski *et al.,* (2003) observed that the fibroblast number that is needed for the optimal HaCaT cell development and for the development of the tissues is precisely specified as 6×10^5 cells/ml for HaCaT cell and 2×10^5 cells/ml for fibroblast development. Additionally, the formation of the epidermal tissues by the HaCaT cells that was delayed for three weeks was unfinished when it was compared with the organotypic cultures of the primary keratinocytes (Maas Szabowski *et al.* 2003; Stark *et al.* 1999).

TGF-α treatment promoted stratification in HaCaT epidermal cell layers. In addition, the double paracrine keratinocytes regulation and fibroblast interaction induces IL-1α expression from keratinocytes and TGF-α, enhancing the HaCaT cells receptors including; keratinocyte growth factor (KGF) receptors and granulocyte macrophage colony stimulating factor (GM-CSF) to improve the epidermal layers differenation in *in vitro* skin models (Maas Szbowaski *et al.,* 2003; 2000). The immunohistochemical analysis performed in this study, demonstrated appropriate keratin expression patterns produced by the HaCaT cells within the epidermal layers of the 3D skin model.

Keratinocyte differentiation was observed by immunopositive staining for PCK, CK10, CK14 and collagen type IV. Similar to previous studies, PCK staining was localised, indicating the surface of the stratum. The production of CK10 by HaCaTs indicates that terminal differentiation was taking place in the epidermal layers (Rosario *et al.*, 1979; Bernerd *et al.* 2008). CK14 was expressed earlier than K10 (Song *et al.* 2001) indicating the proliferation and differentiation of HaCaT cells were ongoing. Collagen type IV positive expression was observed in between the basement membrane and the upper dermal layer of *in vitro* skin models (Bell *et al.*, 1979; Asselineau *et al.*, 1985; Thomas *et al.* 1993). This result indicates that the collagen type IV motivates the proliferation of basal keratinocytes and progress the stratification of epidermal layers in skin models (Matsuura-Hachiya *et al.* 2018). In addition, the lack of caspase 3 immunopositive cells in the epidermal layers in the tissue models indicated low levels of HaCaT cells apoptosis

3.5- Conclusion

The current study demonstrated the optimal HaCaT cell to fibroblast ratio, along with addition of TGFα, to create *in vitro* skin models using DED as a dermal scaffold that structurally resembled native human skin. Higher numbers of $2x10^5$ cells/ml fibroblasts and $6x10^6$ cells/ml HaCaT cells supported an improved 3D skin model. Both histological and immunohistochemical analysis demonstrated morphology and differentiation of appropriate epidermal layers. This model could serve as a good alternative to, or an addition to animal models for burned and/ or infection skin infection layers with the 3D skin model.

Chapter 4

Effect of biocides on *in vitro* burned 3D skin infection with *Staphylococcus aureus* biofilm

4.1- Introduction

Wound infections can be caused by a range of pathogens including viruses, fungi and bacteria and are common in cases of chronic non-healing wounds such as diabetic ulcers and thermal injuries. The management of wound infection presents a challenge to healthcare authorities both in terms of economic burden and the need to reduce the use of antibiotics due to the rising global crisis of antibiotic resistance. Large numbers of the population in western countries have been affected by chronic wounds, especially elderly people (Garcia *et al.* 2006), and in patients with diabetes whose non-healing ulcers are challenging (Boulton *et al.* 2005; Ramsey *et al.* 1999; Ramsey *et al.* 2006). Thus new treatments are required which can address bacterial infection of wounds whilst supporting wound healing. To date, models utilised for investigating new biocidal agents fail to recapitulate the environment of an infected wound within humans.

4.1.1: Animal models of wound infection

In vivo models of wound infections especially using murine and porcine models have been extensively used (Ahrens *et al.* 2011; Sullivan *et al.* 2001; Ansell *et al.* 2014), However, these animal models are not necessarily good representatives of human skin and such investigations have raised concern regarding the use of animals' skins due to differences between human and animal immune systems (Mestas & Hughes, 2004). Moreover, using animals' samples in these models also has ethical issues (Liguori *et al* 2017). Thus, Carlson *et al.*, 2008; Safferling *et al.*, 2013; and Xu *et al.*, 2012 amongst others developed 3D models to better mimic the stracture and responses of skin.

4.1.2 Tissue engineered skin models of infection

Over the last two decades, the tissue-engineered skin models have been developed, which are similar to human skin (Ghosh *et al*. 1997; Chakrabarty *et al*., 1999; Netzlaff *et al*. 2005; MacNeil *et al*. 2007) (See chapter 3). Holland, *et al*. (2008) successfully used a 3D skin model using fibrin populated with fibroblasts to study skin colonisation by human cutaneous skin commensals including *S. epidermidis, Propionibacterium acnes and Malassezia furfur*. However, this model maintained an intact epidermidis as the study was investigating normal flora colonisation rather than pathological ingress which occurs during skin injury (Holland *et al*. 2008).

De Breij *et al.* (2012) studied. *Acinetobacter baumannii* (ATCC 19606) and *A. junii* (RUH2228) skin colonization of a three-dimensional (3D) model. The capacity of the disinfectant chlorhexidine to decolonize the skin equivalents was also evaluated. The findings showed that both strains colonised and expanded on the stratum corneum for more than 72 h, however, no migration into the epidermis was seen. Shepherd, *et al*. (2009) and (2011) also developed three-dimensional models of normal human skin to study infection of *P. aeruginosa* (SOM1), and *S. aureus* (S-235) and *S. aureus* (NCTC6571).

The 3D model developed was reproducible, and showed similar properties to human skin, well defined keratinocyte layers and a complicated epidermal–dermal junction with a clear basement membrane. *S. aureus* is the most common bacteria isolated in infected wounds; it is a transient coloniser of the skin that has an extensive range of virulence factors. Thus, this study utilised the 3D skin model developed in chapter 3 to develop skin model infected with *S. aureus.* This model was utilised to investigate the effects of biocidal agents

investigated in chapter 2 to reduce *S. aureus* bacterial load in infected wounds using tissue engineered skin as an infected-wound model. Importantly the use of this model to determine effects of infection and biocidal agents on native skin cells was also investigated.

4.2- Materials and Methods

To determine the effect of biocides on tissue engineered (TE) skin, a TE skin model was cultured as described in Chapter 3. Briefly, HaCaT cells and human dermal fibroblasts are seeded onto a decellularised dermal scaffold, brought to an air-liquid interface and cultured for 21 days. A full thickness 3D model of human skin is thus generated. Initially, Alamar blue assays were performed on monolayers of HaCaT, fibroblasts and HaCaT, and fibroblasts treated with biocidal agents to determine the effect on cell viability of the skin cells individually. Then, to optimise the 3D model of human skin, the skin model was thermally burned to allow egress of bacteria through the epidermal barrier to create a model of infected skin.

The skin was infected with *S. aureus* (using a range of infection loads) for 24h and both skin morphology and viability were assayed as described above. The viable counts of bacteria with and without treatment were investigated. Infected TE skin was homogenised and bacterial viability determined using CFU counts, and skin also was formalin fixed, paraffin embedded and stained using H&E stains and Gram stains to determine migration and pentration rates. Furthermore the effects of infection and biocidal agents on skin cell viability and phenotype were determined using histology and immunohistochemistry.

4.2.1- Cell viability of 2D cultured fibroblasts and keratinocytes treated with biocidal agents

4.2.1.1- Alamar Blue method

Monolayer cultures of HaCat cells and fibroblasts individually or as a 3:1 HaCat/Fibroblast co-culture were seeded at 15000 cells /well and allowed to adhere overnight. Cells were then treated with 100 µl of the biocidal agents (silver nitrate, isothazolione and hydrogen peroxide) with a range of 0 to 250

μg/ml of biocide for 24 hours. Following treatment with the biocides for 24hrs, wells were thoroughly washed with PBS to remove traces of media and biocides completely. Alamar blue (10 μg/ml) was pipeted to each well and incubated for 4 hours at 37 °C / 5% CO_2. The blue resazurin salt is reduced to red resazurin by mitochondrial enzymes. The absorbance was determined with a *CLAROstar* (BMG Labtech, Offenburg, Germany) microplate reader set at 570nm. The readings were normalized using control non-treated cells.

4.2.2- Wound Model

4.2.2.1- 3 D skin model composites

3D skin models were produced as per the optimised 3D skin model described in chapter 3. Briefly, human dermal fibroblasts and HaCaT cells were obtained from ECACC Company. Sterilized Euroskin tissue was decellularised and prepared as per section (**3.1.2).** DED was seeded with $2x10^5$ fibroblast and $6x10^5$ HaCaT keratinocytes, and cultured in Dulbecco's modified Eagles medium (DMEM) with 10% fetal bovine serum FBS, penicillin and streptomycin and 2ng/ml Transforming growth factor alpha (TGFα), where TGFα was refreshed every 48hrs. 3D skin models were used for experiments after 21days at ALI at 37°C in 5% CO_2.

4.2.2.2- 3D skin burn wound models and bacterial infection

A single bacterial colony of *S. aureus* was suspended in 20 ml brain heart infusion broth (BHI) for 24hours at 37°C in a shaking incubator. Constructs were burnt by application of heated metal rod (4 mm diameter) for 6 seconds (Figure 4.1) with a fixed depth of injury (75-100μm) before infection with $1x10^6$ *S. aureus* cells in 100μl of BHI by pipetting directly onto to the region of the burn.

Infected and non-infected (control) 3D skin models were incubated in antibiotic free 10% v/v FBS DMEM with TGFα at 37°C in 5% CO_2 atmosphere for 24 hours post infection prior to antimicrobial treatment. Alginate gel (1.2% w/v) was utilised to dissolve biocidal agents as described in section (2.2.1). Biocidal agents were utilised at the MICs for planktonic culture determined in chapter 2 (Silver nitrate and 2- Methyle -4- isothiazoline -3-one: 62.5 µg/L; Hydrogen peroxide: 0.046 v/v). One hundred microliters of biocidal gel was added via pipette to the top of the 3D skin construct to ensure coverage of the wound. These constructs were incubated at 37°C in 5% CO_2 atmosphere for 24 hours. Following treatments 3D skin models were bisected with sterile scalpels, half of the construct model was fixed in 10% formalin for ~24 hours prior to processing to paraffin as described previously (Section 3.1.3), immunohistochemical staining was preformed as described previously (Le Maitre, *et al* 2005)(Section 2.1.4) and Gram stained as per standard procedures (Shepherd *et al.* 2009a). The other half was weighed and homogenised in 1ml of BHI broth. The resulting homogenate was serially diluted and used to perform viable counts of bacteria per Gram.
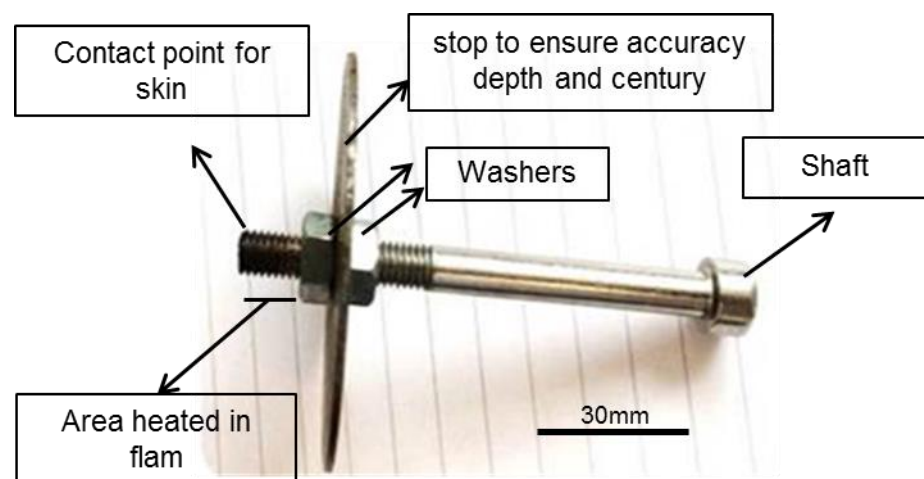
Figure 4.1: Metal rod tool used for burning 3D skin models. Scale 30mm

4.2.2.3- 3D skin model cell death zone

The skin models previously prepared in this study were subjected to infect by *S. aureus* to assess the size of the zone of mammalian cell cytotoxity ('death zone') that forms as a result of the injury/infection. The infected models were then treated with four biocidal agents and the resultant death zone after 24 hours of incubation was assessed, to determine if there was an increase after treatment. The 3D skin models with no biocides were immunohistochemically stained with Caspase 3 (as described in section 3.2.4), to detect the presence of apoptosis in the 3D skin model. Normal skin models, stained with caspase 3 were used as control slides to be compared with burned skin models, burned and *S. aureus* infected skin models and lastly with burned and infected skin models with alginate (the medium used to introduce the biocide). Tissue samples were analysed and zone death measured by microscopy. Sections were analysed using an Olympus BX 51 Microscope and images captured by camera (Microcapture V5.0 RTV digital camera (Q imaging, Buckinghamshire, UK) and capture pro OEM v8.0 software (Media Cybernetics, Buckinghamshire, UK) (Figure 4.2).
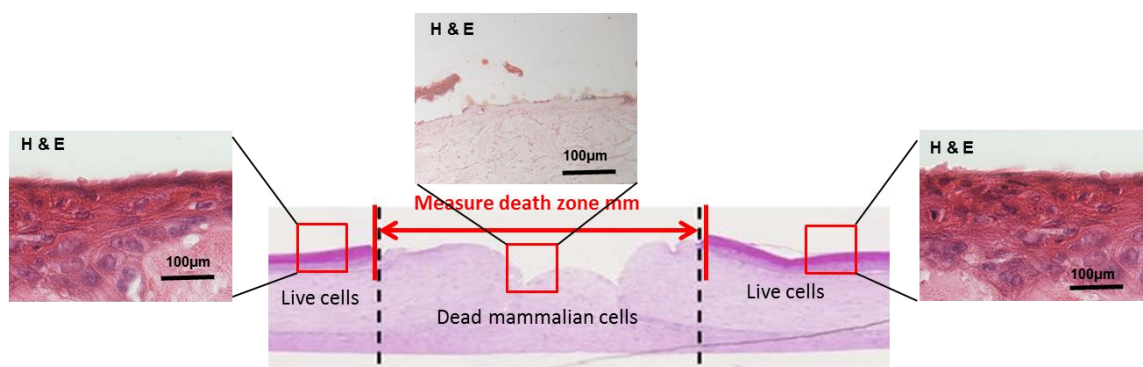
Figure 4.2: Model of 3D skin describing the measurement of mammalian cell death zone. The three pictures are shown in each section of the 3D skin models. The middle one shows the centre of the slide while the peripheral ones show the peripheries of the slide.

4.2.2.4- Bacterial migration and penetration

After investigating the effect of the burned of *in vitro* 3D skin models, bacterial infection and biocidal agent treatment, further experiments were conducted on 3D skin models infected with *S. aureus* with the aim of estimating the degree of bacterial migration and penetration of the bacterial cells. Initially, bacterial migration was measured after skin had been infected for 24 hours. Following this, migration was measured in skin infected for 24 hours then measured the bacterial migration. In addition, the skin infected with *S. aureus* for 24 hours then treated with biocides for 24 hours. Silver nitrate, isothiazolone, hydrogen peroxide and Manuka honey were used. Similarly, the degrees of migration (horizontal spread) across the skin model after the same periods of time were estimated in millimeters.

In order to accurately estimate the depth of penetration and extent of horizontal spread, immunohistochemical staining with specific antibody markers against *S. aureus* proteins was used together with a Gram stain.

Sections were analysed using an Olympus BX 51 Microscope and images captured by camera (Microcapture V5.0 RTV digital camera (Q imaging, Buckinghamshire, UK) and capture pro OEM v8.0 software (Media Cybernetics, Buckinghamshire, UK).

4.2.3- Immunohistochemistry

Anti-Caspase-3, Ani-collagen type IV, Anti-S100A4, anti- Cytokeratin 10 anti-Cytokeratin 14, anti- Pancytokeratin (PCK-26) and anti *S. auerus* antibody, were selected for immunohistochemistry (IHC) investigation to assess variability and differentiation of 3D skin cells models and identification of presence of *S.*

auerus. Sections were prepared as described for histological analysis; IHC was performed as previously described in chapter 3 section (3.2.4).

Sections were analysed using an Olympus BX 51 Microscope and images captured by camera (Microcapture V5.0 RTV digital camera) (Q imaging, Buckinghamshire, UK) and capture pro OEM v8.0 software (Media Cybernetics, Buckinghamshire, UK).

4.2.4- Statistical analysis

All experiments were performed independently at least three times and results are shown using scatter plots with medians. Statistical significance of the experimental results (significance level of $P \leq 0.05$) was calculated. Data did not follow a normal distribution, thus, non-parametric and Kruskal-Wallis with a connover Ingman post hoc test was used to investigate significant differences.

4.3- Results

4.3.1: Effect of biocidal agents on monolayer mammalian cells

Initially the effects of biocides on mammalian skin cells were studied. The biocides used were silver nitrate, isothazoline and hydrogen peroxide as investigated in Chapter 2. The skin cells investigated were HaCaT epidermal cells, fibroblasts and mixture of HaCaT cells and fibroblasts in the ratio of 3:1 respectively. The cells were grown as a monolayer in plates and were treated with gradually increasing concentrations of biocides.

4.3.1.1- The effect of silver nitrate, isothiazolone and hydrogen peroxide on HaCaT cells, fibroblasts and a 3:1 mixture of HaCaT and fibroblasts.

The effects of silver nitrate, isothiazolone and hydrogen peroxide on mammalian monocultures were determined. Furthermore, the concentration determined as the MIC for silver nitate and isothazoline on bacteria (chapter 2)

is indicated as a red, line demonstrating that bacterial MIC against bacteria concentrations also induced decreased metabolic activity in fibroblasts, with a 20 fold decrease in metabolic cell activity (Figure 4.3). Fibroblasts were the most sensitive mamalian cells and HaCaT cells were the most resistant to the effects of silver nitrate, isothazoline and hydrogen peroxide (Figure 4.3). Co-cultures of HaCaT cells and fibroblasts showed sensitivity which was between the individual cultures following treatment with all three biocidal agents (Figure 4.3).
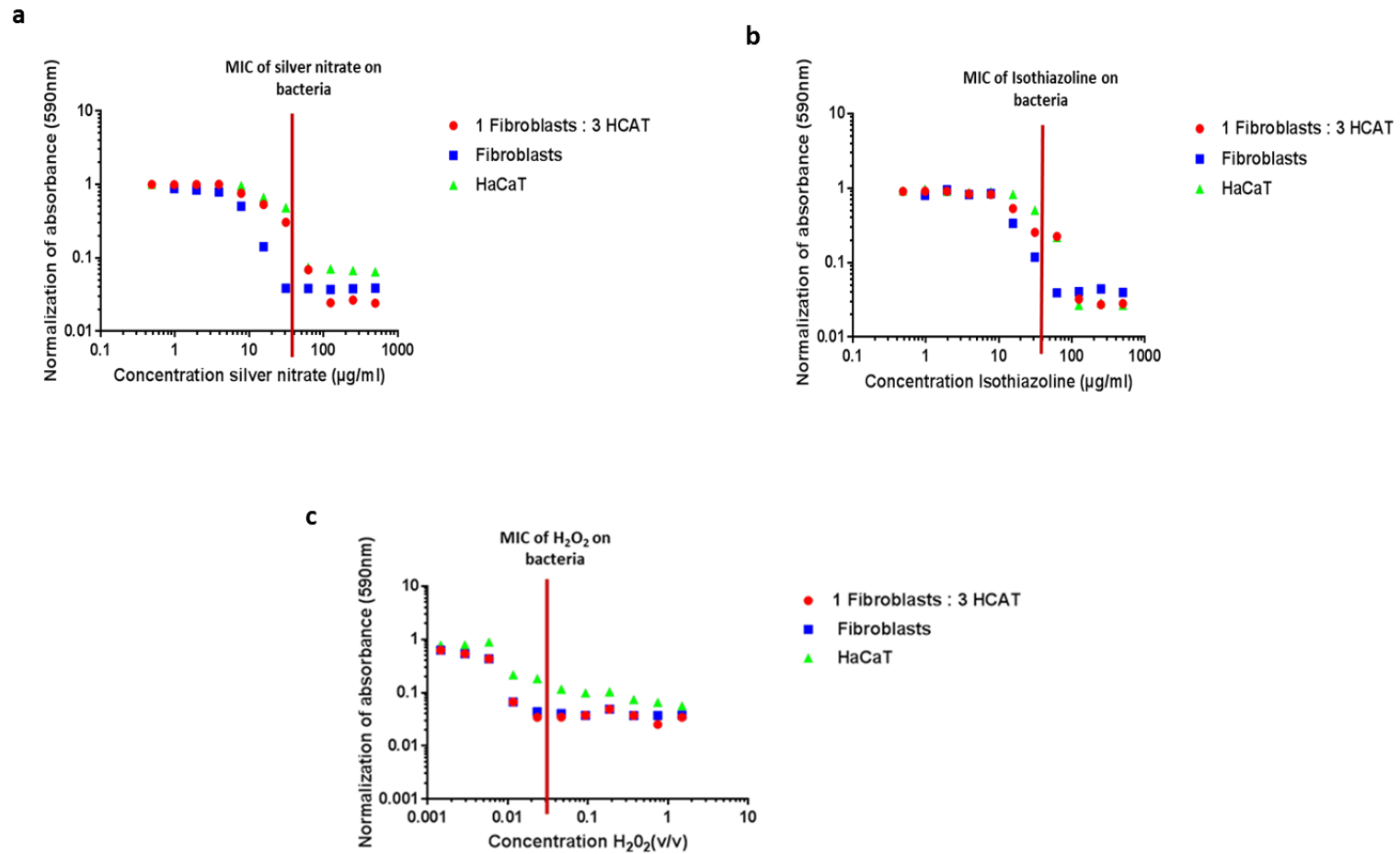
Figure 4.3: Effect biocides at bacterial MIC on monolayers of mammalian cells (fibroblasts, HaCaT cells and a 3:1 mixture of HaCaT and fibroblasts). a; silver nitrate, b; Isothiazolone, c; hydrogen peroxide; red line is the MIC of biocides determined in planktonic bacteria (chapter 2).

4.3.2- Effects of biocidal agents on 3D skin models infected with *S. aureus*

To determine the effect of oxidazing biocides on *S. aureus* skin infections, an *in vitro* surface wound model infected with *S. aureus* was subjected to various biocidal agents: Silver nitrate, isothiazoline (2- Methyl -4- isothiazolin -3-one), Hydrogen peroxide and Manuka honey. In the case of the first three biocides, an alginate treatment was included as a control as alginate was utilised to apply biocides. A non-treated infected skin model was also utilised as a control. There was evident bacterial biofilm growth in both the infected non-treated control and the infected and alginate treated tissue models, following 24 hours of incubation (Figure 4.4). Alginate did not affect the CFU/ml of *S. aureus* recovered from skin models (P value = 0.691) (Figure 4.4). In the test groups, skin models were infected with *S. aureus* and incubated for 24 hours at 37°C prior to treatment with each of the biocides at their pre-determined planktonic MIC, as described in chapter 2 (Section 2.3.2). Silver nitrate and 2- Methyl -4- isothiazoline -3- one significantly decreased the *S. aureus* CFU/ml within 3D skin models by 1.4 $\log_{10}$, compared to infected untreated controls (Figure 4.4). A significant reduction of 1.6 $\log_{10}$ of *S. aureus* in 3D skin models was also seen following Hydrogen peroxide (0.046v/v) treatment (Figure 4.4). The bacterial reduction by hydrogen peroxide was significantly greater than Silver nitrate (P= 0.0047) and 2- Methyle -4- isothiazoline -3-one (P= 0.0047). *S. aureus* was more susceptible to Manuka honey than to other biocidal agents, and showed the highest statistically significant reduction (P =0.0045), with a 1.9, $\log_{10}$ reduction in CFU/ml (Figure 4.4).
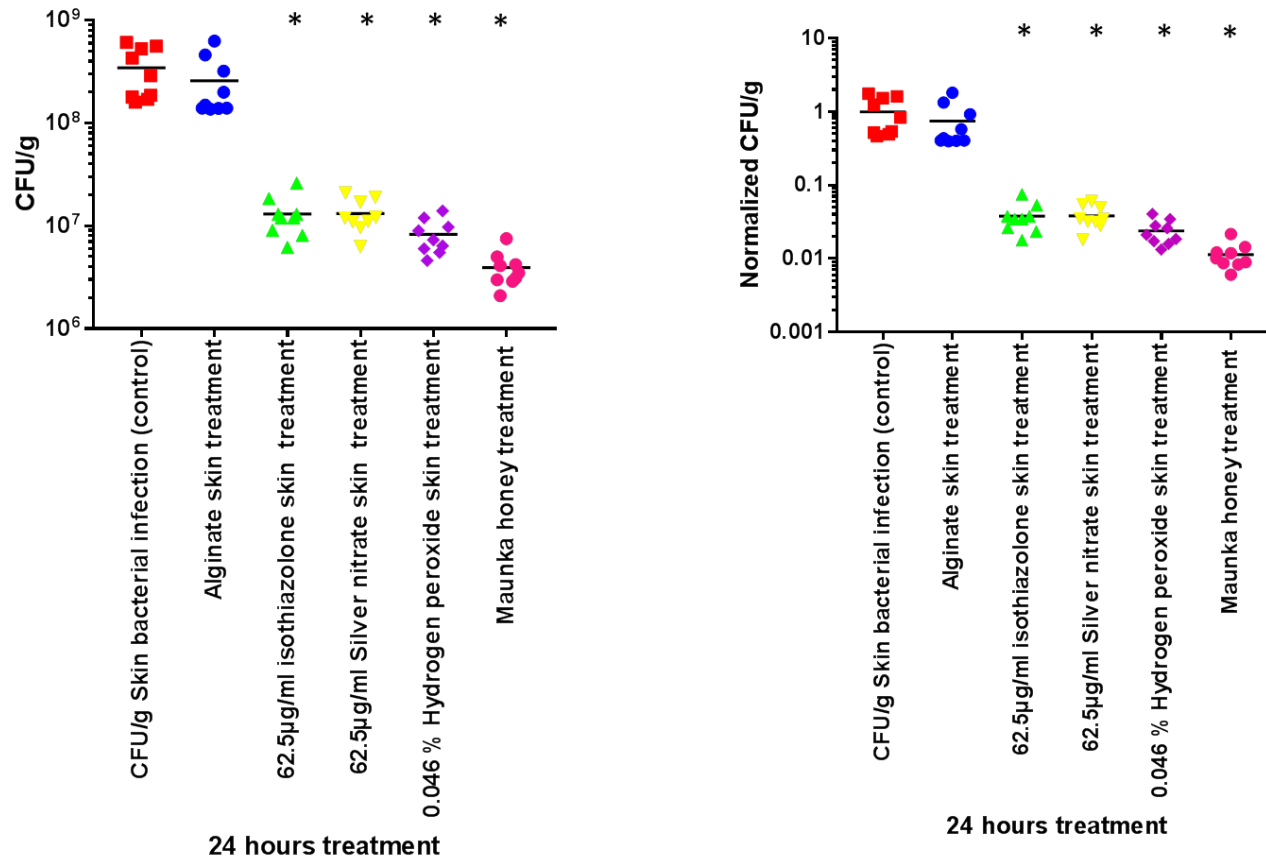
Figure 4.4: Effect of biocides on 3D skin models infection with *S. aureus* (SH1000). CFU/g normalised bacterial counts in skin tissue. *In vitro 3D skin* wound model biofilms grown were treated with Silver nitrate, 2- Methyle -4- isothiazoline -3-one at 62.5 µg/L, Hydrogen peroxide at 0.046 v/v and Manuka honey for 24 hours. *In vitro* wound model biofilms, showing significant inhibition of biofilm of cells following treatment with Silver nitrate, isothiazolone (P≤0.0047),and Hydrogen peroxide (P≤0.0046), with a significant of Honey Manuka (P≤0.0045) for 24h. * = P<0.0.005.

4.3.3 - *S. aureus* skin migration

The 3D skin models were used to demonstrate the degree of migration of *S. aureus* along the surface of skin starting from the infected spot where applied. This was performed by examining sections of the skin in the vicinity of the infected area with Gram stains (Figure 4.5). The skin infection with *S. aureus* lasted for 24 hours and then the skin was treated by biocides for 24 hours. The average size of migration in infected tissue, treated with alginate alone or untreated control tissues was 8.9mm across. Manuka honey significantly reduced the distance that *S. aureus* migrated (P= 0.033) (Figure 4.6). However, other biocidal agents (Silver nitrate, isothiazoline and hydrogen peroxide) did not show any significant reduction in *S. aureus* migration, (Figure 4.6).

4.3.4 - *S. aureus* skin penetration

Burned 3D skin models were infected with *S. aureus* for 24h then treated with biocides, with alginate tratment as a control group. *S. aureus* infection penetrated the 3D skin model in untreated or alginate treatment alone models 58.5 ± 4.3 μm. Treatment of infected models with isothiazoline; hydrogen peroxide and Manuka honey significantly reduced the bacterial penetration depth when compared to controls (P= 0.0357, 0.0462 and 0.0109 respectively) (Figure 4.7). Silver nitrate showed no significant reduction (P = 0.0675) (Figure 4.7).
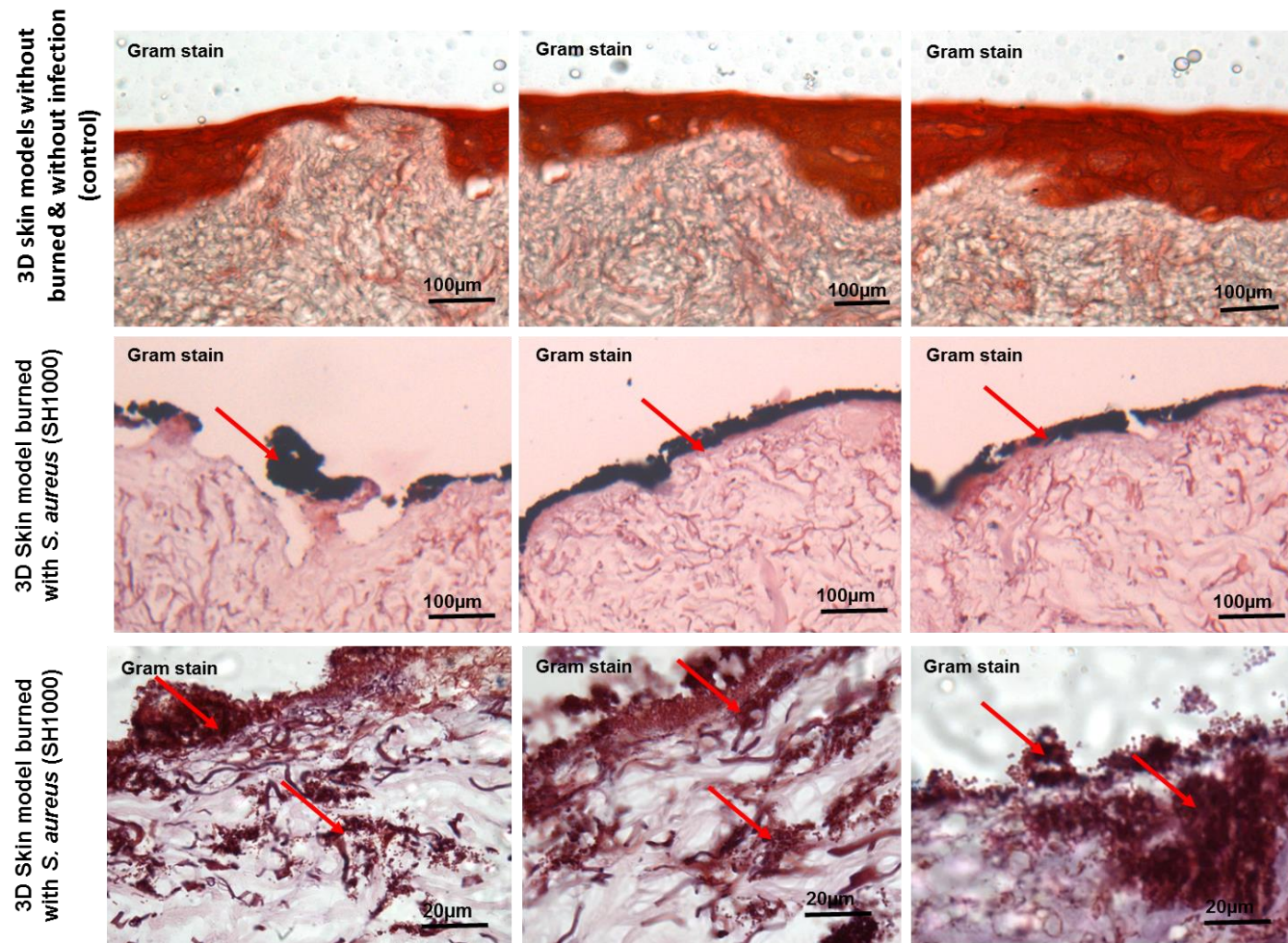
Figure 4.5: Gram stain of 3D skin tissue; Normal 3D skin models, burned with and without *S. aureus* infection. Red arrows indicate *S. aureus* forming biofilm. Scale bar = 100μm and 20μm.
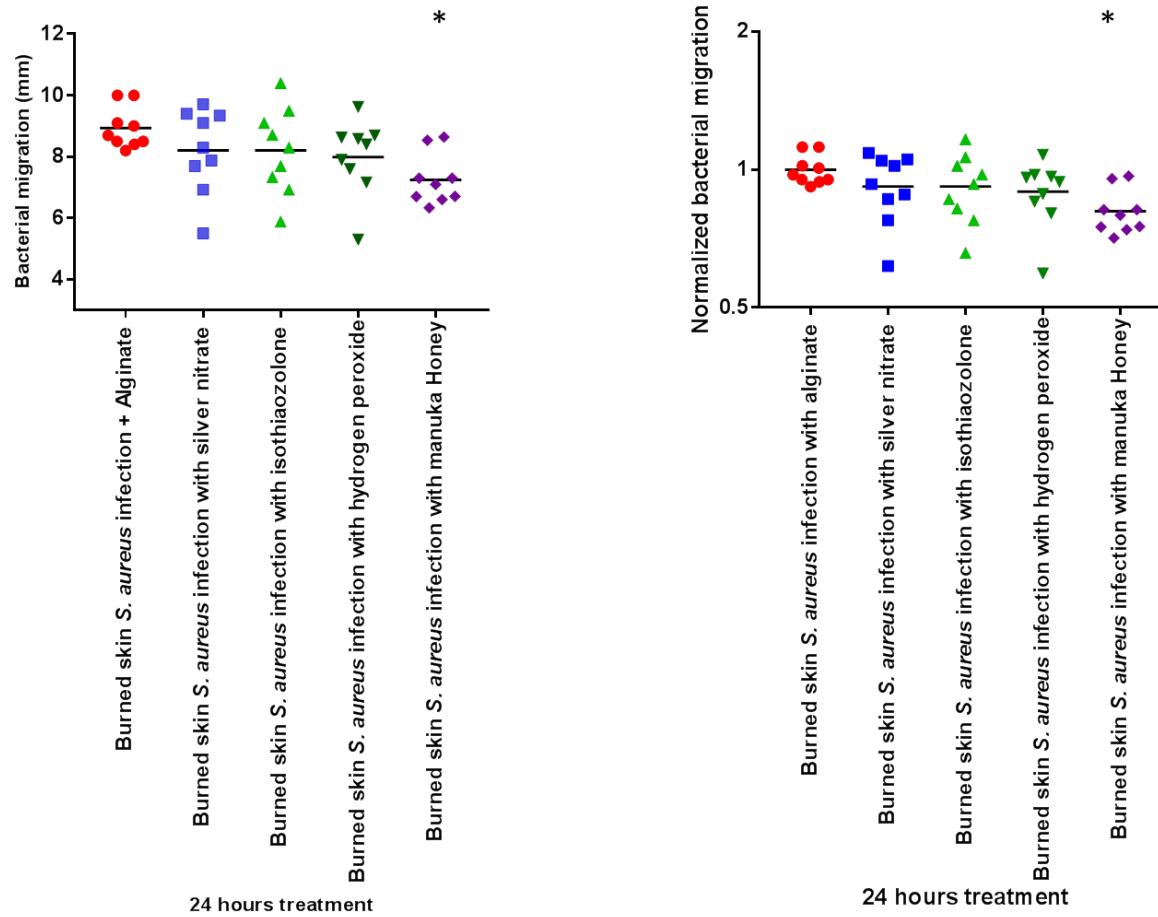
Figure 4.6: Migration of *S. aureus* after 24 hrs of treatment n = 3 separate infected tissue skin models. Infected tissues were treated with Silver nitrate, 2- Methyle -4- isothiazoline -3-one at 62.5 µg/ml, Hydrogen peroxide at 0.046 v/v and Manuka honey for 24 hours. * = P<0.05.
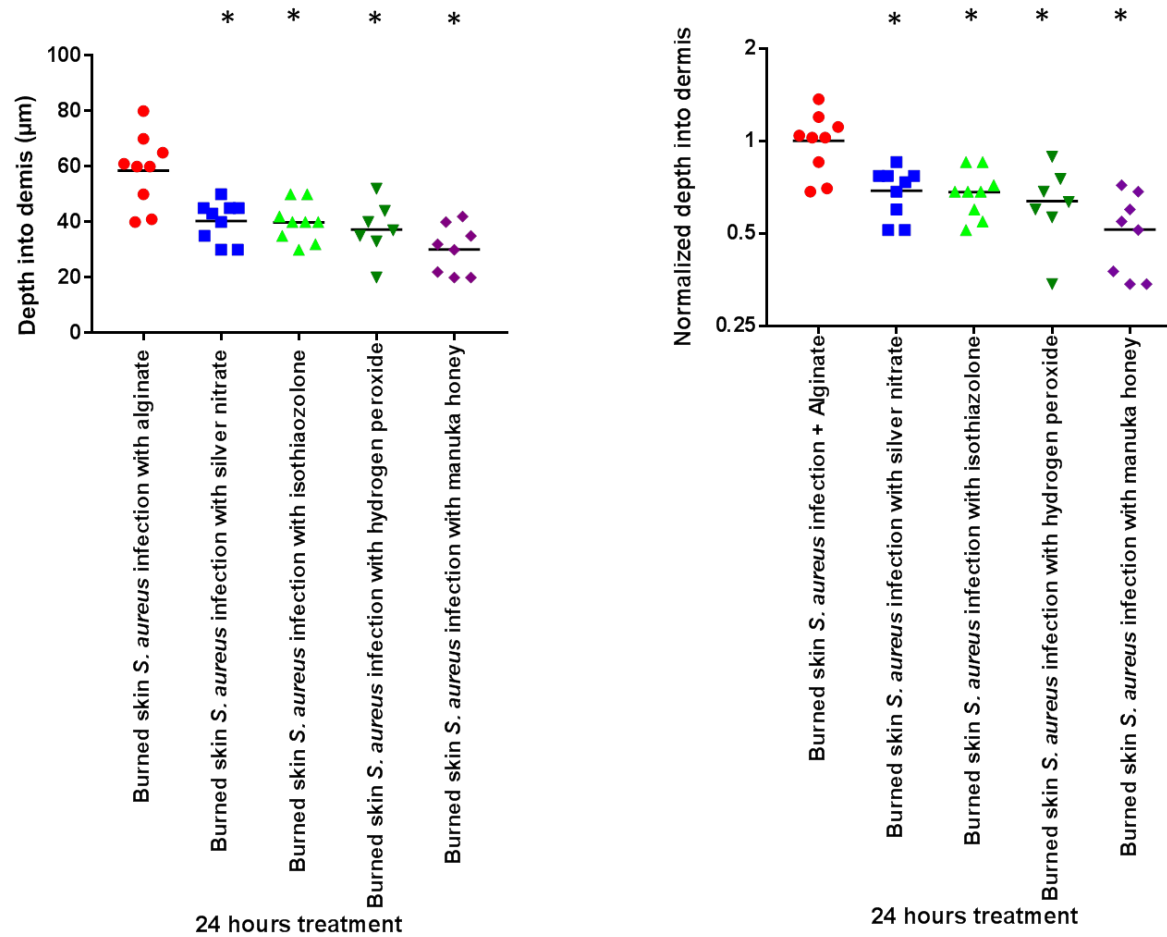
Figure 4.7: Bacteria penetration depth in epidermal layer with skin model. The diaGram showed the depth of *S. aureus* after in 24 hrs of treatment n = 3 separate infected Tissue skin models. Infected tissues were treated with Silver nitrate, 2- Methyle -4- isothiazoline -3-one at 62.5 µg/ml, Hydrogen peroxide at 0.046 v/v and Manuka honey for 24 hours. * = P<0.05.

4.3.5- Anti- *S. aureus* antibody marker:

3D skin models section was infected with *S. aureus* and stained by IgG negative control. It was negative immunohistochemistry. However, tissue sections uninfected models were slightly brown without bacteria forming biofilm on the surface tissue.

When skin models were infected with *S. aureus* for 24 hours, biofilm formation was evident on the surface of the models with considerable penetration into the epidermal and superficial dermal layers. This was evidenced by a thick immunopositive staining for *S. aureus* antibody on the surface of the model (Figure 4.8). *S. aureus* were seen to penetrate into the tissue models (penetration potential) and migrate across the surface of the skin model (migration potential). it was 58.5 ± 4.3 µm penetration of *S. aureus* into dermal layer of the skin model (Figure 4.8).

In models that were subjected to infection with *S. aureus* for 24h and treated by silver nitrate, isothiazoline and hydrogen peroxide. Tissue sections showed brown colour immunopostive *S. aureus* cells was mainly in the center, while in the periphery no such brown coloration was observed (immunonegative) due to bacterial migration. However, the penetration of *S. aureus* into the depth and its migration towards the edges decreases with biocides treatment, rendering the middle brown thicker bacterial biofilm and the peripheral parts moderately stained with the characteristic brown color (Figure 4.8).

When the 3D skin models were treated with manuka honey, the tissues showed less destruction and immunopositivity in the centre of skin tissue Nevertheless, the immunopositivity was less towards the margins due to the relatively lower density of *S. aureus* organisms towards the edges (Figure 4. 8).
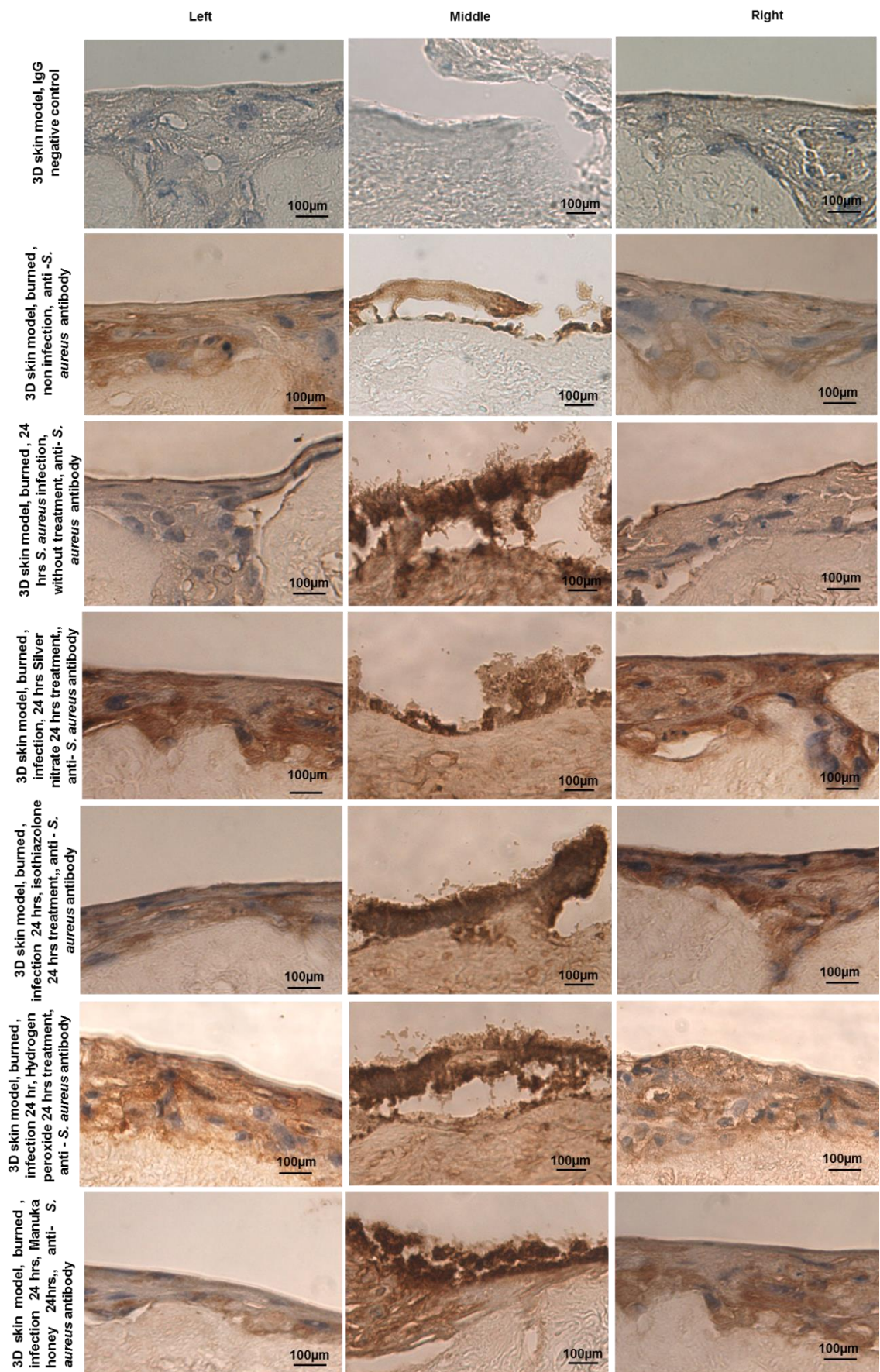
Figure 4.8: Anti *S. aureus* antibody marker, 3D skin models *S. aureus* infection showing biofilm bacteria migration and depth on burned of skin. *S. aureus* antibody marker was compared between burned infected and non-infected controls, burned infected biocidal. These were treated by silver nitrate, isothiazolone, hydrogen peroxide and manuka honey burned skin models for 24 hours). Scale bar=100µm

144

4.3.6- Mammalian cell death zone caused by infection with *S. aureus* alone and with treatment with biocidal agents

Infection of skin by bacteria can cause de-epithelialization of part of the infected skin. This was noticed as an area of absence of keratinocytes in the epidermal layer. The area was described as a cell death zone and was measured in millimetres (Figure 4.9). Unfortunately, the biocides used in the treatment of skin infections also caused cell death.

The death zone associated with a burn was taken as the injured uninfected control; was 4 ± 0.17mm. When the burn was treated with alginate, no significant change in death zone was observed 4.1 ± 0.62 mm, (P = 0.9039), (Figure 4.8). Infection with *S. aureus* caused a death zone that was significantly more than the control (P= 0.0153) (Figure 4.9). Treatment with silver nitrate further increased the zone of death significantly compared with that caused by *S. aureus* infection alone (P= 0.0428) (Figure 4.9).

Similar results were found with 2- Methyl -4- isothiazoline -3- one and hydrogen peroxide, where an increase in the mammalian cell death zone (8.89 ± 0.39 mm) caused originally by the infection (7.2 ±0.52 mm). The further increase in skin death zone by 2- Methyl -4- isothiazoline -3- one (7.2 ±0.52 mm) and hydrogen peroxide (11.3 ±0.75 mm) was significant compared to that caused by *S. aureus* infection alone (9.1 ±0.47 mm) (P values were 0.0428 and 0.0488 respectively) (Figure 4.9). Contrary to the other three biocides, Manuka honey decreased (5.51 ±0.49 mm) rather than increased the death zone caused by *S. aureus* infection (7.2 ±0.82 mm), although this was not significant (P= 0.6554). Accordingly, Manuka honey was considered to be one of the most effective biocides to *S. aureus* with the least toxicity to the mammalian cells in the 3D skin model (Figure 4.9).
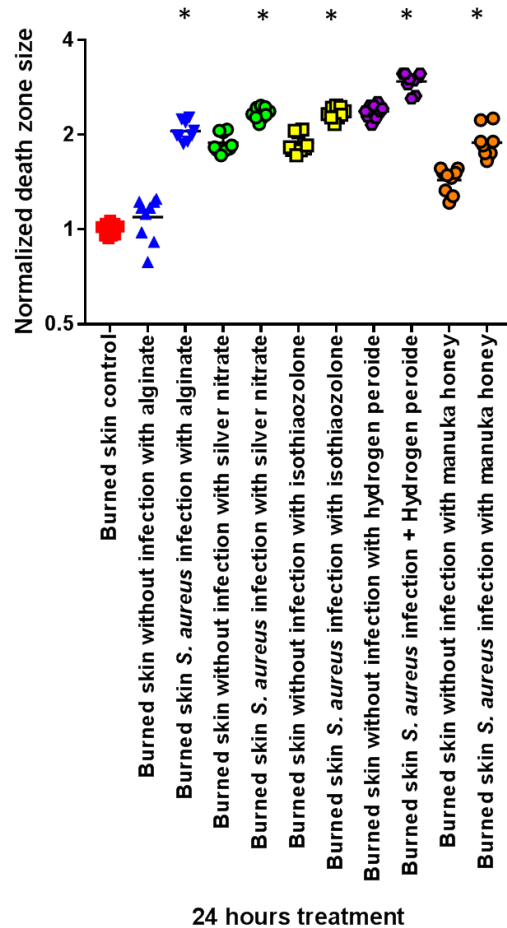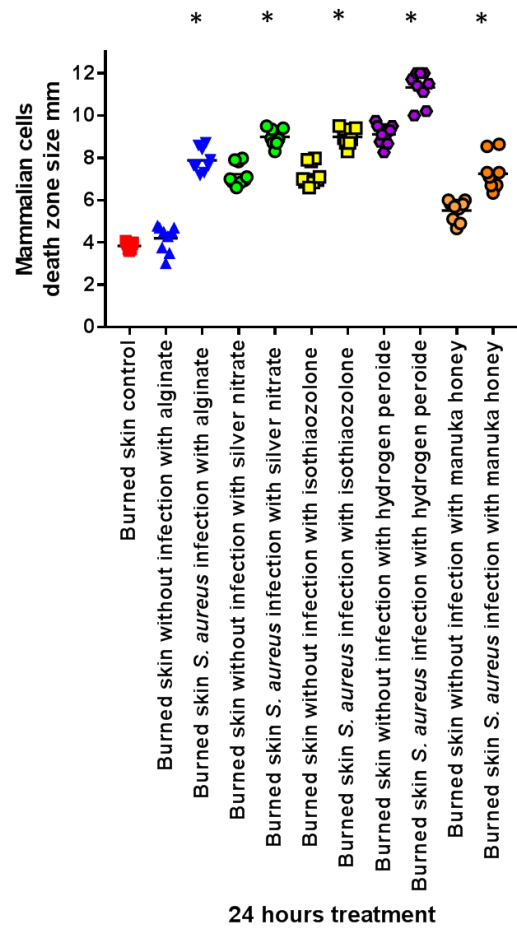
Figure 4.9: Effect of biocidal agents on infected 3D skin models showing death zone of skin following biocidal treatment. The biocidal effect was compared between burned infected controls and burned *S. aureus* infected biocidal treated samples. * = P<0.05.

4.3.7-The effects of biocides on skin models infected with *S. aureus* using immunohistochemical staining.

In order to observe the effect on cellular phenotype of biocides on normal, burned and/or *S. aureus* infected skin models, immunohistochemical staining targeting various antibody markers were used (Caspase 3, Collagen IV, CPK, CK 10 and CK14).

4.3.7.1- Caspase 3

Caspase-3 activity is also needed for producing pluripotent stem cells from human fibroblasts (Li *et al.* 2010), for differentiating stem cells (Fujita et al. 2008; Janzen et al. 2008), and for distinguishing neural stem cells (Fernando *et al.* 2005). Additionally, caspase-3 is required for driving DNA double-strand breaks; it can cleave and it can activate kinases from the constitutive viewpoint, (Fernando *et al.* 2002; Fernando *et al.* 2005; Kanuka *et al.* 2005) or terminate proteins required for maintaining pluripotency and for self-renewal (Fujita *et al.* 2008; Janzen *et al.* 2008).

Astoundingly, caspase-3 activity can also make its contribution to the survival of cells. Early findings propose that this displayed that neuroprotection granted by a preconditioning ischemic event are not found when caspase inhibitors are present (McLaughlin *et al.* 2003). More lately, Khalil *et al.* (2012) proved genetically the moderate caspase-3 activation findings in the cleavage of RasGAP, which, in turn, raises Akt activation and enhances cell survival. Thus, mice that lack caspase-3 need Akt activation. According to Khalil *et al.* (2012), its outspread increased cell death and tissue damage responding to the modest levels of cell stress. These counter-intuitive findings reveal the different activities of the executioner caspases; they highlight the fact that they cannot simply be regarded apoptotic proteases.

4.3.7.1.1- Caspase 3, burned skin models without biocides

In normal control skin model, the majority of HaCat cells which formed the epidermal layers were immunonegative for caspase 3 (blue stained) suggesting they were viable. Some of the uppermost cells were immunopositive for caspase 3 indicating presence of apoptosis (brown stained), denoting the normal formation of the stratum cornum layer (Figure 4. 10). In the burned skin model, some of the epidermal cells were lost in the centre of the skin model where the burn was applied, while cells at the periphery were preserved and immunonegative, suggesting these cells were viable.

The skin model which was burnt and infected with *S. aureus* demonstrated a large number of immunopositive cells in the centre, whereas the peripheral cells were immunonegative suggesting viable cells. While this central apoptotic layer was detached from the underlying dermis in the skin model devoid of alginate, whilst it remained attached to the dermis in the alginate model, suggesting the alginate supported preservation of the architecture of the skin model (Figure 4.10).
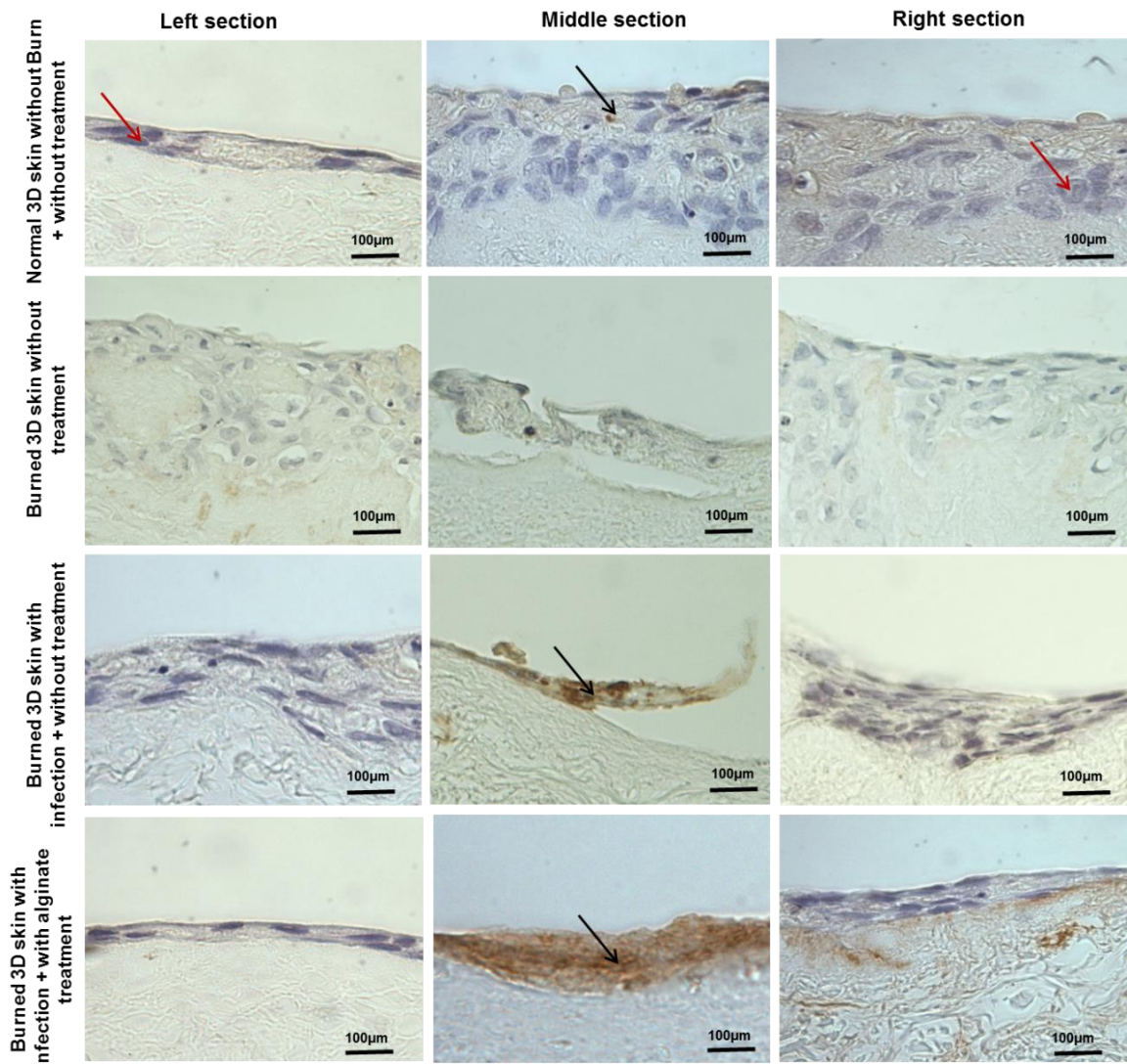
Figure 4.10 : Effect of biocidal agents on 3D skin tissue burned with and without *S. aureus* infection, Caspase 3 antibody marker compared between non burned and non infection, controls , burned non infection without biocidal treated, burned infected without biocidal treated andburned infected with alginate treated.The three pictures shown in each row as left, middle and right tissue. Black arrow is immunopostive; red arrow is immunonpositive with no visible cell nuclei. Scale bar = 100µm.

4.3.7.1.2- Caspase 3, burned skin models with biocides

Burned skin models were treated with biocides and stained with caspase 3 to demonstrate the effect of the biocide by comparing it to the untreated burned skin model (Figure 4.11). This was then repeated within the burned skin model with infection with and without biocidal agents.

4.3.7.1.2.1 Silver nitrate

The burned skin model treated with silver nitrate showed immunopositive epidermal cells in the middle of the tissue and viable cells at the periphery.

149

In burned and *S. aureus* infected skin model treated with silver nitrate, the immunopostive cells were only in the middle sections (Figure 4.11).

4.3.7.1.2.2- Isothiazolone

When the burned skin model was treated with isothiazolone, there was a middle epidermal area stained brown (caspase 3 immunopositive). In the case of burn and *S. aureus* infection together, the middle epidermal layers demonstrated apoptotic immunopositive cells which also showed detachment from the underlying dermis (Figure 4.11).
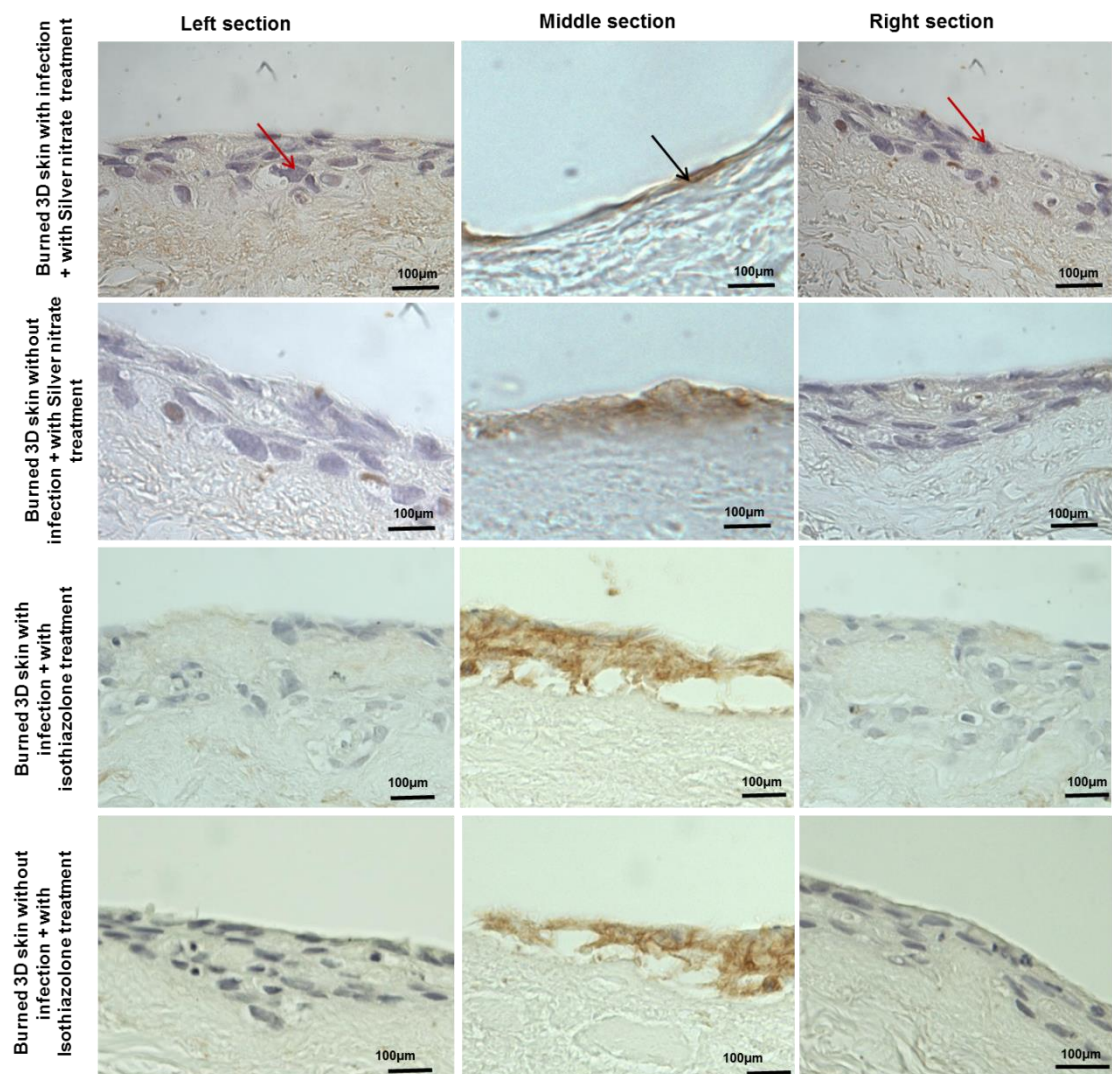
Figure 4.11: Effect of biocidal agents on 3D skin tissue burned with and without *S. aureus* infection, Caspase 3 antibody marker compared between burned,with or without bacterial infection, and silver nitrate treatment; burned,with or without bacterial infection, and Isothazoline treatment.The three pictures shown in each row as left, middle and right tissue. Black arrow is immunopostive; red arrow is immunonnegative with no visible cell nuclei. Scale bar = 100μm.

4.3.7.1.2.3- Hydrogen peroxide

Burned skin models treated with hydrogen peroxide showed a thinning epidermal layer which was partially detached from the underlying dermis in the middle of the section with multiple immunopostive cells. In the peripheral parts the epidermis was normal with immunonegative cells, suggesting viable cells (no apoptosis). The burned *S. aureus* infected skin model treated with hydrogen peroxide showed thinning of epidermis, immunopostive staining for caspase 3 and increased detachment apoptosis cells from the dermis in the middle while the peripheral tissue were almost normal (Figure 4.12).

4.3.7.1.2.4- Manuka Honey

Burned skin model treated with honey showed almost normal thickness epidermal layers, but with partial detachment from the underlying dermis and immunopostive multiple apoptotic cells in the middle tissue. In the *S. aureus* infected burnt skin model treated with Manuka honey, the same observations were noticed but with more detachment from the underlying dermis, whilst morphology was maintained in the periphery (Figure 4.12).

	Left section	Middle section	Right section
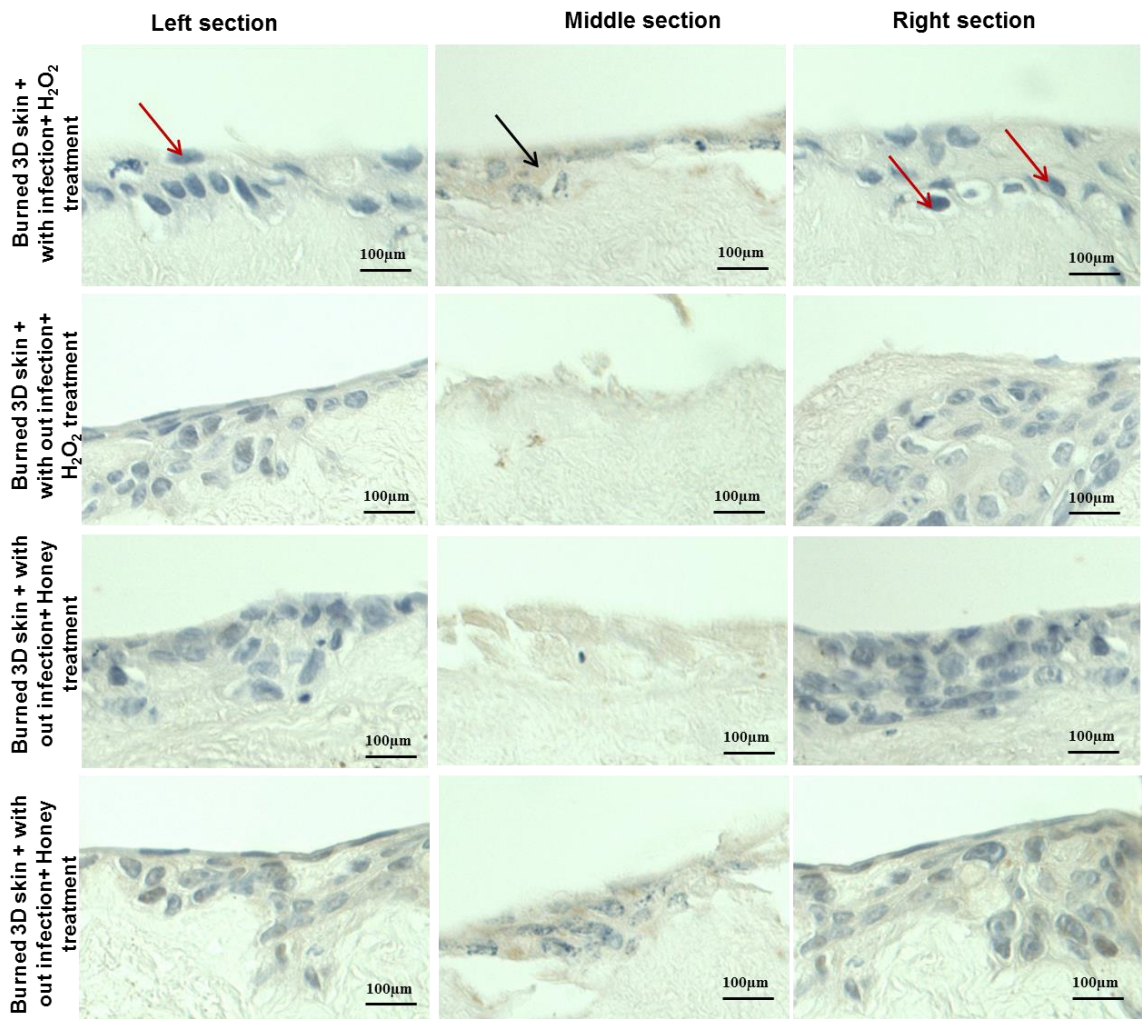
Figure 4.12: Effect of biocidal agents on 3D skin tissue burned with and without *S. aureus* infection, Caspase 3 antibody marker compared between burned,with or without bacterial infection, and H_2O_2 treatment; burned,with or without bacterial infection, and Clinical Manuka honey treatment.The three pictures shown in each row as left, middle and right tissue. Black arrow is immunopostive; red arrow is immunonnegative with no visible cell nuclei. Scale bar = 100µm.

4.3.7.2 - Collagen type IV antibody

4.3.7.2.1- Collagen type IV antibody, burned skin models with and without biocides:

The 3D skin models were investigated with immunohistochemistry for Collagen type IV, to delinate the collagen fibres normally present within the skin architecture. Normal sections showed partial expression of collagen fibres, which were immunopositive between the dermal and epidermal layers (Figure 4.13). In burned skin models, the immunopositive collagen fibres appeared at the basement membrane of the epidermis. This was attributed to the direct effect of burns on collagen. The interrupted collagen layer appeared in the

152

middle of the tissue while it extended continuously at the periphery (Figure 4.13). In burned skin models infected with *S. aureus*, immunopositivity for collagen type IV was decreased particularly within the middle of the skin model where the burn and infection were applied, while still preserved at the peripheries, which characteristically showed thin immunopositive layers at the top of the epidermis. These thin layers of collagen type IV were similar in appearance to collagen fibres in the stratum cornum layer of normal skin. When the skin model was subjected to a burn and infection, and treated with alginate control, preservation of type IV collagen immunopostivity was seen compared to the non-alginate treated model even in the middle, which suggests alginate improves the preservation of the structure of the skin model (Figure 4.13).

	Left section	Middle section	Right section
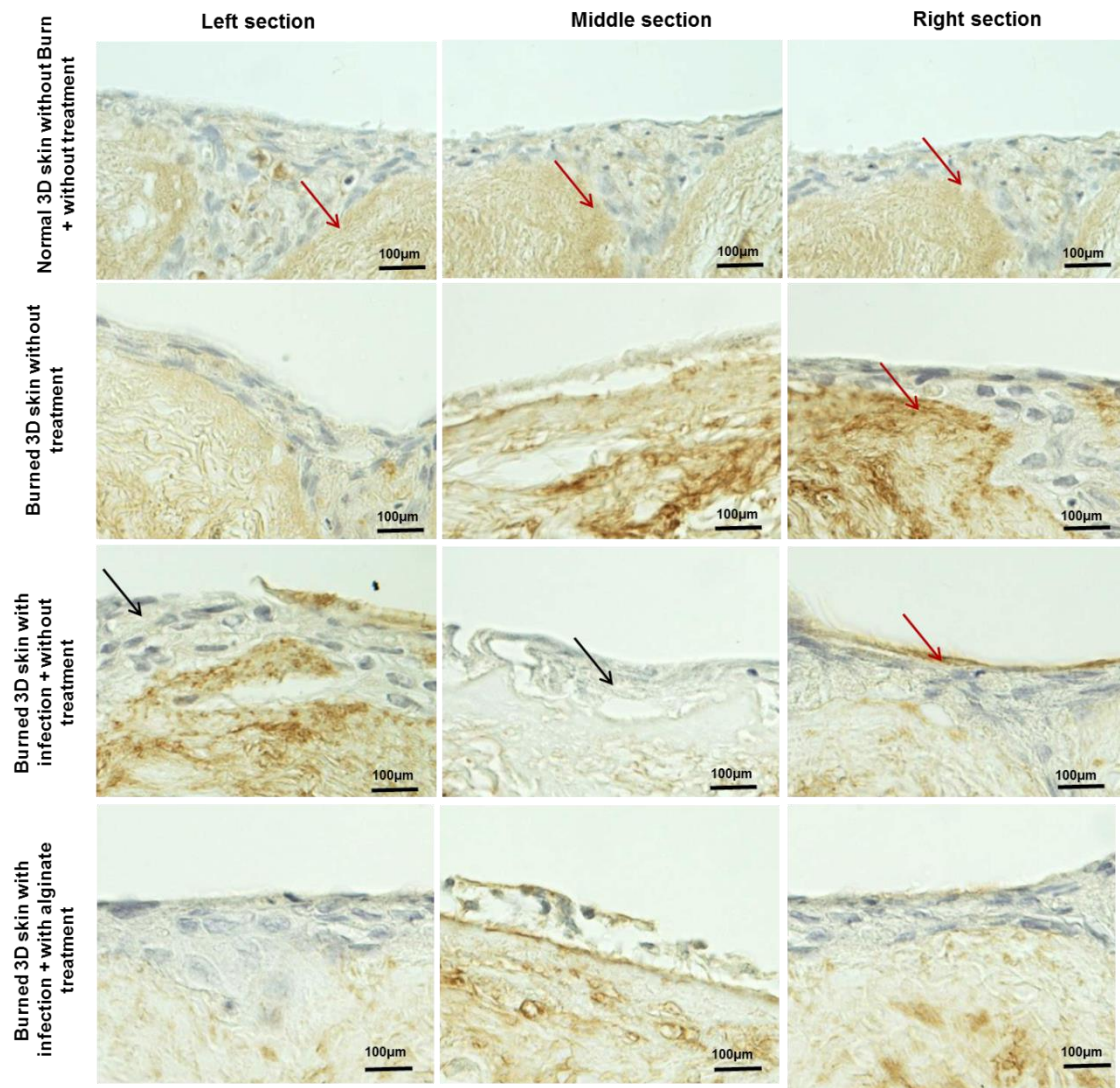
Figure 4.13: Effect of biocidal agents on 3D skin tissue burned with and without *S. aureus* infection, Collagen type IV antibody marker compared between non burned and non infection, controls, burned non infection without biocidal treated, burned infected without biocidal treated and burned infected with alginate treated. The three pictures shown in each row as left, middle and right tissue. Black arrow is immunonegative with no visible cell nuclei; red arrow is immunonpositive. Scale bar = 100µm.

4.3.7.3 - Pancytokeratin (PCK)

4.3.7.3.1-Pancytokeratin, burned skin models without biocides:

The 3D skin models were immunohistochemically stained with Pancytokeratin, the main marker of keratinocytes. Normal skin models, stained with PCK were control slides to compare with burned skin models, burned infected with *S. aureus* infected skin models and lastly with burned and *S. aureus* infected skin models with alginate (Figure 4.14).

In the normal skin model, all the HaCat cells formed epidermal layers with immunopositivity for PCK. The epidermal layer was thick and well formed (Figure 4.14). In the burned skin model, the epidermal layer was shown to be thinner and of darker brown colour, especially in the centre where the effect of burn was maximal. In the peripheries the epidermal layer retained its normal thickness. The skin model that was subjected to both burn and infection showed thinning of the epidermal layer, but with faint and interrupted brownish staining, suggesting increased destruction of this layer. In the alginate model, the epidermis was very thin but compacted and strongly immunopositive (Figure 4.14).
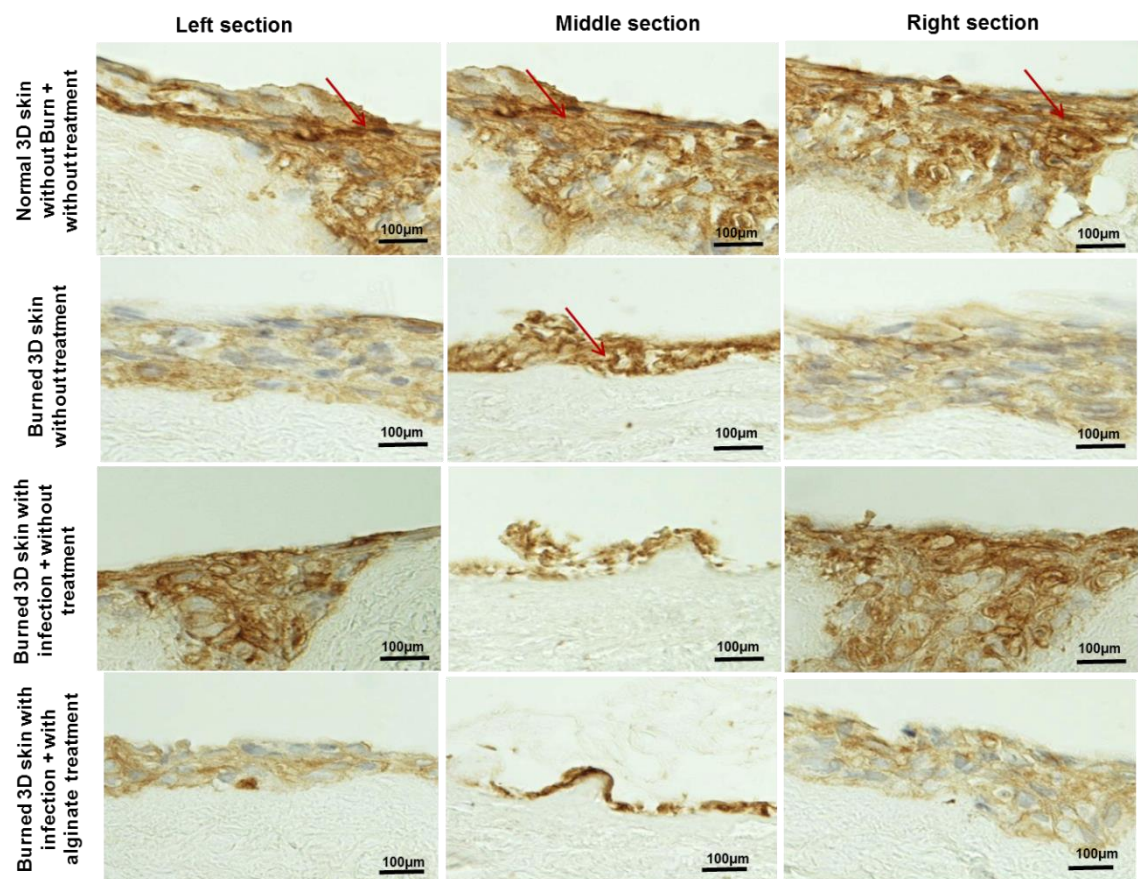
Figure 4.14: Effect of biocidal agents on 3D skin tissue burned with and without *S. aureus* infection, Pancytokeratin antibody marker compared between non burned and non infection, controls, burned non infection without biocidal treated, burned infected without biocidal treated and burned infected with alginate treated.The three pictures shown in each row as left, middle and right tissue. Black arrow is immunonpostive with no visable cell nuclei; red arrow is immunonpositive.Scale bar = 100µm.

4.3.7.4- Cytokeratin 10

4.3.7.4.1-Cytokeratin 10, burned skin models without biocides

The 3D skin models were immunohistochemically stained with cytokeratin 10 which is one of the markers of keratinocytes that are normally expressed in the terminally differentiated keratinocytes among the basal and suprabasal layers of the epidermis. Normal skin models, stained with Cytokeratin 10 were used as positive control slides to be compared with skin models subjected to burns and *S. aureus* infections and both of them were compared to treated models (Figure 4.15).

In normal skin models, the epidermal cells showed immunopostive staining for cytokeratin 10, mainly within basal cells of the epidermis. In burned skin models, there was faint immnuopostive expression of the marker in the middle of the tissue model at the main site of the burn compared to the periphery in both right and left parts of the model. In the infected burned skin, there was no immnuopositive staining for cytokeratin 10, denoting decreased differentiation of basal keratinocytes. This observation was similar in the infected burned alginate model (Figure 4.15).
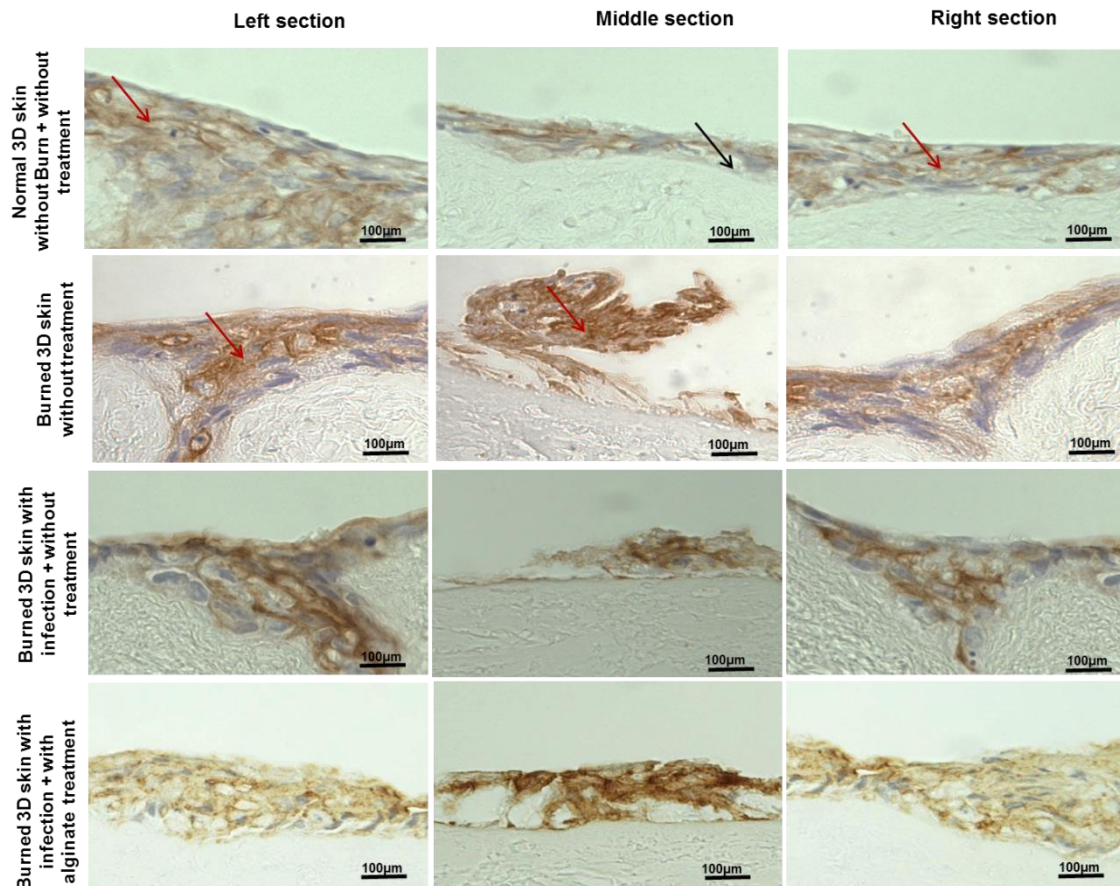
Figure 4.15: Effect of biocidal agents on 3D skin tissue burned with and without *S. aureus* infection, Cytokeratin 10 antibody marker compared between non burned and non infection, controls, burned non infection without biocidal treated, burned infected without biocidal treated and burned infected with alginate treated. The three pictures shown in each row as left, middle and right tissue. Black arrow is immunonegative with no visible cell nuclei; red arrow is immunonpositive. Scale bar = 100µm.

4.3.7.5- Cytokeratin 14

4.3.7.5.1- Cytokeratin 14, burned skin models with and without biocides

The 3D skin models were immunohistochemically stained with cytokeratin 14, a marker for keratinocytes mostly expressed in the basal levels forming the stratum basale. In uninfected untreated skin models, the epidermal cells showed immunopositive expression of cytokeratin 14, mainly at the basal cells of the epidermis, but extending through the whole epidermis to the apical layer (Figure 4.16). In burned skin models, the brown stained cells (expressing cytokeratin 14) formed a thinner layer which was partially detached from the

underlying dermis in the middle of the model where the burn effect was maximal. In the peripheral parts of the model, immunopostive cells formed a thin layer at the basal parts of the epidermis (Figure 4.16). In burned, *S. aureus* infected models and in models treated with alginate, the stained cell layer was thin and there was complete detachment of it from the underlying dermis. This was immunonegative in the middle part of the tissue model only. The peripheral parts showed immunopostive cells in the basal epidermal layer (Figure 4.16).
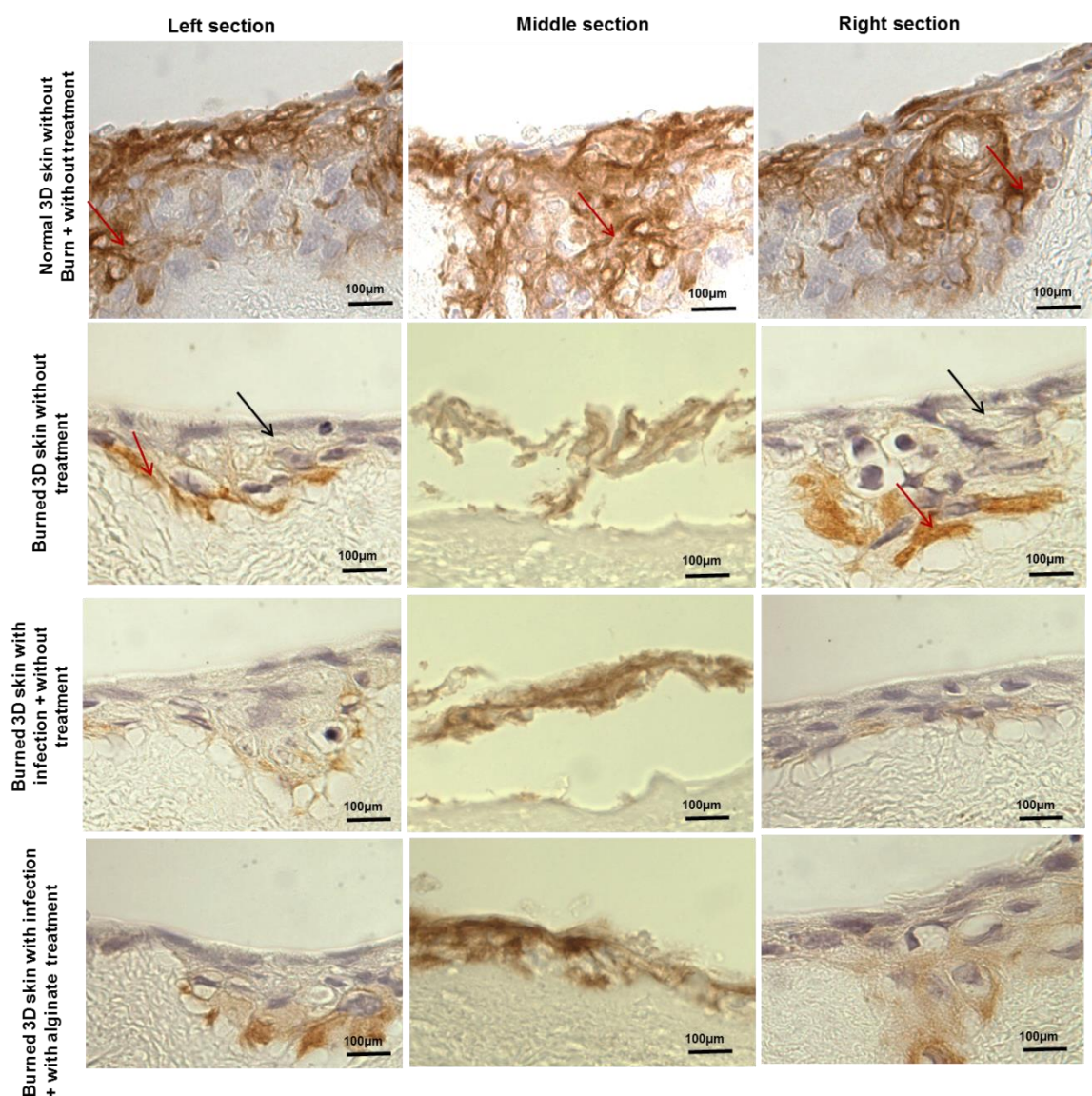
Figure 4.16: Effect of biocidal agents on 3D skin tissue burned with and without *S. aureus* infection, Cytokeratin 14 antibody marker compared between non burned and non infection, controls , burned non infection without biocidal treated, burned infected without biocidal treated and burned infected with alginate treated.The three pictures shown in each row as left, middle and right tissue. Black arrow is immunnegative with no visible cell nuclei; red arrow is immunonpositive. Scale bar = 100µm.

4.3.8 - Phenotypic assessment of 3D skin models following infection and treatment with biocidal agents.

Burned infected skin models infected with *S. aureus* and treated with silver nitrate, isothiazolone and hydrogen peroxide immunopositivity for collagen type IV showed an interrupted collagen layer, especially in the middle of the model. Whilst the collagen type IV layer at the interface between the dermis and epidermis was partially immunonegative (Figure 4.17 & Figure 4.18). PCK, cytokeratin 10 and cytokeratin 14 were immunopositive within the epidermal layer as evidenced by the small immunopostive area expressed in the middle compared to the normal thick immunopostive layer in the peripheral regions (Pancytokeratin: Figure 4.19 & Figure 4.20; CK 10: Figure 4.21 & Figure 4.22 ;CK 14: Figure 4.23 & Figure 4.24). In the presence of *S. aureus* infection, collagen type IV protein was disrupted and faint (Collagen type IV: Figure 4.12 & Figure 4.13). PCK, cytokeratin 10, cytokeratin 14 immunopositivity was decreased in the epidermal layer and detachment of the cell layer of the tissue was seen. A thin layer of immunopositive staining and detachment from the underlying dermis with no upper epidermal cells as well in the middle model was observed. In the periphery cells were maintained normal distribution immunopositive stain (PCK: Figure 4.15 & Figure 4.16; Cytokeratin10 Figure 4.18 & Figure 4.19; Cytokeratin 14: Figure 4.21 & Figure 5. 22). Whilst burned *S. aureus* infected skin model treated with honey, displayed improved maintenance of immunopositive staining for collagen type IV, PCK, cytokeratin 10, cytokeratin 14 within the centre of the model, with only minimal decrease in staining seen (Collagen type IV: Figure 4.13; PCK: Figure 4.16; Cytokeratin 10 Figure 4.19; Cytokeratin 14 Figure 4.22).
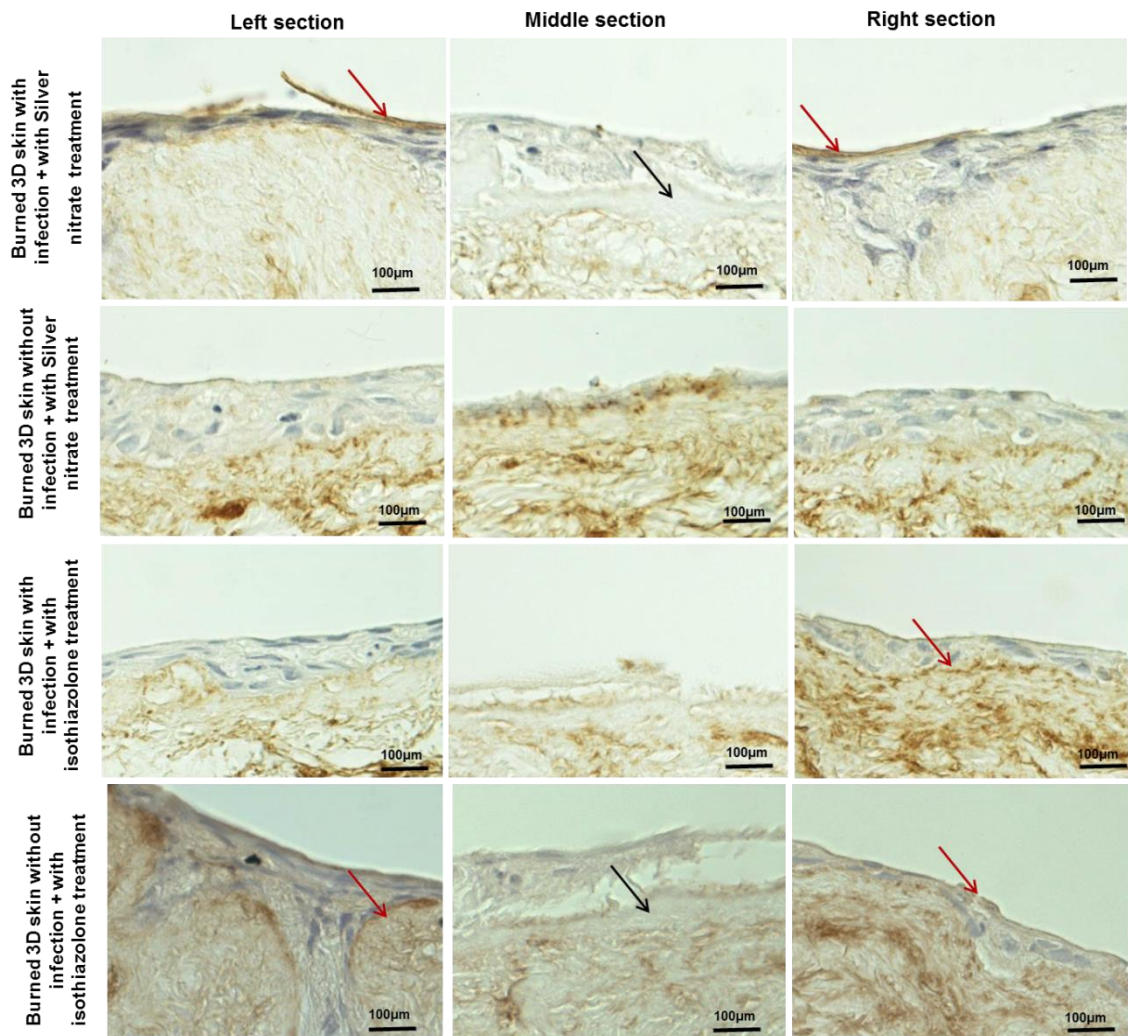
Figure 4.17: Effect of biocidal agents on 3D skin tissue burned with and without *S. aureus* infection, Caspase 3 antibody marker compared between burned, with or without bacterial infection, and silver nitrate treatment; burned, with or without bacterial infection, and Isothiazolone treatment. The three pictures shown in each row as left, middle and right tissue. Black arrow is immunonegative with no visible cell nuclei; red arrow is immunonpositive. Scale bar = 100µm.
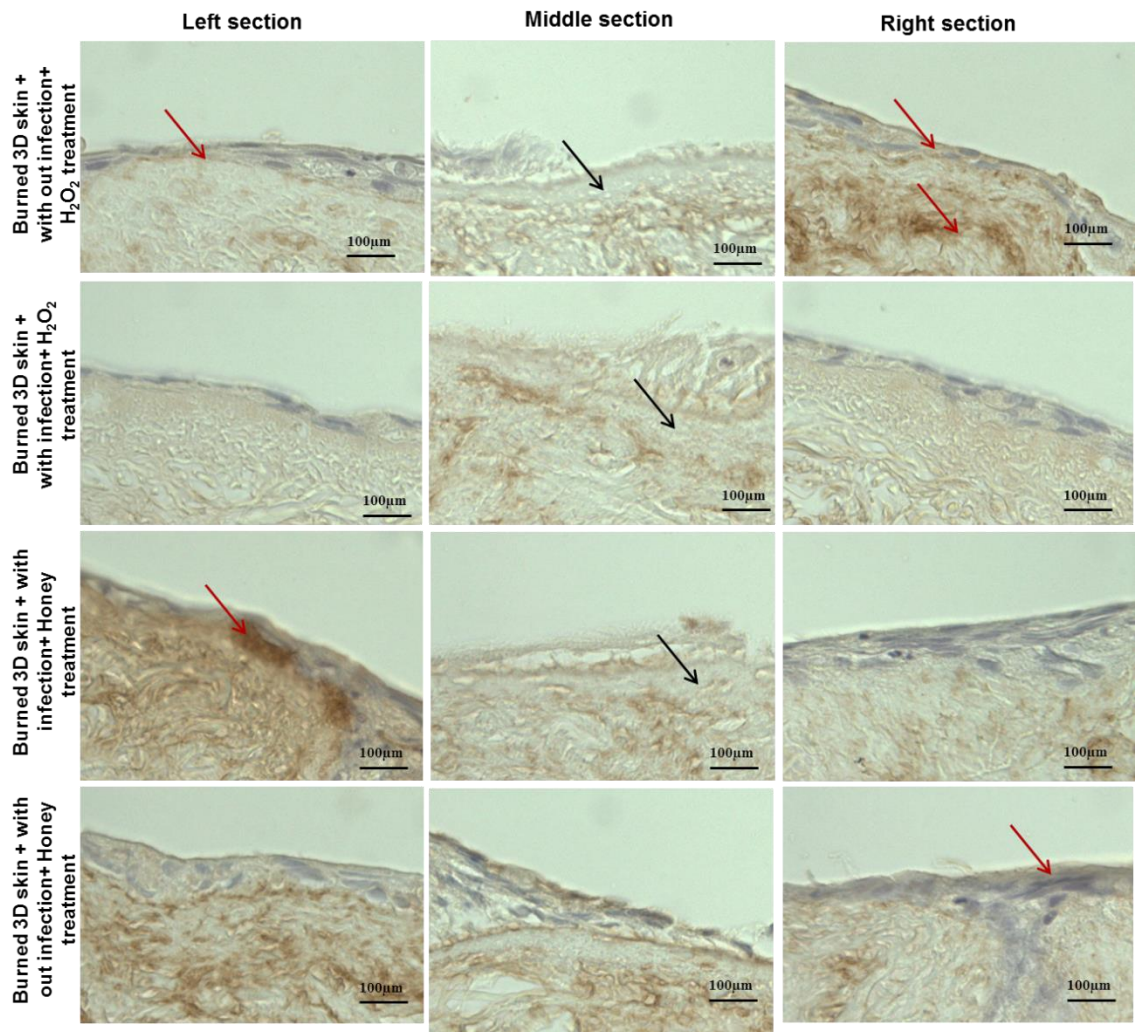
Figure 4.18: Effect of biocidal agents on 3D skin tissue burned with and without *S. aureus* infection, Collagen type IV antibody marker compared between burned, with or without bacterial infection, and H_2O_2 treatment; burned, with or without bacterial infection, and Clinical Manuka honey treatment. The three pictures shown in each row as left, middle and right tissue. Black arrow is immunonegative with no visible cell nuclei; red arrow is immunonpositive. Scale bar = 100μm.
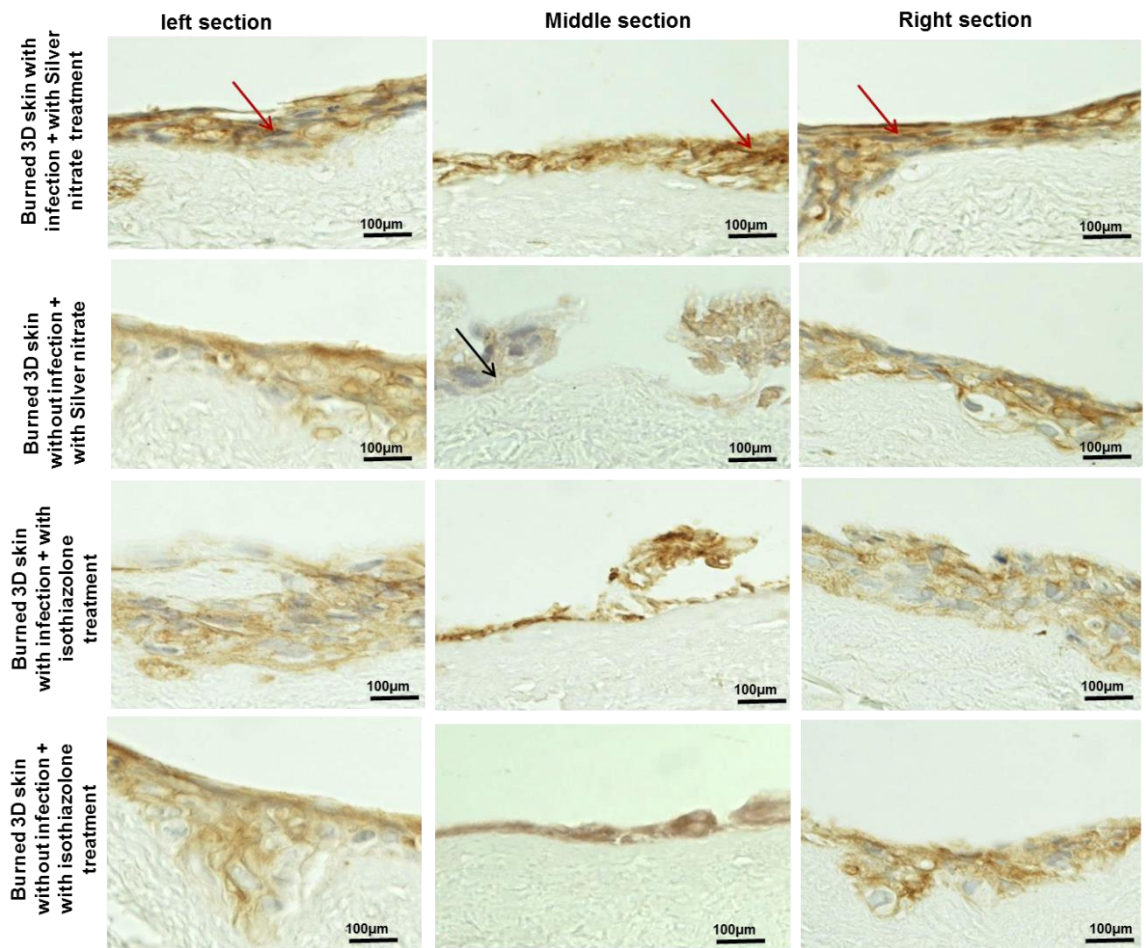
Figure 4.19: Effect of biocidal agents on 3D skin tissue burned with and without *S. aureus* infection, Pancytokeratin antibody marker compared between burned, with or without bacterial infection, and silver nitrate treatment; burned with or without bacterial infection, and Isothiazolone treatment. The three pictures shown in each row as left, middle and right tissue. Black arrow is immunonegative with no visible cell nuclei; red arrow is immunonpositive. Scale bar = 100µm.
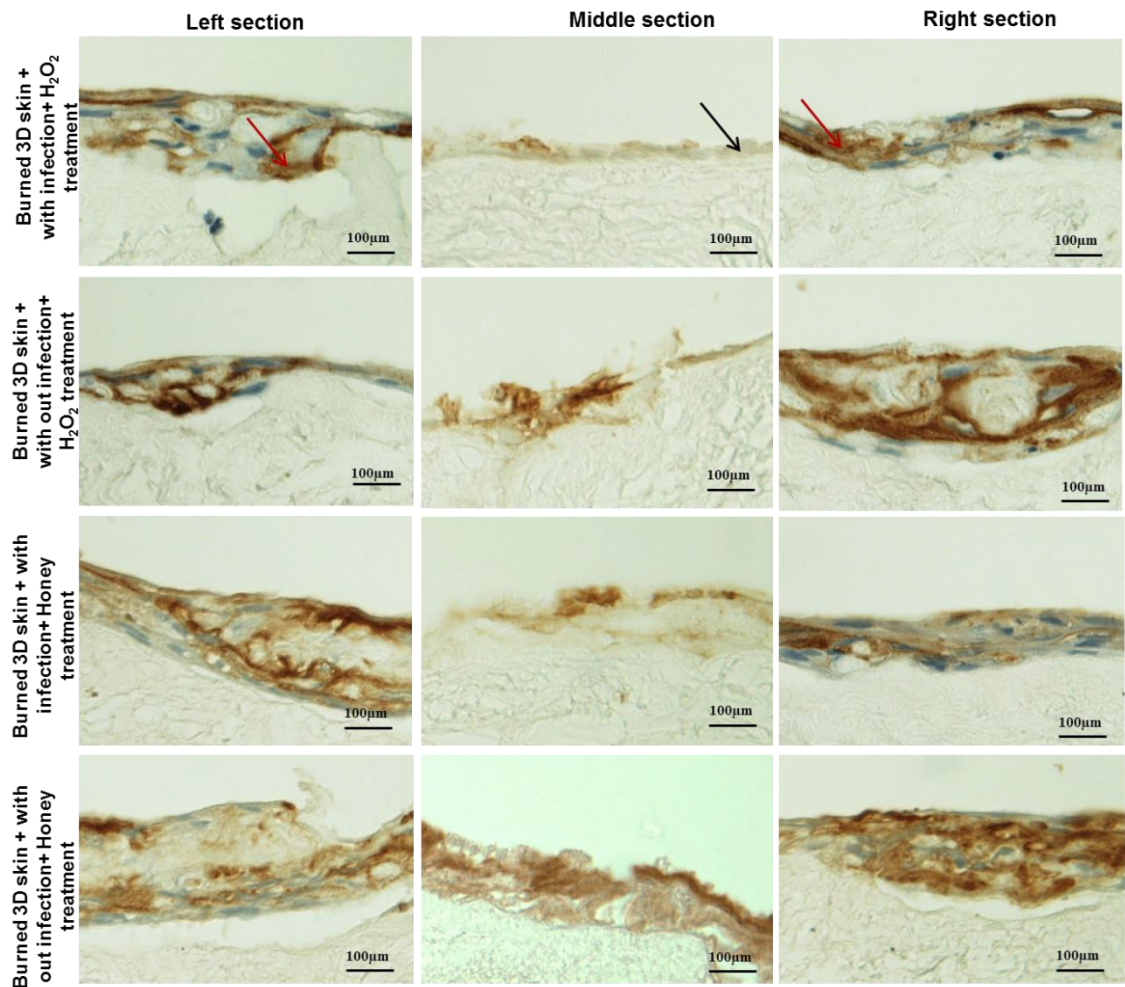
Figure 4.20: Effect of biocidal agents on 3D skin tissue burned with and without *S. aureus* infection, Pancytokeratin antibody marker compared between burned, with or without bacterial infection, and H₂O₂ treatment; burned with or without bacterial infection, and clinical manuka honey treatment. The three pictures shown in each row as left, middle and right tissue. Black arrow is immunopostive with no visible cell nuclei; red arrow is immunonpositive. Scale bar = 100μm.
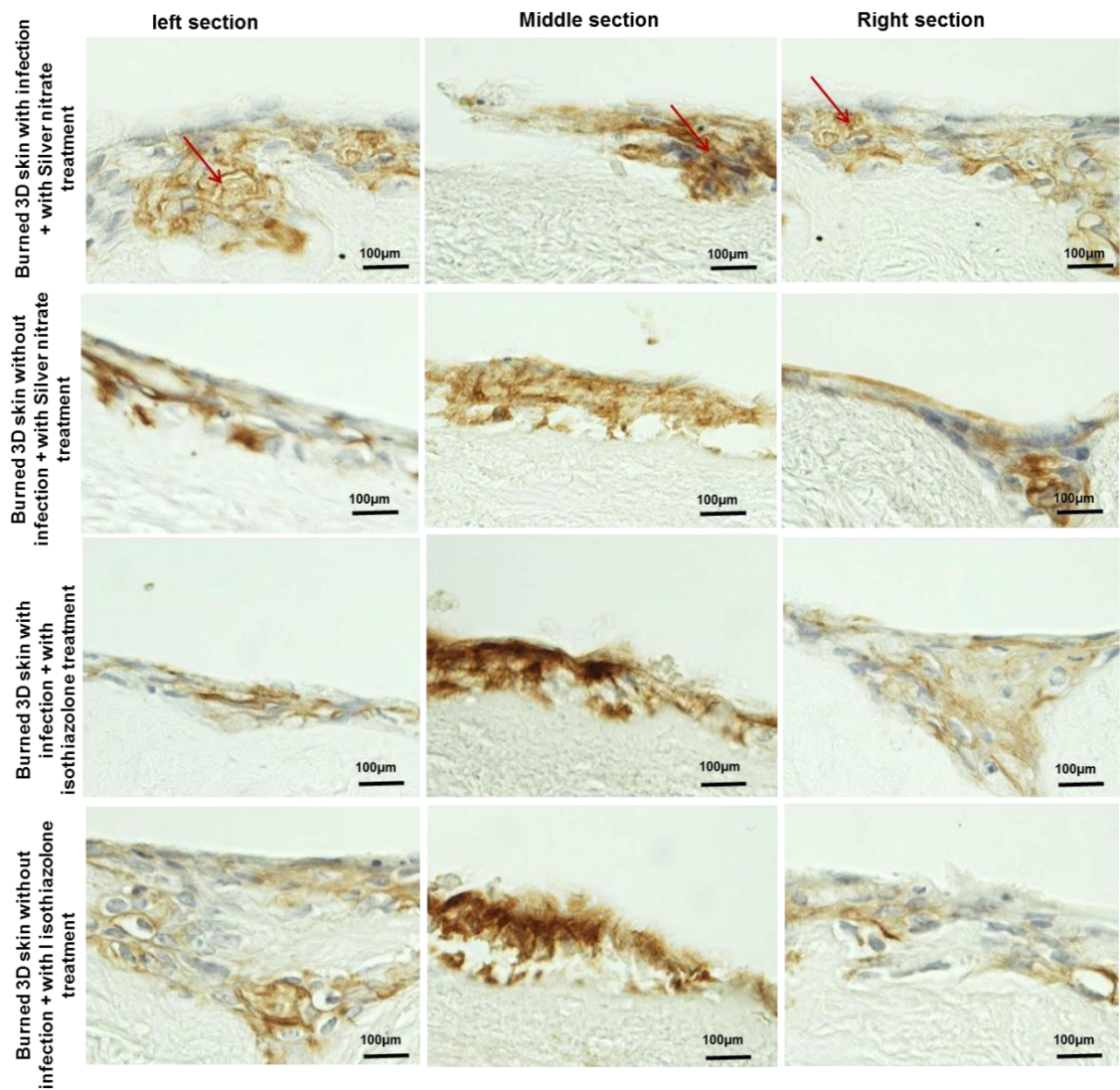
Figure 4.21: Effect of biocidal agents on 3D skin tissue burned with and without *S. aureus* infection, Cytokeratin 10 antibody marker compared between burned with or without bacterial infection, and silver nitrate treatment; burned, with or without bacterial infection, and Isothazoline treatment. The three pictures shown in each row as left, middle and right tissue. Black arrow is immunonegative with no visible cell nuclei; red arrow is immunonpositive. Scale bar = 100µm.
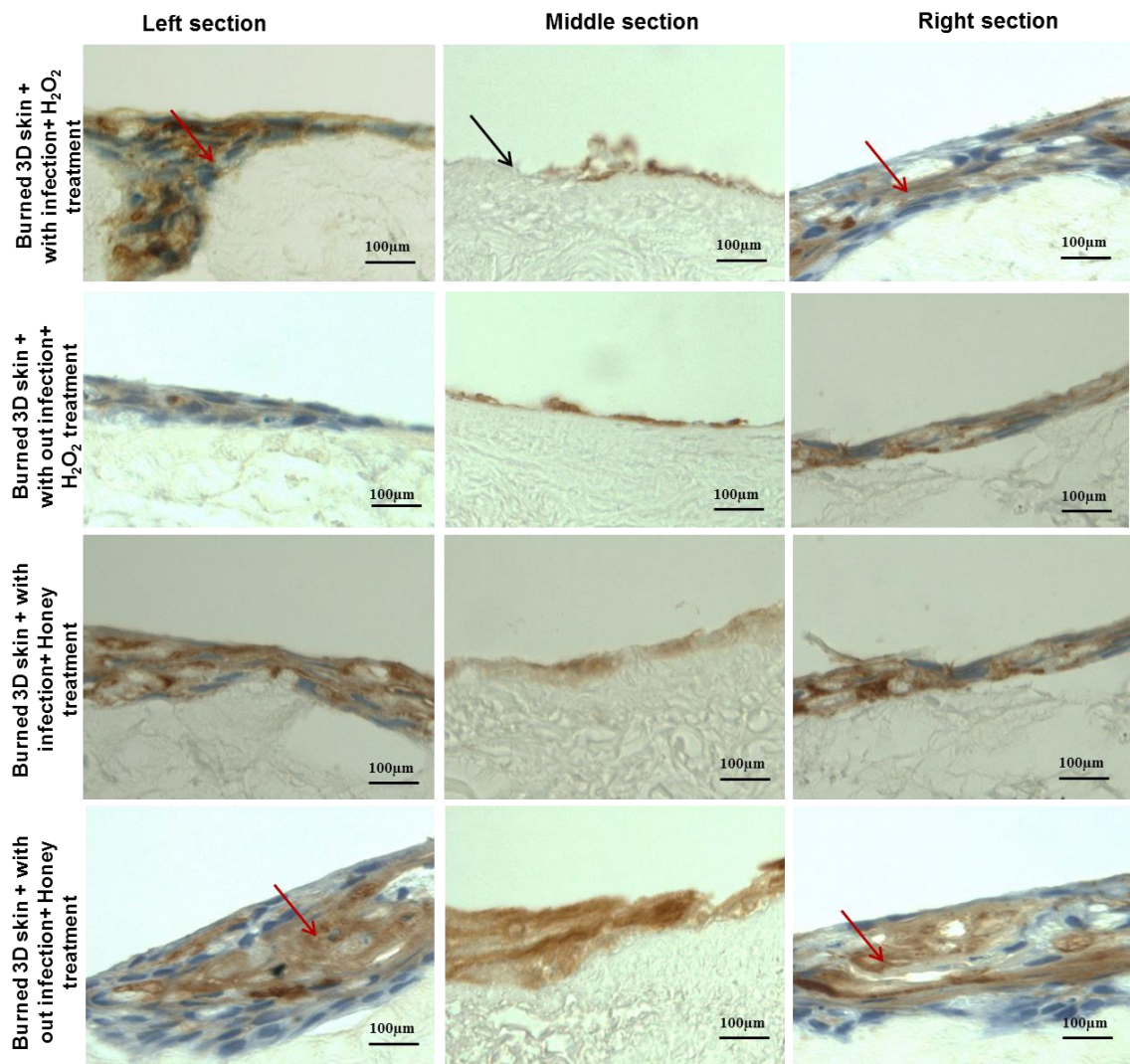
Figure 4.22: Effect of biocidal agents on 3D skin tissue burned with and without *S. aureus* infection, Cytokeratin 10 antibody marker compared between burned with or without bacterial infection, and H$_2$O$_2$ treatment; burned, with or without bacterial infection, and clinical manuka honey treatment. The three pictures were shown in each row as left, middle and right tissue. Black arrow is immunonegative with no visible cell nuclei; red arrow is immunonpositive. Scale bar = 100µm.
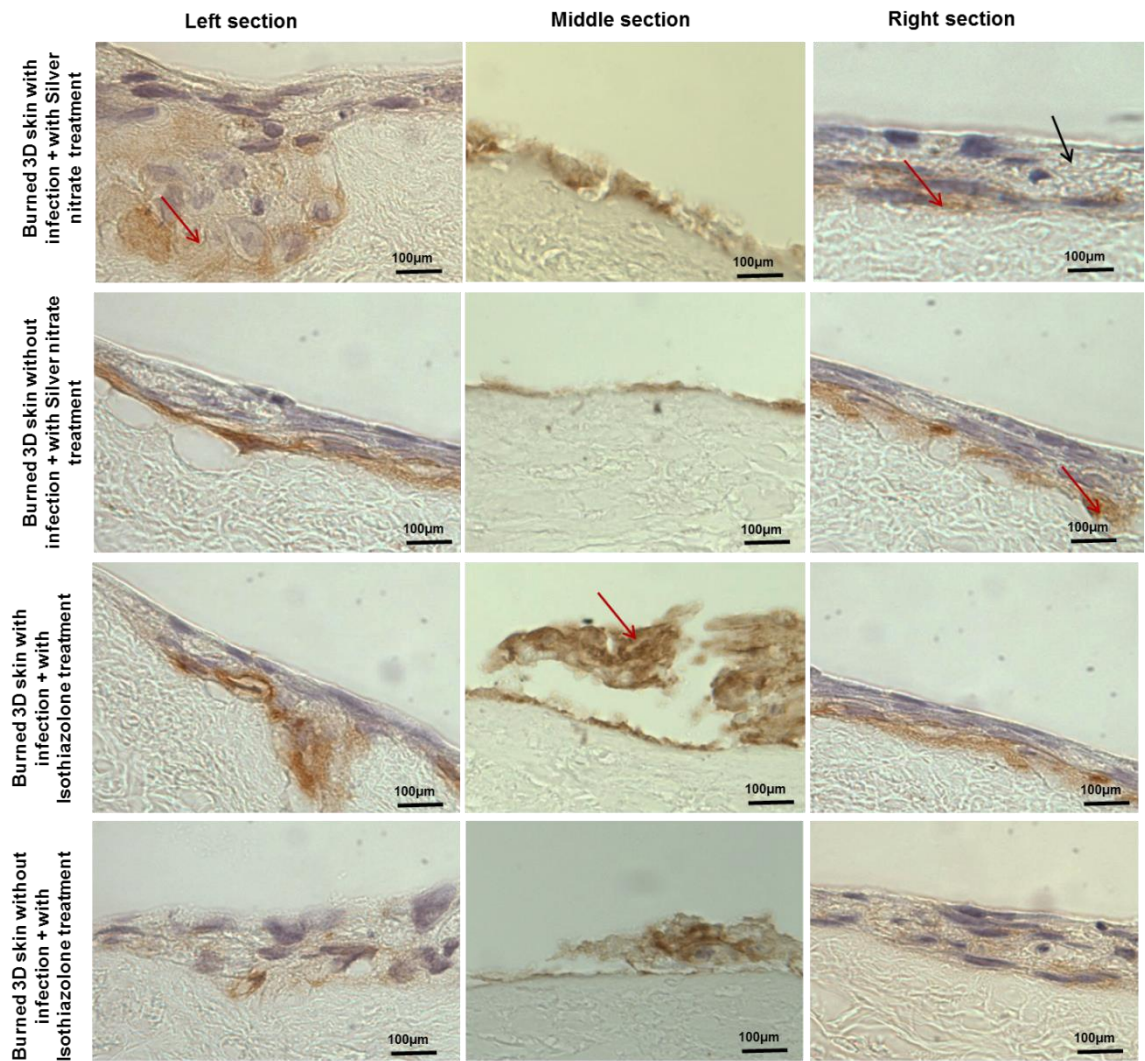
Figure 4.23: Effect of biocidal agents on 3D skin tissue burned with and without *S. aureus* infection, Cytokeratin 14 antibody marker compared between burned with or without bacterial infection, and silver nitrate treatment; burned, with or without bacterial infection, and isothiazolone treatment. The three pictures shown in each row as left, middle and right tissue. Black arrow is immunonegative with no visible cell nuclei; red arrow is immunonpositive. Scale bar = 100µm.
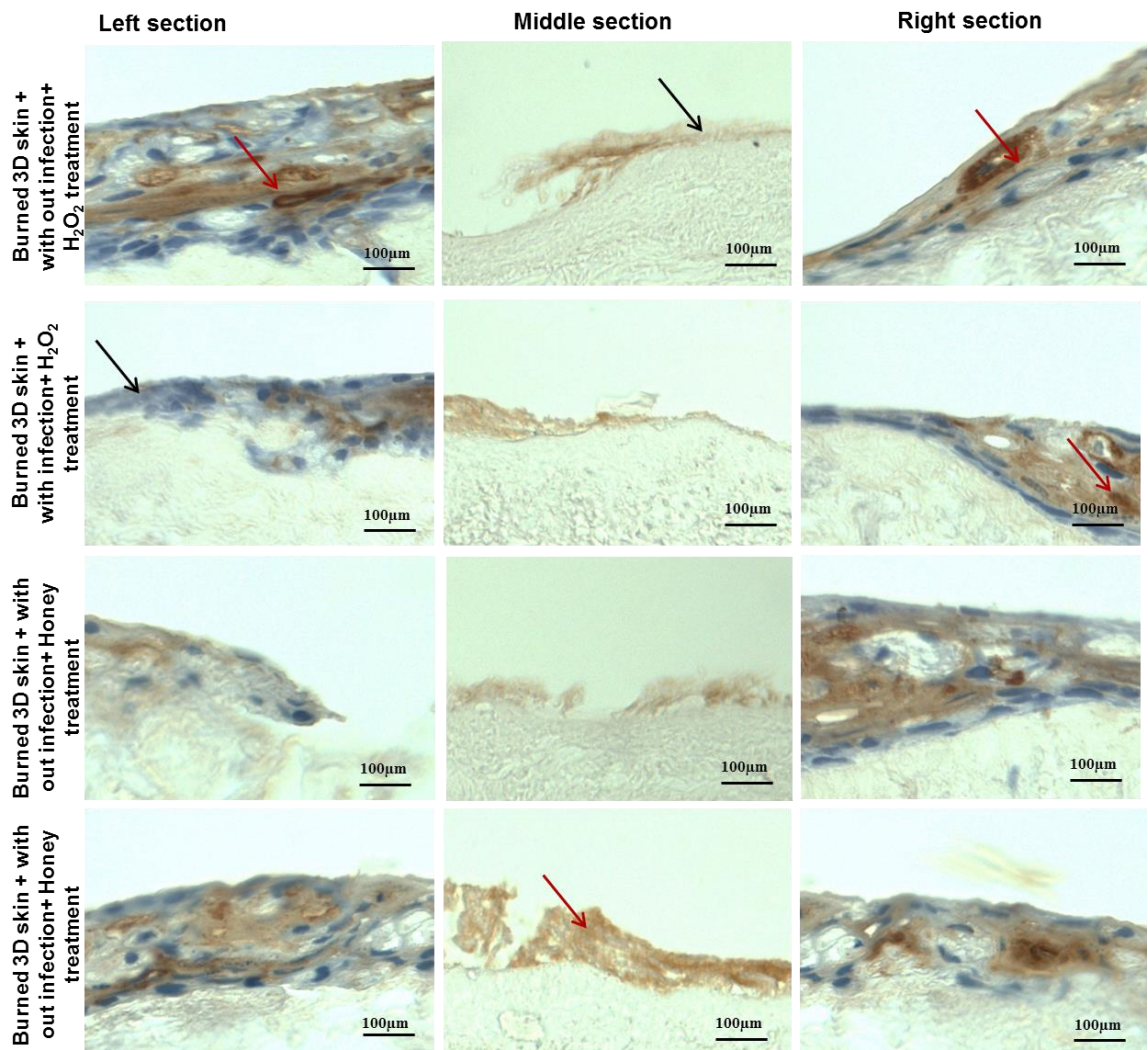
Figure 4.24: Effect of biocidal agents on 3D skin tissue burned with and without *S. aureus* infection, Cytokeratin 14 antibody marker compared between burned, with or without bacterial infection, and H_2O_2 treatment; burned, with or without bacterial infection, and Clinical Manuka honey treatment. The three pictures shown in each row as left, middle and right tissue. Black arrow is immunonegative with no visible cell nuclei; red arrow is immunonpositive. Scale bar = 100µm.

4.4- Discussion

Wounds to the skin are a significant cause of pain and discomfort for patients, as well as increasing healthcare cost, and presenting a problem globally because of frequent failure to heal in the short term. Bacterial biofilms are extremely important in wounds infections, with biofilm bacteria demonstrating strong resistance to defensive mechanisms to protect the host, including antibiotic agents. This means that it is challenging to eliminate biofilm infections in chronic wounds using standard interventions with antibiotics (Costerton 1999; Donlan & Casterton 2002; Parsek & Singh 2003).

Prior to the application of new or less conventional therapies for burn wounds, there is a need to explore the way in which biofilms form using 3D skin models. Based on this need, the current study utilised an *in vitro* human skin model in order to imitate the formation in biofilms in infected burns in humans. The study also sought to uncover simple markers capable of identifying the occurrence of bacterial biofilm infections for burn wounds through the model developed. Furthermore, the effects of infection and potential treatments on the native skin cells in addition to effects on bacterial cells were investigated.

Applying a 3D human skin model enhances the ability to imitate infections in human skin (Mertz *et al*. 1987; Svedman *et al*. 1989; Sullivan *et al*. 2001; Davis *et al*. 2008). However, there are limitations to this approach, such as the high cost involved. Greater knowledge about the ways in which skin-bacterial interaction will lead to new approaches being developed for the promotion of healing in burns wounds. One limitation of the current *in vitro* human skin model for biofilm bacteria and chronic wounds is that immunological functions are not included in the modelled wound beds, meaning that immune activity cannot be

explored through this model. However, the model shows its suitability for testing the effectiveness of biocidal treatments.

The model used here was utilised to investigate ways of reducing bacterial load within wound infections, and further work might include this technique in developing anti-bacterial treatments which target specific situations, as well as improving diagnoses.

S. aureus was applied in the *in vitro* skin model based on its suitability to be used to model and assess the growth of a simple bacterial biofilm. *S. aureus* in a biofilm was formed effectively by application of 1×10^6 CFU/ml. The bacterial biofilm matured successfully in the burned skin models. Bacterial biofilms showed formation following culturing for 24 hours, with multiple clusters of bacteria embedded in a biofilm matrix. *S. aureus* infections were localised wounds and did not appear to cause infection across the full 3D skin model. The model demonstrated that at 24 hours post introduction of the infection, *S. aureus* was localised mainly to the skin's upper layers.

The results are in agreement with those of Shepherd (2009 and 2011), who reported a bacterial inoculum rate for *S. aureus* of 1×10^7cfu/ml at 24 hours (Shepherd *et al.* 2009, Shepherd *et al.* 2011). In addition, when modelling infection in pigs, Mertz *et al.*, (1987) reported an optimal inoculum rate of 1×10^8 cfu/mL for *P. aeruginosa* or *S. aureus* which gave the best bacteria-wound bed adherence, and the current work followed this concentration rate (Mertz *et al.* 1987).

Based on the modelling performed, silver nitrate, isothiazolone, hydrogen peroxide, and medical grade manuka honey showed potential efficacy for topical application to human skin as biocide agent. Due to the extensive application of biocides within medicine, the possible impacts of these were

examined *in vitro* using HaCaT human keratinocyte and fibroblast cell culture. The minimum inhibitory concentration (MIC) of biocides determined from planktonic cultures (Chapter 2) was applied on mammalian monocultures. The viability of cells was reduced for both keratinocyte and fibroblast cultures. However, HaCaT cells were more resistant to biocides than fibroblasts.

In agreement with this, Drewa *et al.* (2008) reported use of low concentrations of $AgNO_3$ 3 & 15 x 10^{-4} M/dm^3 in comparison to concentrations applied when treating patient's 31 x 10^{-4} M/dm^3, as toxicity was found at these smaller concentrations, triggering apoptosis in human keratinocytes and fibroblasts. Thus, Nitrate ions from silver nitrate may have a negative impact on the healing of such wounds (Drewa *et al.* 2008).

In addition, research established by Hidalgo *et al.* (1998) found that concentrations of $AgNO_3$ which were 100–700 less concentrated than applied clinically remained successful in inhibiting certain microbes discussed previously. However, at these concentrations' cytotoxicity was still seen in cultured fibroblasts. Therefore, silver nitrate can be applied in dilutions of 100 times greater than 0.5% of normal dilution, based on the inhibition of bacteria at this level and the lowered cytotoxicity healing of wounds would be supported (Hidalgo *et al.* 1998).

In comparison, when normal human keratinocytes (NHK) were exposed to 5-chloro-2-methyl-4-isothiazolin- 3-one (CMI) and 2-methyl-4-isothiazolin-3-one (MI) CMI/MI at low concentrations (0.001- 0.05%), pathways of apoptosis are activated within healthy NHK cell (Ettorre *et al.* 2003). Rivalland *et al.* (1994) reported that CMI/MI had cytotoxic effects within single-layer cultures of human cells and fibroblasts, which was demonstrated using MTT (3-(4, 5

dimethylthiazol- 2-yl)-2, 5-diphenyltetrazolium bromide) test (Rivalland *et al.* 1994).

Loo *et al.,* (2012) reported that keratinocytes showed high resistance to hydrogen peroxide (250 and 500 µM) toxicity, but fibroblasts were observed to be less viable, which agrees with the sensitivity shown in the current study. Moreover, a scratch-wound model which is based on cultured keratinocytes demonstrated promotion by hydrogen peroxide of the mobility of keratinocytes using lower concentrations; approximately 500 µM did not affect cell viability. The keratinocytes which received the lower concentration of hydrogen peroxide treatment showed better activation of epidermal growth factor as well as phosphorylation of Extracellular signal-regulated protein kinases ERK1/2, and this accounts for their greater migratory potential (Loo *et al.* 2012).

Martinotti *et al.,* (2017), reported the impact of honey on scratch models of wound healing *in vitro* using fibroblasts and keratinocytes. Honey has the capability to enhance the closing of wounds through both cell migration and proliferation on fibroblasts and keratinocytes (Martinotti *et al.* 2017). However, this study was applied to monolayers in a scratch injury model, in contrast; the current study utilized a 3D skin model and burn injury.

Within the current study an alginate derived from seaweed was utilised to enable biocidal agent application, and an alginate model was used as the treatment control in order to assess bacterial growth in those groupings. After incubating the samples for 24 hours, it was found that the bacterial agents remained viable, with no effect from the alginate.

The present study investigated the impact of biocidal agents on biofilm skin tissue infection, by introducing a range of agents, including Silver nitrate, 2-Methyle -4- isothiazolin -3-one, hydrogen peroxide and manuka honey to a

bacterially infected skin wound modelled *in vitro*. Silver nitrate, 2- Methyle -4-isothiazolin-3-one and Hydrogen peroxide each significantly reduced the modelled *S. aureus* infection, but Manuka honey showed the most significant effect. Silver nitrate at the planktonic MIC of 62 .5 µg/ml decreased in the skin by 1.4 $\log_{10}$ reduction CFU/ml. Sütterlin (2012) reported that the silver nitrate MIC were ≤ 32 mg/l and MBC > 512 mg/l for *S. aureus* in planktonic and that it was found to have a predominantly bacteriostatic impact on *S. aureus* (Sütterlin *et al.* 2012). This could be part of the explanation why the performance of silver nitrate has been high MIC both *in vitro* as planktonic and *in vivo* on leg skin ulcer patients with *S. aureus* infection (Carter *et al.* 2010; Yin *et al.* 1999; Tredget 1998).

The study measured a lower efficacy of hydrogen peroxide against biofilm bacteria following 24 hours in comparison with planktonic forms. The finding is in line with results showing that use of hydrogen peroxide causes a reduction of 1.4 $\log_{10}$ to eliminate biofilms when low concentrations are used. Tote *et al.* (2009) found an active effect of hydrogen peroxide against viable mass and biofilm matrix in a microplate-based assay, using resazurin as viability indicator, with approximately similar results for biofilms of *P. aeruginosa* and *S. aureus.*

In this study, the treatment of biofilms with medical grade manuka honey resulted in a significant reduction of viable *S. aureus* cells, with significant decrease in biofilm formation when culturing strains with manuka honey. Our results are in agreement with those of Henriques *et al.* (2010), who reported that *S. aureus* NCTC 10017 showed susceptibility to comparatively low concentrations of manuka honey, even though these bacteria can tolerate significant osmolarity changes. Based on cell viability assessments manuka

honey was found to act bactericidally and $\log_2$ decreases occurred at approximately 427 minutes (Henriques *et al.* 2010).

Reversibility testing showed no viable microbes were recovered following 8 hours, confirming the non-reversible nature of the inhibitory effect (Henriques *et al.* 2010).

Histological analyses conducted on skin sections in the current study showed that for the infected sections high numbers of *S. aureus* bacteria remained, particularly in the skin's surface layers. Counts of viable microbes within tissue sections after treating the membrane were also conducted, and bacterial viability counts demonstrated that fewer bacteria remained for samples receiving treatments with biocidal agents.

Following this, an investigation of 3D skin cells within the cell death zone of the burn and bacterial migration and penetration considered whether microbes binding to 3D skin tissue were dying or had simply become immobile and membrane bound. While bacterial numbers were significantly decreased, a proportion of bacteria in the tissues still showed viable bacteria after the biocidal agents had been applied.

This study investigated the impacts of silver nitrate, isothiazolone, hydrogen peroxide and manuka honey on a 3D skin model with a mature infection of bacteria. *S. aureus* showed significant adherence to the control skin tissue model sections, meaning that larger numbers of the microbe successfully penetrated the dermal layer to become isolated from the skin tissue. Moreover, Manuka honey was observed to reduce the area where skin cells died following infection with *S. aureus,* in contrast the other biocidal agents resulted in increased toxcitiy. Manuka honey also decreased the extent to which *S. aureus* penetrated the dermis.

The impact of the biocidal agents on cell phenotypes for burned and/or *S. aureus* infected skin models, immunohistochemical staining was applied which targeted a range of antibody markers (Caspase 3, Collagen type IV, CPK, CK 10 and CK14). The findings indicate immunopositive stain of phenotypes of epidermal cells. In the infected 3D skin models, *S. aureus* was quantified following 24h of treatment of membranes, the middle of tissue showed strong immunopositivity for *S. aureus* demonstrating the capability of *S. aureus* to form biofilm. Although the biofilm occupied mainly the centre of the tissue, there was extensive immunopositive staining throughout the model. In addition, infection of skin by bacteria caused de-epithelialization of part of the infected 3D skin models. A similar result was seen by Shepherd *et al.* (2009), who reported that *S. aureus* caused detachment of the epidermal layer within a 3D skin tissue after 24 hours.

However, biofilms which form during skin infections are not normally a single bacterial species; there are usually several strains of bacteria. Thus, the proposed model should involve other common pathogenic bacteria in order to construct a complex biofilm containing multiple bacterial species, and thus this model could be applied to other infective agents to build a more complex biofilm.

4.5- Conclusion

This study utilised decellularised human dermis (created from Euroskin), HaCaT cells and human dermal fibroblasts to create a 3D skin model which was burned and infected with *S. aureus*, demonstrating migration and penetration of bacteria through the skin model. Infection resulted in increased toxicity to the mammalian cells which were further increased by some of the biocidal agents

investigated. Manuka Honey was found to be the most effective agent investigated with greatest effects on reducing numbers of bacteria, migration and penetration of bacteria and reducing mammalian cell death zones. This model system has shown promise to increase the understanding of the effect of antimicrobial biocides on bacteria and skin models. However alternative infective agents should be investigated to develop more complex biofilms.

Chapter 5

Effect of biocides on *in vitro* burned 3D skin models infected with *Pseudomonas aeruginosa* biofilm

5.1- Introduction

5.1.1- *P. aeruginosa* in wound infections

P. aeruginosa is one of the most common organisms involved in wound infection (Akinjogunla *et al*. 2009; Fazli *et al*. 2009; Cooper *et al*. 2009) (Agnihotri *et al.* 2004). It is characteristically common in wound infections of patients with underlying health problems like diabetes (Ako-Nai *et al*. 2006) or burns (Bielecki *et al*. 2008). Often responsible for opportunistic, chronic, severe wound infections of large ulcers and resistant wound infection with biofilm formation (Malic *et al*. 2009; James *et al*. 2008). As discussed previously the biofilm protects against phagocytosis and other host immune mechanisms (Leid *et al*. 2002). The chronicity of pseudomonas wound infection was evidenced by the findings of James and colleagues in 2008, when *P. aeruginosa* was isolated from 35% of chronic wound infections in the 50 cases investigated. Malic *et al.,* (2009), also found that *P. aeruginosa* was the predominant species in the multispecies chronic wound infections they investigated. Kirketerp-Møller *et al*, 2008, demonstrated that *P. aeruginosa* was particularly embedded deep in the niche of chronically infected wounds (Kirketerp-Moller *et al*. 2008).

Furthermore, *P. aeruginosa* has been shown to be the most common isolated organism in cases of bacteraemia secondary to wound infection (92% of isolated organisms, according to the 2006 England and Wales survey). With an increase in prevalence and mortality of *P. aeruginosa* infection observed, particularly in patients with long term hospital stays (Lautenbach *et al*. 2006, Onguru *et al*. 2008).

5.1.2- Pathogenicity and virulence factors of *P. aeruginosa* infections

P. aeruginosa is a severe pathogenic organism affecting plants, animals and humans. This organism contains different types of colonies at different isolation sites, and can also cause many devastating infections due to the strong adherence through pili and high production of virulence factors, including phospholipase C, elastase, exotoxin A, and the exoenzyme S. Other virulence factors include lipopolysaccharides, proteases, and alginate (Lyczak *et al.* 2000; Van Delden *et al.* 1998; Jia *et al.* 2006). Some of these virulence factors act at a local level, while others diffuse away from bacteria and act at remote sites. Their effects result in bypassing the host immunity which can lead to tissue damage, multiple organ failure, systemic infections and even death if the infection is not cleared (Tang *et al.* 1996). The elastase enzyme produced by *P. aeruginosa* induces breakdown of host elastin and other extracellular matrix proteins of the in connective tissue such as laminin and collagen type III and IV (Yanagihara *et al.* 2003). This enzyme impairs the arterial structure thus causing a hemorrhage and the degradation of the surfactant proteins A (SP-A) and D (SP-D) (Komori *et al.* 2001), these destructive enzymes aid invasion (Malloy *et al.* 2005). *P aeruginosa* is known to secrete the exotoxin S that induces the apoptosis pathway in the host organism (Jia *et al.* 2006).

The effect of the toxins of this pathogen on the host tissues in combination with the host immune response can lead to septic shock, morbidity and mortality due to the *P. aeruginosa* infection. The host immunity is further initiated by the smooth LPS O-antigen (Hancock *et al.* 1983; Vitkauskiene *et al.* 2005). The microbial LPS can be recognised by the host Lipopolysaccharide Binding Protein (LBP).

This LBP-LPS complex can react with the CD14 and TLR4 which is expressed on the macrophages and the keratinocytes (Wright *et al*. 1990). The macrophages internalise the pathogen by phagocytosis, forming the phagolysosome and generates nitric oxide (NO) (Inohara *et al*. 1999).

The keratinocyte cells detect the bacterial presence in the cell cytoplasm with the help of the Nucleotide-binding oligomerisation domain (NOD) proteins. The NOD2 proteins recognise the muramyl dipeptide, from the peptidoglycan layer and then activate the receptor-interacting protein kinase (RICK). The activation of RICK then switches on the NF-α signalling pathway, thereby causing the cells to generate and release cytokines, chemokines and antimicrobial peptides (AMPs) (Frantz *et al.* 2001).

The later infectious stage and the host immune responses to the bacteria can be coordinated by the activated T helper (Th1) cells that secrete the IFNγ and CD40 ligands, which is an important event in the host immune response. The macrophages containing *P. aeruginosa* are prevented from activation. The pathogenic organisms also impair the host immune defense by blocking the INF (Andonova *et al.* 2013).

5.1.3- Aim of this study

This study applied the 3D skin model developed in chapters 3 and 4 to evaluate its use as a model for *P. aeruginosa* infection as an important infective agent in infected burns. This model was then applied to investigate the effects of different types of anti-microbial strategies which generate active free radicals to reduce *P. aeruginosa* load in infected wounds. Furthermore this model was utilized to investigate the effect of *P. aeruginosa* infection and biocidal agents on native skin cells.

5.2- Materials and Methods

5.2.1- Experimental design

In this chapter, the effects of biocides were investigated on *P. aeruginosa* infected 3D skin models. TE skin models were cultured as described in chapter 4 but instead of infection by *S. aureus,* skin models were inoculated with *P. aeruginosa* at 1×10^6 at different time points (6, 12, 24 hours), with and without biocidal agent treatments as described in chapter 4. Tissues were formalin fixed, paraffin embedded, histologically stained and assayed by immunohistochemistry to determine cell morphology and viability. In addition, the infected skin models were homogenized and bacterial loads (in CFU/mg tissue) determined by the Miles and Misra technique (Miles *et al.* 1938). 3D skin models infected with *P. aeruginosa* were investigated to determine the degree of migration and penetration of the bacterial cells into the skin models. The migration and penetration rates of *P. aeruginosa* grown on 3D skin models were studied by observing the histological damage as a result of infection in 3D skin models. Generally, the depth of the tissue damage reflected the penetration potential of bacteria whereas the horizontal spread of damage towards the margins indicated the migration potential. Specific antibody markers of *P. aeruginosa* were used to estimate the penetration and migration rates of bacteria, in a more precise and objective manner. The use of specific bacterial antibody markers, for staining infected tissues, gives a more accurate estimation of migration and penetration as they indicate the extent of the bacterial spread itself rather than the tissue damage. Immunohistochemical stains targeting bacterial proteins (markers) were first applied to normal skin models and to burnt non-infected models as negative controls. They were then applied to burned skin models that were infected with *P. aeruginosa* bacteria for

24 hours. Finally, the immunohistochemical stains were applied to burned skin models which were infected with bacteria for 3, 6 and 24 hours followed by 24 hours of treatment with Manuka honey.

5.2.2- Wound Model

5.2.2.1- 3D skin model composites

The 3D skin models were prepared as described in Chapter 3 section (3.1.2), and incubated at 37°C in 5% CO_2 for 21days

5.2.2.2- 3D skin wound models and bacterial infection

Infection of the skin models was established as described in chapter 4 (4.2.2.2). All skin models were transferred to media without antibiotic supplements. Skin models were subjected to burns using a heated metal rod 4 mm in diameter and the epidermal 3D skin tissue surface was infected with $1X10^6$ *P. aeruginosa*. Following infection for 3,6 and 24 the effect of biocidal agents (silver nitrate, isothiazoline and hydrogen peroxide) on bacterial infection were investigated, they were dissolved in 1.2% alginate gel as described in chapter 2, and models treated for 24hrs (2.2.3.1), whilst Manuka honey was applied directly as described in Chapter 2 section (2.2.4). Following treatment with biocidal agents for 24hrs the models were bisected into two halves; each were assessed as follows: a) the first half was fixed in 10% v/v formalin for 24 hours. After that, it was processed to paraffin and 4µm sections mounted on slides. The histological sections were stained with Gram stain (Section 4.2.2.4) or immunohistochemical stains to determine phenotype (Section 3.2.4) of cells and presence of *P. aeruginosa* and its virulence factors section (5.2.2.3) (Table 5.1).

b) the other half was weighed and homogenized in 1 ml of BHI broth. The resultant homogenate was diluted, several times if required, and the viable

bacterial organisms (measured in CFU) were counted via the Miles and Misra method (Miles *et al.*1938). Consequently, the viable bacterial count per Gram of tissue was determined and compared to untreated infected controls.

5.2.2.3- Bacterial migration and penetration

Migration and penetration of bacteria was determined in infected untreated models and those treated for 24 hours with biocidal agents: silver nitrate; isothiazoline; hydrogen peroxide and Manuka honey as described in section 4.2.2.4. Furthermore, the effect on bacterial migration and penetration following treatment with Manuka honey was further investigated following 3, 6 and 24 hours of bacterial infection to determine different effects during maturation of biofilms. In order to accurately estimate the depth of penetration and extent of horizontal spread, immunohistochemical staining with specific antibody markers against *P. aeruginosa* proteins were used including a specific *P. aeruginosa* antibody, IHC was performed as described previously section (3.2.4) (Table 5.1), and Gram stain as described in chapter 4 section 4.2.2.4.

Table 5.1: Target antibodies marker used in IHC and antigen retrieval methods.

Target antibody	Clonality	Optimal dilution	Antigen retrieval	Secondary antibody	Serum block	Cat No.
Anti- *P. aeruginosa*	Mouse monoclonal	1:400	None	Rabbit anti mouse	Rabbit	ab35835
Anti- Flagellin	Rabbit polyclonal	1:400	None	Goat anti- rabbit	Goat	ab93713
Ant- Exoenzyme S	Chicken polyclonal	1:400	None	Goat anti- chicken	Goat	ab20031
Ant- Exotoxin A	Rabbit polyclonal I	1:400	None	Goat anti- rabbit	Goat	P2318

5.2.3-Statistical analysis

All experiments were performed independently at least three times and results presented using scatter plots with medians. Statistical significance of the experimental results (significance level of P≤0.05) was calculated by using Stats Direct. Data did not follow a normal distribution, thus, non-parametric Kruskal-Wallis test was used with a Connover Ingman Post hoc test to determine significant differences.

5.3 Results

5.3.1- Effect of biocides on burned *P. aeruginosa* infected skin

To determine the effect of biocides on *P. aeruginosa* infected skin tissue. Before applying the biocide, bacterial infection was applied to a control infected untreated group and a biocide-free alginate gel treated infected group to test the growth of bacteria in burned 3D skin models and effects of alginate treatment. There was evident bacterial biofilm growth in both the control burned infected skin and the infected skin models treated with alginate, following 24hr incubation, with no difference in CFU/ml seen between untreated and alginate treated models (Figure 5.1). Following 24-hour biocide treatment, all biocides, (silver nitrate, isothiazolone, hydrogen peroxide and Manuka honey), significantly decreased the CFU of *P. aeruginosa* with 1.26, 1.28, 1.39 and 1.99 $\log_{10}$ reduction CFU/ml of *P. aeruginosa* observed (P<0.05), respectively (Figure 5.1). Manuka honey was found to be the most effective of all the tested biocides in reduction of CFU/ml *P. aeruginosa* in biofilms (1.99 $\log_{10}$ CFU/ml), compared with alginate treated controls (P= 0.0046) (Figure 5.1).
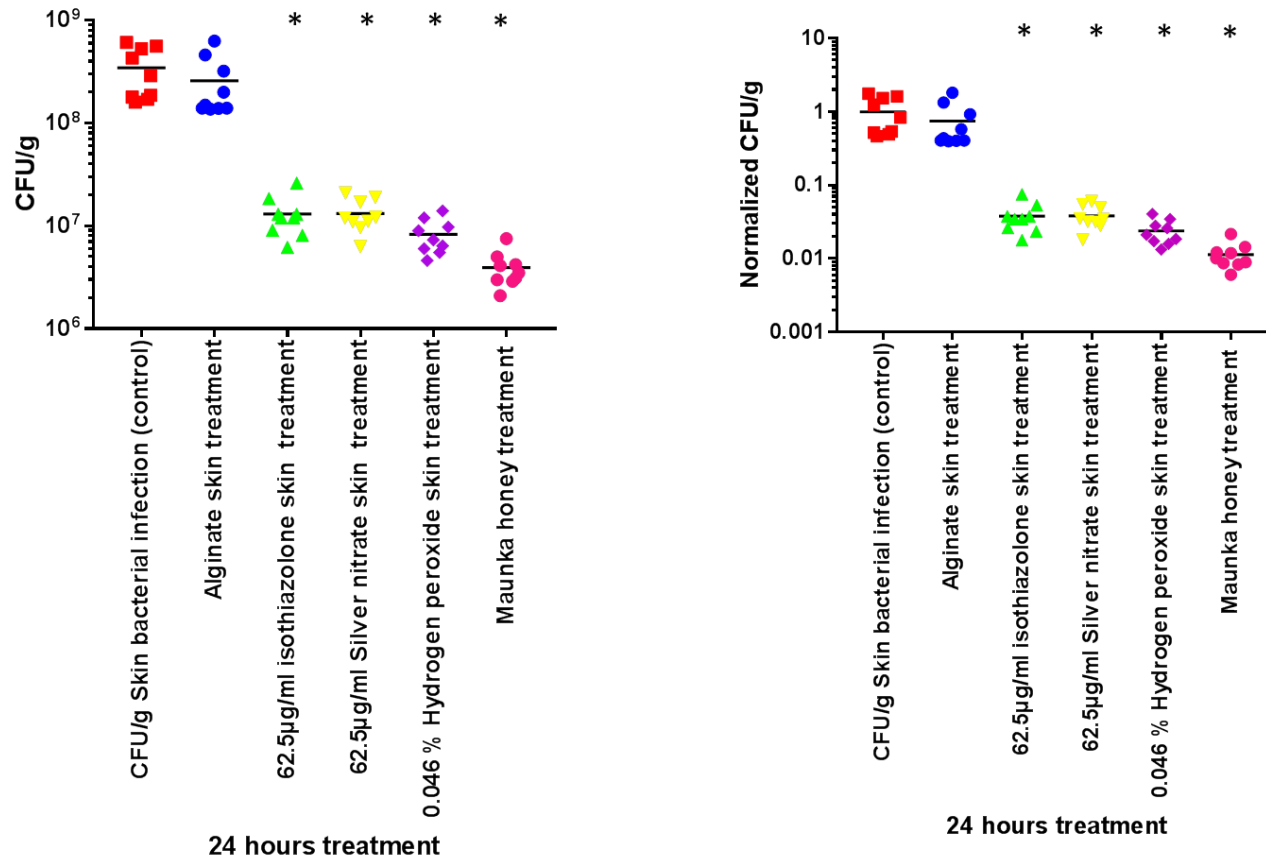
Figure 5.1: Biofilm ability of *P. aeruginosa* (8295), viable bacterial counts in skin tissue per Gram. *in vitro 3D skin* wound model biofilms grown were treated by Silver nitrate, 2- Methyle -4- isothiazoline -3-one are 62.5 µg/L , Hydrogen peroxide is 0.046 v/v and Manuka honey for 24 hours. wound model biofilms, showed significant (P<0.05) inhibition of biofilm of cells following treatment with Silver nitrate, isothiazolone, Hydrogen peroxide and Manuka honey for 24 hours. * = P<0.05.

5.3.2- *P. aeruginosa* skin migration 3D burned skin model infection

Migration of bacteria on infected skin was assessed to investigate the analysis and histological effects of bacterial infection on the tissue. Histological examination using Gram stains showed clear migration of bacteria across the whole epidermal layer (Figure 5.2). *P. aeruginosa* was found to migrate large distances of up to 15.8 ±0.58 mm from the infection site in untreated infected models. Silver nitrate, isothiazoline and hydrogen peroxide did not significantly affect the migration distance of *P. aeruginosa* ($P>0.05$) (Figure 5.3). However, Manuka honey significantly reduced the migration of *P. aeruginosa* ($P = 0.0372$) compared with the burned skin infected with *P. aeruginosa* treated with alginate control (Figure 5.3).

5.3.3- *P. aeruginosa* skin penetration

3D skin models were infected with *P. aeruginosa* and the depth of bacterial penetration was estimated by microscopically examining sections of infected skin after being stained with Gram stain and antibody markers. *P. aeruginosa* tissue infection, the depth of penetration in the alginate culture (control) was 341.8 ± 21 µm, which was far deeper than *S. aureus* penetration seen in chapter 4. This might be attributed to the higher motility which characterizes *P. aeruginosa*, probably due to its possession of active motility structures like flagella. *P. aeruginosa* has previously been shown to migrate for a longer distance across the skin causing spreading of infection horizontally. The four biocides in this study were shown to significantly restrict and decrease the penetration of *P. aeruginosa*.

The penetration depth of *P aeruginosa* in the presence of silver nitrate, isothiazolone, hydrogen peroxide and Manuka honey were measured to be 219 ± 9 µm, 206 ± 6.7 µm, 183 ± 7.3 µm and 170 ± 8.8 µm respectively (Figure 5.4).

These values were shown to be significantly less than the depth of penetration in the control cultures (P values= 0.001, 0.0008, 0.0007 and 0.0007 respectively) (Figure 5.4). Manuka honey was shown again to be the most effective biocide at hindering the penetration of *P. aeruginosa* in this model (Figure 5.4).
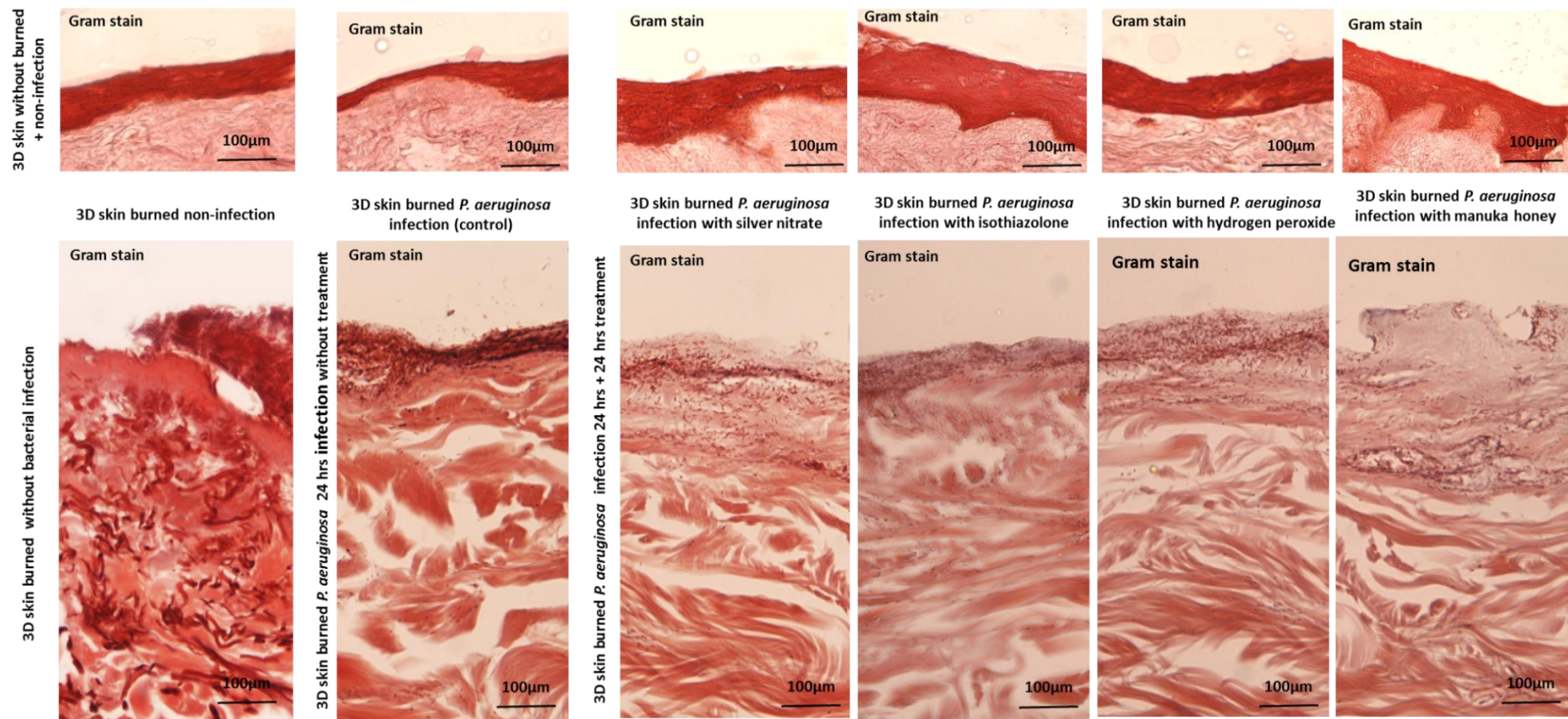
Figure 5.2: Gram stain section of *P. aeruginosa* burned skin infection. The sections showed the infection, migration and penetration of *P. aeruginosa* biofilm formation for 24 hrs of silver nitrate, isothiazolone, hydrogen peroxide and manuka honey treatment for 24 hrs n = 3 separate infected Tissue skin models. Scale bar = 100 and 20μm.
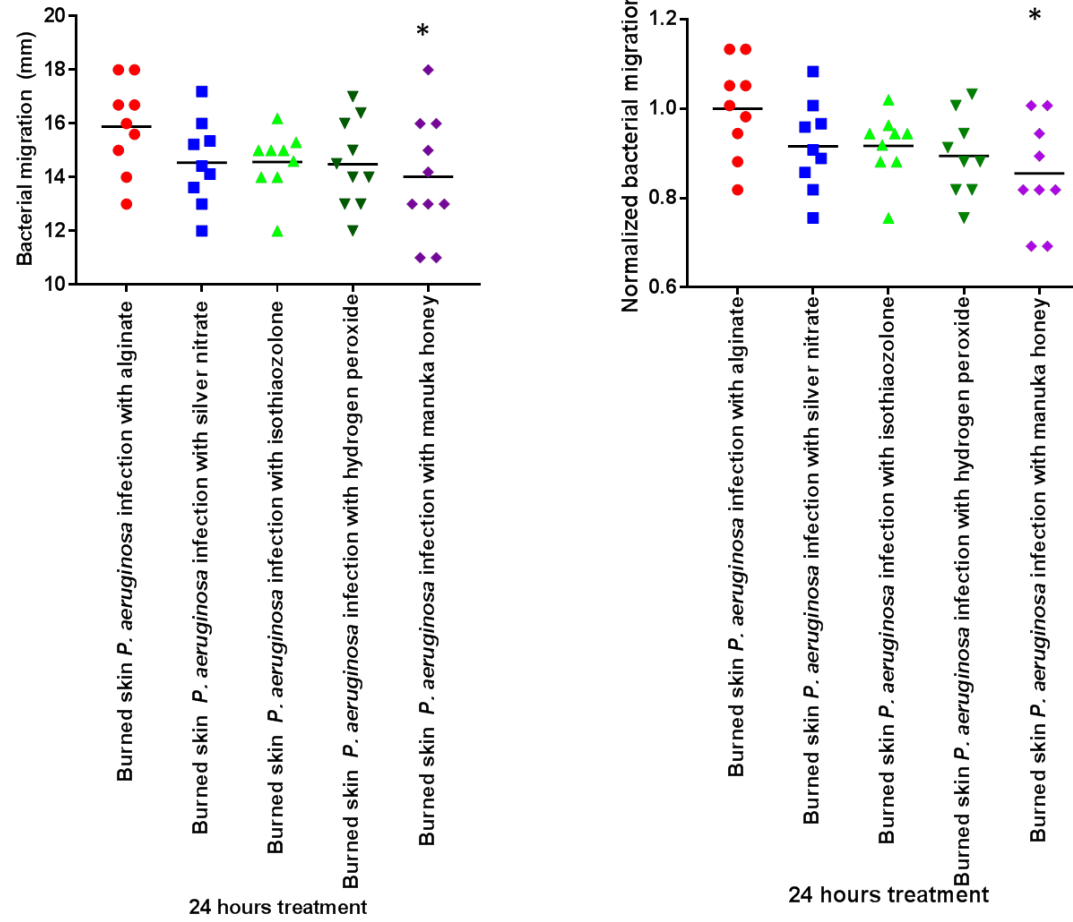
Figure 5.3: Migration of *P. aeruginosa* following 24hr biofilm formation and 24 hrs of treatment n = 3 separate infected Tissue skin models. * = P<0.0. 05.
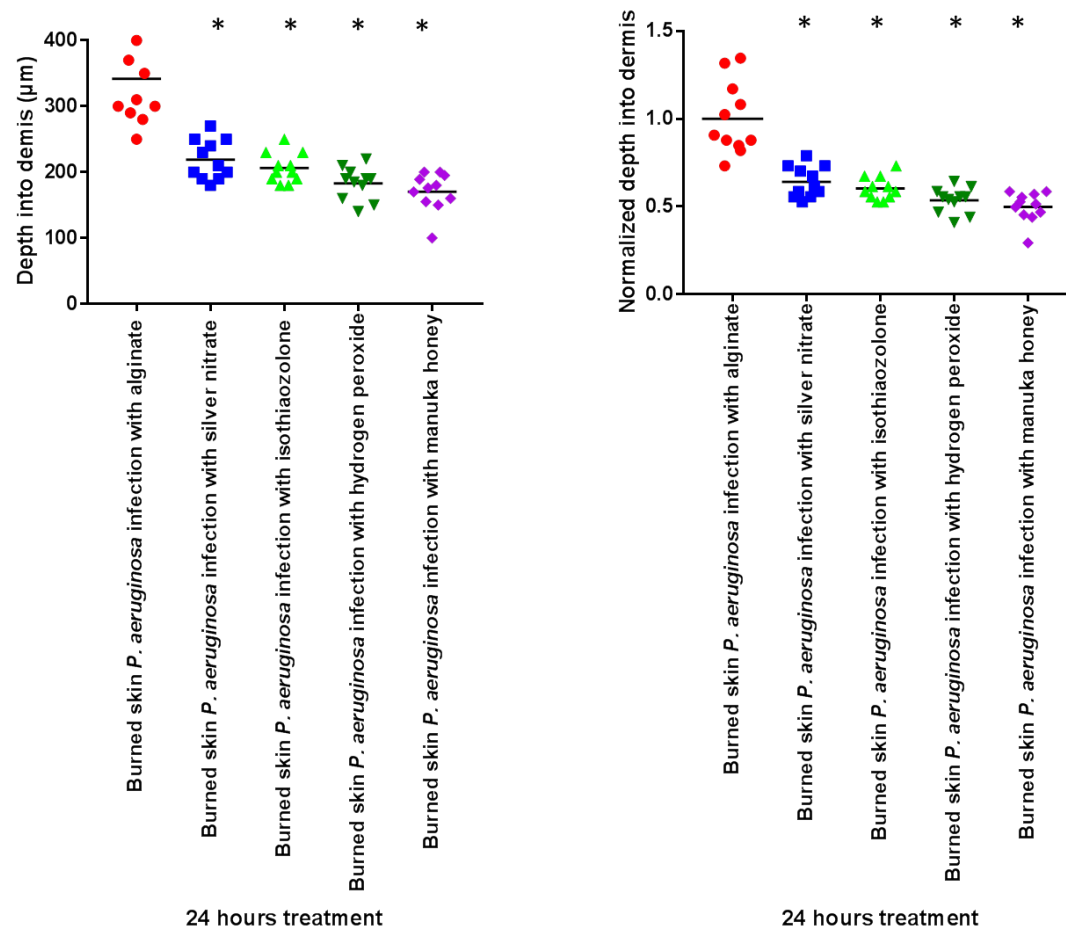
Figure 5.4: Depth of penetration of *P. aeruginosa* into 3D skin models following 24hrs infection and after 24 hrs of treatment of biocides n = 3 separate infected tissue skin models. * = P<0.05.

5.3.4- Effect of biocides on *P. aeruginosa* biofilm *in vitro* nitrocellulose model biofilms formed over 3, 6 or 24hrs

Biofilm forming bacteria are typically more resistant to treatment than planktonic bacteria. However, it takes bacteria variable periods of time to form a mature forming biofilm. In order to investigate the effect of honey on biofilm forming bacteria during various stages of biofilm formation, a nitrocellulose filter paper was created that enables bacteria to grow on it in a medium of BHI broth. The bacterial growth was calculated after 3, 6 and 24 hours. After that, honey was applied for 24 hours to all of the samples. Bacterial counts were determined following treatment to investigate the inhibitory effect of honey on the various stages of bacterial biofilm formation. The bacteria chosen for this study was *P. aeruginosa*.

It was shown that the *P. aeruginosa* bacterial count (CFU/ml) after 3 hours of growth on the nitrocellulose filter paper was 2.3×10^5. When the filter was placed on an agar plate and overlayed with Manuka honey for 24 hours, there was a significant decrease in bacteria (2.5 $\log_{10}$ kill) (P= 0.0001) following treatment, suggesting the bacteria did not have enough time to form a biofilm (Figure 5.5). Consequently, Manuka honey was able to pass through and eliminate a large proportion of the *P. aeruginosa* bacterial cells.

The bacterial count following 6 hours of incubation on the nitrocellulose filter paper was 1.9×10^6, which was higher than that of the previous experiment of 3 hours as expected due to proliferation of bacteria. Following treatment with Honey for 24hrs a significant decrease in bacterial CFU was seen (2.2 $\log_{10}$ kill rate) which was lower than the kill rate attained following 3hr biofilm formation. This can be attributed to the fact that the biofilm formation became more

established after the longer period of growth with more protection and support of the included bacterial cells (Figure 5.5).

Following 24 hour biofilm formation on nitrocellulose filter paper, the bacterial count reached 1×10^8. When the grown *P. aeruginosa* were treated with Manuka honey for 24 hours, a significant decrease in CFU was observed with a 1.95 $\log_{10}$ kill rate, which was less effective than treatment of less established biofilms (P= 0.0001) (Figure 5.5).
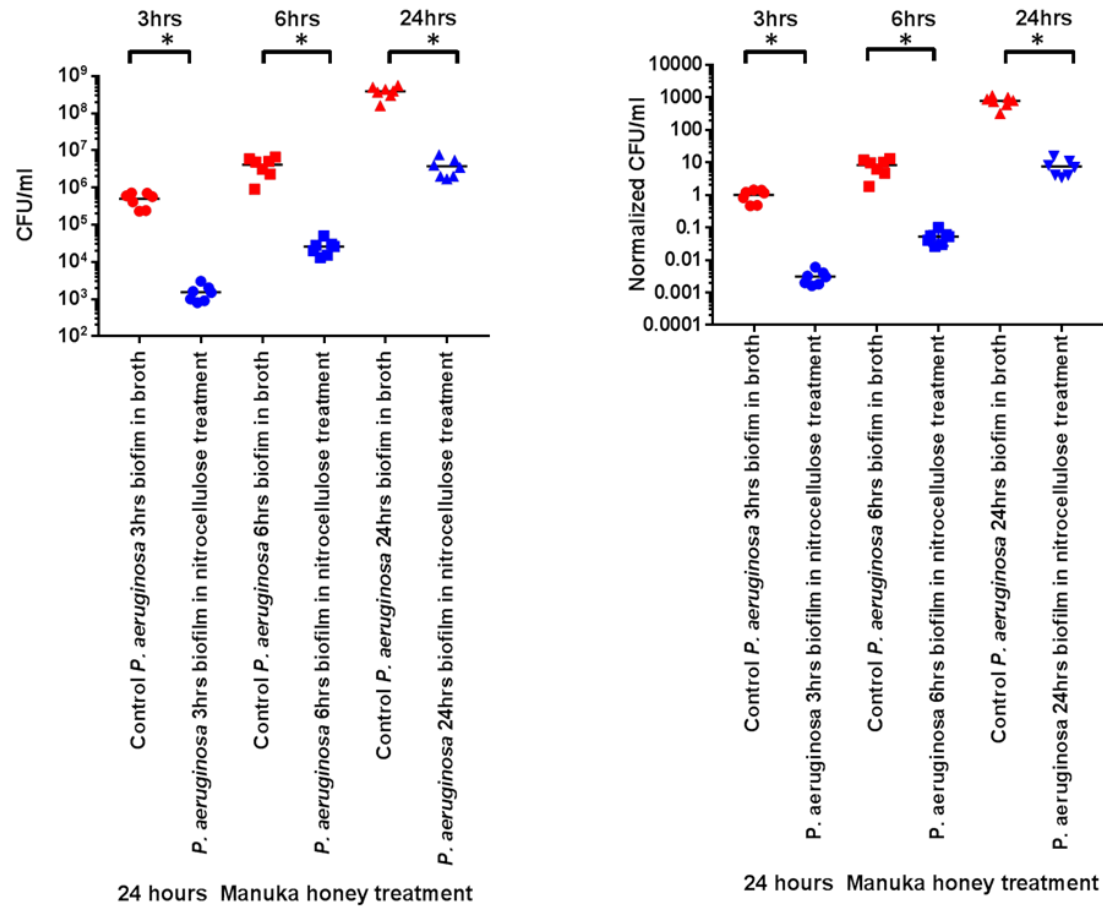
Figure 5.5: Biofilm ability of *P. aeruginosa* (8295), bacterial counts in nitrocellulose *in vitro* model biofilms grown in difference time point 3,6,24 hours were treated by Manuka honey for 24 hours. *In vitro* nitrocellulose model biofilms showed significant inhibition of biofilm of cells following treatment with Manuka honey for all different time points' hours. * = P<0.05

5.3.5- Effect of biocides on *P. aeruginosa* biofilm *in vitro* 3D skin model biofilms formed over 3, 6 or 24hrs

In order to investigate the effect of honey on biofilm-forming bacteria during various stages of biofilm formation, *in vitro* 3D skin models were created that allowed bacteria to grow on burned skin model. The bacterial growth was investigated after 3, 6 and 24 hours. Following which time, honey was applied for 24 hours to all tissue models. Bacterial counts were determined following treatment to investigate the inhibitory effect of honey on the various stages of bacterial biofilm formation. The bacteria chosen for this study was *P. aeruginosa*.

When a skin model was infected with *P. aeruginosa* for 3, 6, and 24 hours, biofilm formation was evident on the surface of the skin model with considerable penetration into the epidermal and superficial dermal layers of skin.

In models that were exposed to infection with *P. aeruginosa* for three hours, it was shown that the *P. aeruginosa* bacterial count (CFU/g) on the burned skin model bacterial infection was 6 x10^5 CFU/g. When skin tissue was overlayed with Manuka honey for 24 hours, there was a significant decrease in bacteria (3 $\log_{10}$ kill) (P= 0.0001) following treatment, signifying the bacteria did not have sufficient time to form a biofilm (Figure 5.6). Thus, Manuka honey was able remove a large quantity of the *P. aeruginosa* bacterial cells.

After 6 hours of infection, the bacterial count was 4.6x10^6 CFU/mg, which was more than 3 hrs infection as predicted owing to proliferation of bacteria. Following treatment with Honey for 24hrs a noteworthy decrease in bacterial CFU/mg was seen (2.46 $\log_{10}$ kill rate) which was lower than the kill rate attained following 3h biofilm formation. This can be attributed to the fact that the forming of biofilm developed after the extended period of growth (P= 0.0001) (Figure 5.6).

Following 24 hour forming of biofilm on *in vitro* tissue skin models, the bacterial count was reached 1.5×10^8. When the skin burned skin *P. aeruginosa* infection treated with Manuka honey for 24 hours. CFU/mg bacterial count was significant decrease with a 1.8 $\log_{10}$ kill rate, which was less effective than seen on less established biofilms (P= 0.0001) (Figure 5.6).
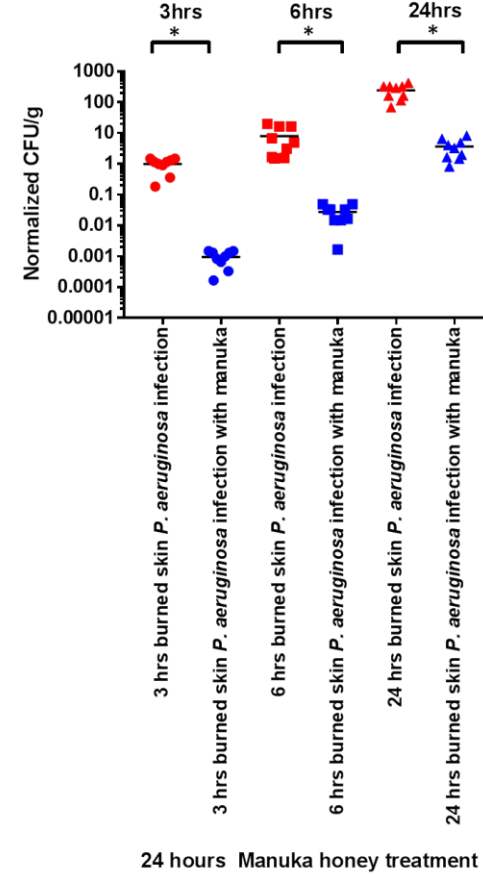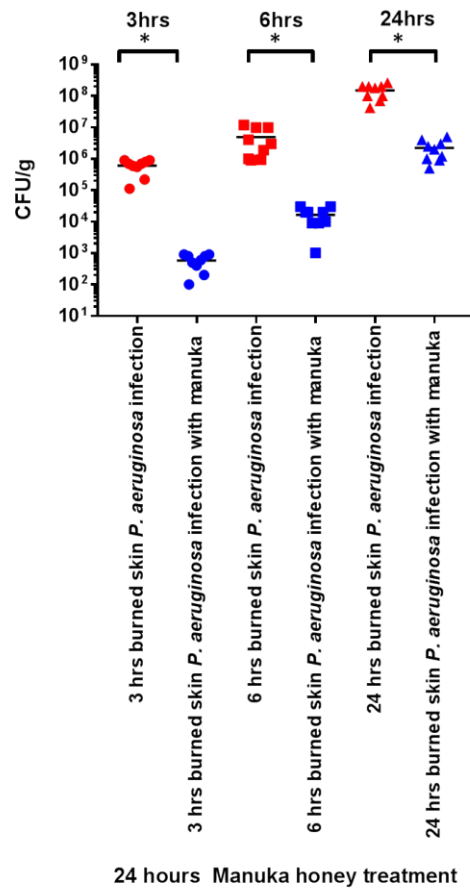
Figure 5.6: Biofilm ability of *P. aeruginosa* (8295), bacterial counts *in vitro* model biofilms grown in difference time point 3,6,24 hours were treated by Manuka honey for 24 hours. *In vitro* skin model biofilms showed significant inhibition of biofilm of cells following treatment with Manuka honey for all different time points' hours. * = P<0.05

5.3.6- Anti *P. aeruginosa* antibody

All skin models stained with IgG controls were shown to be immunonegative suggesting primary antibodies bound specifically to their antigen targets (Figure 5.7). In the burned non-infected skin models, there was no evidence of immunohistochemical staining for bacterial markers (immunonegative) (Figure 5.7). Whereas the infected non-treated models, there was a strongly immunopositive thick brown layer representing a well-formed biofilm of *P. aeruginosa*. The biofilm occupied mainly the centre of the tissue, but there was also extension of the bacteria towards the peripheral parts seen via immunopositive staining; the less dense the bacteria the lighter the immunopositive staining (Figure 5.7).

In models subjected to 3h of *P. aeruginosa* infection, the immunopositive staining for *P. aeruginosa* was mainly in the centre, whereas the peripheral parts were immunonegative demonstrating limited migration. There was also slight penetration of bacteria to the epidermal and dermal layers (Figure 5.7).

After 6h of infection, *P. aeruginosa* spread both vertically into the depth of the epidermal and dermal layers and horizontally into the periphery, making the central brown area thicker from *P. aeruginosa* biofilm and the peripheral areas scattered with brownish spots (Figure 5.7). In the 24h infected models, the tissues showed more destruction due to the migration of *P. aeruginosa* across the tissues, evidenced by the strong immunopositivity in most of bacteria in the tissues. The peripheral parts were also destructed but the staining was less dense (Figure 5.7).
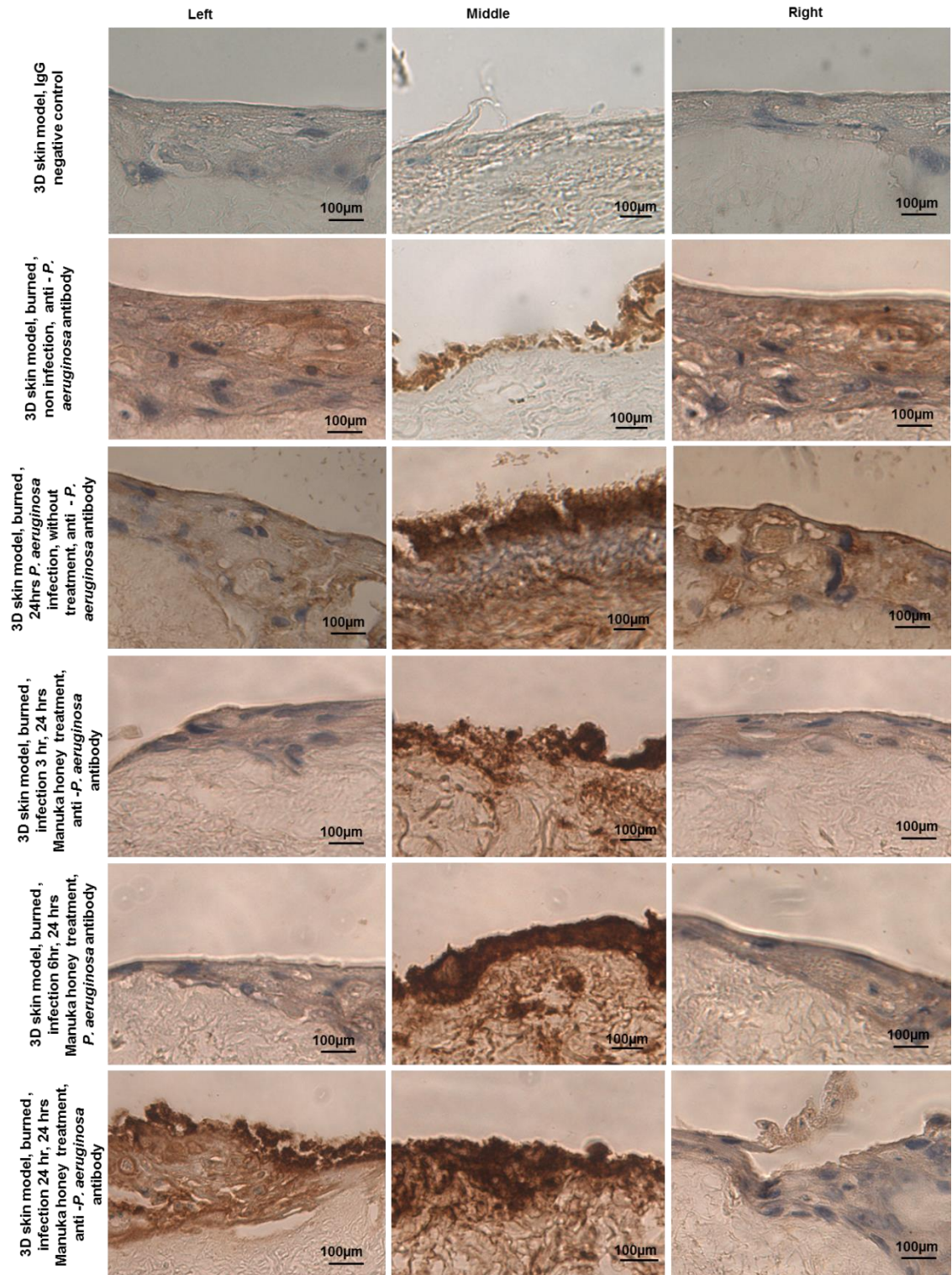
Figure 5.7: Anti *P. aeruginosa* antibody marker, 3D skin models *P. aeruginosa* infection showing of biofilm bacteria migration and depth on burned of skin. *P. aeruginosa* antibody marker was compared between burned infected and non-infected controls, burned infected biocidal treated samples and Manuka honey burned skin models in 3 time point bacterial infection 3, 6 and 24h). Scale bar=100µm

5.3.7- Penetration of *P. aeruginosa* into skin models following 3, 6 and 24 biofilm formation and effect of 24 hours of honey treatment:

After 3 hours of biofilm showed in antibody marker and Gram stain tissue section (Figure 5.8), the penetration of *P. aeruginosa* into the skin models was estimated to be 75.6 μm. After 24 hours of treatment with honey, the depth of penetration significantly decreased to 54 μm (P= 0.005) (Figure 5.9). Following 6 hours biofilm formation, *P. aeruginosa* cells penetrated into a depth of 97.1 μm Treatment with honey decreased the depth of penetration to 79.1 μm achieved by *P. aeruginosa*, which was significant (P= 0.005) (Figure 5.9). Following 24 hours of *P. aeruginosa* biofilm formation, the penetration into the skin model was markedly increased when compared with shorter timeframes to 396.6 μm and was then reduced to 376.6 μm following 24hr honey treatment which was not significant (P = 0.3) (Figure 5.9).
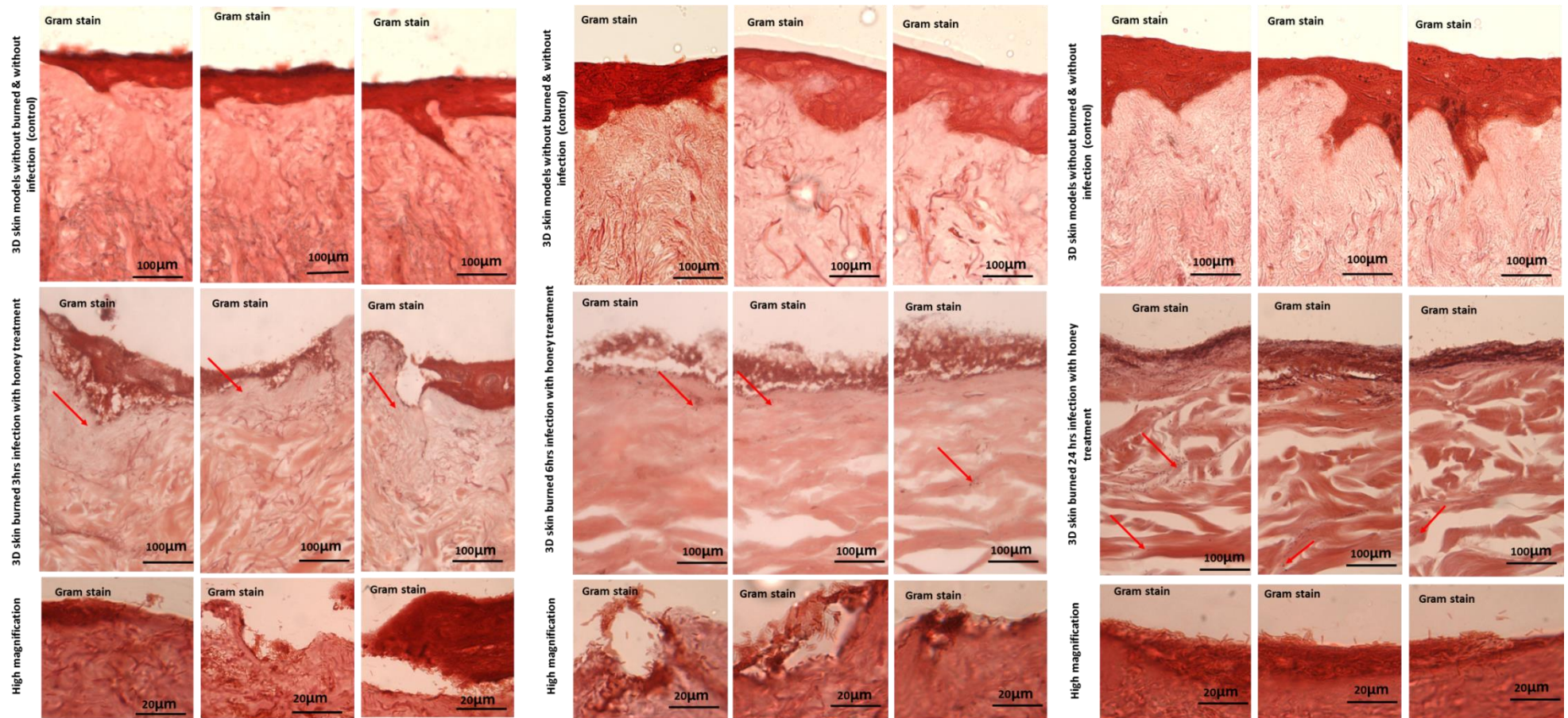
Figure 5.8: Gram Stain of 3D burned skin *P. aeruginosa* infection, 3D skin models *P. aeruginosa* infection showing of biofilm bacteria migration and depth on burned of skin. Gram Stain was compared between non burned and non-infected controls, burned infected biocidal treated with Manuka honey burned skin models in 3 time point bacterial infection 3, 6 and 24h). Scale bar=100 & 20 µm
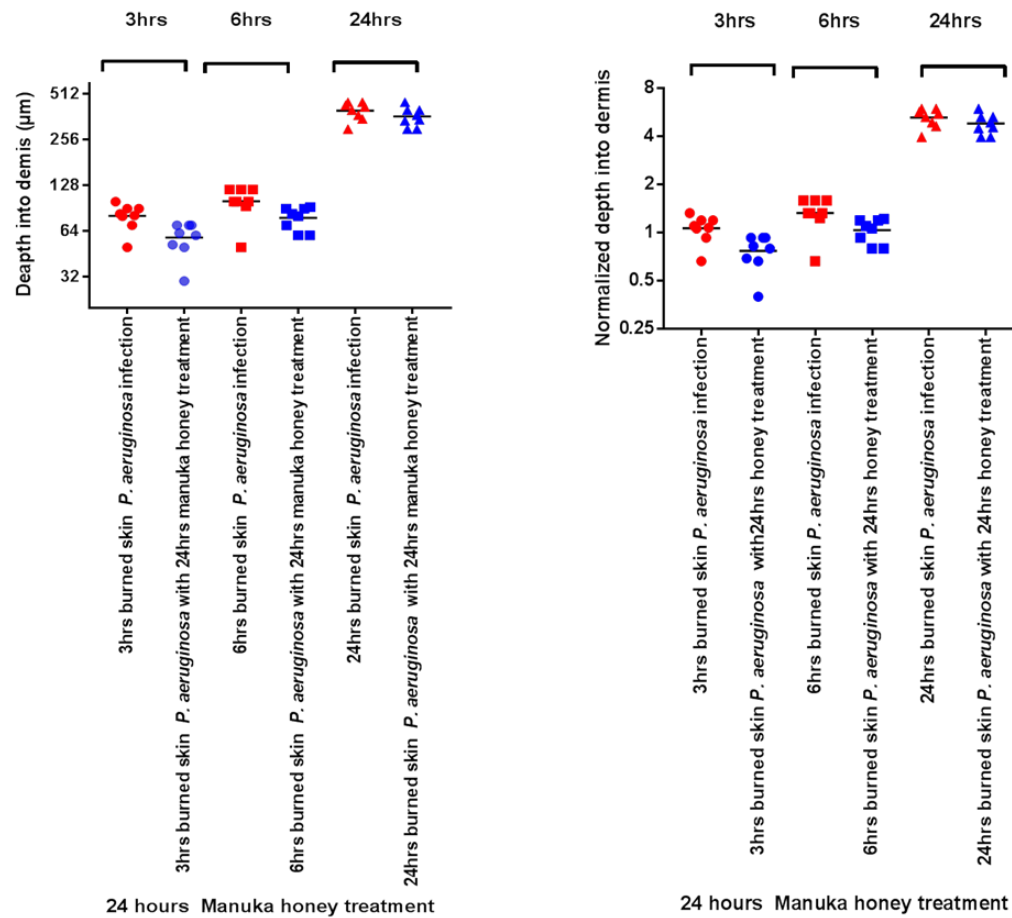
Figure 5.9: Bacteria penetration depth in epidermal layer with skin model. The diaGram showed the depth of *P. aeruginosa* after in difference time point 3, 6, 24 hrs of treatment n = 3 separate infected Tissue skin models. * = P<0.0. 05.

5.3.8- Migration of *P. aeruginosa* across the skin models after 3, 6 and 24 hours of biofilm formation and after 24 hours of honey treatment

After 3h of 3D skin biofilm infection, the *P. aeruginosa* spread across the skin models was estimated to be 11.57 mm. After 24h of treatment with honey, the spread significantly decreased to 8.7mm (P = 0.02) (Figure 5.10).

The *P. aeruginosa* cells migrated across the skin model to reach an extent of 13.18 mm after 6h of biofilm formation. Treatment with honey significantly decreased the migration distance of pseudomonas to 10.5mm (Figure 5.10) (P = 0.01).

Following 24h of *P. aeruginosa* biofilm formation, the pseudomonas bacteria migrated to a distance of 15.12 mm which was greater than that seen in 3 and 6h treatments. Treatment with honey decreased the bacterial migration extent, but the decrease was less than seen with less mature biofilms (3 and 6h) and the decrease was not significant (P= 0.4) (Figure 5.10).
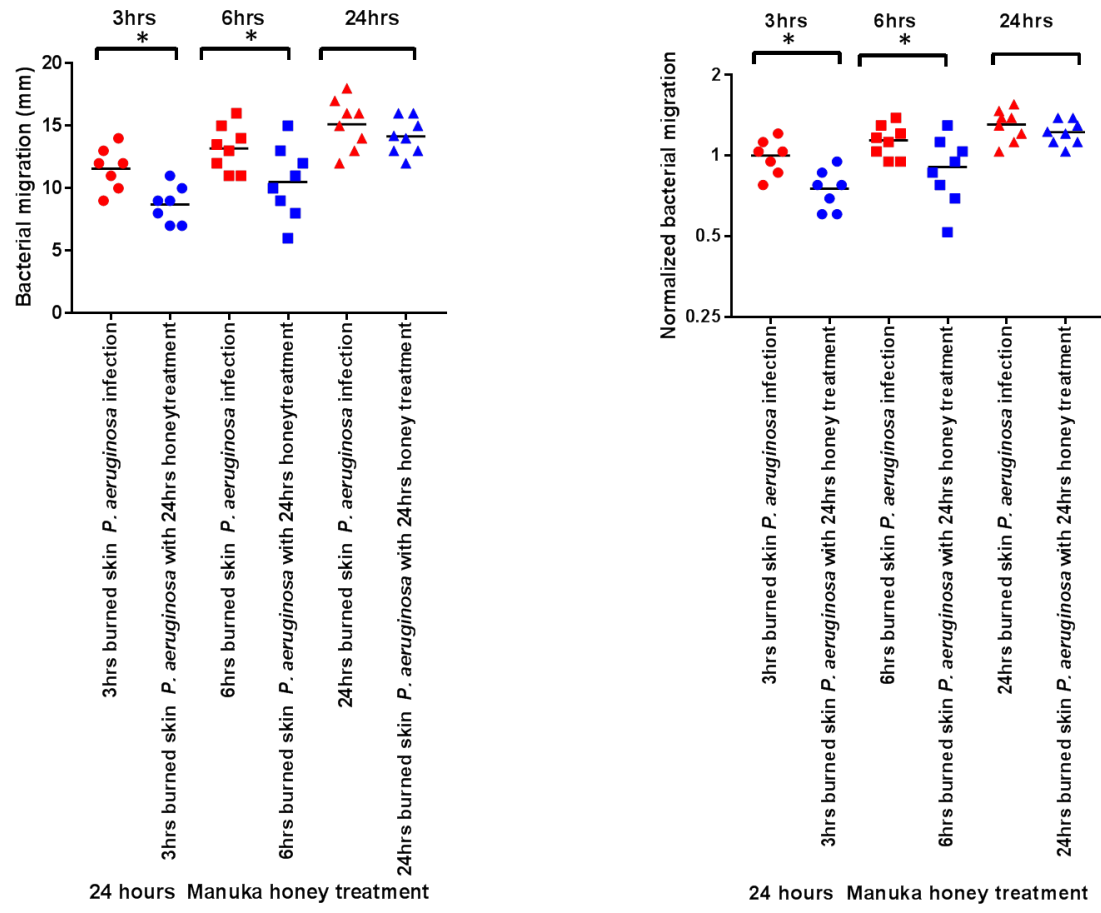
Figure 5.10: Migration of bacteria in epidermal layer with skin model. The diaGram showed the migration o*f P. aeruginosa* following biofilm formation for 3, 6, 24 h of treatment n = 3 separate infected Tissue skin models. * = P<0.05.

5.3.9- Bacterial antibodies marker of infected burned skin models with *P. aeruginosa*

The antibody markers targeted with immuno-histochemical stains were anti *P. aeruginosa* antibody, anti-Flagellin and anti-Exoenzyme S and Exotoxin A of *P. aeruginosa* with all the antibody directed stains, there was no staining of tissues in normal and burnt non-infected skin models, since they were devoid of the bacterial organisms; sections were immunonegative (Figure 5.11).

In cases of infected models with *P. aeruginosa*, whatever the period of infection (3, 6 or 24h) and whether they were associated with treatment or not, brown staining of the tissues represented the presence of bacteria or one of its products.

5.3.9.1- Anti-Flagellin antibody of *P. aeruginosa*

In the 24h infected skin models with *P. aeruginosa*, a thick brown biofilm layer was apparent in the centre of the slide with extension of the brownish staining towards the periphery. This links to the characteristic ability of *P. aeruginosa* to spread and migrate by flagella. In models where biofilms were formed over 3h *P. aeruginosa* flagella immunopositivity was constrained to the infection site in the middle of the tissue. The penetration of bacteria to the epidermal and dermal was also limited (Figure 5.11). After 6 hours of infection, *P. aeruginosa* migrated considerably into the depth of the tissues resulting in greater immunopositivity staining for flagella than 3h biofilm formation. Similarly, the horizontal spread covered a wider area (Figure 5.11). In the 24 hour biofilm infection models, the migrating bacteria across the tissues caused more destruction. This was confirmed by the strong immunopositivity for *P. aeruginosa* flagella. Although the peripheral parts were also damaged, immunopositivity for flagella was lower than the middle suggesting a lower bacterial density in the periphery (Figure 5.11).
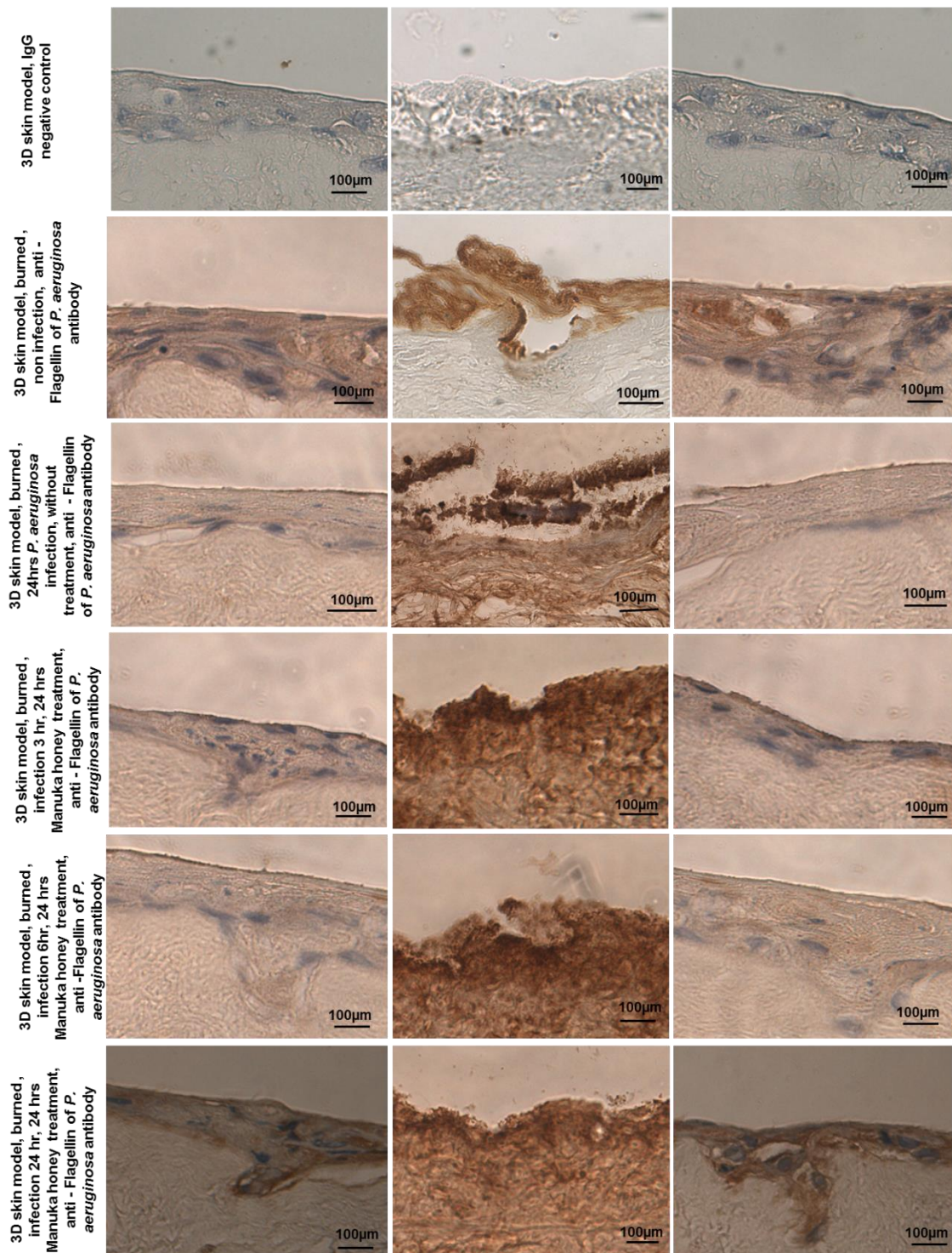
Figure 5.11: Anti Flagellin antibody marker, 3D skin models *P. aeruginosa* infection showing of biofilm bacteria migration and depth on burned of skin. Anti Flagellin antibody marker was compared between burned infected and non-infected controls, burned infected biocidal treated samples and Manuka honey burned skin models in 3 time point bacterial infection 3, 6 and 24h). Scale bar=100μm

5.3.9.2- Anti Exoenzyme S antibody of *P. aeruginosa*

In the infected models, a central area of strong immunopositivity denoted the capability of *P. aeruginosa* to form a well-formed biofilm layer. Although the biofilm occupied mainly the centre of the model, there was extension of the immunopostive staining towards the peripheral parts. In models subjected to 3h of *P. aeruginosa* infection, the immunopositivity for Exoenzyme S was mainly in the middle. There was also moderate penetration Exoenzyme S to the epidermal and dermal layers (Figure 5.12). However following 6h of infection, *P. aeruginosa* exoenyme S immunopositivity was observed through the depth of the epidermal and dermal layers. Horizontal extension of the immunopositivity for exoenzyme S was seen throughout the tissue towards the edges of the model (Figure 5.11). Following 24h of infection, tissues showed more destruction due to both the migration of *P. aeruginosa* across the tissues and the spread of the immunopositivity for exoenzyme S was extensive (Figure 5.12).
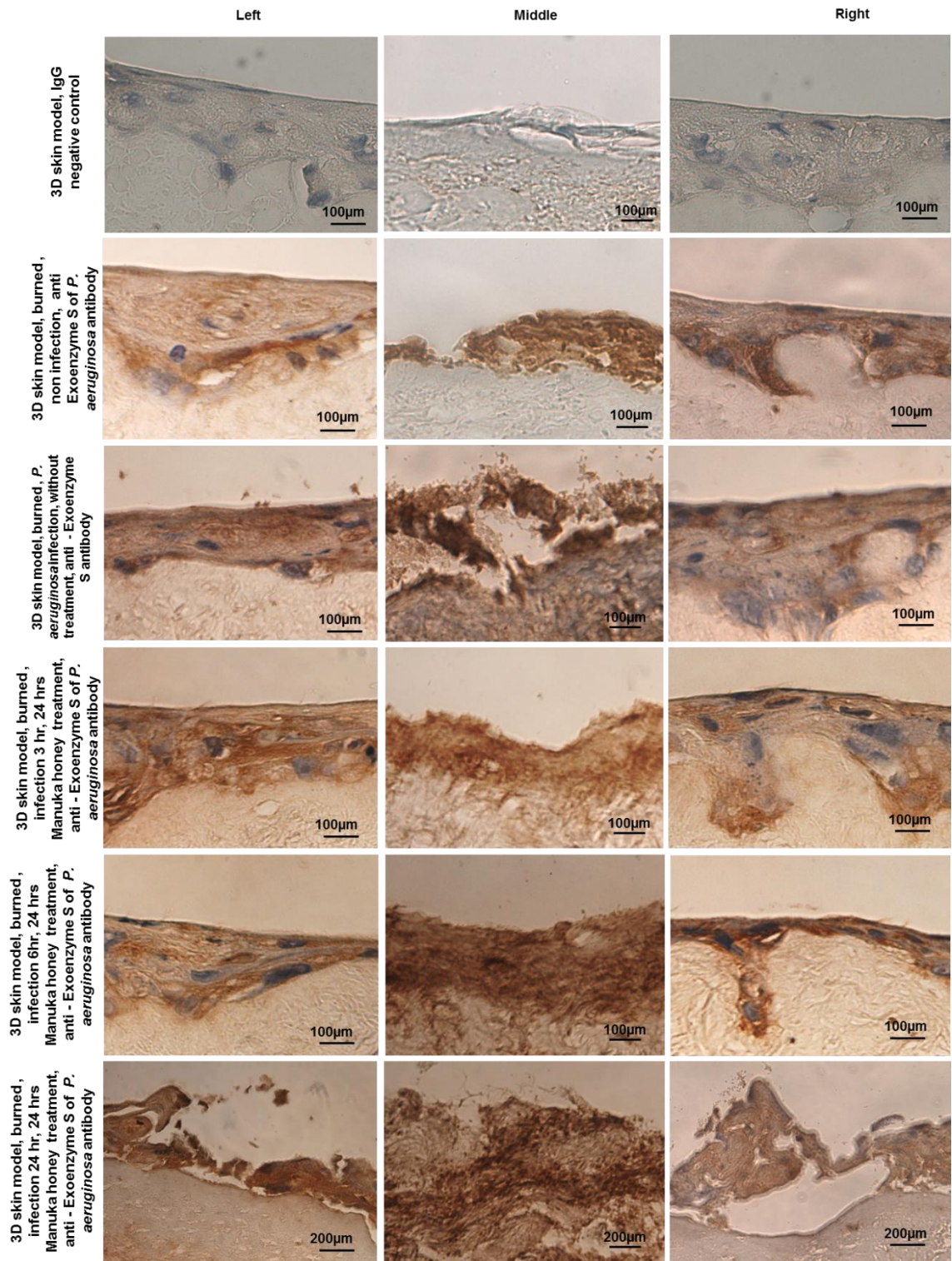
Figure 5.12: Anti Exoenzyme S antibody marker, 3D skin models *P. aeruginosa* infection showing of biofilm bacteria migration and depth on burned of skin. Exoenzyme S antibody marker was compared between burned infected and non-infected controls, burned infected biocidal treated samples and Manuka honey burned skin models in 3 time point bacterial infection 3,6 and 24h). Scale bar= 100μm.

5.3.9.3- Anti Exotoxin A antibody of *P. aeruginosa*

In models subjected to 3h of *P. aeruginosa* infection, the brown immunopositive colour of *P. aeruginosa* Exotoxin A was mainly in the middle of the 3D skin model, whereas the peripheral parts were immunonegative (Figure 5.13). Following 6h of infection, immunopositive staining for *P. aeruginosa* exotoxin A was seen throughout the epidermal and superficial layer of dermis. *P. aeruginosa* Exotoxin A immunopositivity was seen together with extension to the edges of the 3D skin model (Figure 5.13). Following 24h infection extensive immunopositive staining for exotoxin A was observed (Figure 5.12).
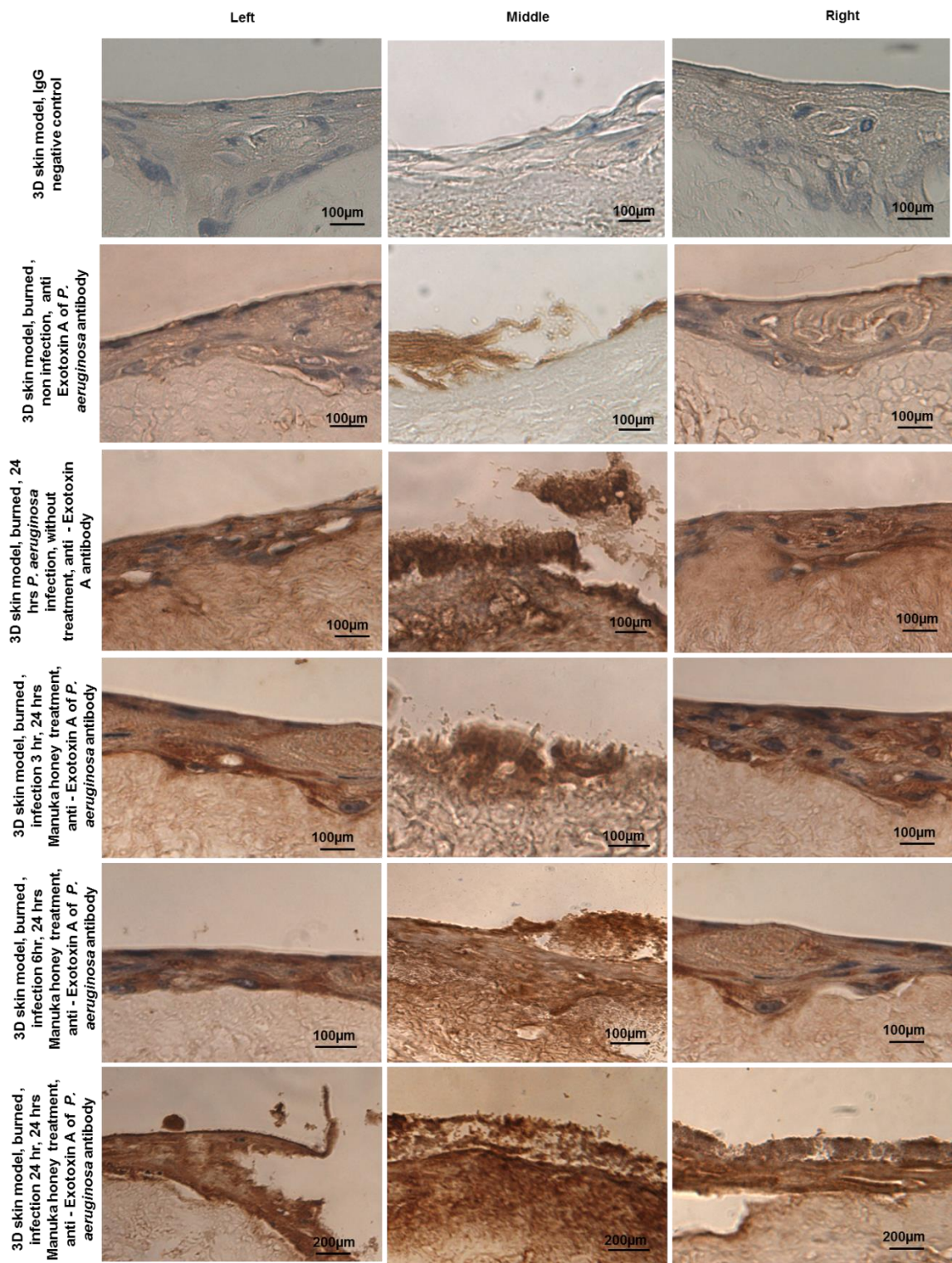
Figure 5.13: Anti Exotoxin A antibody marker, 3D skin models *P. aeruginosa* infection showing of biofilm bacteria migration and depth on burned of skin. Exotoxin A antibody marker was compared between burned infected and non-infected controls, burned infected biocidal treated samples and Manuka honey burned skin models in 3 time points bacterial infection 3, 6 and 24h). Scale bar=100µm

5.3.10- Death zone in the skin model caused by infection with *P. aeruginosa* alone and with treatment with various biocides

Infection with *P. aeruginosa* caused a mammalian cell death zone in the skin model which was significantly greater than the uninfected control (P<0.05) (Figure 5.14). Silver nitrate and hydrogen peroxide further increased the death zone caused by *P. aeruginosa* infection alone (P=0.0322 and 0.0318 respectively) (Figure 5.12). 2- Methyl -4- isothiazolone -3- one did not change the death zone caused by *P. aeruginosa* infection alone significantly (P = 0.0775) (Figure 5.14).

Manuka honey decreased the death zone caused by *P. aeruginosa* infection alone, although this was not significant (P=0.8698) (Figure 5.14). Manuka honey was shown to be the least toxic of the biocides tested in this study; yet, it was still effective in reducing CFU for *P. aeruginosa* and its migration and penetration into 3D skin models (Figure 5.1, 5.3, 5.4).
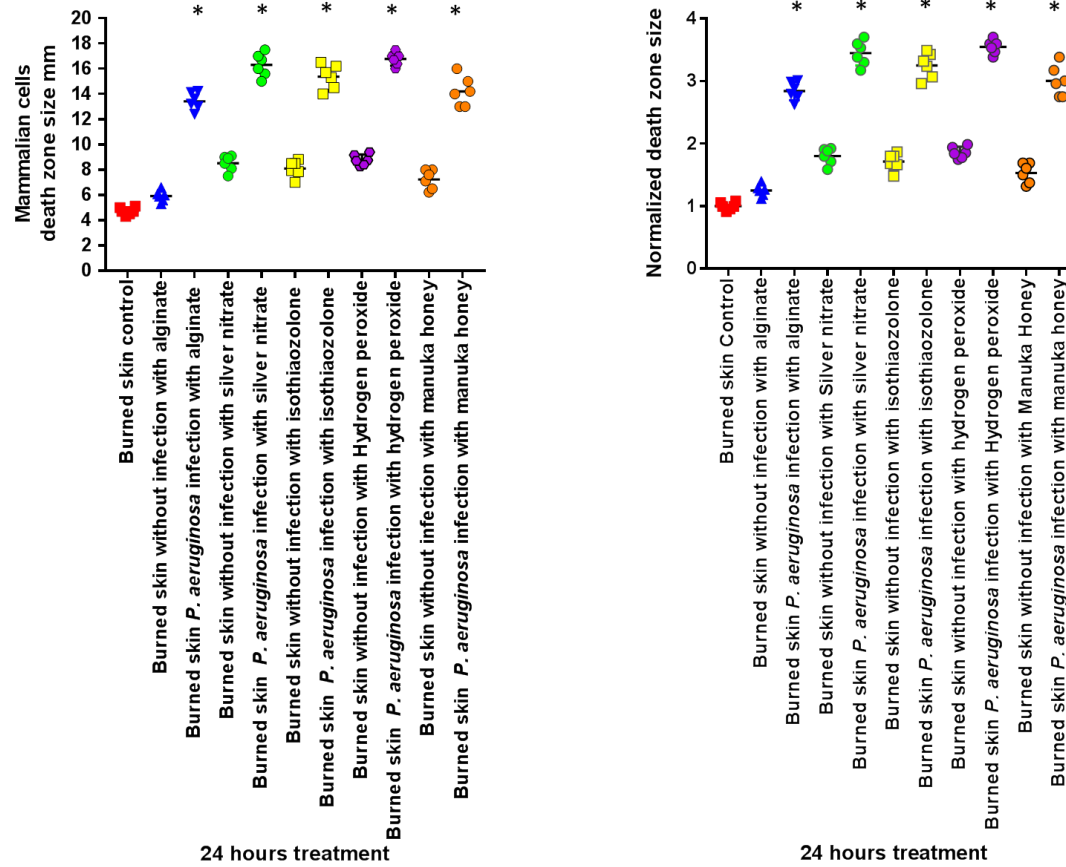
Figure 5.14: Death zone in 3D skin models, effect of biocidal agents on infected 3D skin models showing death zone of skin following biocidal treatment. The biocidal effect was compared between burned infected controls and burned *P. aeruginosa* infected treated with biocidal agents.* = P<0.05.

5.3.11- The effects of biocides on skin models infected with *Pseudomonas aeruginosa* using immunohistochemical staining.

The effects of biocides on skin models infected with *P. aeruginosa* were studied by immunohistochemical stains targeting various markers (Caspase 3, Collagen IV, CPK, CK 10 and CK 14). Normal control skin and burned non-infected skin models with and without biocidal agents were described within chapter 4, these controls were comparable to those for the *P. aeruginosa* infected skin models and thus in this chapter the infected models with *P. aeruginosa* will be discussed with and without biocidal agent treatment only.

5.3.11.1- Caspase 3

5.3.11.1.1- Caspase 3, burned skin models with and without biocides:

The burned skin model infected with *P. aeruginosa* showed immunopositive caspase 3 cells in the middle of skin models with complete detachment of the epidermis in parts of tissue from the underlying dermis leading to de-epidermisation of the skin model. Even in the peripheral parts, apoptotic cells were observed denoting the widespread effect of infection by *P. aeruginosa* (Figure 5.15).

In the alginate model, whilst the majority of the cells were immunonegative for caspase 3 even in the middle of the tissue, the epidermal layer was lost in these models denoting that the destructive effect of *P. aeruginosa* infection on the epidermis overcame the protection that alginate was seen to offer to the architecture of the skin models including the epidermis in chapter 4 following *S. aureus* infection.
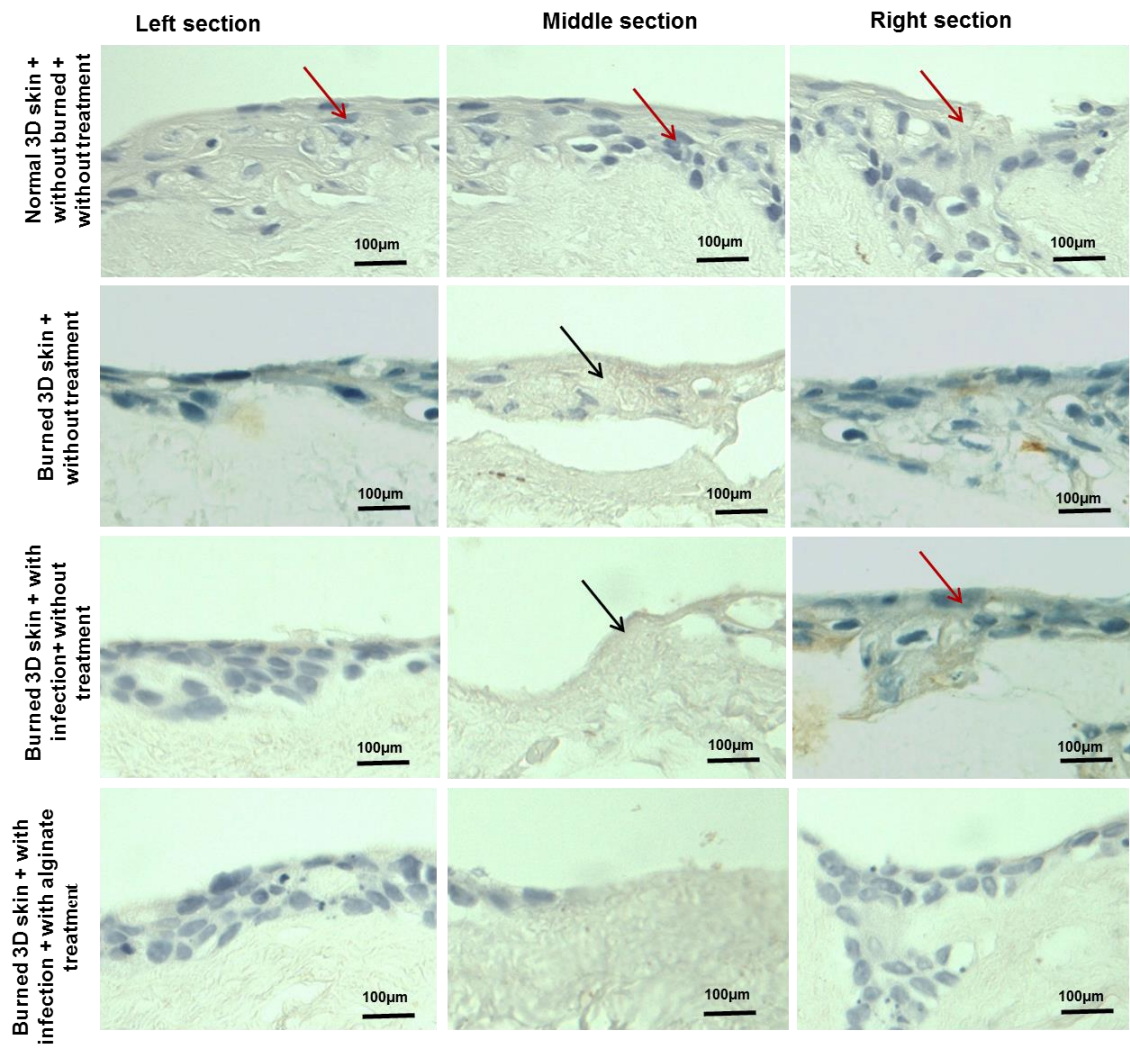
Figure 5.15: Effect of biocidal agents on 3D skin tissue burned with and without *P. aeruginosa* infection, Caspase 3 antibody marker compared between non burned and no infection, controls , burned non infection without biocidal treated, burned infected without biocidal treated and burned infected with alginate treated. The three pictures shown in each row are left, middle and right tissue. Black arrow is immunopostive; red arrow is immunonegative. Scale bar = 100µm.

5.3.11.1.2- Caspase 3, burned skin models with biocides

The effect of biocides on burned non-infected skin models, in terms of density of apoptotic cells as demonstrated by Caspase 3 staining, was discussed in the previous chapter. Only the biocidal effects on burned infected skin models infected with *P. aeruginosa* will be discussed here. These effects can be compared to those of burned non-infected models or to the burned models infected with *S. aureus* described in chapter 4.

5.3.11.1.2.1- Silver nitrate

Burned infected skin models infected with *P. aeruginosa* treated with silver nitrate, showed a large loss of epidermal cells in the middle of the tissue; in this region there was immunopositive staining for caspase 3. Whilst the peripheral parts of the model were immunonegative and suggested cell viability, although the epidermis was not completely detached there was considerable apoptosis within epidermal cells in the middle of the model in proximity to the infection (Figure 5.16).

5.3.11.1.2.2- Isothiazolone

Burned infected skin models infected with *P. aeruginosa* treated with isothiazolone, showed immunopositive staining for caspase 3 and total loss of the epidermal layer in the middle part of the tissue model. In the peripheral parts, the epidermis was mainly immunonegative with very few apoptotic cells (Figure 5.16).

5.3.11.1.2.3- Hydrogen peroxide

The burnt *P. aeruginosa* infected skin model treated with hydrogen peroxide showed immunopositive caspase 3 cells and complete loss of the epidermal layer in the middle of the skin model, while in the peripheral parts the epidermal layer was immunonegative (Figure 5.17).

5.3.11.1.2.4- Manuka Honey

Infected burnt skin model with *P. aeruginosa* treated with honey showed immunopositive caspase 3 cells and deficient epidermal layers cell in the middle of tissue. In the peripheral parts the epidermis was preserved but with few apoptotic caspase 3 immunopositive cells (Figure 5.17).
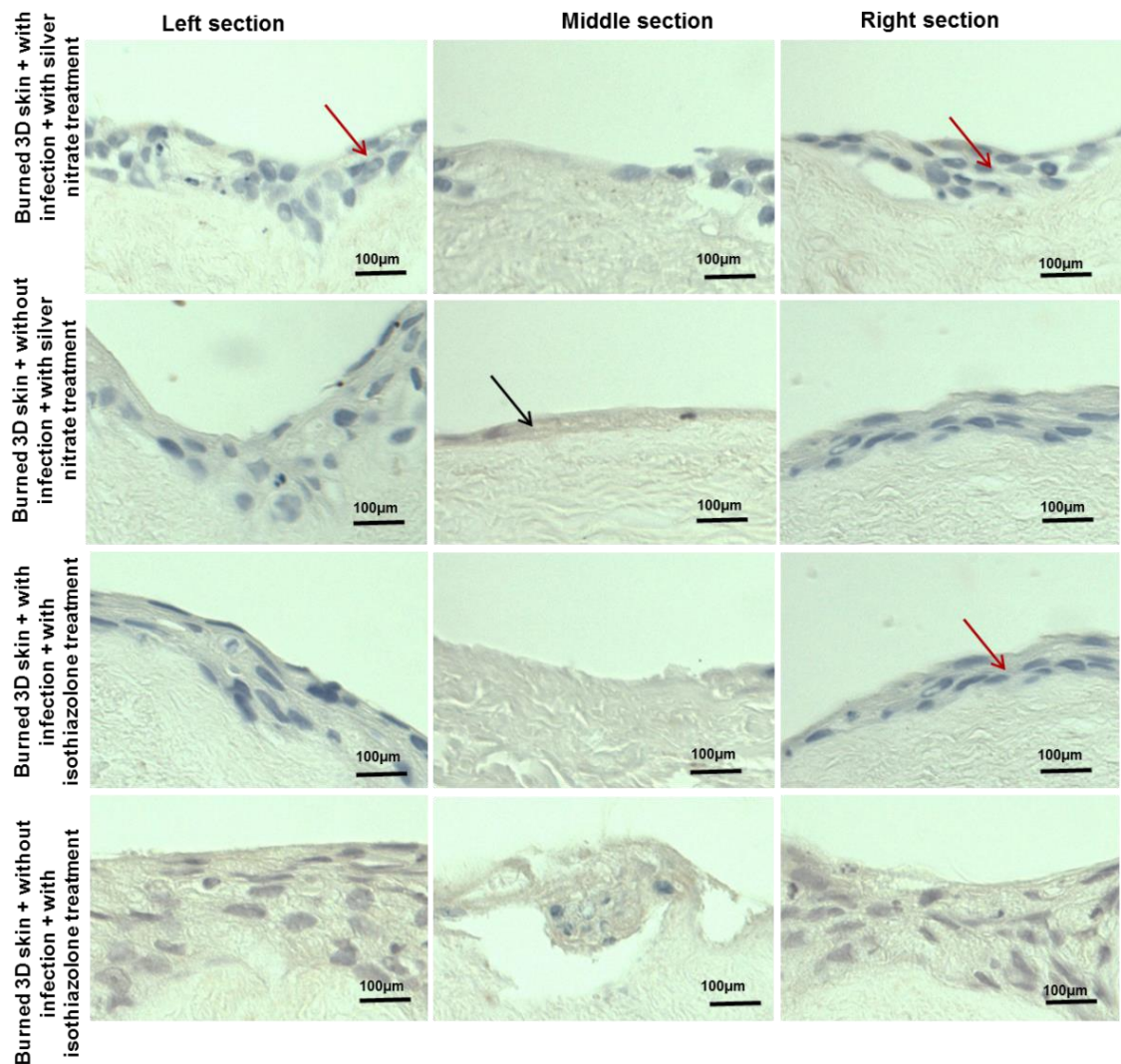
Figure 5.16: Effect of biocidal agents on 3D skin tissue burned with and without *P. aeruginosa* infection, Caspase 3 antibody marker compared between burned, with or without bacterial infection, and silver nitrate treatment; burned, with or without bacterial infection, and Isothiazolone treatment. The three pictures shown in each row are left, middle and right tissue. Black arrow is immunopostive; red arrow is immunonegative. Scale bar = 100μm.

	Left section	Middle section	Right section
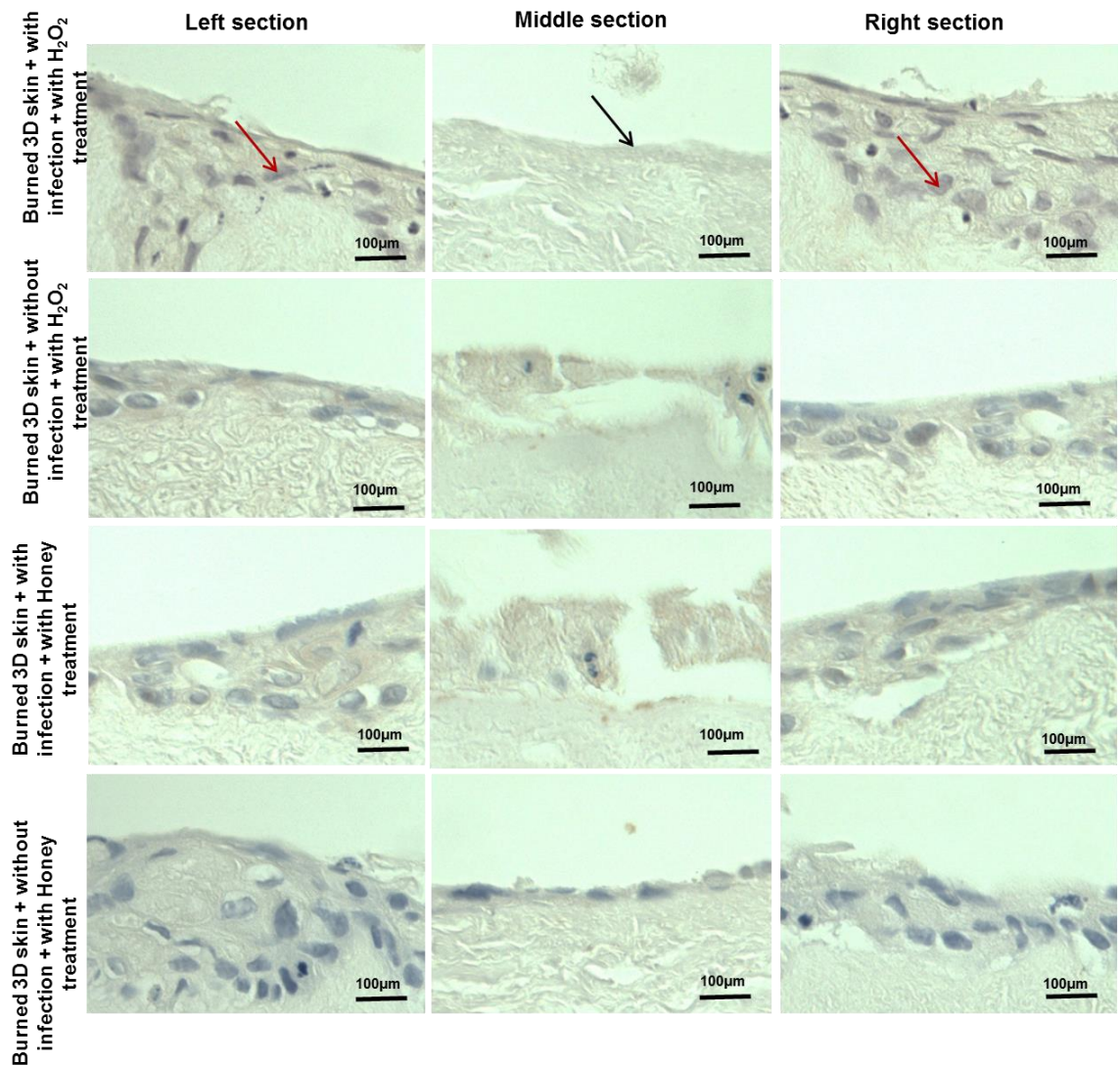
Figure 5.17: Effect of biocidal agents on 3D skin tissue burned with and without *P. aeruginosa* infection, Caspase 3 antibody marker compared between burned, with or without bacterial infection, and H$_2$O$_2$ treatment; burned, with or without bacterial infection, and Clinical Manuka honey treatment. The three pictures shown in each row are left, middle and right tissue. Black arrow is immunopostive; red arrow is immunonegative. Scale bar = 100µm.

5.3.12. - Phenotypic assessment of 3D skin models following infection

5.3.12.1- Collagen type IV antibody, burned skin models without biocides

In burned and infected skin models infected with *P. aeruginosa*, the collagen type IV layer was decreased particularly in the middle of the model denoting that *P. aeruginosa* effect did not only affect the epidermal layer which was completely lost, but also extended into the depth of the skin model. The

peripheral parts showed slight immunopositive disruption among the layers of the collagen type IV with preservation of the collagen layer as a whole.

The overlying epidermal layers in the peripheries were thinner than in the control skin model (Figure 5.18).

In burned and *P. aeruginosa* infected skin models treated with alginate, the collagen layer was preserved, though slightly disrupted and the overlying epidermis was partially preserved in the middle. This can be attributed to the protective nature of alginate on the skin model structures. In the peripheral parts less collagen disruption was seen and Collagen IV immunopositive staining of the overlying epidermal layers was maintained (Figure 5.18).

5.3.12.2- Pancytokeratin, burned skin models without biocides

The 3D skin models were immunohistochemically stained with Pancytokeratin which is the main marker of keratinocytes; thus, normal skin models can be compared with burned skin models, burned and infected skin models with *P. aeruginosa*, with and without alginate (Figure 5.21).

The skin model that was subjected to both burn and infection with *P. aeruginosa* showed stronger immunopositive staining for PCK in the epidermal layer in the middle zone of the 3D model compared with the peripheral parts of model. Similar staining patterns were observed in the burned, infected and treated with the alginate control (Figure 5.21).

5.3.12.3-Cytokeratin 10, burned skin models without biocides

The 3D skin models were immunohistochemically stained with cytokeratin 10 which is a keratinocyte marker that is normally expressed in the terminally differentiated keratinocytes in epidermis.

In the burned skin model infected with *P. aeruginosa*, there was a thin layer of epidermis which was immunopositive for cytokeratin 10 in the middle part of the

tissue denoting decreased differentiation of basal keratinocytes with loss of the upper layers of the epidermis. In the peripheral parts, both the basal layers and the overlying layers displayed cytokeratin 10 immunopositive staining. In the alginate model, the epidermal layer was immunopositive in the centre (Figure 5.24).

5.3.12.4- Cytokeratin 14, burned skin models without biocides

The 3D skin models were immunohistochemically stained with cytokeratin 14 which is the keratinocyte marker of the epidermal cells forming the stratum basale. In burned infected skin models with *P. aeruginosa*, there was a thin layer of epidermal brown cells, immunopositive for cytokeratin 14 in the middle as compared to the peripheral parts of the model. With immunopositive stained cells observed within the periphery of the epidermis. The stains were light brown in general denoting a probable role of *P. aeruginosa* decreasing the expression of cytokeratin 14. In the alginate model, although the epidermal layer was abnormal in thickness, it was disrupted and partially detached from the underlying dermis (Figure 5.27).

5.3.13 - Phenotypic assessment of 3D skin models following infection and treatment with biocidal agent

Burned infected skin models infected with *P. aeruginosa* and treated with silver nitrate, isothiazolone and hydrogen peroxide, immunopositivity for collagen type IV, PCK, cytokeratin 10 and cytokeratin 14 were moderately disrupted with complete detachment of the overlying epidermis in middle of tissue. In the peripheral parts of the tissue model collagen type IV immunopositivity was decreased and the overlying epidermis was detached in some sites and preserved in others (Collagen type IV: Figure 5.19 & Figure 5.20; PCK: Figure 5.22 & Figure 5.23; Cytokeratin 10: Figure 5.25 & Figure 5.26; Cytokeratin 14: Figure 5. 28 & Figure 5. 29). Whilst burned *P. aeruginosa* infected skin model

treated with honey, displayed improved maintenance of immunopositive staining for collagen type IV, PCK, cytokeratin, cytokeratin within the centre of the model, with only minimal decrease in staining seen (Collagen type IV: Figure 5.20; PCK: Figure 5.23; Cytokeratin Figure 5.26; Cytokeratin Figure 5. 29). The edges of the 3D skin model infected with *P. aeruginosa* maintained expression comparable to control models (Collagen type IV: Figure 5.20; PCK: Figure 5. 23; Cytokeratin Figure 5.26; Cytokeratin Figure 5.29).
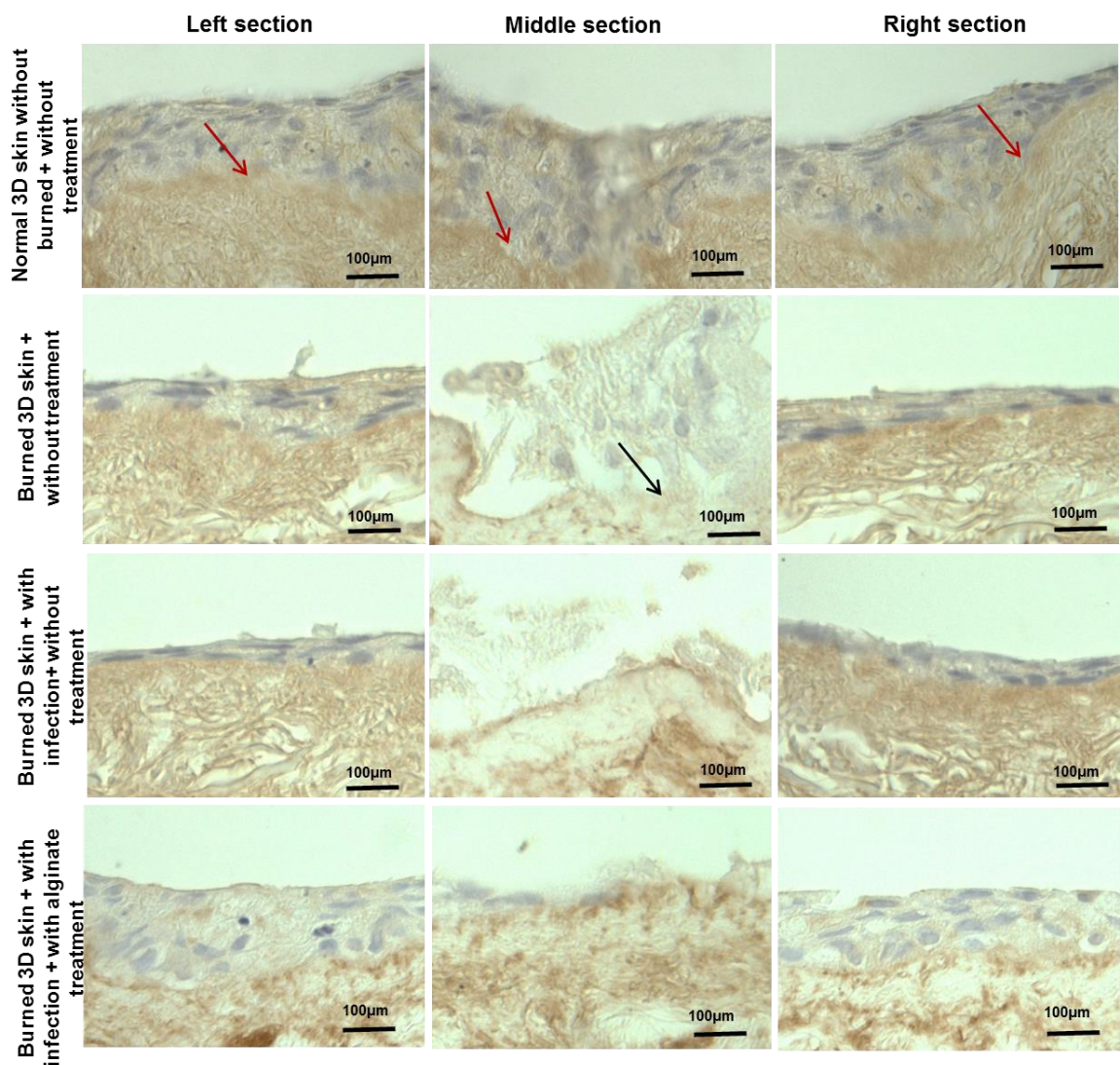
Figure 5.18 : Effect of biocidal agents on 3D skin tissue burned with and without *p. aeruginosa* infection, Collagen type IV antibody marker compared between non burned and no infection, controls , burned non infection without biocidal treated, burned infected without biocidal treated and burned infected with alginate treated. The three pictures shown in each row are left, middle and right tissue. Black arrow is immunonegative; red arrow is immunopositive. Scale bar = 100µm.
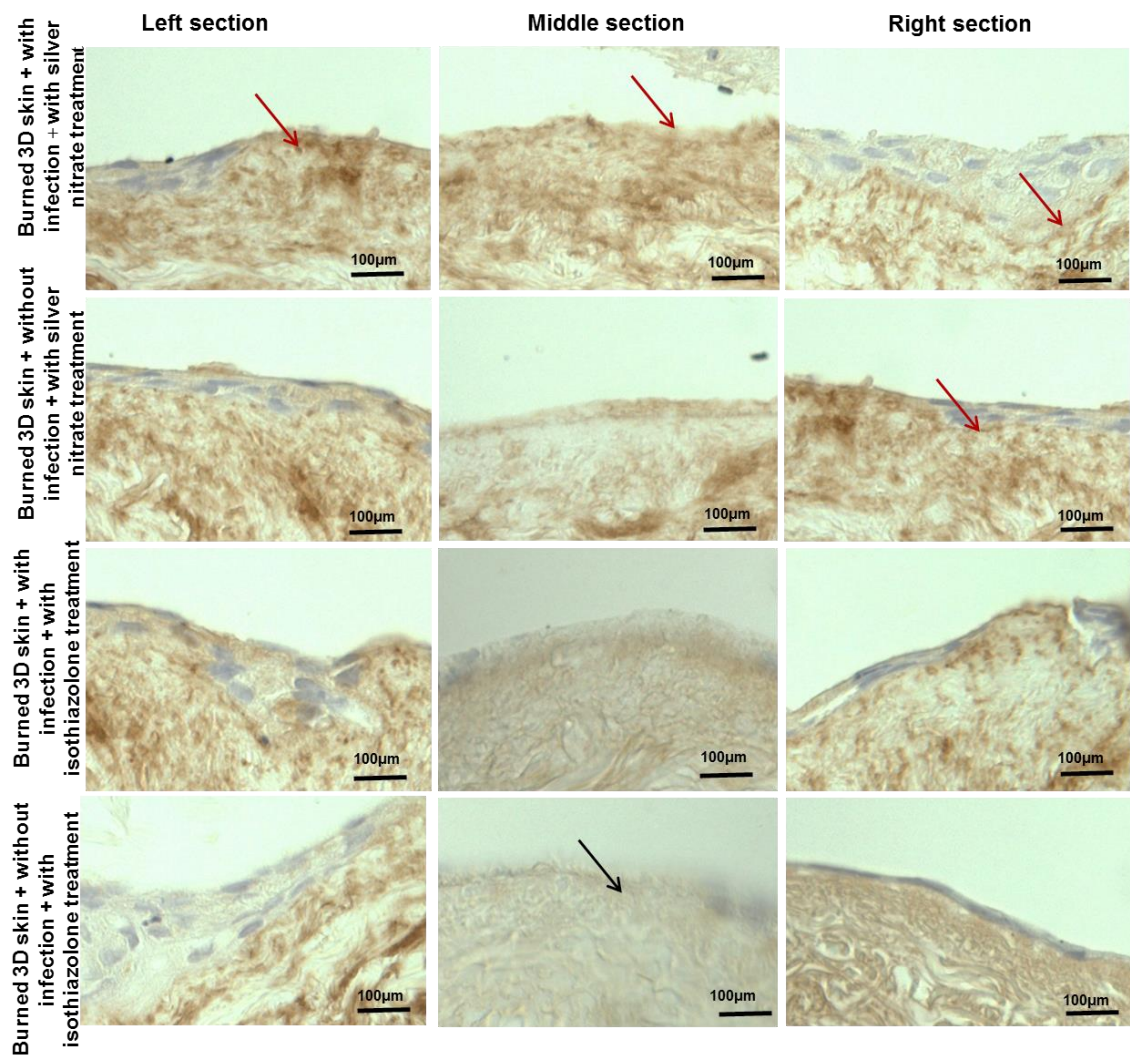
Figure 5.19: Effect of biocidal agents on 3D skin tissue burned with and without *P. aeruginosa* infection, Caspase 3 antibody marker compared between burned, with or without bacterial infection, and silver nitrate treatment; burned, with or without bacterial infection, and Isothiazolone treatment. The three pictures shown in each row are left, middle and right tissue. Black arrow is immunonegative; red arrow is immunopositive. Scale bar = 100µm.
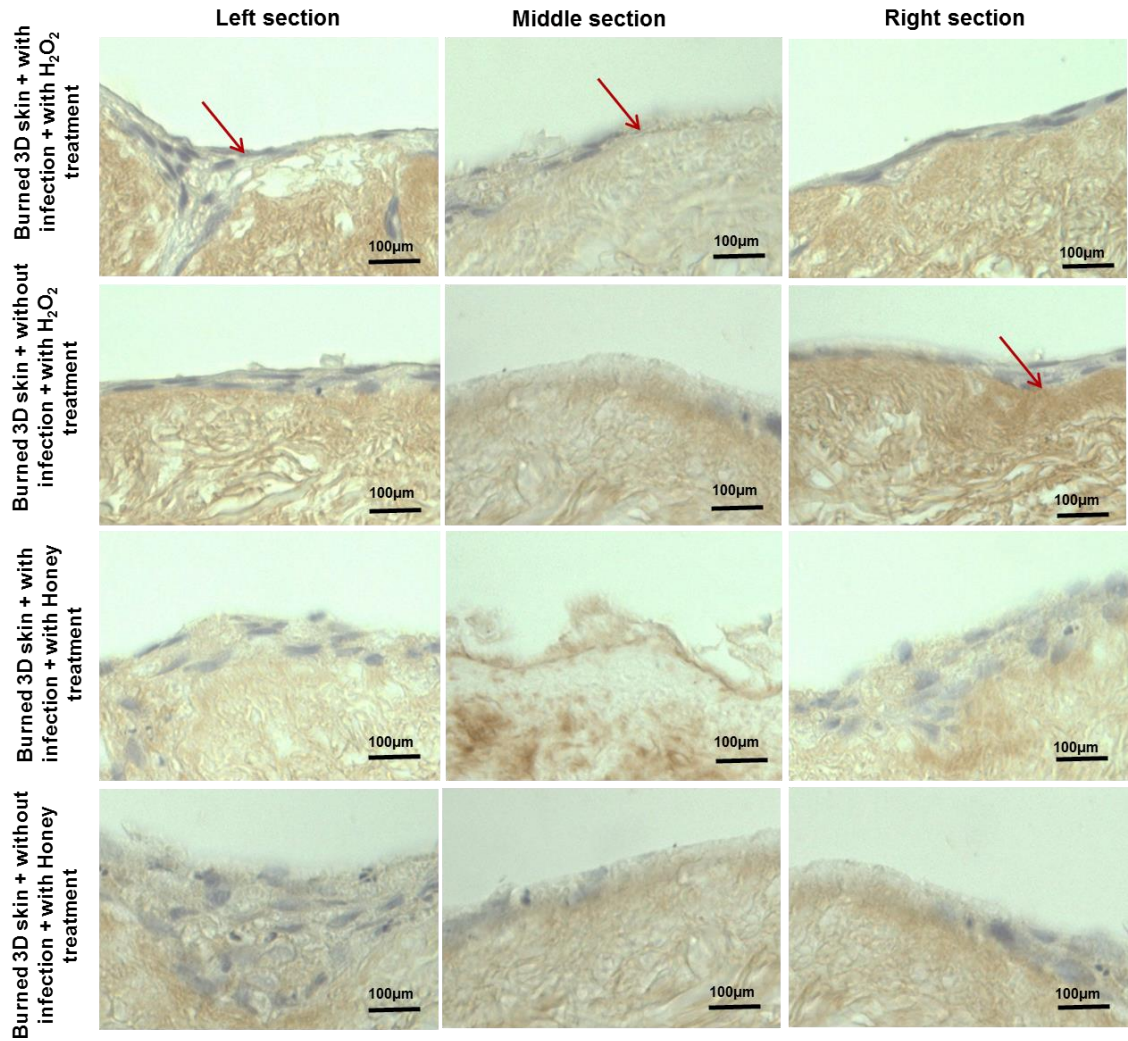
Figure 5.20: Effect of biocidal agents on 3D skin tissue burned with and without *S. aureus* infection, Collagen type IV antibody marker compared between burned, with or without bacterial infection, and H_2O_2 treatment; burned, with or without bacterial infection, and Clinical Manuka honey treatment. The three pictures shown in each row are left, middle and right tissue. Red arrow is immunopositive with no visible cell nuclei. Scale bar = 100µm.
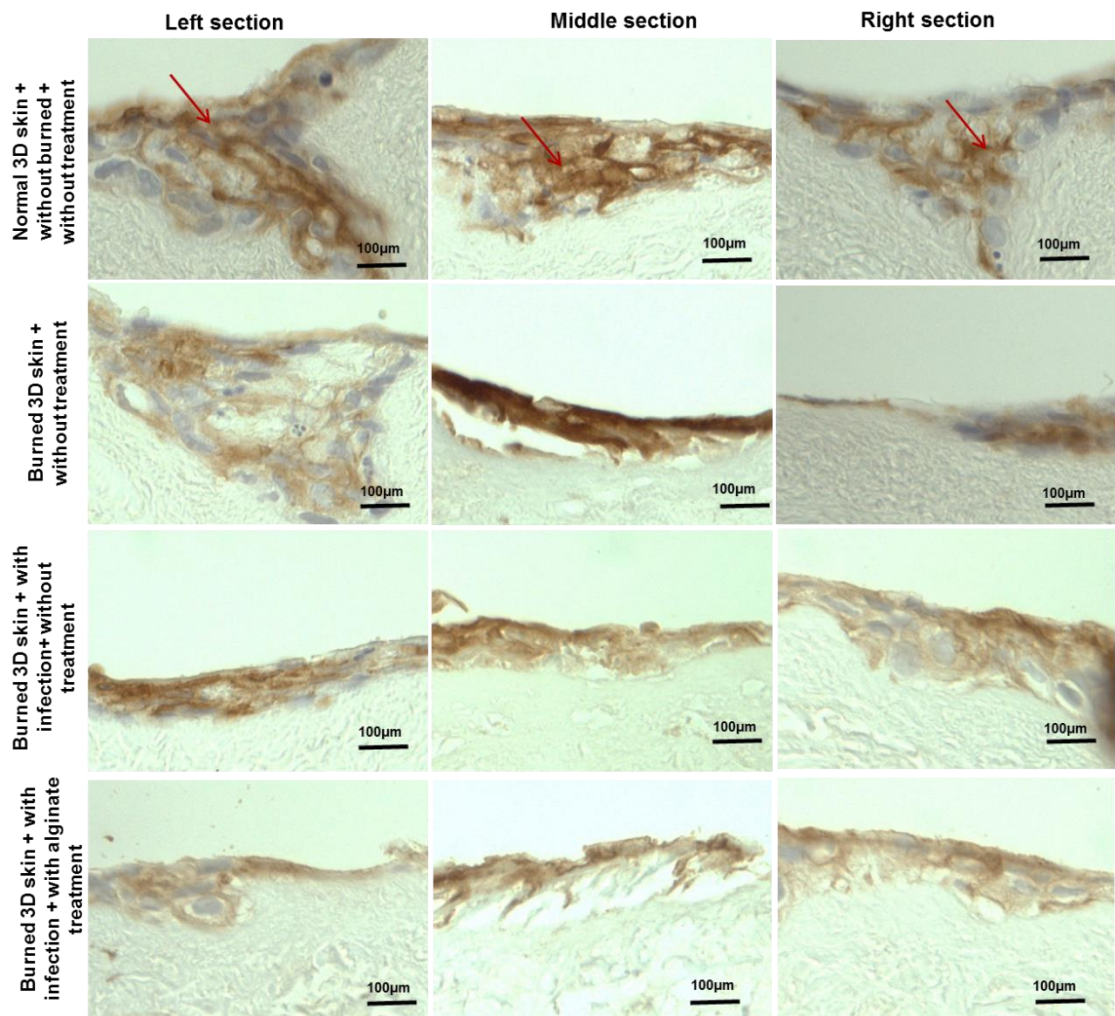
Figure 5.21: Effect of biocidal agents on 3D skin tissue burned with and without *P. aeruginosa* infection, Pancytokeratin antibody marker compared between burned, with or without bacterial infection, and silver nitrate treatment; burned, with or without bacterial infection, and Isothiazolone treatment. The three pictures shown in each row are left, middle and right tissue. Red arrow is immunopositive. Scale bar = 100µm.
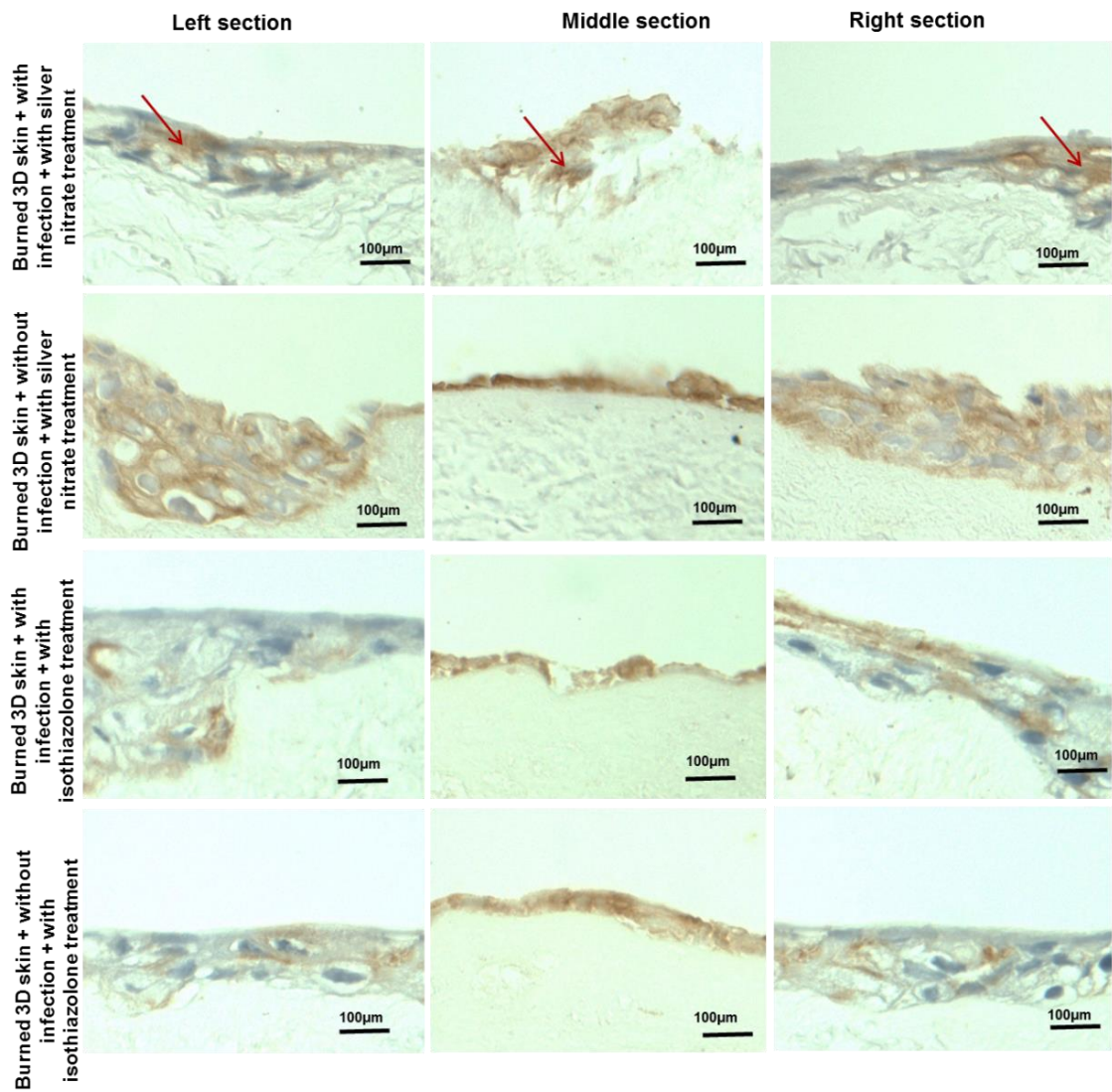
Figure 5.22: Effect of biocidal agents on 3D skin tissue burned with and without *P. aeruginosa* infection, Pancytokeratin antibody marker compared between burned, with or without bacterial infection, and silver nitrate treatment; burned, with or without bacterial infection, and Isothiazolone treatment. The three pictures shown in each row are left, middle and right tissue. Red arrow is immunopositive Scale bar = 100µm.
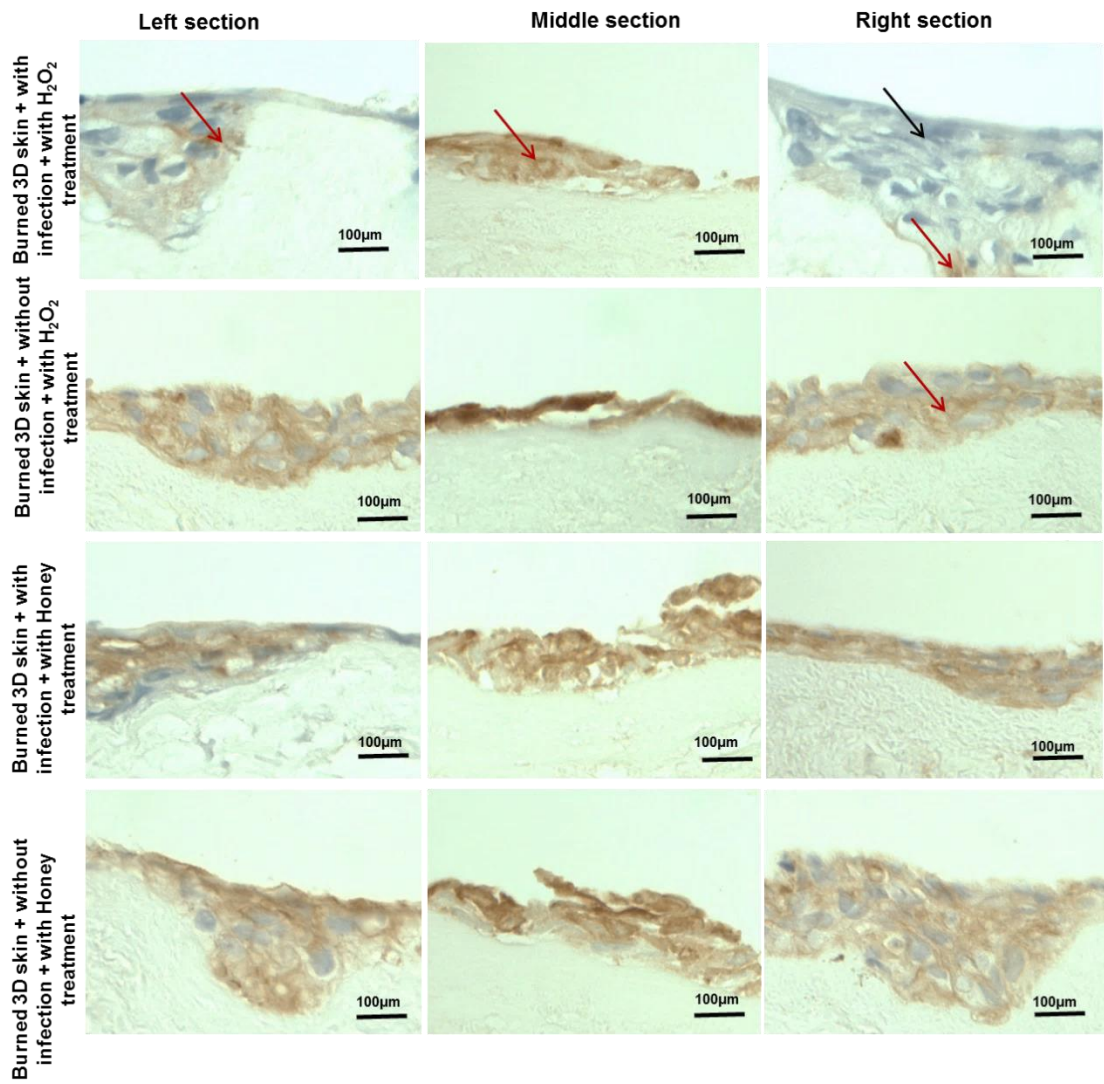
Figure 23: Effect of biocidal agents on 3D skin tissue burned with and without *P. aeruginosa* infection, Pancytokeratin (PCK) antibody marker compared between burned, with or without bacterial infection, and H$_2$O$_2$ treatment; burned, with or without bacterial infection, and Clinical Manuka honey treatment. The three pictures shown in each row are left, middle and right tissue. Black arrow is immunonegative; red arrow is immunopositive. Scale bar = 100µm.
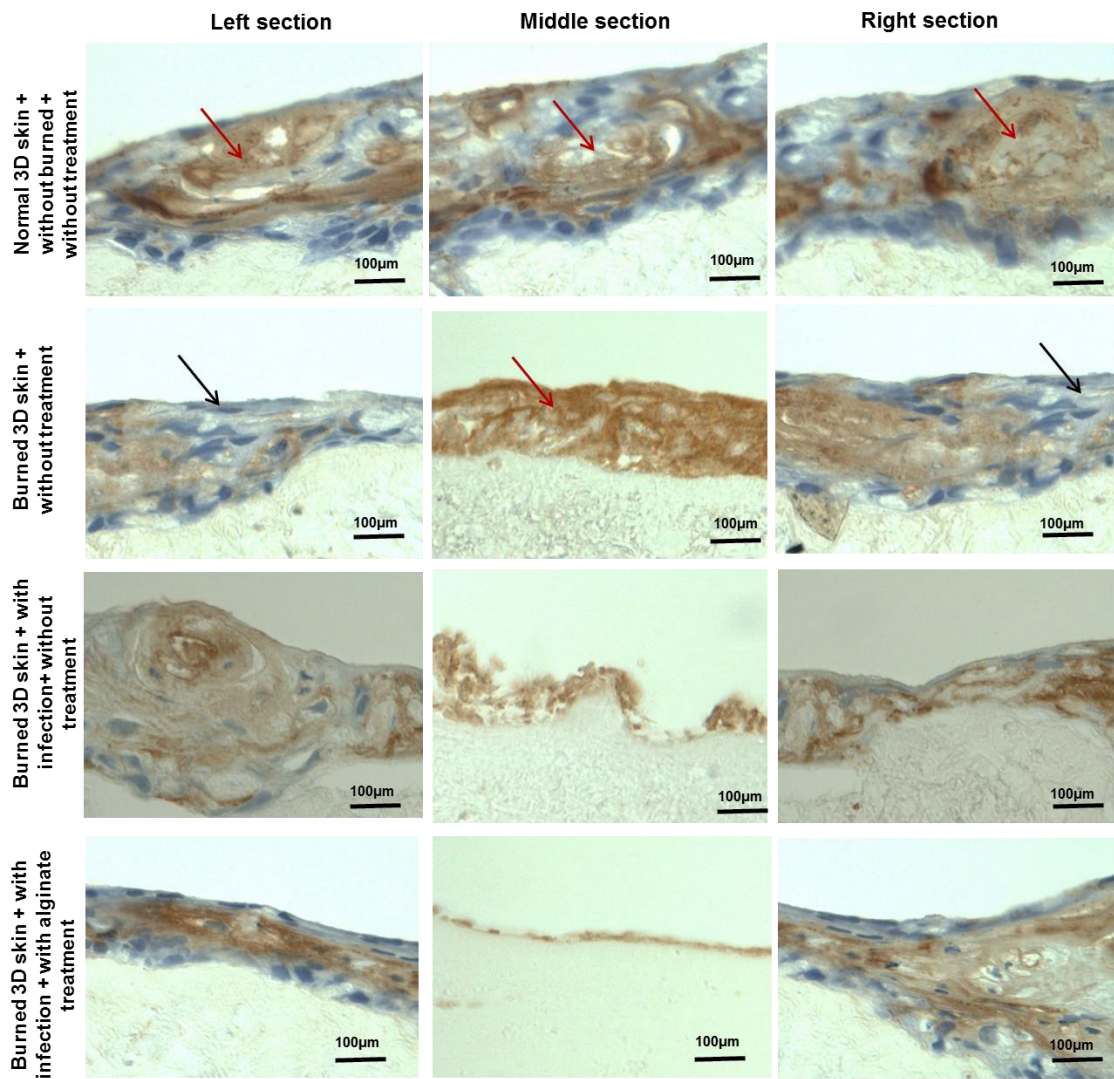
Figure 5.24: Effect of biocidal agents on 3D skin tissue burned with and without *P. aeruginosa* infection, Cytokeratin 10 antibody marker compared between non burned and no infection, controls , burned non infection without biocidal treated, burned infected without biocidal treated and burned infected with alginate treated. The three pictures shown in each row are left, middle and right tissue. Black arrow is immunonegative with no visible cell nuclei; red arrow is immunopositive Scale bar = 100µm.
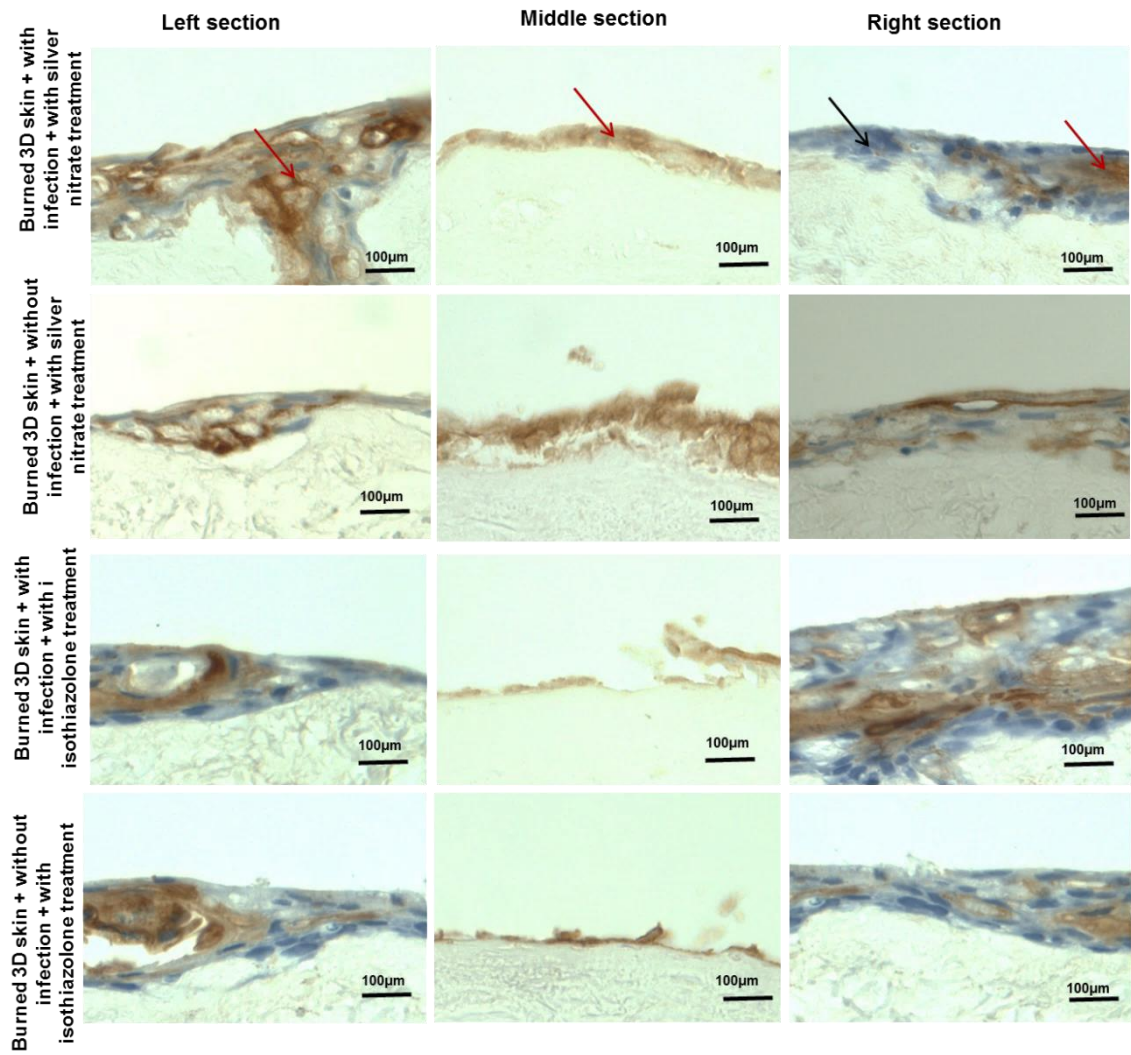
Figure 5.25: Effect of biocidal agents on 3D skin tissue burned with and without *P. aeruginosa* infection, Cytokeratin 10 antibody marker compared between burned, with or without bacterial infection, and silver nitrate treatment; burned, with or without bacterial infection, and Isothiazolone treatment. The three pictures shown in each row are left, middle and right tissue. Black arrow is immunonegative; red arrow is immunopositive Scale bar = 100µm.
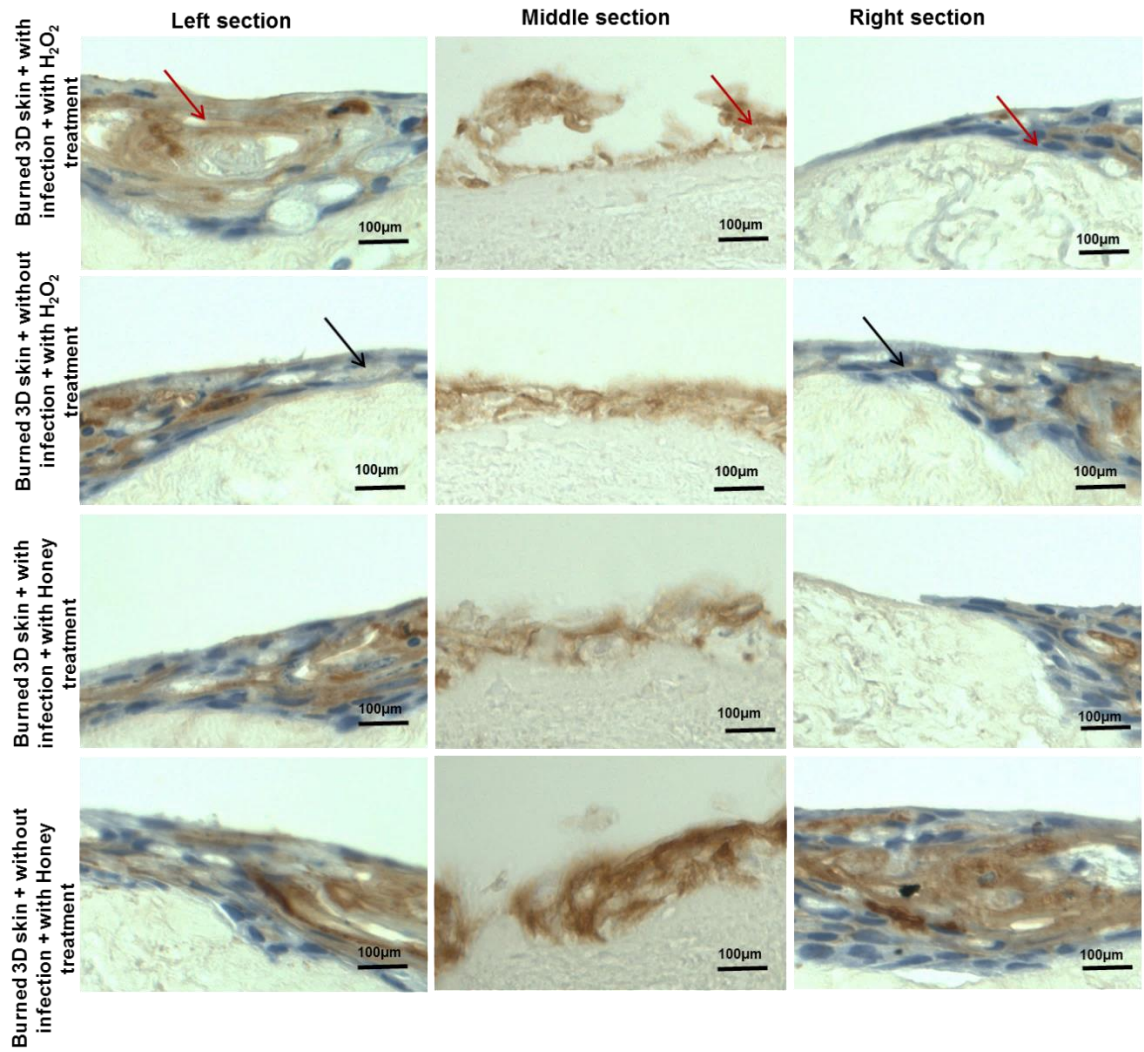
Figure 5.26: Effect of biocidal agents on 3D skin tissue burned with and without *P. aeruginosa* infection, Cytokeratin 10 antibody marker compared between burned, with or without bacterial infection, and H_2O_2 treatment; burned, with or without bacterial infection, and Clinical Manuka honey treatment. The three pictures shown in each row are left, middle and right tissue. Black arrow is immunonegative; red arrow is immunopositive Scale bar = 100µm.
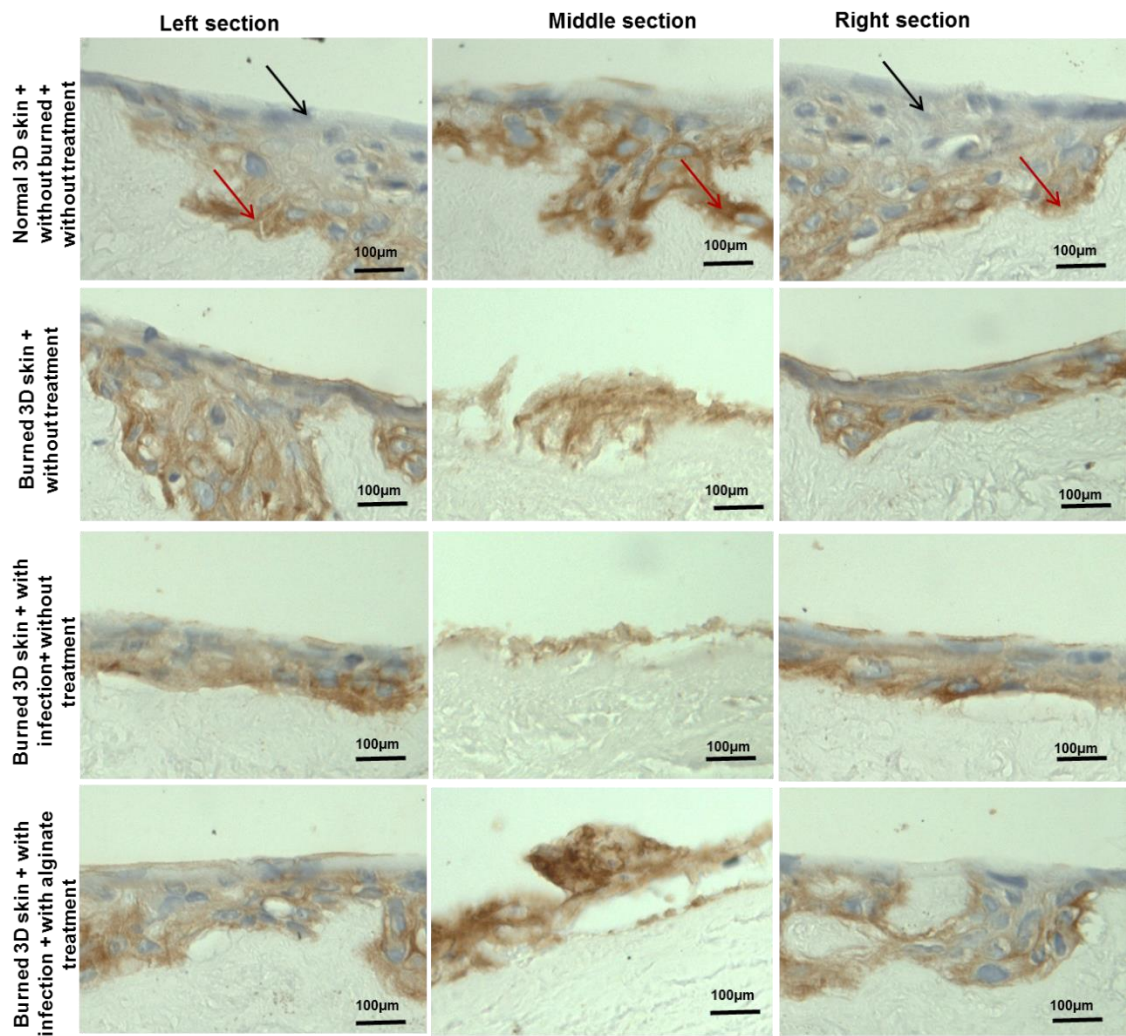
Figure 5.27: Effect of biocidal agents on 3D skin tissue burned with and without *S. aureus* infection, Cytokeratin 14 antibody marker compared between non burned and no infection, controls , burned non infection without biocidal treated, burned infected without biocidal treated and burned infected with alginate treated. The three pictures shown in each row are left, middle and right tissue. Black arrow is immunonegative; red arrow is immunopositive. Scale bar = 100µm.

227
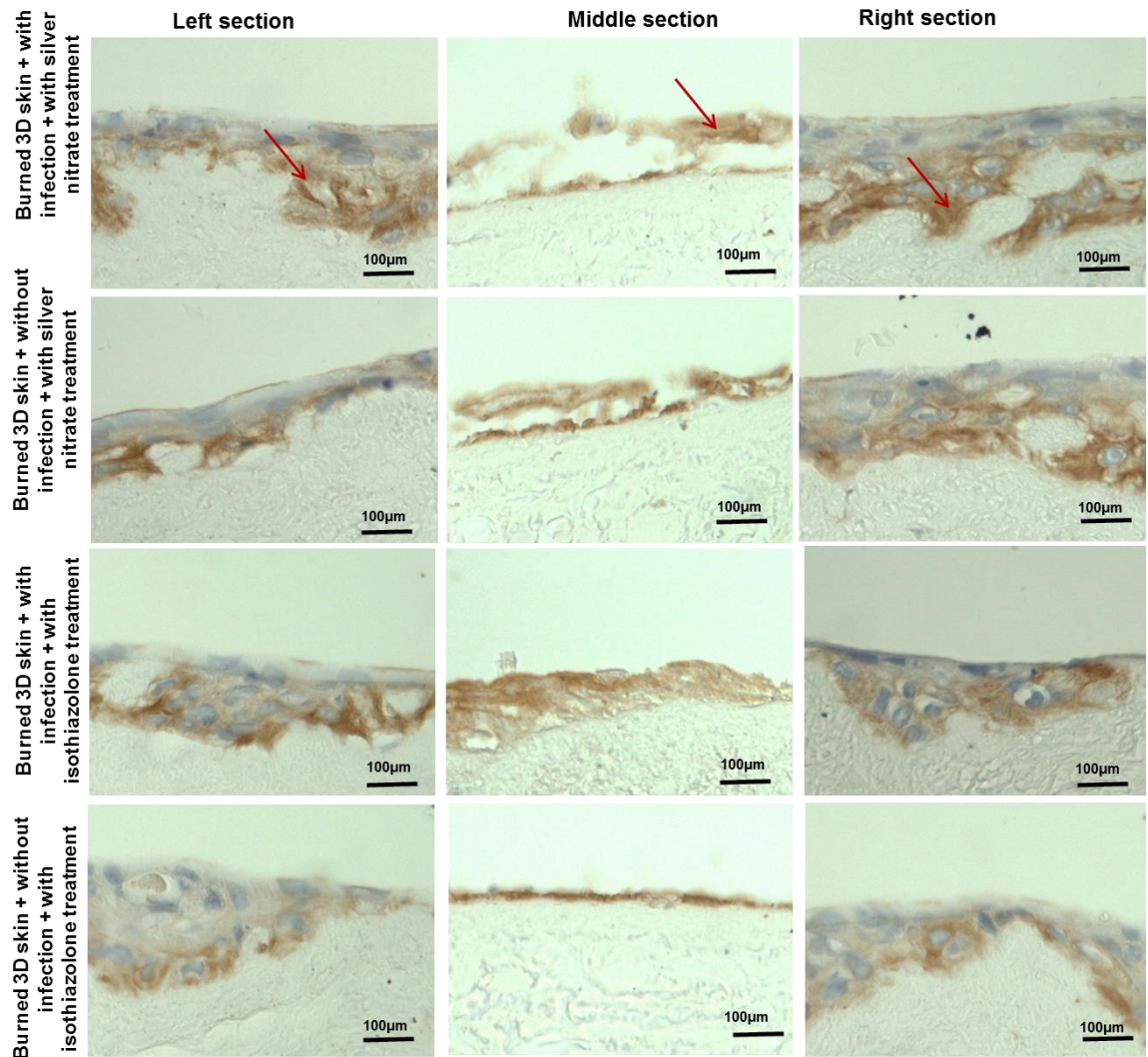
Figure 5.28: Effect of biocidal agents on 3D skin tissue burned with and without *S. aureus* infection, Cytokeratin 14 antibody marker compared between burned, with or without bacterial infection, and silver nitrate treatment; burned, with or without bacterial infection, and Isothazoline treatment. The three pictures shown in each row are left, middle and right tissue. red arrow is immunopositive. Scale bar = 100µm.
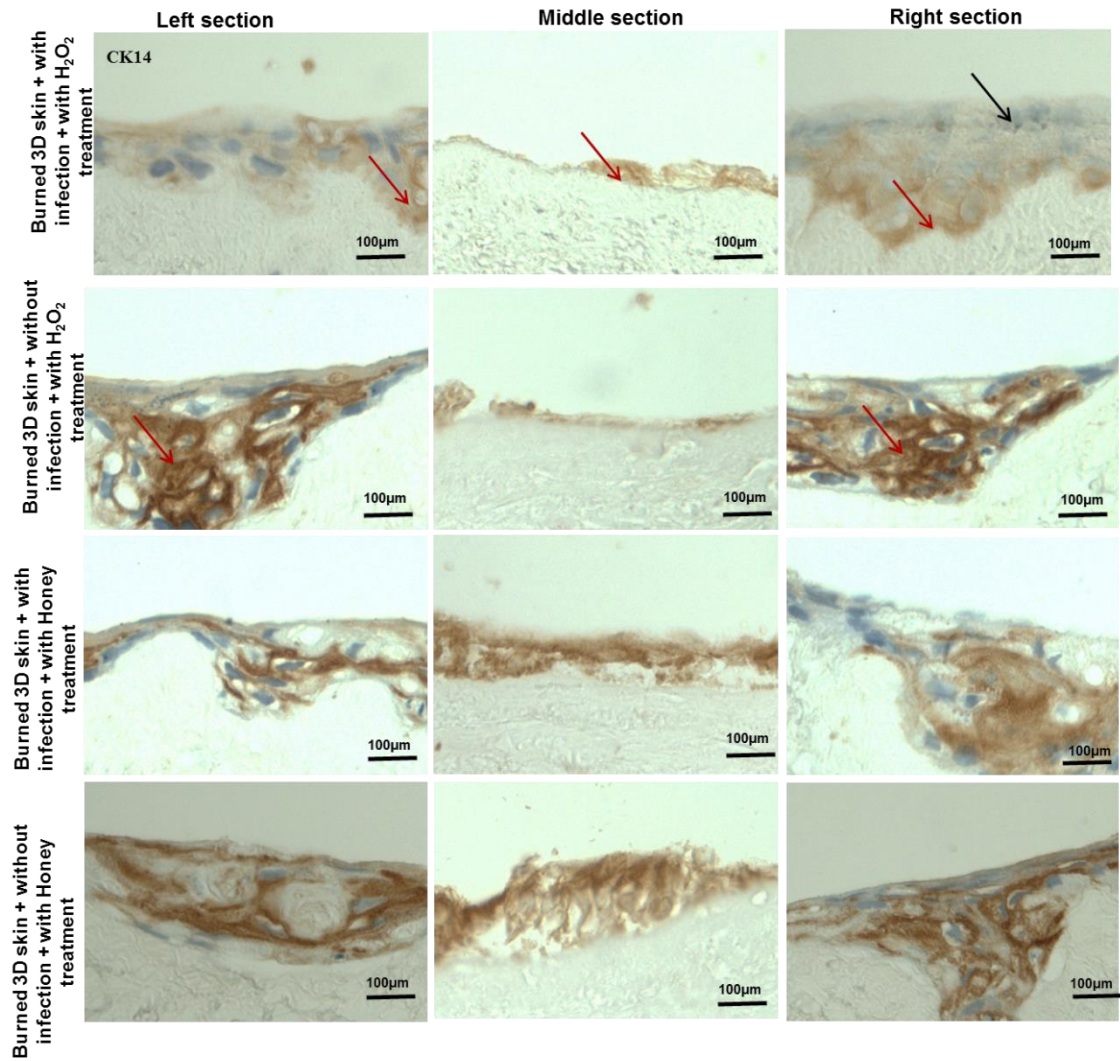
Figure 5.29: Effect of biocidal agents on 3D skin tissue burned with and without *P. aeruginosa* infection, Cytokeratin 14 antibody marker compared between burned, with or without bacterial infection, and H_2O_2 treatment; burned, with or without bacterial infection, and Clinical Manuka honey treatment. The three pictures shown in each row are left, middle and right tissue. Black arrow is immunonegative; red arrow is immunopositive. Scale bar = 100µm.

5.4- Discussion

This chapter developed a 3D burned skin model infected with *P. aeruginosa*. While *P. aeruginosa* colonizes both the skin and anterior nares in approximately 22% (Palavutitotai *et al.* 2018) of individuals in good health compared to 25-30% of individuals with *S. aureus* (Kluytmans *et al*, 1997; Zanelli *et al.* 2002; Kuehnert *et al.* 2006), the microbe is one the most frequent agents responsible for infections of the skin and soft tissues (Dou *et al.* 2017). Further, carrying this pathogen has been reported as a risk factor for a range of types of morbidity and mortality, including possible infections following surgery (Kluytmans *et al.* 1997).

As antibiotic resistant forms of *P. aeruginosa* have emerged, simultaneously with failures in treating infections through antibiotics, this suggests that new approaches to treatment are needed. The skin infection model developed in this chapter could be used as a key tool in developing these treatments. Prior work on skin infections have mainly utilised small mammals to model such infections (Khavari 2006; Malachowa *et al.* 2013). However, while these studies provide large quantities of data, the skin of humans and animals such as rodents differ in many ways. Mature mice have thin layers in the epidermis in comparison to human skin, and these have a far greater concentration of hair follicles (Khavari 2006). Using a 3D human skin model comes closer to imitating human skin infections (Mertz *et al.* 1987; Svedman *et al.* 1989; Davis *et al.* 2008; Hirsch *et al.* 2008), although it presents limitations, such as the high cost and doesn't contain an immune system. Further, animal models come with ethical concerns, including the quantity of animals required for research purposes, and *in vitro* modelling can usefully decrease the numbers used for experiments, by introducing pre-screening.

To date, no study has been reported which has investigated the direct antibacterial effects of biocides using 3D skin tissue models. In our model, burned infected skin models were created. These utilized the 3D model developed in chapter 2 together with methodology utilised by Shepherd *et al.*, 2009, where 3D skin models were infected with *S. aureus* (Chapter 4) and *P. aeruginosa*. However, this project used Euro skin bank DED and HaCaT cell line, rather than using primary keratinocytes human cells and donor hospital skin as scaffold, which could be a model which could easily be utilised in a wide number of laboratories.

In this chapter *P. aeruginosa* was applied in the *in vitro* skin model based on its suitability to be used to model and assess the growth of bacterial biofilms. *P. aeruginosa* in a young biofilm was formed on the burned skin models using an inoculum of 1×10^6 and 24hr culture. The bacterial biofilm matured successfully in the burned 3D skin model. The *P. aeruginosa* biofilm showed rapid growth following culture for 24 hours, with multiple clusters of bacteria observed within a biofilm matrix.

The number of bacteria used in the 3D skin model is similar to the number of bacteria used in 3D skin models presented in chapter 4. Following 24h of biofilm culture the bacterial counts observed (approximately 1×10^8), were similar to those reported by Shepherd (2009 and 2011), who reported a bacterial inoculum rate for *P. aeruginosa* of 1×10^7 bacteria at 24 hours. In contrast, Mertz *et al.*, (1987) demonstrated optimal bacteria-wound adherence when they modelled infection in pigs. The researchers reported an optimal inoculum rate of 1×10^8 cells for *P. aeruginosa* or *S. aureus.*

Based on the 3D model developed, a number of biocidal agents were investigated to inhibit the load of *P. aeruginosa* within 3D skin models. The alginate gel served as a medium to hold biocides; it was used as a treatment control in order to assess bacterial growth. The findings demonstrated that the bacterial agents remained viable, not being affected by the alginate while each of the silver nitrate, 2- Methyl -4- isothiazolone -3-one and hydrogen peroxide significantly reduced *P. aeruginosa* in skin model infection. However, Manuka honey showed the most significant effect.

This study assessed the efficiency of 62 .5 µg/ml of silver nitrate which was the planktonic MIC determined in chapter 2 applied to the 3D skin model infected with *P. aeruginosa*. Silver nitrate decreased *P. aeruginosa* colonies on the skin by 1.26 $\log_{10}$. Whilst Schierholz *et al.*, (1999) investigated an *in vitro* biofilm model on catheter tubing inoculated with *E. coli* ATCC 11229, *S. aureus* ATCC 6538 and *S. epidermidis* DSM 3269. Treatment of these bacterial biofilms on catheter tubes with silver nitrate (for *E. coli*, 32 µg/ml; for *S. aureus* and *S. epidermidis*, 256 µg/ml), incubated for 24 or 48 h at 37°C resulted in 5 $\log_{10}$ reduction in bacterial counts after 48 hours (Schierholz et al., 1999). These results suggest increased sensitivity seen compared to the current study, however biofilms on skin and cathers are likely to be very different, furthermore concentrations and duration of treatment in Schierholz *et al., (*1999) study were higher and longer than those investigated in the current study.

The current research project found the H_2O_2 (0.046v/v) on biofilms lasting for 24 hours in comparison with planktonic forms. The finding is in line with the results displaying the use of H_2O_2 which caused a reduction of 1.39 $\log_{10}$ to eliminate biofilms when low concentrations were used. Stewart *et al.*, (2000) found incomplete penetration of 50 mM H_2O_2 against *P. aeruginosa* biofilms and

a minor loss of viable cells in biofilms. Biofilms were formed by the *katA* mutant; the result was that biofilm was partially killed, while in case of *katA* mutant, the biofilms were fully penetrated by H_2O_2. *katA* mutant was significantly less susceptible to H_2O_2 in the biofilm (Stewart *et al*. 2000). Stewart *et al*. (2000) found that hydrogen peroxide had the same effect on both viable mass and biofilm matrix in *P. aeruginosa* and *S. aureus* biofilm.

Many studies have reported that antibacterial activity of honey differs with respect to the source of honey plants (Lusby *et al.* 2005; French *et al.* 2005; Wilkinson & Cavanagh 2005). In this study, it was found that the treatment of biofilm with honey significantly reduced the *P. aeruginosa*, when the culturing strains were used with medical grade manuka honey. The reduction of *P. aeruginosa* was 1.99 log_{10} which was similar to that seen with *S. aureus* (1.9, log_{10}) (Chapter 4, section 4.3.2).

These results are in agreement with those reported by Lusby *et al.*, (2005), French *et al.*, 2005 and Wilkinson *et al.*, (2005), who demonstrated that *P. aeruginosa* and *S. aureus* were affected by honey concentrations ≥ 3%, with the bactericidal effect of medical grade Manuka honey being dependant on the concentration and type of bacteria.

To determine the efficacy of biocides with respect to maintenance of mammalian cell phenotypes, and hence potential wound healing following burn injury and *P. aeruginosa* infected skin models. Immunohistochemistry was used to investigate phenotypic markers of the cells. Immunonegative cells were generally seen in all infected models in the middle of the models with complete detachment of the epidermis in parts of the tissue, whilst the peripheral parts of the model were immunopositive for the keratinocyte and fibroblast markers. However improved maintenance of tissue structure and phenotype was seen

following Manuka Honey treatment. Shepherd *et al.*, (2009) also reported loss of the epidermal layers and normal keratinocytes layer following *P. aeruginosa* infection. In addition, the pentation of *P. aeruginosa* reported in this thesis of 341.8 ± 21 µm, was similar to the 400- 500 µm shown by Shepherd *et al.*, 2009. Within the current study *P. aeruginosa* was quantified at 3h, 6h, and 24h to investigate the formation of the biofilm and the efficacy of Manuka Honey during biofilm formation. Manuka honey decreased CFU/ml at all time points however effects were greatest in the more immature models, where migration and penetration were also inhibited.

The immunohistochemical staining was applied to the target of *P. aeruginosa*: (Anti Exotoxin A, Anti *P. aeruginosa*, Anti Flagellin and Exoenzyme S). When the histological investigation was carried out on immunochemical 3D skin sections, it was found out that *P. aeruginosa* which infected 3D skin tissue attached to the upper layer of keratinocytes, resulting in removal of the epidermal layers, with infiltration into and across the dermis layer seen with increasing infectivity time. This might be explained by the fact that the *P. aeruginosa* had enough time to develop a mature forming biofilm. Increased time of infection supported the development of bacterial biofilms, augmented the migration and penetration potential, and reduced the effectivness of the Manuka Honey.

The data presented in this thesis demonstrated silver nitrate, 2- methyle -4-isothiazolone -3-one and hydrogen peroxide had a toxic effect on mammalian cells in the tissue, which was not seen following Manuka honey treatment. Furthermore Manuka honey was seen to inhibit bacterial penetration although this was most effective in immature biofilms. Roberts *et al.*, (2014) demonstrated that Manuka honey reduced *P. aeruginosa* swimming motility due to de-flagellation of *P. aeruginosa*. They attributed that to fact that flagellin

associated gens: *fliA, fliC, flhF, fleN, fleQ* and *fleR* were inhibited (Roberts *et al.,* 2014). This could be the mechanism reducing migration of *P. aeruginosa* bacteria across the skin models, but this would need further investigation. Histological investigation of the tissue showed that a high number of *P. aeruginosa* persisted on the surface and deep into the tissue section. Viable *P. aeruginosa* appeared in skin sections treated with honey but their number was fewer than those of the bacteria within untreated controls. *P. aeruginosa* bacterial numbers were significantly decreased by manuka honey. A proportion of bacteria in the tissues still showed viability after the biocidal agents were applied. Moreover, Manuka honey treatment of bacterial infected 3D skin model showed a decrease in the death zone where the skin was infected by *P. aeruginosa* when compared with the control test.

5.5- Conclusion

This study applied a 3D skin model which was burned and infected with *P. aeruginosa*, demonstrating migration and penetration of bacteria through the skin model. Infection resulted in toxicity to the mammalian cells, which was further increased by some of the biocidal agents investigated. Manuka Honey however, reducing mammalian cell death zones and was found to be the most effective agent at reducing numbers of bacteria, migration and penetration of bacteria. Thus, this model system has shown promise to increase the understanding of the effect of antimicrobial biocides on bacteria and skin models. Manuka honey was shown to be the most promising biocidal agent investigated, however the high toxicity of biocides (silver nitrate, 2- methyle -4- isothiazolone -3-one and hydrogen peroxide) on the mammalian cells demonstrate that alternative antimicrobial strategies may be required.

Chapter 6

Effect of low frequency ultrasound on planktonic bacteria

6.1- Introduction

Management of wound infection presents a challenging problem to healthcare authorities and represents a significant healthcare burden financially. The development of wound infection is dependent on several complex factors including, but not limited to, patient age, preoperative stays in hospital for surgical wounds, subcutaneous oxygen tension and early colonisation by biofilm-forming bacteria and host immune response (Mishriki *et al.* 1990, Hopf *et al.* 1997), and can seriously affect the quality of life of affected individuals. Skin infections can be caused by a range of pathogens including viruses, bacteria, and fungi (O'Dell 1998) and are common in cases of thermal injuries (Church *et al.* 2006) and in chronic wounds such as diabetic ulcers (Jeffcoate & Harding 2003). Currently, there is a global rise in bacterial infection of wounds that, at least in part, correlates with the increasing number of elderly patients encountered in our health system, exacerbated by their increased risk of injury as well as the increase in certain medical conditions such as diabetes combined with the rise in antibiotic resistant bacteria (Sen *et al*. 2009). However, the increase in antibiotic resistance coupled with the increase in hospital acquired infections such as healthcare acquired methicillin resistant *Staphylococcus aureus* (HA-MRSA) has led to the search for alternative therapies.

Studies have shown that ultrasound can be used in conjunction with antibiotics to treat infection (Ensing *et al*. 2006; Carmen *et al*. 2004; Rediske *et al*. 1998; Williams & Pitt 1997; Rediske *et al*. 2000; Yua *et al.* 2011).

This method relies on ultrasound causing an increase in membrane permeability allowing large molecules such as antibiotics to enter the infected cells (Runyan *et al*. 2006) which increases efficacy of antibiotic delivery and

aids wound healing. Acoustic cavitation caused by ultrasound at lower frequencies, in which tiny bubbles form in surrounding liquids and rapidly collapse with a huge increase in local pressure and shear stresses is one mechanism by which ultrasound itself may have antibacterial properties (Erriu *et al.* 2014; Scherba *et al.* 1991).

Previous chapters in this thesis have demonstrated that biocidal agents, whilst showing promise for antibacterial properties also affect mammalian cells. Thus, alternative less toxic methods such as ultrasound were investigated within this chapter to determine novel therapies which could be used alone or in combination with biocidal agents. This chapter aims to discuss the current understanding of ultrasound and its potential use in skin therapies.

6.1.1- Nature of ultrasound (US)

Ultrasound is a wave of rapidly moving molecules, which are generated by a vibrating source causing pressure variation in the surrounding medium (gas, liquid or solid). The pressure variation leads to consecutive mechanical compression and rarefaction on the molecules of the medium in close contact to the source, causing movement of these molecules in the exact pattern of the source (Figure 6.1). This movement pattern is propagated outwards through the rest of the molecules of the medium with the same pattern, forming ultrasound waves (O'Brien 2007), in a similar way to sound waves.

Sound waves are audible (mechanical waves of frequencies between 20 Hz and 20 KHz – that is, 20 cycles per second to 20,000 cycles per second.

The waves below 20 Hz (infrasound) or greater than around 20 KHz (Ultrasound) are inaudible to humans, though they are still 'sounds' in the sense of still being mechanical waves of the same nature propagating in a medium, and may still be audible to certain animals e.g. bats and whales. (O'Brien 2007).

Ultrasound waves are modified by the medium they pass through, whether biological or non-biological. The medium properties impose influences on the ultrasound waves, thus change its original pattern. The medium affects ultrasound waves by either absorption or scattering. Absorption is associated with temperature changes in the medium, due to the change conversion of the kinetic energy of the ultrasound waves into heat, an effect which is described as a thermal effect. The longer the distance the wave travels through the medium, the lower the amplitude of the wave and the higher the temperature of the medium. Scattering deviates the direction of the ultrasound wave, and is not associated with energy transfer, thus, has a non-thermal effect. Yet, both absorption and scattering are associated with attenuation of ultrasound waves (O'Brien 2007).

6.1.2- Diagnostic and therapeutic ultrasound

6.1.2.1: Diagnostic ultrasound

Since US waves are absorbed or scattered when passing through living tissues with variable degrees according to the density of these tissues, the resultant modulations in US can delineate these tissues. This phenomenon is used to visualise internal organs including the liver, spleen, kidneys, heart or blood vessels. In case of disease, the size and/or the density of these organs change, thus US has been exploited as a diagnostic tool (Fikri *et al.* 2011).

6.1.2.2: Therapeutic US

Therapeutic US is exploiting US to produce changes in living tissues, as opposed to simply imaging them. They are usually continuous rather than being delivered in pulses (Figure 6.1). Therapeutic ultrasound is categorised into two classes, low intensity, up to 3 W/cm^2, which serve to stimulate or accelerate

biological processes and high intensity, over 5 W/cm^2, aiming to selectively destroy tissues (Ter Haar 1999; Xin *et al.* 2016).

High intensity ultrasound is further classified into low frequency ultrasound (LFU), ranging from 20 kHz to a few hundred kHz and high frequency US of 1 MHz and above (Ter Haar 1999). Another classification is based on whether ultrasound waves are passed via a coupling medium directly from the transducer into the target tissues directly or indirectly, where the transducer is coupled to another tool for a specific application for the required task (Ter Haar 1999). Therapeutic uses of ultrasound are numerous; for instance, in cancer therapy, ultrasound is used to increase the drug absorption and to reduce the tumour cell burden (Kremkau 1979; Wood *et al.* 2015; Hsiao *et al.* 2016).

6.1.3- Mechanism of action of therapeutic ultrasound

The therapeutic effects of US on tissues are attributed to either the mechanical or the thermal effects, but the two effects usually co-exist, except in lithotripsy and other related situations. Mechanical effects or non-thermal occur where high power pulsed waves are applied for shorter than 1 second). But even then, some thermal effects will occur, especially with devices which produce continuous waves (Baker 2001, O'Brien *et al.* 2007. As a consequence, there is no concrete evidence that the biological effects are exclusively due to one mechanism rather than the other (Baker *et al.* 2001; O'Brien *et al.* 2007).
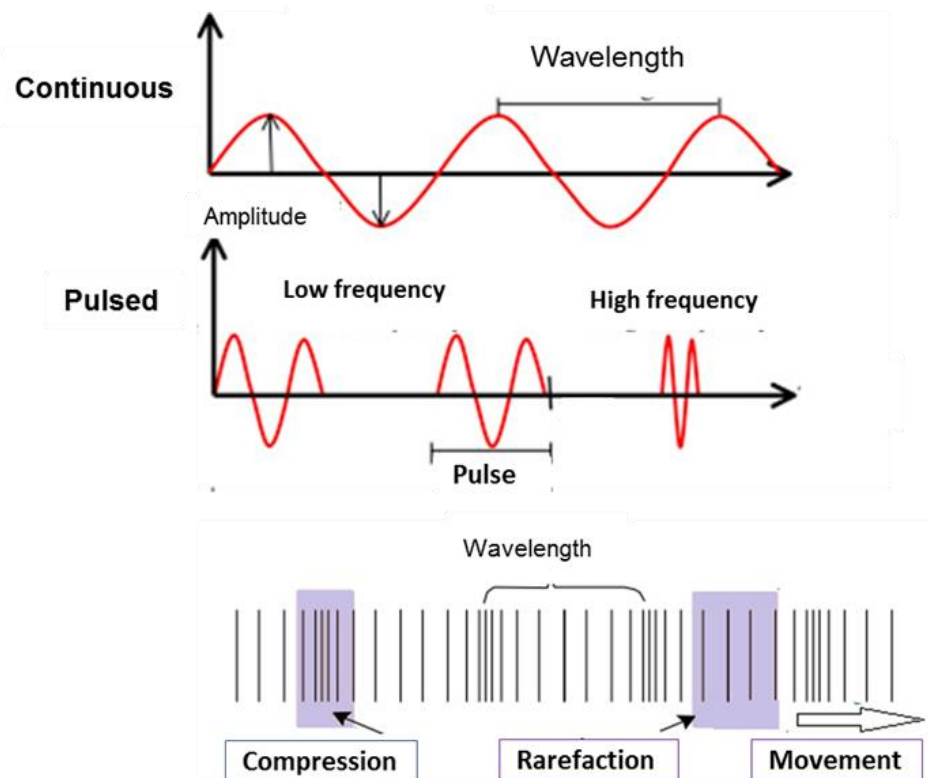
Figure 6.1: Mechanism of action of therapeutic ultrasound, the pressure variation lead to consecutive mechanical compression and rarefaction on the molecules of the medium in close contact to the source of wave.

6.1.4- Effect of Ultrasound on mammalian cells and wound healing

The therapeutic effects of ultrasound on injured or infected soft tissues have largely been controversial. While some studies denied the healing effects of ultrasound, others confirmed ultrasounds role in enhancing the rate of healing (Table 1). Some of the supporting studies showed that ultrasound treatment increased the strength of Achilles tendons of rats after being subjected to partial rupture (Frieder *et al*. 1988; Jackson *et al*. 2002). Along the same line, Byl *et al.,* (1993) found that ultrasound treatment increased collagen deposition and, hence, the tensile strength of skin tissues that have been subjected to wounds in Yucatan pigs (Byl *et al*. 1993).

Webster *et al.,* 1980 identified that ultrasound had an activating effect on fibroblasts inducing them to synthesise collagen. When fibroblasts subjected to

ultrasound, at 3 MHz, a space-time peak intensity of 0.5 Wcm^2 in the tissues underwent active molecular processes and morphological changes similar to those accompanying the synthesis of collagen, which is essential for healing. Doan *et al.* (1999) showed that *in vitro* cultures of human fibroblasts from muscle tissue subjected to ultrasound (15 and 30 mW/cm^2 for the 45-kHz continuous ultrasound, and 0.1 and 0.4 W/cm^2 for the 1 MHz pulsed ultrasound) were able to synthesize proteins in large amounts, as compared to non-sonicated control fibroblasts, and the fibroblast collagen production and glycosaminoglycan removal by ultrasound stimulation at the frequency of 1 MHz and an intensity of 0.2 W/cm^2 with a 20% duty cycle (Bohari *et al*. 2015).

Samuels *et al.,* (2013) were able to improve ulcer healing in both human skin ulcer and *in vitro* fibroblast models by subjecting them to 20 kHz of ultrasound for 15 minutes. They reported that their treatment was more effective than using higher frequency ultrasound for the same period (100 kHz for 15 min) or using the same frequency for longer duration (20 kHz for 45 min)(Samuels *et al* . 2013).

Wollina *et al* confirmed the increased healing potential of low frequency ultrasound; 34 kHz ultrasound was associated with significantly higher oxygen saturation and superficial concentration of haemoglobin at the ultrasound exposure site than ultrasounds of 53.5 and 75 kHz. Supporting the same view was the finding that residual burns showed complete healing with 25 kHz low-frequency ultrasound applied to the wounds every other day for a period of two weeks (Wollina *et al*. 2011).

Chang *et al.,* (2017) showed that low frequency ultrasound (20- 60 kHz), through the microsized gas bubbles they produce, enhanced wound healing by selectively emulsifying dead tissues, a process that can be considered as

micro-debridement. Debridement is the removal of dying and dead tissue which is crucial in the process of wound healing. In doing so, ultrasound waves stimulate the membranes of the adjacent healthy tissues.

Table 6.1; Effect of ultrasound on keratinocytes and fibroblasts

Authors	Mammalian cell	Frequency	Intensity	Conclusion
Zhou *et al.* 2004	Human fibroblasts	1.5 MHz	30 mW/cm^2	Reorganization of actin cytoskeleton and promoting of bigger DNA
Lai and Pittelkow 2007	Fibroblasts foreskin	40 kHz	0.002 W/cm^2	Biological effects as promote and amplification of vacuoles in cytoplasm.
Chen *et al.* 2007	(Embryonic mouse fibro-blast	1 MHz;	0.5 to 2 W/cm^2	Increase in gene transfer rate and a significant decrease on the number of cells.
Oliveira *et al.* 2008	Mouse fibroblast	1 MHz;	0.2 and 0.6 W/cm^2	Significance decrease on the number of cells.
Oliveira *et al.* 2008	Mouse fibroblast	1 MHz;	0.1, 0.2, 0.6, 0.8, 1.0 and 2.0 W/cm^2	Significant decrease on the number of cells.
Tomankova *et al.* 2009	NIH3T3 (mouse fibroblast cells) and B16FO (mouse melanoma cells)	1 MHz;	2 W/cm^2	Significance increase of cell proliferation.
Mostafa *et al.* 2009	Human gingival fibroblasts (HGF	1.5 MHz	30 mW/cm^2	Potential of osteogenic differentiation and absence of significant alterations on the Collagen-I expression.
Pires-Oliveira *et al.* 2009	Mouse fibroblast (L929)	1 MHz	0.2 and 0.6 W/cm^2	Promoting protein and endoplasmic reticulum activity.
Hauser *et al.* 2009	Human foreskin fibroblasts	1.5 MHz	30 mW/cm^2	Endocytic cell activity.
Scarponi *et al.* 2009	Human keratinocytes	42 KHz	0.15W/cm^2	Did not affect extracellular-signal regulated kinase (ERK) 1/2 activation, cell viability, or expression of adhesion molecules in cultured keratinocytes. US at these frequency and intensity did not influence the keratinocyte expression and release immunomodulatory molecules.
Tsukamoto *et al.* 2011	Mouse fibroblast (L929)	1 MHz	Non	Absence of significant alterations on the Collagen expression on the rupture of cell membrane
Oliveira *et al.* 2011	Mouse fibroblast (L929)	1 MHz	0.2 and 0.6 W/cm^2	Significance increase of cell proliferation.
Grimaldi *et al.* 2011	Murine fibroblasts (NIH-3T3)	1 MHz	307 and 46 mW/cm^2	Induaction of possible genotoxic damage by using 1mHz as frequency.

Authors	Mammalian cell	Frequency	Intensity	Conclusion
Roper *et al.* 2012	Mouse embryonic fibroblasts	1.5 MHz	30 mW/cm^2	Induction of focal adhesion.
Bohari *et al.* 2012	3T3 mouse fibroblasts	1 MHz	0.2 W/cm^2	Significant decrease on the number of cells.
Zhang *et al.* 2012	Mouse embryonic fibroblast cells (NIH3T3)	50–50.000 Hz	0–11 W/cm^2	Significance decrease on the number of cells.
Domenici *et al.* 2013	Murine fibroblasts (NIH-3T3)	1 MHz	11.8, 15.2 and 19.3 mW/cm^2	Significance increase of cell proliferation.
Duvshani-Eshet *et al.* 2013	Human foreskins fibroblasts and baby hamster kidney	1 MHz	2 W/cm^2	Absence of significant alterations on the Collagen expression19, on the observed morphology or on the actin fibres.
Samuels *et al.* 2013	3T3 mouse fibroblasts	20 kHz	50 and 200 mW/cm^2	Significant increase of cell proliferation
Udroiu *et al.* 2014	Murine fibroblasts (NIH-3T3)	1 and 3 MHz	7.1, 11.8, 15.2 and 19.3 mW/cm^2 1.0, 4.9 and 7.0 mW/cm^2	Significant decrease on the number of cells.
Domenici *et al* ., 2014	Murine fibroblasts (NIH-3T3)	1 and 3 MHz	0.11, 0.12 and 0.09 W/cm^2 0.01, 0.04 and 0.06 W/cm^2	Significant increase of cell proliferation.
Li *et al.* 2015	Fibroblasts of rabbit ears scar	Non	0.5 W/cm^2	Significant decrease on the number of cells.
Oliveira *et al.* 2015	Mouse fibroblast (L929)	1 MHz	0.3 e 0.5 W/cm^2	Significant increase of cell proliferation.
Domenici *et al.* 2017	HaCaT cell line.	1 MHz	7 and 16 mW/cm^2, 100 mW/cm^2	Keratinocytes undergoing low US doses can uptake drug model molecules with size and efficiency which depend on exposure parameters - By increasing US doses, they observed a reduced cells viability.
Leng *et al.* 2018	HaCaT cell line.	0.5 MHz	voltage was set at 150 MVpp	Cell viability was the highest after LUS stimulation. Promoting of a migration, - regulation of MMP-2 and MMP-9. Phosphorylation levels of kinase pathways.

6.1.5- Effect of ultrasound on bacteria

Ultrasound can be used in the bacterial field, as a double-edged sword. On the one hand, it can be used to stimulate bacterial growth. On the other hand, it can be used as an antibacterial agent in a similar way to antibiotics (Table 6.2 & 6.3). The effect is determined by the magnitude and types of ultrasound waves used. Generally, low intensity US (2-4 W/cm^2) is metabolic and growth stimulating, while high intensity US (above 5 W/cm^2) selectively destroys biological tissues.

6.1.5.1- Ultrasound as stimulators of bacterial growth

Ultrasound was shown to stimulate bacterial growth (Pitt *et al.* 1994). In 2003, Pitt and Ross showed enhanced growth of *S. epidermidis*, *P. aeruginosa* and *E. coli* when subjected to US of 40 kHz frequency and an intensity of 2 to 4 W/cm^2. They assessed the effect on bacteria through testing bacterial quantification and their adhesion ability (Pitt & Ross, 2003). The enhanced growth was observed in both planktonic and biofilm bacteria.

In biofilms, it was suggested that US enhanced nutrient and waste transport within the biofilm (Stewart *et al.* 1998; Xu *et al.* 2000; Hornemann *et al.* 2008). Within these biofilms' bacteria proliferation increased following exposure to low intensity and low frequency US while the growth of planktonic cultures was also enhanced by US.

6.1.5.2- Ultrasound as an antibacterial agent

6.1.5.2.1- Mechanism of antibacterial action of US on planktonic bacteria

The effect of US on planktonic bacteria has been investigated by a number of studies (Table 6.3). The bactericidal activity of US on bacteria was first attributed to the cavitation produced by the US waves (Scherba *et al.* 1991).

In their study on planktonic *E. coli, S. aureus*, *B. subtilis* and *P. aeruginosa*, Scherba *et al.*, 1991 showed that, when exposed to low frequency US (26 KHz), bacterial killing was directly proportional to the intensity of US waves and the duration of exposure, notwithstanding the type of bacteria (Gram negative or positive bacteria). They also showed that the main cause of bactericidal activity at this frequency was cavitation (Scherba *et al.* 1991).

Cavitation is defined as the formation of tiny gas bubbles in tissues or liquids due to the US vibration. The gas bubbles expand and shrink with the cycles of low and high acoustic pressures of US waves, causing shear flow around the bubbles (Figure 6.2). There are two types of cavitation: stable cavitation where the oscillating bubbles do not collapse in the low cycles and collapsing cavitation where they collapse at the end of the low (contraction) cycle (Guzmán *et al.* 2003; Kodama *et al.* 2006).

In the latter, the oscillation causes an outgoing shock wave that can fragment water and other substances into free radicals (Pitt *et al.* 2003; Bigelow *et al.* 2009).

Figure 6.2: Mode of action of cavitation low frequency ultrasound.
Modified from (Izadifar *et al.,* 2019)
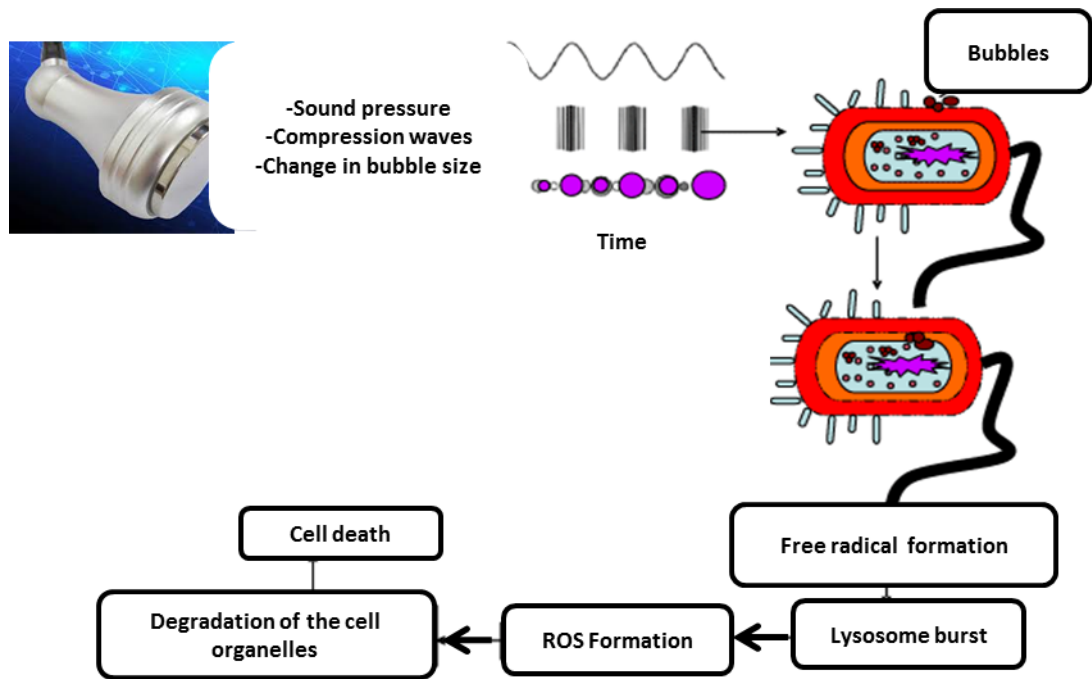
Figure 6.3: Mode of action of low frequency ultrasound planktonic bacteria. Modified from Mahvi, 2009)

Thus, the antimicrobial activities of cavitation are due to physical and chemical effects. The physical effects are either mechanical (resonance of the bacterial cells as a result of the oscillating bubbles on the bacterial solutions at or near the cell wall and the shear forces also derived from these oscillations around the bacterial cells, causing damage to the bacterial cell membranes or organelles) (Runyan *et al.* 2006; Joyce *et al.* 2003), or thermal (directly destroyed by the heat produced as a result of transfer of the accompanying kinetic energy). The mechanical effects are attributed to free radicals and the hydrogen peroxide produced by the degradation of water and other substances in the bacterial cells. Both free radicals and hydrogen peroxide produce by ultrasound that is capable of reacting with and destroying vital compounds within the bacterial cells like DNA and cell organelles (Piyasena *et al.* 2003).

Table: 6.2. Effect of LFU combined with Antibiotic on Planktonic and biofilm bacteria.

Reference	Year	Frequency used	Intensity used	Objective of study	Bacteria tested	Conclusions
Scherba *et al.*	1991	26 kHz	Low (1.1, 0.2 and 0.1) W/cm2, Medium (2.0, 0.3, 0.4) W/cm2 High 3.0 0.4 0.5) W/cm^2	Investigating bactericidal effect of US	*E. coli, S. aureus, B. subtilis, P. aeruginosa*	The mechanism of bacterial damage is cavitation on both Gram positive and Gram negative bacteria.
Pitt *et al.*	1994	67 kHz	0.3 W/cm^2	Investigating the antibiotic effect of US on biofilm bacteria.	*P. aeruginosa, E. coli, S. epidermidis, S. aureus*	Ultrasound treatment might make biofilm bacteria susceptible to antibiotics.
Phull *et al.*	1997	38 kHz, 800 kHz	5 to 30 W/cm^2	Studying the biocidal effect of US with chemical disinfectant and without.	*E. coli*	US can be used in water disinfection. High frequency US has higher biocidal activity. US improves chemical disinfection.
Williams and Pitt	1997	70 kHz	0.01– 4.5 W/cm^2	Would gentamycin activity be enhanced by ultrasonication?	*E. coli*	The more the energy of US, the more its bactericidal activity would be. Maximum effect was observed at 4.5 W/cm^2. No bactericidal activity was noted at 10m W/cm^2.
Rapoport *et al.*	1997	80 kHz	0.68, 3.2 W/cm^2	The antibacterial effect of erythromycin on planktonic *P. aeruginosa*	*P. aeruginosa*	The antibacterial activity of erythromycin increased exponentially with concomitant use of US. US is not able to kill the cells by itself. It rather augments erythromycin.
Rediske *et al.*	1998	70 kHz	3 W/cm^2	The effect of US as a bactericidal when used alone or in combination with an antibiotic.	*E. aerogenes, S. marcescens, S. derby, S. mitis, S. epidermidis*	US combined with antibiotics effectively reduced bacterial viability in both Gram positive and negative bacteria similarly.

Reference	Year	Frequency used	Intensity used	Objective of study	Bacteria tested	Conclusions
Rediske *et al.*	1999	70 kHz	2.2 W/cm^2	The combined effect of erythromycin and US on reducing *P. aeruginosa* viability.	*P. aeruginosa*	Combined use of erythromycin and US reduced *P. aeruginosa* viability double to quadruple times the antibiotic alone. This was effective even with antibiotic concentrations below the MIC.
Rapoport *et al.*	1999	80 kHz	0.8–2.4 W/cm^2	Spin- labelled gentamycin penetration was not changed with insonation less than the threshold of cavitation.	*P. aeruginosa* *E. coli*	LFU lethal effect on Gram negative bacteria was not the consequence of increased antibiotic penetration into the bacterial cells.
Singer *et al*	1999	20–50 kHz	Non	LFUs effects on Staphylococcus epidermidis cell counts.	*Staphylococcus epidermidis*	US intensity and the size of the US probe seemed to affect the counts of bacteria. Temperature also played a role.
Peterson and Pitt	2000	70 kHz, 500 kHz	2 to 200 mW/cm^2	The effect of combined use of antibiotic and US on bacteria.	*E. coli*	The combined use of US and antibiotic was highly effective. High intensity with low frequency gave better results than high frequency US.
Joice *et al.*	2003	20 kHz, 38 kHz, 512 kHz, 850 kHz	0.064 and 0.071 W /cm^3	US effect on Bacillus subtilis using various powers and frequencies.	*B. subtilis*	US caused two different effects on bacteria, namely killing and declumping. The net result will be the sum of these two effects.
Pitt and Ross	2003	70 kHz	<2 W /cm^3	Does US enhance the growth of bacterial cells?	*S. epidermidis, P. aeruginosa, E. coli*	Low frequency and intensity US did increase the bacterial growth rate.
Carmen *et al.*	2005	28.5 kHz	500 mW/cm^2	The effect of combined use of US and antibiotics on biofilm infections *in vivo*.	*E. coli, P. aeruginosa*	Combined use of US and antibiotics effectively reduced *P. aeruginosa* count after 48 h, compared to antibiotic alone which failed to do so within the same time

Runyan et al.	2006	70 kHz	500 mW/cm^2 and 4.7 W/cm^2	Effect of US on bacterial membrane	*P. aeruginosa*	US performed holes in the lipid bilayer outer bacterial membrane through which large molecules like antibiotics can pass.
Ayan et al.	2008	1.5MHz	0.03 – 0.161 W/cm^2	Comparing the effects of LFU to antibiotics alone on bacterial colonies.	*S. aureus*	LFU was superior to antibiotics alone in decreasing the number of bacterial colonies. Partial bacterial destruction was noted using electron microscopy.
Kirzhner et al.	2009	20 kHz	2.7 W/cm^2 to 81.4 W/cm^2	US effect on microbial biofilms.	*Wastewater heterotrophic aerobic bacteria*	US effect was more than two fold higher in removing biofilm bacteria adherent to roots
Declerck et al.	2010	36 kHz	Non	Investigating the effect of US in disinfecting certain species of bacteria.	*L. pneumophila, A. castellanii*	US can theoretically be used to control both types of studied bacteria, but due to the high energy required if US were to be used alone, its general use as microbial decontamination is not recommended.
Conner-Kerr et al.	2010	35 kHz	500 mW/cm^2	*In vitro* effect of LFU on bacteria viability, cell wall stracture and coloy characteristic	MRSA	.LFU decreased CFU of bacteria, caused destruction of cell walls and changed MRSA traits including methicillin resistance.
Liu et al.	2011	40 kHz	1 W/cm^2	The effect of adding LFU to floxacins (cipro and levo) in enhancing their antibacterial effect against E.coli.	*E. coli*	LFU activate fluoroquinolones through producing free oxygen radicles, e.g. superoxide and hydroxyl radicles, which are destructive to bacteria.
E. Joyce et al.	2011	20, 40 and 580 kHz	0·012 and 0·013 W/cm^3	Effect of US of variable frequencies and intensities on two micro-organisms.	*Escherichia coli and Klebsiella pneumonia*	The effect of US depends in intensity and frequency. Generally it may either cause declumping or inactivation of bacteria.

Reference	Year	Frequency used	Intensity used	Objective of study	Bacteria tested	Conclusions
Shengpu Gao *et al.*	2013	20 kHz	Non	Comparing the degree of bacterial deactivation by US according to the physiochemical properties of various strains of bacteria.	*Enterobacter aerogenes, Bacillus subtilis, Staphylococcus epidermidis, S. epidermidis SK and Staphylococcus pseudintermedius*	Although the enzyme activity was considerably deactivated, the outcome was positive all the time.
Zhu *et al.*	2014	46.5 kHz	Non	The effect of microbubble mediated LFU on gentamycin efficacy in comparison to LFU only.	*E. coli*	Microbubble-mediated LFU was more effective in destroying the bacterial cell membrane than other groups as evidenced by the images of transmission electron microscopy.
Jiao Li *et al.*	2016	18 kHz and 100 kHz	60 to 300 W · cm^2	Application of flow cytometry and transmission electron microscopy in investigating the effect of US on E coli and Staph aureus.	*Escherichia coli Staphylococcus aureus.*	US was effective in damaging bacteria. However, the mechanism of damage varied according to the type of bacteria (e.g. In Gram -ve *E. coli*, US effect was initially on the outer membrane; Then on the cytoplasmic membrane).
Liaoa, *et al.*	2018	20 kHz	252 W/cm^2	The mechanism of action of US on Gram +ve (S. *aureus*) and Gram -ve (*E.coli*) on the molecular level.	*Eshcerichia coli and Staphylococcus aureus*	Proportion of bacteria subpopulation suffered from serious damage of intracellular components (e.g. DNA and enzymes) but with intact cell envelopes.

An additional cause of antibacterial activity of US has been shown to be its effect on bacterial motility. US, at 67 kHz, have been found to reduce flagella motility in *P. aeruginosa* after 9 hours of exposure (Mitchell & Kogure 2006). Motility is crucial to bacterial function and viability because it enables bacterial cells to move towards their targets of nutrition and migrate away from immune cells (Bardy *et al.* 2003).

6.1.5.2.2- Mechanism of antibacterial action of US on biofilm bacteria

Biofilm bacteria are bacteria extending along living and non-living surfaces. They are capable of forming colonies which flourish within an extracellular polymeric substance (EPS). Usually, the ecology of the biofilm is complex encompassing multiple bacterial species and strains which often co-operate with each other under the control of quorum sensing molecules (QSMs), which allow them to undergo intercellular communication (Donlan & Casterton 2002). The effects of US on biofilms have been investigated in several studies (Table 6.3). In addition to that, US exert a destructive effect on the EPS forming the matrix of the biofilm, through inducing cavitation. EPS is well known to play an important role in protecting the bacteria harboured within against the surrounding hostile environment and in preventing antibacterial agent penetration by binding them directly (Sutherland 2001; Donlan & Casterton 2002; Olson *et al.* 2002). The EPS destructive effect is specifically performed by high intensity and low frequency US. Unfortunately, stripping of bacteria from the surfaces they grow on is not complete, usually, the bacterial detachment percentage range between 85 to 90 %. With the highest power density of 38 kHz, no more than 95% was achieved (Oulahal-Lagsir *et al.* 2000).

6.1.6- Applications of antibacterial activity of ultrasound

6.1.6.1- Single US applications

The antibacterial activity of US has been used in combating infection caused by bacteria in the human body. This has been achieved by the non-thermal effects of US (Sonication), thermal plus heat (thermosonication), thermal plus pressure (manosonication) or thermal plus heat and pressure (manothermosonication). Spores and, to a lesser extent, bacteria are resistant to sonication alone; thus, to obtain a lethal effect, thermosonication, manosonication or manothermosonication should be applied (Piyasena *et al.* 2003).

One application of US is for the treatment of bacterial infections of the skin (especially wounds) and mucous membranes (e.g. oral infections) (Ioannou *et al.* 2009). Furthermore, in periodontal therapy, ultrasonic scalers are used to combat bacteria biofilms; these are vibrating mechanical devices which allow removal of root-surface accretions. They achieve similar results to manual scaling in achieving probing depth reduction and in ameliorating clinical inflammation (Oda *et al.* 2004; Ioannou *et al.* 2009; Zucchelli *et al.* 2009).

Ultrasonic debridement has the advantages of being faster than its manual counterpart with minimal operator fatigue, but it is associated with some hazards both to the patient and the operators that need to be guarded against to ensure safe dental practice. These include heating temperature effects and cavitation process which lead to platelet damage, which cause pulp death (Walmsley *et al.* 1984; Walmsley 1988). In spite of wide spread use in the US for the treatment of oral bacteria, very few studies are found in this respect (O'Leary *et al.* 1997; Oda *et al.* 2004; Ioannou *et al.* 2009).

6.1.6.2- Combined US applications with antibiotics

Synergism between US and antibiotics has been confirmed by a number of studies (Rediske *et al.* 1998; Rediske *et al.* 1999) (Table 6.3). Pitt *et al*, (1994) has demonstrated synergism between US and antibiotics in combating biofilm bacteria such as (*P. aeruginosa*, *E. coli*, *S. epidermidis* and *S. aureus*). While US alone, at 67 kHz was stimulatory to bacterial growth, it was bactericidal when combined with an antibiotic, with increased bactericidal activity compared with the antibiotic alone. The paradoxical increase in growth was attributed to the stress-induced bacterial stimulation and not to the higher concentration of oxygen (Pitt *et al.* 1994).

In the treatment of infections caused by *S. epidermidis* biofilms with vancomycin, Carmen *et al.*, (2004), demonstrated that exposure of bacterial biofilms to US (28, 48 kHz) for 48 hours significantly reduced the number of viable bacteria in the biofilm than treatment with vancomycin alone.

Carmen *et al.* applied the same combination was delivered using a 28.5 kHz ultrasound with gentamycin treatment to *E. coli* ATCC 10798 and *P. aeruginosa* ATCC 27853 biofilms on rabbits *in vivo*. While *E. coli* responded well to treatment, *P. aeruginosa* biofilms did not show any reduction in viable bacterial count. The resistance of *P. aeruginosa* biofilms was attributed to the extreme outer membrane impermeability of this strain (Carmen *et al.* 2005).

In 2005, Ensing showed that *E coli* treated with gentamycin and 70 kHz US resulted in higher bacterial killing effect than when gentamycin alone was used (Ensing *et al.* 2005). In 2006, Ensing *et al.* extended their work on *P. aeruginosa* and *S. aureus*.

These results showed that *P. aeruginosa* biofilm was resistant to the combination treatment of US and antibiotic, thus confirming the earlier results of Carmen *et al.* and Ensing *et al.* 2006.

In 2006, Runyan *et al* were able to overcome the *P. aeruginosa* biofilm resistance *in vitro* by applying US of 70 kHz of frequency and intensity of 4.6 W/cm^2 coupled with antibiotics (Runyan *et al.* 2006). The applied US has been shown to create perturbations or holes in the outer membrane of bacteria enough to allow the large hydrophilic molecules of antibiotics to pass and kill the bacteria in biofilms. Nevertheless, it remained unresolved why the previous *in vivo* experiments failed to overcome *P. aeruginosa* resistance.

6.1.7- Aims and objectives

The aim of the present study was to investigate the effects of ultrasound coupled with a non-antibiotic approach to reduce bacterial planktonic culture and determine effects on biofilms in an infected sample using tissue engineered skin developed in chapters 4 and 5. Low frequency ultrasound combined with biocides at sub MIC was used to investigate whether combination treatments could increase the toxicity of biocidal agents alone to *S. aureus, P. aeruginosa, S. epidermidis* and MRSA.

Table 6.3: Effect of LFU combined with Antibiotic on bacterial biofilm

Reference	Year	Frequency used	Objective of study	Intensity used	Bacteria tested	Conclusions
Qian *et al.*	1996	500 kHz	Effect of LFU on gentamycin antibacterial activity of *P. aeruginosa* biofilm of 24 h growth *in vitro*.	10 mW cm^2	*P. aeruginosa*	LFU did not disrupt neither the biofilm nor the bacteria itself.
Qian *et al.*	1997	70, 500 kHz 2.25, 10MHz	Effect of ultrasound alone and combined with gentamycin on *in vitro* biofilm.	10 mW/cm^2	*P. aeruginosa*	US significantly increased the efficacy of gentamycin in killing bacteria of biofilms. However, US alone did not have any lethal antibacterial effect. LFU is more effective than high frequency US in reducing biofilm bacterial viability.
Johnson *et al.*	1998	70, 500 kHz	The effect of combined use of US of 70 kHz and antibiotic on *in vitro* biofilm.	20, 100 mW/cm^2	*E. coli*	The combined use of 70 kHz US and antibiotic had more antibacterial effectiveness than antibiotic alone (killing 97% in about 2 h). 500 kHz US, when combined with antibiotic, caused insignificant slight reduction in bacterial killing than the antibiotic alone.
Rediske *et al.*	1999	28.48 kHz	Effect of US alone on biofilm infected rabbit model.	300 m W/cm^2	*E. coli*	US alone did not affect bacterial viability. US of 300 m W/cm2 caused significant reduction of bacterial viability. US of 100 m W/cm2 caused insignificant reduction of bacterial viability.
Qian *et al.*	1999	44 kHz–10MHz	Effect of sonication combined with antibiotic on *in vitro* biofilms.	100–300 mW/cm^2	*P. aeruginosa*	US enhanced the antibacterial efficacy of antibiotic. This enhancement was inversely proportional to the frequency (the more the frequency the less the enhancement) and directly proportional to the energy (the more the energy the more the enhancement e.g. 10 m W/cm2 intensity was more enhancing than 1 m W/cm2).
Rediske *et al.*	2000	28.48 kHz,	Effect of LFU on *in vivo* biofilm in a rabbit model	600 mW/cm^2	*E. coli*	Pulsed US of 300 m W/cm2 decreased bacterial viability from 2.94 to 0.99 log 10 CFU/cm2. However, Pulsed US of 600 m W/cm2 decreased bacterial viability from 2.93 to 1.69 log 10 CFU/cm2. No concomitant skin damage occurred.

Reference	Year	Frequency used	Objective of study	Intensity used	Bacteria tested	Conclusions
Carmen *et al.*	2004	28.48 kHz	The effect of LFU on vancomycin efficacy against *S. epidermidis In vivo* study of biofilm-infected.	500 mW cm^2	*S. epidermidis*	LFU was found to enhance the efficacy of vancomycin against *S. epidermidis* as evidenced by the significant decrease in viable bacterial count after 48 hours of US.
Carmen *et al.*	2004	70-kHz	Effect of US on the transport of gentamycin through vitro biofilms.	1.5 W/cm^2	*P. aeruginosa E. coli*	Ultrasonication significantly increased transport of gentamycin ac biofilms that normally blocked or slowed gentamycin transport when not exposed to ultrasound. US was found to significantly increase the transport of gentamycin through biofilms that resisted this transport without being exposed to US.
Carmen *et al.*	2005	28.5 kHz	Effect of LFU on *In vivo* rabbit biofilms alone and combined with antibiotics.	500 mW/cm^2	*P. aeruginosa E. coli*	When US for 48 h was combined with gentamycin for 72 h, the viable bacterial count in E coli decreased significantly to 0.011 ± 1.02 log 10 CFU/cm2; With 72 h of gentamycin alone the count reduced to 2.29 ± 0.40 log 10 CFU/cm2. There was no such enhancement of US in case of *P. aeruginosa*.
Li *et al.*	2015		Investigating the bacterial load of a biofilm on titanium surface *In vivo* mice (Biofilm densities, viable bacterial count and proportions of live cells) and how these are affected by US.	200mW/cm^2	*S. epidermidis S. aureus*	Microbubble-mediated US combined with HBD-3 significantly decreased the biofilm densities, the proportion of live cells as well as the viable counts on titanium surface in mice.
Liu *et al.*	2016	40 kHz	Effect of vancomycin combined with colistin and LFU on *in vitro* biofilm.	600 mW/cm^2	Pan-resistant *A. baumannii*	Colistin combined with vancomycin and LFU for 12 h reduced bacterial counts more than 2 log CFU/mL than without LFU. The reduction continued for 24 h to 3.77 log CFU/mL with LFU than in case where LFU was not applied.

6.2- Material and methods:

6.2.1- Experimental design

The effect of low frequency ultrasound on two common bacterial species, *S. aureus* and *P. aeruginosa* were studied. Both of these pathogens are known to be amongst the major causes of wound infections, particularly following burns (Lawrence, 1994) and were therefore used as a model for Gram-positive and Gram-negative bacterial infection respectively. Previous studies conducted by Shepherd & Rose (unpublished) demonstrated that low frequency ultrasound (20 and 38 kHz) can reduce bacterial viability in pure culture suspensions and reduce bacterial load in a tissue engineered model of bacterially infected skin. Here, the effect of ultrasound at a frequency of 40 KHz was investigated. Bacteria were grown both as planktonic cultures and biofilm cultures on nitrocellulose filters as described in chapter 2 and subjected to either single ultrasound treatment or multiple ultrasound treatments and over a range of times (0-15 minutes). Cell viability was determined by counting the number of colony forming units (CFU) after treatments. For planktonic cultures, the effects of ultrasound treatment on both bacterial species at stationary phases of growth were investigated. Finally, the effect of biocides at sub MIC and LFU co-treatment on planktonic bacterial viability was measured. In addition, the effects of LFU on mammalian skin cells (HaCaT Cells, dermal fibroblasts) were determined to identify potential toxicity to mammalian cells.

6.2.2- Low frequency ultrasound as an anti-bacterial strategy

In this study, several types of commercial US systems together with an in-house system were investigated to determine their antibacterial properties.

6.2.3- Preparation of bacterial samples

Four bacterial strains were used in this study: *S. aureus* (SH1000), *S. epidermidis*, *P. aeruginosa* (NCIMB 8295) and MRSA (EMRSA-16) as described in chapter 2, section (2.2.1.2).

6.2.4- Ultrasound waves application

Two milliliters of the bacterial suspension containing $1x10^8$ CFU/ml and $1X10^6$ CFU/ml were added to each well of six well plates and subjected to ultra-sonication. The US waves were delivered by US transducers to deliver waves of the required frequency and intensity utilising 3 different US machines as detailed below.

6.2.5- Determination of bacterial viability in CFU/ml

After being subjected to US waves, CFU/ml were calculated as described in chapter 2 (section 2.2.2).

6.2.6- US system optimisation

6.2.6.1- Commercial US system

The Desktop Ultrasonic Liposuction Equipment Cavitation GS8.2E (Shenzhen, China) delivers US waves of 40 kHz frequency (Figure 6.4), however the intensity was not able to be determined utilising this system.

Figure 6.4: Desktop Ultrasonic Liposuction Equipment Cavitation GS8.2E

Bacterial suspensions (1×10^8 CFU/ml) were placed in a sterile microbiological Petri dish, on ice to prevent an increase in temperature, and subjected to 40kHz US waves for 0, 5 and 10 minutes. CFU/ml were determined and compared with untreated controls. A significant decrease of *S. aureus* CFU/ml following both 5- and 10-min US treatment (P=0.0049) was observed (Figure 6.5a). However, the decrease was less than one $\log_{10}$ reduction in CFU/ml. US stimulation significantly reduced *P. aeruginosa* CFU/ml following 5 and 10 minutes (P= 0.003 and P =0.0005) (Figure 6.5b). However, again US failed to reduce CFU/ml by more than one $\log_{10}$ (Figure 6.5b). These results are close to has been reported in previously published studies, which have shown that LFU alone significantly drop the cell bacterial numbers in planktonic broth culture by 1 $\log_{10}$.

Most studies to date have controlled the intensity and exposed for longer periods than reported in the current study. Joyce *et al.,* 2010 showed that low frequency ultrasound between 20-38 kHz and 0.013 W/cm^3 for 15 minutes reduced viable number 1.2 $\log_{10}$ from 2×10^8 to 1×10^7 CFU/ml of *Klebsiella pneumonia* and *E. coli* bacteria. In contrast, Singer *et al.,* (1999) showed a major significant reduction of *S. epidermidis* bacteria at frequency 20- 50 kHz, experimentally with and without ice plate immersion. They found out that LFUS has less effect on bacterial counts in case of ice plate immersion.
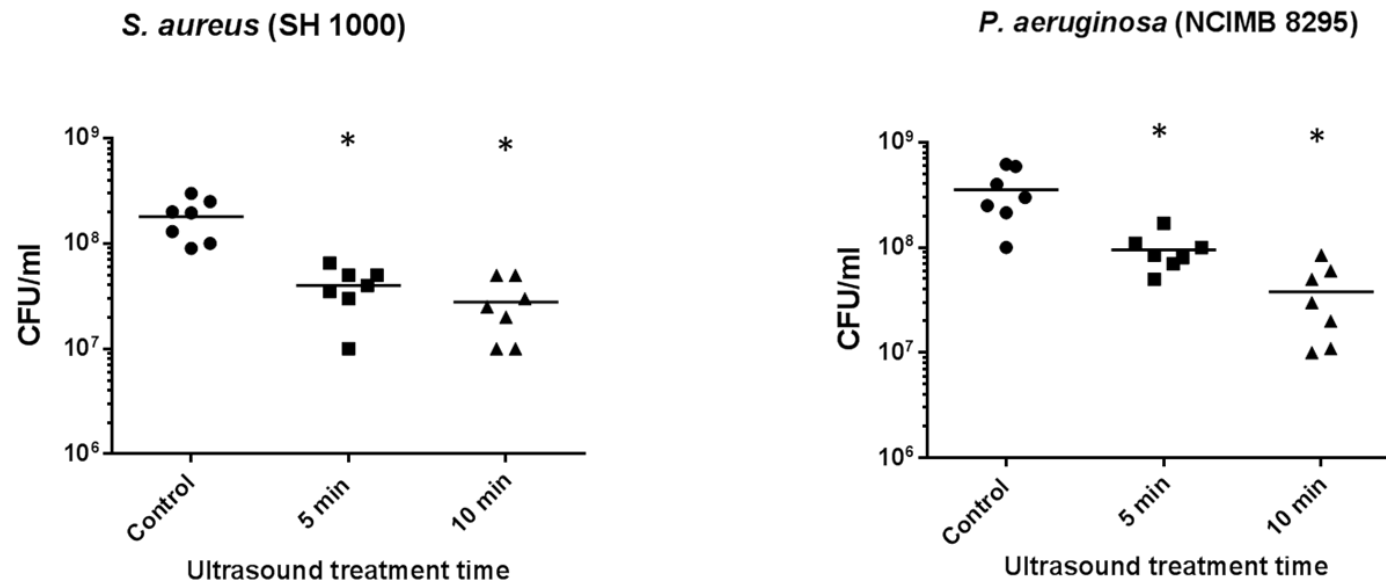
Figure 6.5: Effect of LFU of Desktop Ultrasonic Liposuction Equipment Cavitation GS8.2E on planktonic bacteria. *S. aureus* (SH1000) and *P. aeruginosa* (NCIMB 8295), were all exposed to 40 KHz at an intensity W/cm^2 ultrasound for 0, 5 and 10 min. * P < 0.005.

6.2.6.2- Commercial US system 2

As the first US system utilised only resulted in low kill rates for bacteria and the intensity could not be determined or altered a second commercial US system was identified. The system is call Cavitation 40kHz ultrasound (Quirumed, Spain); it was selected as this system could deliver differential US intensities and measure these accurately. The US wave intensities chosen were 5, 25 and 47 W/cm^2, as difference levels of intensity, while the frequency was kept constant at 40 kHz. The US waves were applied to the bacterial solutions in the bacterial petri dish plates for the same periods (5 and 10 minutes), but with a variable intensity in each experiment to determine the effect of US intensity on bacteria CFU/ml.

P. aeruginosa CFU/ml was decreased following LFU stimulation for 5 and 10 minutes at a frequency of 40 kHz with 5, 25 and 47 W/cm^3 intensity. The reduction in viable cell numbers was less than 1 log_{10} CFU/ml when the intensities were 5, 25 and 47 W/cm^3 within 5 minutes treatment and 1 log_{10} CFU/ml bacterial reduction when the intensity was 47 W/cm^3 within 10 minutes treatment (Figure 6.6). *S. aureus* numbers were decreased by less than 0.3 log_{10} CFU/ml at when the intensities were 5, 25 and 47 W/cm^3 within 5 and 10 minutes treatment (Figure 6.6). The bactericidal effect of ultrasound was significantly greater for *P. aeruginosa* compared with *S. aureus*. However, these results were varied from those reported in the literature (Table 6.2).
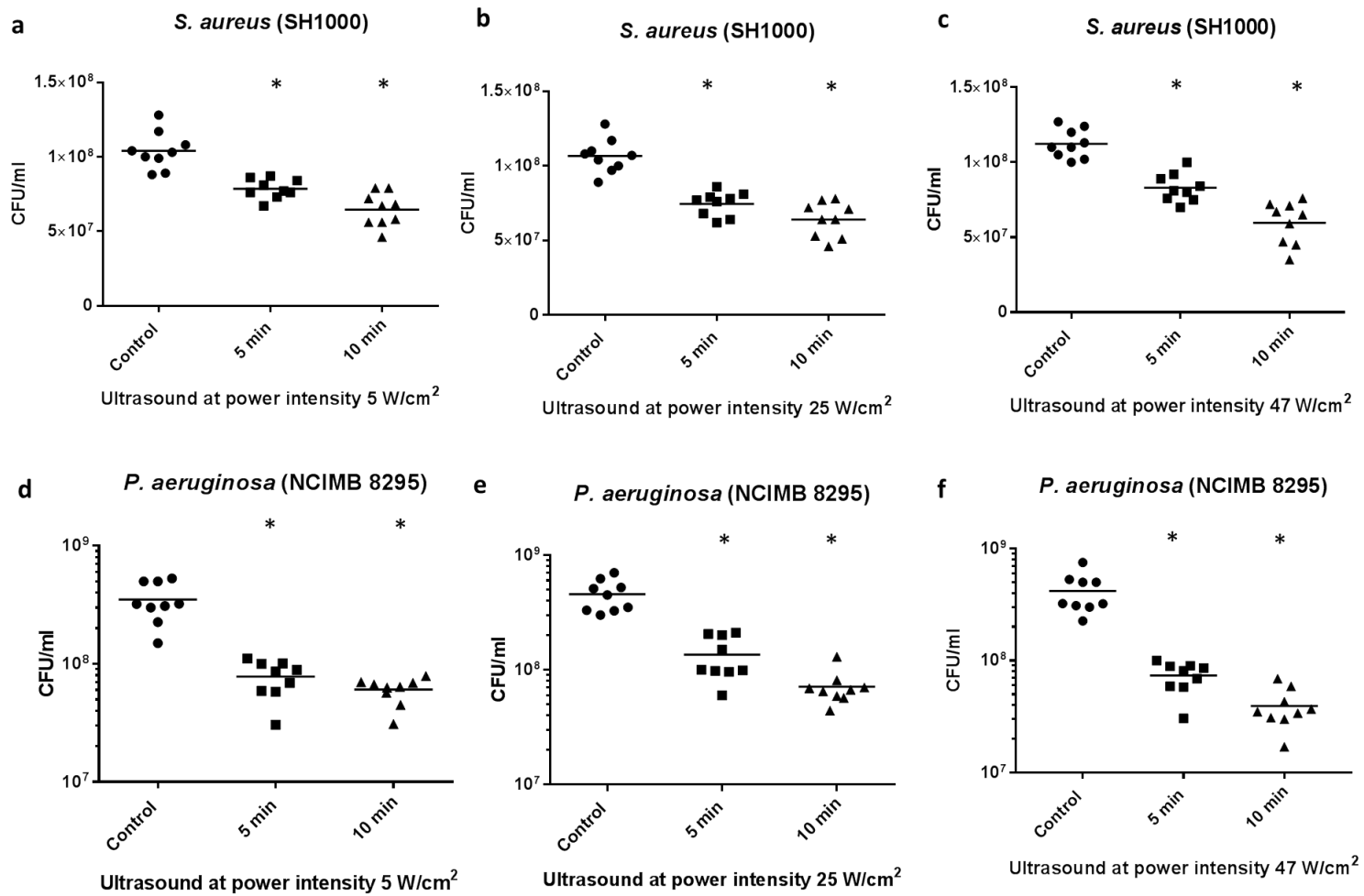
Figure 6.6: Effect of LFU of ultrasound on planktonic bacteria. *S. aureus* (SH1000) and *P. aeruginosa* (NCIMB 8295), were all exposed to 40 KHz at deference intensity 5, 25 and 47 W/cm^2 ultrasound for 0, 5 and 10 min. * P < 0.005.

6.2.6.3- Ultrasound system 3: In house designed

Whilst the second commercial LFU system did show improved kill rates at higher intensities the kill rates were still lower than Desktop ultrasound at 40kHz with high intensity. The system did not have any capability to ensure the reported intensities and frequency were delivered to the sample and thus levels could not be verified. Thus, an in house system was developed by collaborators at the University of Sheffield (Ms. Olivia Manfredi, Prof. Rob Dwyer-Joyce, Department of Mechanical Engineering). This system was designed to enable the transduction of US waves of variable frequency and intensity to each of the wells of a 6 well plate, via 6 individual transducers. Furthermore this system was developed to enable monitoring of the US wave forms via a sensor linked to computer software and thus enable validation of the delivered US dose (Figure 6.7).
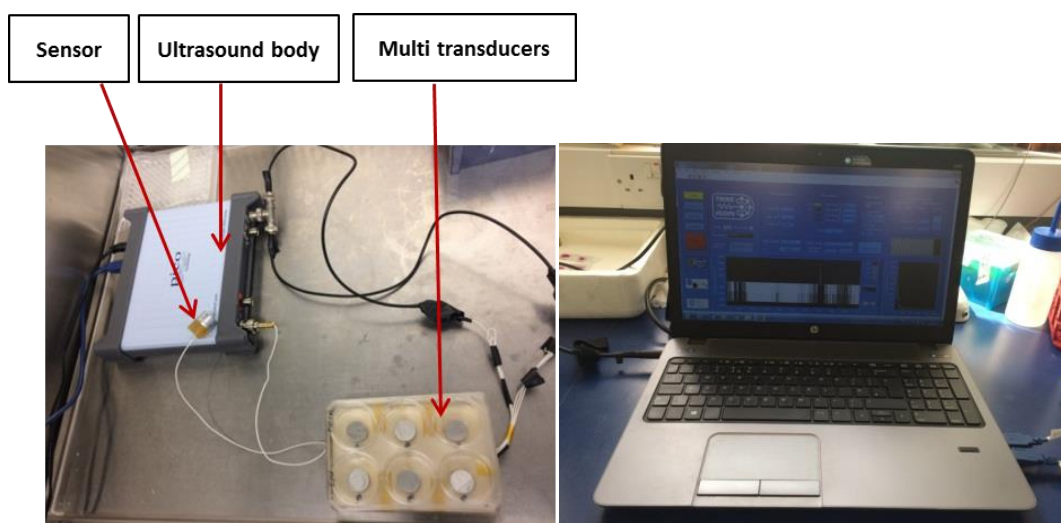
Figure 6.7: Lab management ultrasound, multiple transducers, computerised with software to control the ultrasound.

Initial experiments with this system discovered that the intensity of the US waves delivered was 150 mW/cm^2, with a voltage of ≤ 1.6 volts/ well. This US application was tested on all four bacterial strains (*S. aureus, P. aeruginosa, S.*

epidermidis and MRSA) for 0, 10, 15 and 20 minutes. Following ultrasound treatment by using a range of times could be reducing of bacterial load.

6.2.3.3.1- High Planktonic suspensions CFU/ml

Initially, bacterial suspensions of *S. aureus, P. aeruginosa, S. epidermidis* and MRSA were seeded at 1×10^8 CFU/ml in PBS and treated with 150 mW/cm^2 ultrasound for 10, 15 and 20mins. A significant decrease in viable counts of all bacteria was seen following 10 min LFU treatment, with similar effects seen following 15 and 20 minutes with ~ 1 $\log_{10}$ CFU/ml reduction ($P<0.05$) (Figure 6.8).

6.2.3.3.2: Low Planktonic suspensions CFU/ml

To determine if US treatment was more effective if the bacterial load was reduced the seeding concentration was reduced to 1×10^6 CFU/ml. However all bacteria were still only reduced approximately 1 $\log_{10}$ following LFU treatment for 10 minutes, which whilst significant ($P<0.05$)(Figure 6.8) were lower than that observed in previous studies. Interestingly, these low intensity US waves (150 mW/cm^2) (Figures 6.8 & 6.9) resulted in similar kill rates to those seen with higher intensities (47W/cm^2) (Figure 6.8) utilised in the 2nd US systems, suggesting that the reported intensity given on the 2nd system was inaccurate and could explain why results varied from those reported in the literature. Joyce *et al.*, (2011) reported that 1 $\log_{10}$ CFU/ml reduction at 40 kHz and 2 $\log_{10}$ CFU/ml reduction at 20 kHz and intensity were 0·012 and 0·013 W/cm^3
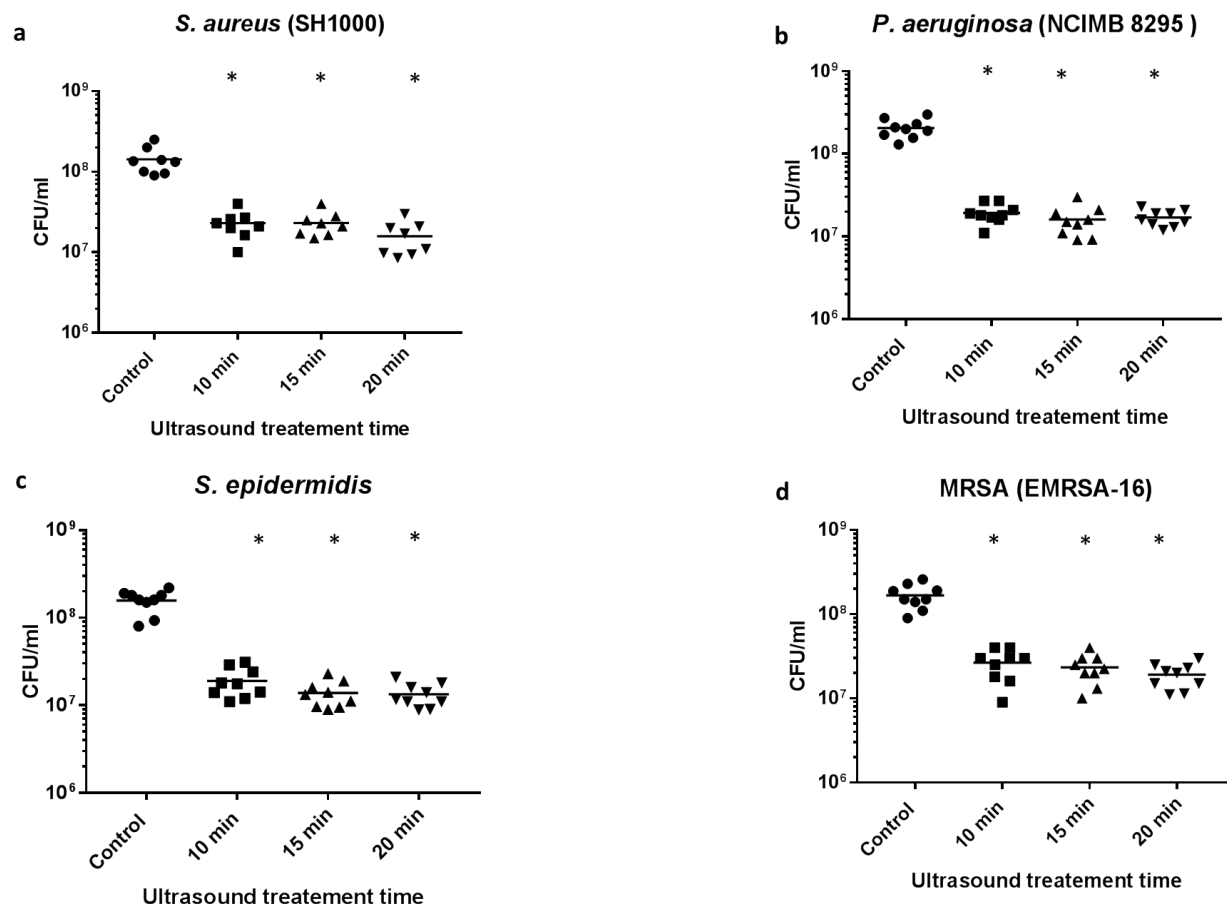
Figure 6.8: Effect of low frequency ultrasound on planktonic bacteria. (A) *S. aureus* (SH1000) and (B) *P. aeruginosa* (NCIMB 8295), *S. epidermidis* and MRSA were all exposed to 40 KHz at an intensity W/cm² ultrasound for 0, 10, 15 and 20 min. * P < 0.005.
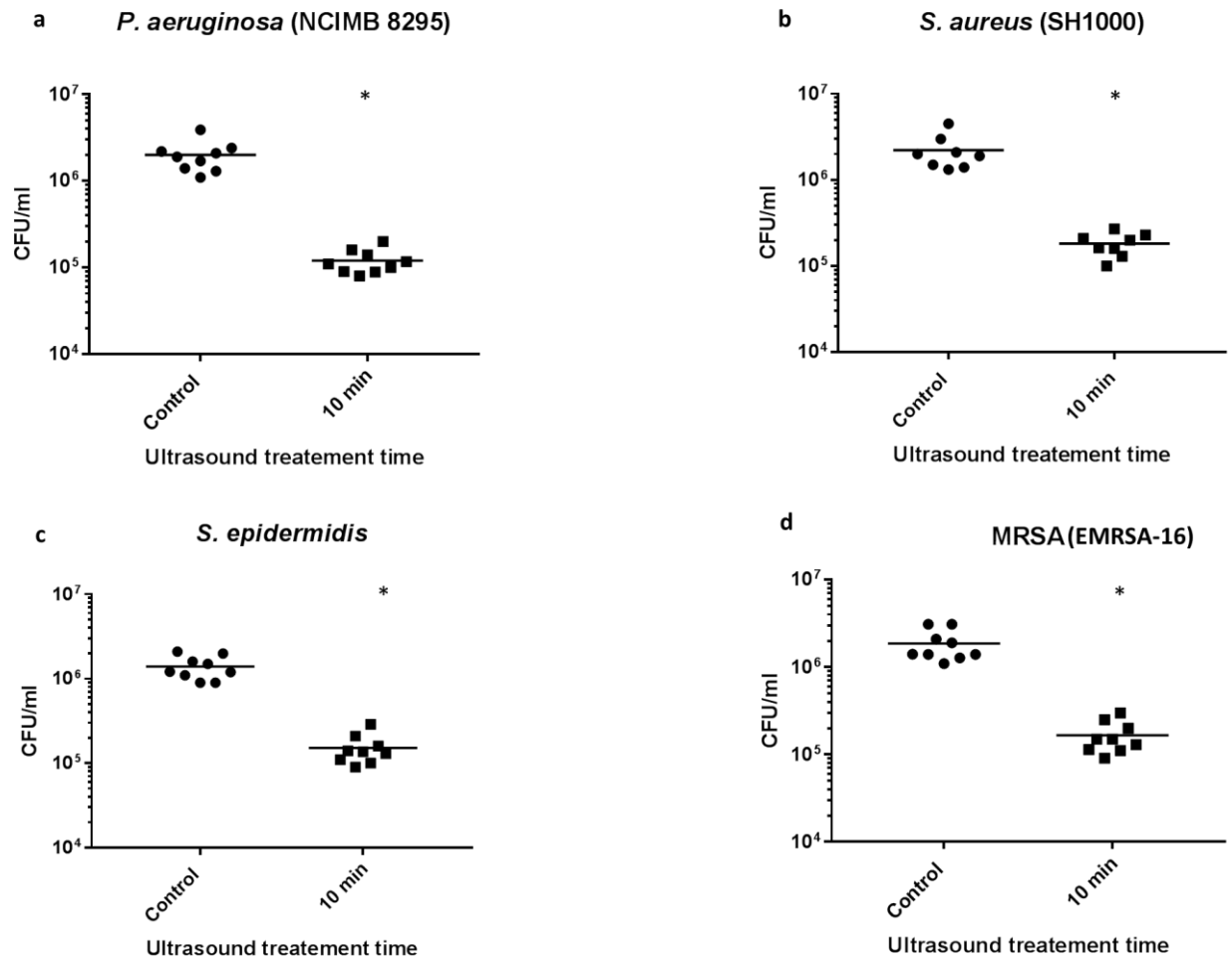
Figure 6.9: Effect of low frequency ultrasound on planktonic bacteria. (a) *S. aureus* (SH1000) and (b) *P. aeruginosa* (NCIMB 8295), (c) *S. epidermidis* and (d) MRSA were all exposed to 40 KHz at an intensity W/cm^2 ultrasound for 0, 10 min. * P < 0.005.

6.2.7- Effect of co treatment of biocides and low frequency ultrasound on planktonic bacteria

To investigate whether pre-treatment of planktonic bacteria with biocidal agents increased the effectiveness of ultrasound treatment, planktonic bacteria suspensions were treated with biocides at sub MIC concentrations before treatment with ultrasound. Planktonic bacteria, untreated or treated with sub MIC concentrations of biocides and not exposed to ultrasound were used as control. CFU/ml was calculated for these control samples as well as samples treated with US for 0, 5, and 10 minutes. MIC concentrations shown in chapter 2 demonstrate a high kill rate for bacteria and thus combination effects with LFU would not be visible. Furthermore biocidal agents at these concentrations showed toxicity to mammalian cells (Chapters 3, 4 and 5); hence here biocidal agents used were at 50% of the MIC.

6.2.7.1- Effect of sub MIC of Siver biocide and LFU on *S. aureus and P. aeruginosa*

The four bacteria species *S. aureus, P. aeruginosa, S. epidermidis* and MRSA were treated by the sub MIC biocides including 31.25 µg/ml silver nitrate, 31.25 µg/ml isothiazolone and 0.023 v/v hydrogen peroxide. Bacteria were cultured at 1×10^4 CFU/ml and treated with biocides for 24 hours. They were then treated with 150 mW/cm^3 intensity and 40 kHz ultrasound frequency for 5 and 10 minutes and the viable bacteria remaining were enumerated.

The co-treatment of sub MIC of silver nitrate (31.25 µg/ml) with ultrasound at 40 kHz reduced the CFU/ml of *S. aureus* by 1.96 and 2.27 log$_{10}$ after 5- and 10-minutes treatment respectively compared with the untreated bacterial control (P =0.001 for both) (Figure 6.10).

When the sub MIC silver nitrate biocide and LFU on *P. aeruginosa* were used the bacterial count significantly decreased compared with untreated controls. The CFU/ml showed a 2 and 2.5 $\log_{10}$ reduction CFU/ml for 5- and 10-minutes ultrasound treatment respectively (P=0.001) for both times respectively compared to the untreated bacterial control) (Figure 6.11).
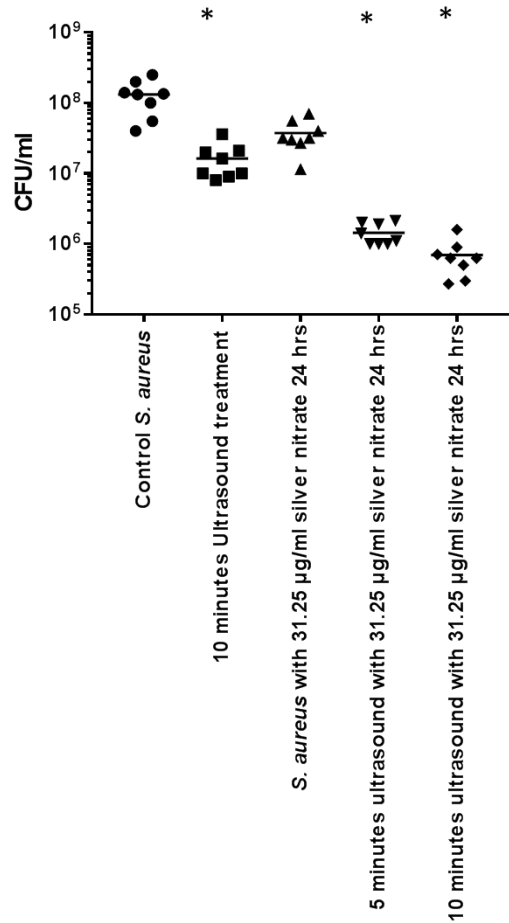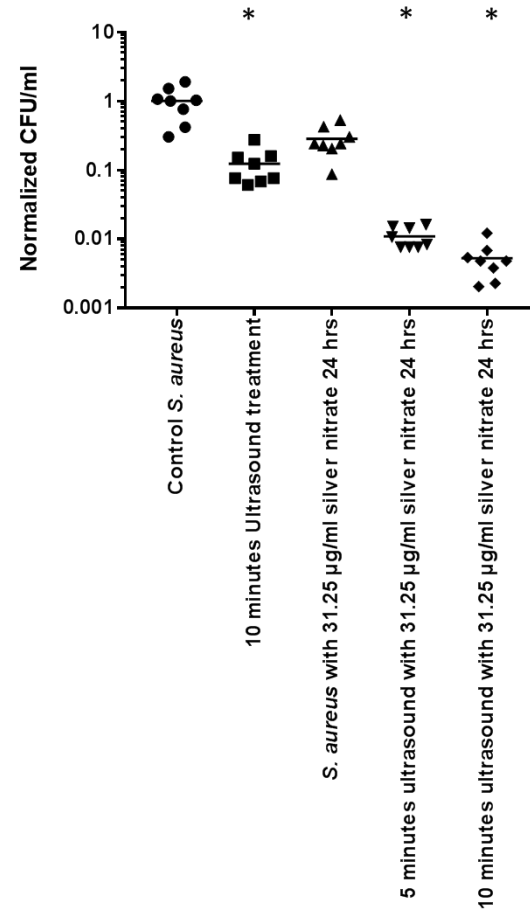
Figure 6.10: Effect of co treatment of sub MIC of biocides and low frequency of ultrasound on planktonic. *S. aureus* (SH1000) was treated by 24hrs of sub MIC of silver nitrate and exposed to 40 KHz at an intensity W/cm^2 ultrasound for 0, 10 min. * P < 0.005.
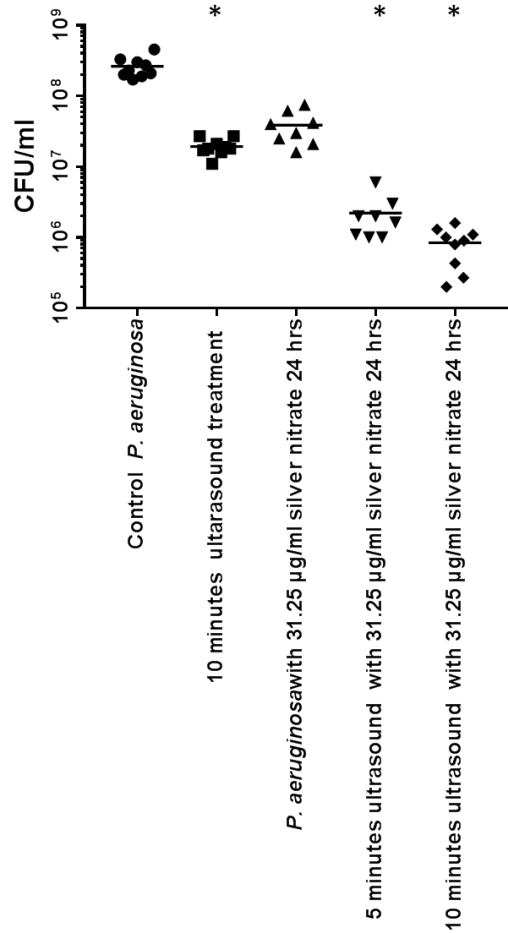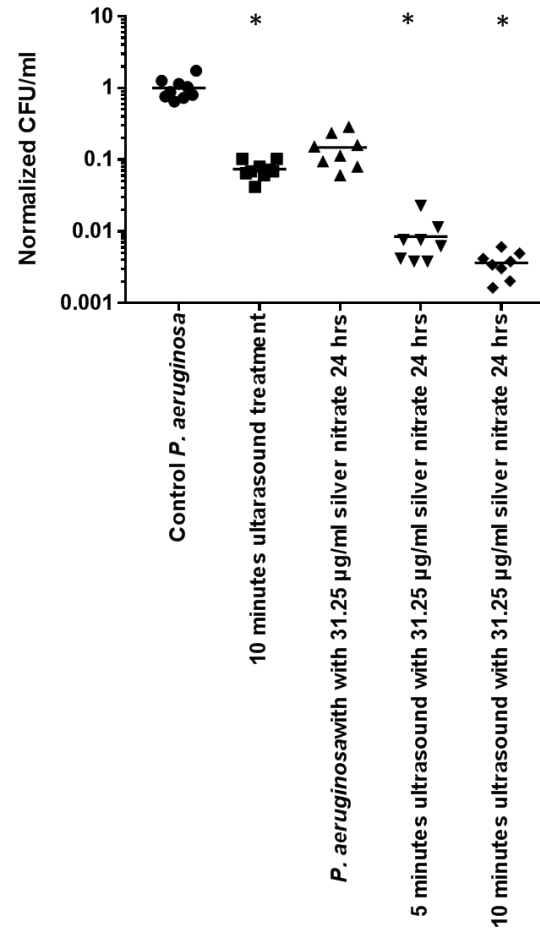
Figure 6.11: Effect of co treatment of sub MIC of biocides and low frequency of ultrasound on planktonic. *P. aeruginosa* (NCIMB 8295) was treated by 24hrs of sub MIC of silver nitrate and exposed to 40 KHz at an intensity W/cm^2 ultrasound for 0, 10 min. * $P < 0.005$.

6.2.7.2- Effect of sub MIC of isothiazolone biocide and LFU on *S. aureus and P. aeruginosa,*

Following treatment with US for 5 and 10 minutes after 24h sub MIC treatment with isothiazolone, the numbers of viable *S. aureus* were reduced by 1.66 and 2 $\log_{10}$ respectively (P< 0.0001) (Figure 6.12). Co treatment of *P. aeruginosa* resulted in a 2 to 2.5 $\log_{10}$ CFU/ml reduction following 5- and 10-minutes US exposure. (P< 0.0001) (Figure 6.13).

6.2.7.2- Effect of sub MIC hydrogen peroxide (H_2O_2) and LFU on *S. aureus and P. aeruginosa*

 The decrease of the bacterial count was proportionally related to the period of US application. *S. aureus* viable bacterial counts decreased by 1.6 to 2 $\log_{10}$ CFU/ml after US application for 5, 10 minutes respectively (P< 0.0001) (Figure 6.14). The bacterial count for *P. aeruginosa* decreased by 2 to 2.2 $\log_{10}$ CFU/ml following H_2O_2 and US co-treatment application for 5 and 10 minutes, respectively (P< 0.0001) (Figure 6.15).
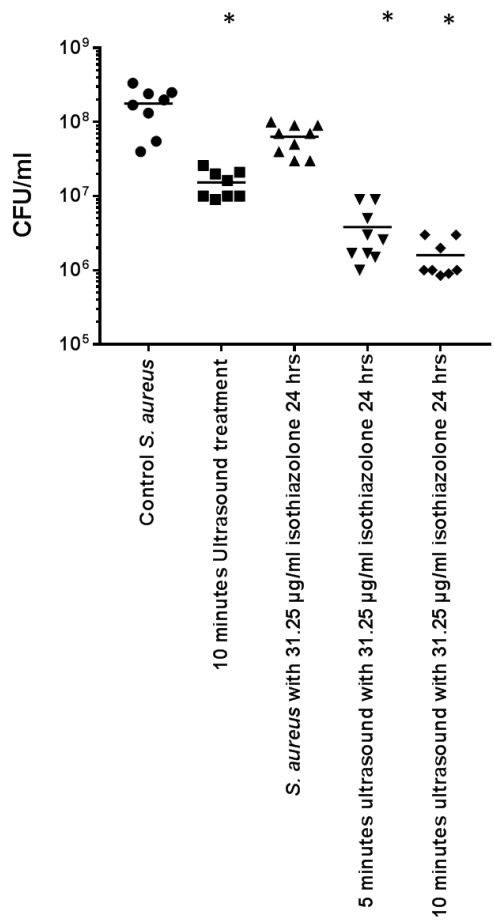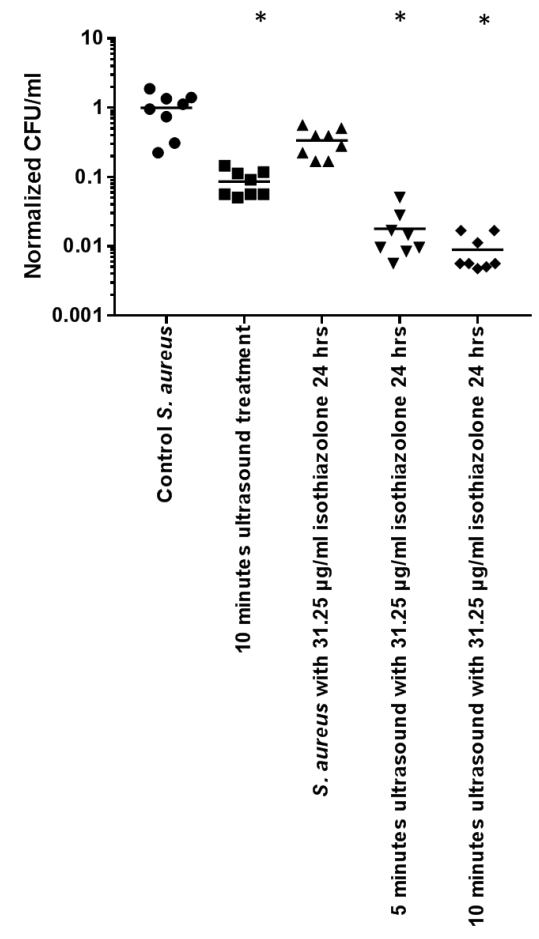
Figure 6.12: Effect of co treatment of sub MIC of biocides and low frequency of ultrasound on planktonic. *S. aureus* (SH1000) was treated by 24hrs of sub MIC of isothiazolone and exposed to 40 KHz at an intensity W/cm^2 ultrasound for 0, 10 min. * P < 0.005.
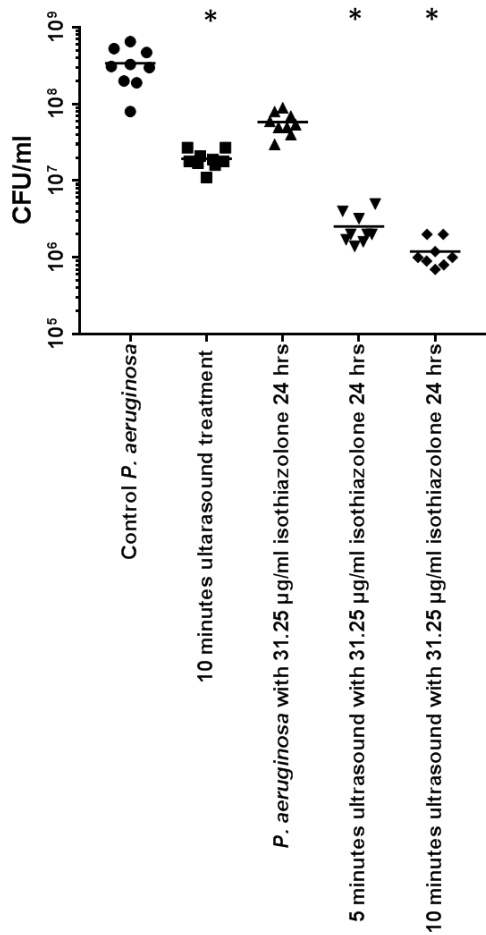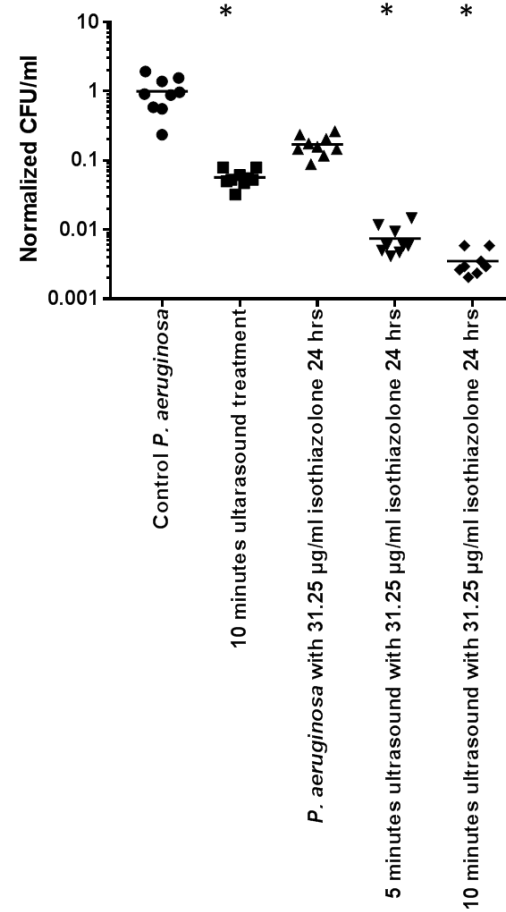
Figure 6.13: Effect of co treatment of sub MIC of biocides and low frequency of ultrasound on planktonic. *P. aeruginosa* (NCIMB 8295) was treated by 24hrs of sub MIC of isothiazolone and exposed to 40 KHz at an intensity W/cm^2 ultrasound for 0, 10 min. * P < 0.005.
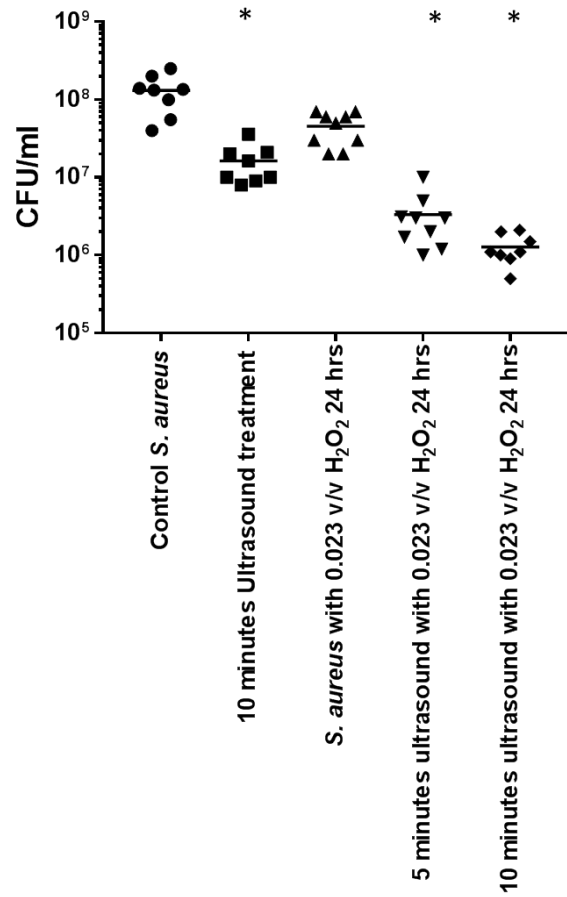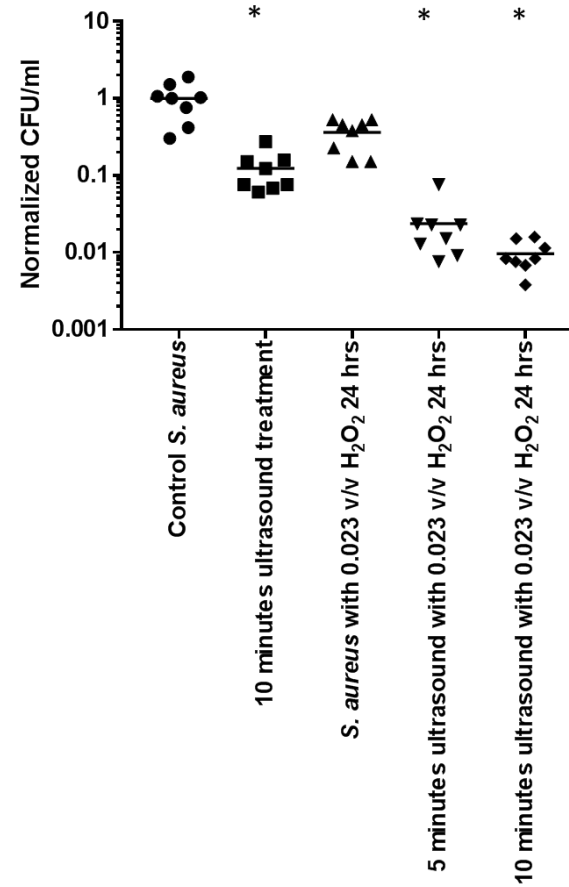
Figure 6.14: Effect of co treatment of sub MIC of biocides and low frequency of ultrasound on planktonic. *S. aureus* (SH1000) was treated by 24hrs of sub MIC of hydrogen peroxide and exposed to 40 KHz at an intensity W/cm^2 ultrasound for 0, 10 min. * $P < 0.005$.
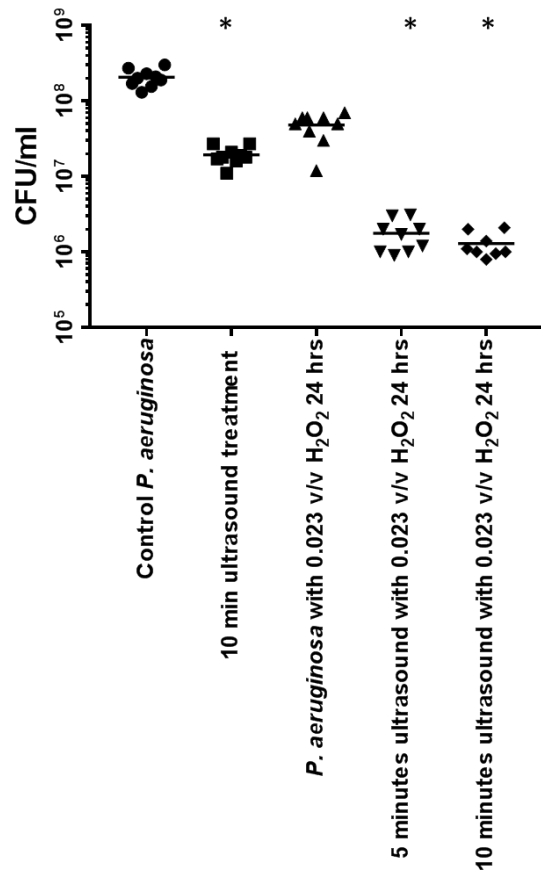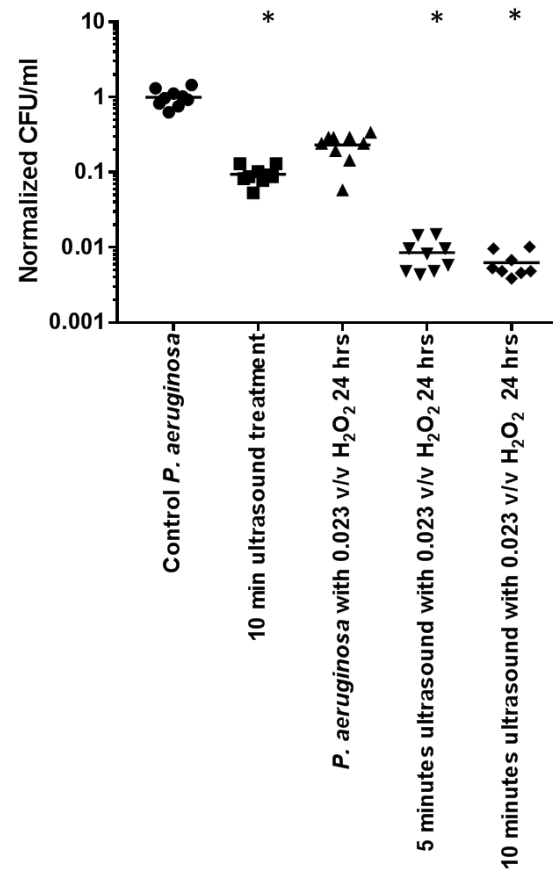
Figure 6.15: Effect of co treatment of sub MIC of biocides and low frequency of ultrasound on planktonic. *P. aeruginosa* (NCIMB 8295) was treated by 24hrs of sub MIC of hydrogen peroxide and exposed to 40 KHz at an intensity W/cm^2 ultrasound for 0, 10 min. * $P < 0.005$.

6.2.8- Effect of Ultrasound on mammalian cells

6.2.8.1- Cell culture

A keratinocyte cell line (HaCaT) and human dermal fibroblasts were cultured as described previously (section 4.2.1.1), ratios of HaCaT and fibroblasts were seeded at 1.5×10^4 cell/ml HaCaT alone, fibroblasts alone or a 3:1 ratio of HaCaT to fibroblasts in 6 well plates. Cells were allowed to settle overnight prior to LFU treatment at 40 kHz frequency and 150 mW/cm^2 intensity for 5, 10, 15 and 20 minutes. Following treatments metabolic cell activity was determined using an alamar blue as described previously (Section 4.2.1.1). Absorbance readings were normalised to untreated controls. HaCaT cells, fibroblasts and a mixture of HaCaT cells and fibroblasts monolayers treated with LFU showed a non-significant decrease in metabolic activity (Figure 6.16).
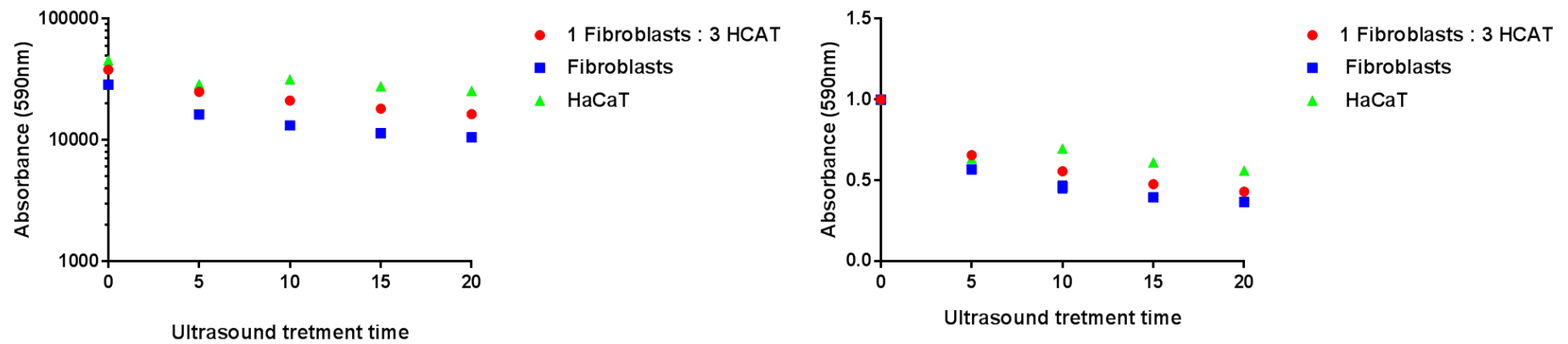
Figure 6.16: Effect of low frequency ultrasound at 40 kHz on mammalian cells monolayer; HaCaT cells, fibroblasts and a mixture of HaCaT cells and fibroblasts were all exposed to 40 KHz at an intensity 150 mW/cm^2 of ultrasound for 0, 5, 10, 15 and 20 min.

6.4- Discussion

The effect of low frequency ultrasound on *S. aureus, P. aeruginosa, S. epidermis* and MRSA were investigated. These pathogens are known to be amongst the major causes of skin infections, particularly in burns (Lawrence, 1994). With increasing failure of antibiotic treatment due to antibiotic resistance, novel treatments are urgently needed. Therefore alternative treatment options should be employed in order to overcome antibiotic resistance. The aim of this study was to investigate the effects of low frequency ultrasound (LFU) as an anti-microbial strategy for wound infections.

Several studies have demonstrated potential effects for LFU on different types of microorganisms (e.g. bacteria, spores, and fungi) using higher intensities and longer periods of exposure of US than those mentioned in the present study (Declerck *et al.* 2010; Dong *et al.* 2013; Runyan *et al.* 2006; Yu *et al.* 2012). However, unfortunately the systems used in this study were not able to generate higher intensities than those investigated.

This study showed that commercial ultrasound cavitation GS8.2E ultrasound treatment at 40 kHz reduced viability of both planktonic *S. aureus* and *P. aeruginosa*, when the bacteria were exposed to ultrasound for 5 and 10 minutes. These results are consistent with those of Scherba, *et al.* (1991) who used LFU at a frequency of 26 kHz in order to assess the antimicrobial efficacy of ultrasound on four types of bacteria (*E. coli, S. aureus, B. subtilis* and *P. aeruginosa*). They found a significant effect of low frequency ultrasound on *B. subtilis, S. aureus, P. aeruginosa* and *E.coli* (Scherba *et al.* 1991). However, in the current study the bacteria decreased approximately 1 $\log_{10}$ reduction in

CFU/ml. The findings of the present research are in agreement with those found by Singer *et al.*, (1999), who applied 20–50 kHz on LFU to *S. epidermidis*, with a significant decrease in bacteria observed. However, they attributed the reduction in the bacteria to the increase in temperature of the medium which exceeded 45°C. In the current study, the effects of LFU took place with no increase in the medium temperature due to the use of ice during LFU application to maintain temperature, suggesting results were due to acoustic cavitation generated active free radicals rather than a thermal effect. Joyce *et al.*, (2011) investigated US between 20 - 40 and 580 kHz frequency and an intensity of 0·012 and 0·013 W/cm^3 on *E. coli* and *K. pneumonia,* with a reduction in bacteria cell counts seen in low-frequencies (20 and 38 kHz). Higher frequencies (512 and 850 kHz) increased bacteria cell counts (Joyce *et al.*, 2011).

The frequency of the commercial ultrasound cavitation GS8.2E device gave unexpected results compared with the results of the previous studies. Furthermore, information about the intensity was not available for this device. The second device utilised was reported to vary intensities between 5 and 47 W/cm2. However, whilst an increase in effectiveness was observed with increased intensies effects were lower than those reported in the literature (Ganesan *et al.*, 2015). Since the intensity could not be verified a third device was utilised which could measure the delivered intensity with computerised software connected to the ultrasound device to determine the intensity and frequency precisely. The software was an in-house system developed by collaborators at the University of Sheffield. This system was intended to be used on each of the 6 well plates, through 6 individual frequency and intensity

transducers. Moreover, this system could also monitor the US wave forms. In the preliminary experiments, the intensity150 mW/ cm^2 with ≤1.6 volts /well voltage were utilised.

The ultrasound was applied to four types of bacteria: *S. aureus*, *P. aeruginosa*, *S. epidermidis* and MRSA. Significant decreases in viable numbers were seen in all bacteria investigated following 5- or 10-minutes US treatment. However, a limited increase in effectiveness was seen with increased treatment time. Interestingly, the in-house ultrasound system which generated 150 mW/cm^2 gave results similar to those given by the second commercial US system which was reported to have an intensity of 47W/cm^2, suggesting the reported levels may have been incorrect; alternatively the effects of LFU could be intensity independant. However, the results of the second commercial system did show increasing effectiveness with increasing intensity investigates.

The in-house ultrasound of Sheffield system at 150 mW/cm^2 was then utilised to determine the combined effects of biocidal agents and US. An increase in bactericidal effect was shown for *S. aureus* and *P. aeruginosa* when combined treatments were applied. In an attempt to reduce the use of chlorine, Phull *et al.* (1997) showed that when ultrasound at frequency 38 kHz and 800 kHz with intensities of 5 to 30 W/cm^2 were used with chemical disinfection, more bacteria in water samples were killed by using chemical disinfection combined with ultrasound than by using disinfection alone.

Carmen *et al.,* (2005), Liu *et al.,* (2011) and Zhu *et al.,* (2014) used ultrasound combined with antibiotics to increase the effectiveness of antibiotics via improved penetration. Frequency ≤ 70 kHz with different intensity could increase bacterial reduction which was enhanced by antibiotics (Table 6.2, 3).

Following these promising results, which suggested ultrasound could be utilised to decrease the concentration of biocidal agents, thus potentially reducing the toxic side effects on mammalian cells, this system was then to be utilised for the skin models developed in chapters 4 and 5. However a number of the transducers on the ultrasound machine became faulty and different values were identified from the six transducers, and the system deemed unreliable for future use.

6.5- Conclusion

This research has highlighted the effect of different intensities of LFU on planktonic bacteria. More than one type of ultrasound machine was utilised to determine the effects of frequency and intensity. It was found that the in-house system ultrasound produce better results (in terms of reducing numbers of viable bacteria) compared to the other devices although the intensities were very low compared to published papers. The preliminary findings of our study suggested that LFU could significantly reduce the number of viable bacterial in the planktonic culture and that US combined with biocidal agents could work in an additive manner.

Chapter 7

General Discussion and Future Directions

7.1- Key findings

Infection Burn skin is type of wound, which requires specific treatment to reduce bacterial infection, morbidity and mortality. Furthermore, the rise in prevalence of diabetes, coupled with advancing age of the population, has led to an increase in bacterial infection of wounds, with limited studies investigating in detail the effects of treatments on mammalian cell responses. Alternative methods of treating infection have become more widely used in order to circumvent these problems. However, there is an urgent need for new antimicrobial strategies to counteract the development of antibiotic resistance and to minimise local toxicity to skin cells, which hinders wound healing. Therefore, the aim of the current thesis was to examine the impact of a number of potential antimicrobial strategies to decrease the bacterial load in a 3D model of infected wounds, whilst determining the effects of these strategies on mammalian skin cells.

Firstly, the effects of potential antimicrobial strategies which are thought to act via generation of free radicals were determined on four common bacteria involved in skin infections. These studies demonstrated that biocidal agents (silver nitrate, isothiazolone, hydrogen peroxide and medical grade Manuka honey) reduced CFU/ml of bacteria in planktonic and biofilm cultures. They could be useful in treating infections. Nitrocellulose membranes were utilised initially as a bacterial biofilm model to examine biocidal agents; however, this model is a simple biofilm and fails to model interactions with skin cells. Thus, it was essential to determine the efficacy of biocidal agents on a more representative model for skin infections.

Moreover, the effects of biocidal agents on native skin cells are an important consideration to define possible side effects and local toxicity. Thus, this thesis went on to establish an *in vitro* tissue engineered skin model utilising a cell line (HaCaT) and commercially available primary fibroblasts which can be accessed easily allowing application in most laboratories. This model was utilised to determine the effects of the biocidal agents on the 3D skin model as a more representative screening model prior to animal model testing and clinical application beyond this thesis.

This 3D skin model was burned and infected individually with *S. aureus* and *P. aeruginosa* and the migration and penetration of bacteria assessed using the skin model. Bacterial infection resulted in increased toxicity to the mammalian cells, which further increased following biocidal treatments. Interestingly, the most effective agent was Manuka Honey which produced the greatest impact on reducing numbers of bacteria, decreasing the migration and penetration of bacteria and minimising mammalian cell death zones. *P. aeruginosa*, toxicity was higher than that seen for *S. aureus*, furthermore *P. aeruginosa*, penetration and migration was deeper and more extensive compared to *S. aureus.* However, all the biocides investigated induced toxic effects on the mammalian cells thus an alternative antimicrobial strategy of application of ultrasound was investigated to determine if decreased doses of biocidal agents could be used to reduce toxic side effects. This research illustrated the influence of diverse types of low frequency ultrasound on planktonic bacteria; with a variety of intensities investigated. Several types of ultrasound machines were tested including commercial systems and an in-house system.

The in house ultrasound system was shown to be more controllable and yielded improved results when compared with some of the commercial devices, however, the intensities used were lower than those reported by other research studies (Scherba *et a.l* 1991; Rediske *et al.* 1998). Furthermore, the ultrasound intensity on the current study is similar to intensity was reported by E. Joyce *et al.* (2003 and 2011). The initial findings of the current study suggested that LFU could significantly decrease the bacterial load in the planktonic culture and that the ultrasound co-treatment with biocidal agents could further reduce the bacterial number. This raises the possibility of decreasing the concentration of biocidal agents which could reduce toxic side effects on mammalian cells.

7.2- Future directions

Although the *in vitro* burned 3D skin model developed here for single bacterial biofilm infection with *S. aureus* or *P. aeruginosa* could be applied for investigating alternative biocidal agents for novel therapies and may serve as a useful alternative to animal models. There remain a number of key areas which should be addressed in the near future. These include:

7.2.1- Developing physiologically relevant biofilm models

In the present study, research on the bacterial pathogens dealt with a single species of bacteria to develop the skin biofilms. However, most chronic wound infections are multi microbial, where individual species may exhibit synergistic interactions with the broader community of microorganisms promoting virulence, persistence, or microbial tolerance (DeLeon *et al.* 2014). These synergistic interactions are challenging to study, in part due to the difficulties involved in growing different bacterial species together *in vitro* (Palmer *et al.* 2007). This is

evident with *S. aureus* and *P. aeruginosa*, though they are often found together in human skin infections, *P. aeruginosa* rapidly kills *S. aureus* when they are placed together in planktonic co-cultures *in vitro* (Palmer *et al.* 2007; Palmer 2005).

Several *in vitro* model systems have been developed to examine complex communities of clinically relevant bacteria under controlled conditions (Sun *et al.* 2008; Sun *et al.* 2009; Wright *et al.* 2015). Most of these models use abiotic surfaces to examine the growth of biofilms and are generally categorised as closed or open systems that are based on the nutrient supply approach (section 1.1.8.1).

Thus, future research needs to focus on biofilms formed by polybacterial species in 3D skin wound model, such as:

7.2.1.1- The Lubbock Chronic Wound Model (LCWM)

The LCWM was developed by Sun *et al.* (2008) to simulate the wound environment by utilising bovine plasma, horse red blood cells and Bolton Broth (Sun *et al.* 2008). As a consequence of staphylocoagulase activity, the media plasma components clot after they are inoculated with a coagulase-positive bacterial species (like *S. aureus*) converting the liquid media into a solidified mass. The bacteria then stick to strands of insoluble fibrin making a biofilm inside the host-derived matrix. Alternatively, a sterile pipet tip, or a different surface type can be added to create biofilm adherence where a coagulase positive strain is not used. LCWM have been used to demonstrate how the diverse combination of common wound pathogens can influence tolerance to various antibiotics and to pinpoint how interactions between species change in the wound environment (Sun *et al.* 2008; Dalton *et al.* 2011; DeLeon *et al.*

2014). According to Dowd and Sun (2009), the chronic wound model, (LCWM) is beneficial for studying interactions between microbes that are isolated from clinical wounds incorporating aerobic species in the biofilm. DeLeon *et al.* (2014) discovered that *P. aeruginosa* totally eliminated *S. aureus* after co-culture in standard laboratory media; however, these two strains could form a biofilm in the LCWM for up to seven days.

7.2.1.2- Microfluidic devices

Microfluidic devices such as the Bioflux systems (Wright *et al.* 2015) are dynamic models that have microfluidic platforms, allowing for the controlled visualisation and determination of a mature biofilm in real time extending over a specific period. The customisable chips permit complete control of the environmental conditions, for example, different substratum properties, the hydrodynamic variables, and the foundation of chemical gradients (Wright *et al.* 2015; Li *et al.* 2015). The model can analyse host-bacteria interactions with real-time visualisation of biofilm growth on human cells (Kim *et al.* 2010).

7.2.2- Developing a physiologically relevant skin model

This thesis reports the development of a functional full-thickness tissue-engineered skin model from human HaCaT cell lines which generated a differentiated epidermis on top of a DED dermis layer and closely resembled the morphology of native skin. However, HaCaT cells are aneuploidy cells, which contain an abnormal number of chromosomes (Boukamp *et al.* 1988). Furthermore HaCaT cells produce abnormal cornfield envelope proteins, such as involucrin, loricrin and filaggrin. These cells are also derived from cancerous tissues and thus may behave differently to normal skin cells and thus alternative

models utilising non-cancerous cells are needed. Development of a 3D skin model using hTERT immortalized keratinocytes, poses a number of advantages for an *in vitro* skin model. Such as the continuous supply of easily amplified cells which are not derived from cancerous cells, no donor variation, and no logistical (transport from the clinic to laboratory) and ethical issues from using primary human cells or animal cells (Smits *et al.* 2017; Jung *et al.* 2016; Raijnder *et al.* 2015).

hTERT cells have the potential to be an important tool to study skin physiology with multiple applications, and may contribute to the replacement, and reduction of animal models in the future. Preliminary investigations towards the end of this thesis investigated the feasibility of a 3D skin model using hTERT immortalized keratinocytes in place of HaCaT cells as described in Chapter 3 section (3.2.2). Histological analysis established that hTERT immortalized keratinocytes showed clear proliferation of multilayers of keratinocytes and pink viable nuclei (Figure 7.1). These data indicate that hTERT immortalized models could be utilised to mimic more closely *in vivo* skin, however phenotypic investigation is required to determine whether appropriate differentiation was induced.
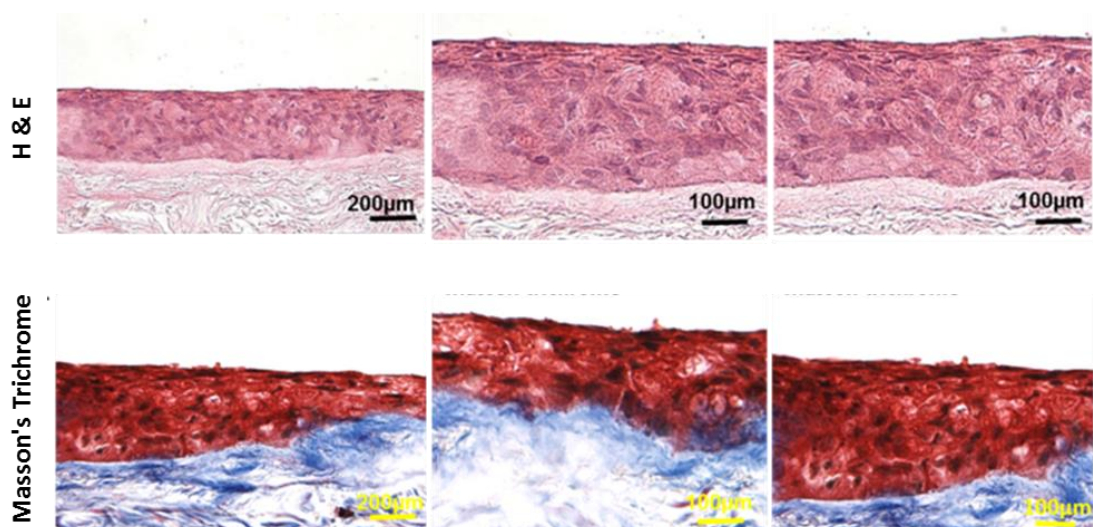
Figure 7.1: 3D skin models with different hTERT immortalized keratinocytes (6×10^5) cells and fibroblast (2×10^5) cells, Stained with Masson Trichrome & H & E.

Reijnders *et al.,* (2015) and Smits, *et al.,* (2017) have also described 3D skin models utilising hTERT-immortalised keratinocytes. The human hTERT-HSEs showed good epidermis on the fibroblast-collagen matrix consisting of fully differentiating multi-epidermal layers. The immortalised keratinocytes could be exploited to develop *in vitro* tissue skin models which could be utilised to investigate novel therapies for burned skin infections.

However, these models lack the dermal layers because the scaffold inside it is made of collagen matrix and are thus difficult to investigate full thickness injury and infection. Thus the application of hTERT keratinocytes and potentially fibroblasts to the 3D skin model developed in this thesis could provide an ideal easily accessible skin model for use in investigating new anti-infective therapies.

7.2.3- Effect of ultrasound on 3D skin model

This thesis demonstrated within planktonic culture ultrasound was able to reduce bacterial load with limited toxicity to mammalian cells in monolayer culture. Thus the application of ultrasound on full thickness 3D skin model at particular frequency and intensity would be important to investigate. In particular it is necessary to test the viability cells in the epidermal layer. Following ultrasound treatment of uninfected skin (using a range of frequencies and times), cell viability of the TE skin model could be determined using the Alamar Blue assay and histological assessment. To determine the effect of ultrasound on bacterially infected skin, a model of infection could be developed using the tissue engineered skin model reported in this thesis. The skin could be infected with *S. aureus* or *P. aeruginosa* for 12h, 24h and 48h and both skin morphology

and viability determined. To effect of ultrasound treatment on biofilms within the wound could then be investigated using both single and multiple treatments. Finally, the effects of ultrasound treatment on TE skin infected with a mix of bacterial species should be investigated to mimic the biofilm infection of wounds *in vivo* more closely.

7.2.4- Combinatorial approaches to biofilm eradication

The results obtained in this thesis demonstrated the effect of the ultrasound with sub MIC biocides on planktonic bacteria demonstrated a promising approach to biofilm eradication, where combination therapies could decrease the concentration of biocides required. However to determine if this is a viable option these treatments should be investigated on biofilm models, in particular infected and uninfected wounds within 3D skin models using sub MIC biocides prior to treatment or in combination with ultrasound need to be investigated. Pre-treated infected/uninfected skin not exposed to ultrasound would be utilised as a control. The effects following infection with mixed biofilms would also be explored to more closely mimic the biofilms formed on infected wounds.

7.3- Conclusion

The pathogenic polybacterial biofilm models could help in identifying new treatments for skin infections. The hTERT immortalized keratinocytes and Euro-skin as 3D skin models together with TGFα revealed that epidermal layer was thick, which holds promise for the *in vitro* 3D skin model. Furthermore, it would be interesting to investigate low frequency ultrasound effect either alone or in combination with biocidal agents on 3D skin burned infection.

Chapter 8

References

8.1- References

Abbas, A. K., Lichtman, A. H., & Pober, J. (2003). Antigen processing and presentation to T lymphocytes. *Cellular and Molecular Immunology,* 115-137.

Abdulkhaliq, A., & Swaileh, K. M. (2017). Physico-chemical properties of multi-floral honey from the west bank, palestine. *International Journal of Food Properties, 20*(2), 447-454.

Adams, C. J., Boult, C. H., Deadman, B. J., Farr, J. M., Grainger, M. N., Manley-Harris, M., & Snow, M. J. (2008). Isolation by HPLC and characterisation of the bioactive fraction of new zealand manuka (leptospermum scoparium) honey. *Carbohydrate Research, 343*(4), 651-659.

Adra, S., Sun, T., MacNeil, S., Holcombe, M., & Smallwood, R. (2010). Development of a three-dimensional multiscale computational model of the human epidermis. *PloS One, 5*(1), e8511.

Agnihotri, N., Gupta, V., & Joshi, R. (2004). Aerobic bacterial isolates from burn wound infections and their antibioGrams a five-year study. *Burns, 30*(3), 241-243.

Ahn, S., Yoon, H., Kim, G., Kim, Y., Lee, S., & Chun, W. (2009). Designed three-dimensional collagen scaffolds for skin tissue regeneration. *Tissue Engineering Part C: Methods, 16*(5), 813-820.

Ahrens, K., Schunck, M., Podda, G., Meingassner, J., Stuetz, A., Schröder, J., Proksch, E. (2011). Mechanical and metabolic injury to the skin barrier leads to increased expression of murine β-defensin-1,-3, and-14. *Journal of Investigative Dermatology, 131*(2), 443-452.

Akinjogunla, O., Adegoke, A., Mboto, C., Chukwudebelu, I., & Udokang, I. (2009). Bacteriology of automobile accident wounds infection. *International Journal of Medicine and Medical Sciences, 1*(2), 023-027.

Ako-Nai, A., Ikem, I., Akinloye, O., Aboderin, A., Ikem, R., & Kassim, O. (2006). Characterization of bacterial isolates from diabetic foot infections in ile-ife, southwestern nigeria. *The Foot, 16*(3), 158-164.

Alberts, B., Johnson, A., Lewis, J., Raff, M., Roberts, K. and Walter, P., 2002. Lymphocytes and the cellular basis of adaptive immunity. *In Molecular Biology of the Cell.* 4th edition. Garland Science.

Alexander, J. W. (2009). History of the medical use of silver. Surgical Infections*, 10*(3), 289-292.

Almasaudi, S. B., Al-Nahari, A. A., El Sayed, M., Barbour, E., Al Muhayawi, S. M., Al-Jaouni, S., Harakeh, S. (2017). Antimicrobial effect of different types of honey on *staphylococcus aureus. Saudi Journal of Biological Sciences, 24*(6), 1255-1261.

Alumia, R. (2013) Improving outcomes with noncontact low-frequency ultrasound. Wound Care Advisor, Vol. 2 (5), available at http://woundcareadvisor.com/wp-content/uploads/2013/09/BP_IMPROVE_S-O13.pdf

Andersen, A., Joergensen, B., Bjarnsholt, T., Johansen, H., Karlsmark, T., Givskov, M., & Krogfelt, K. A. (2010). Quorum sensing regulated virulence factors in *Pseudomonas aeruginosa* are toxic to lucilia sericata maggots. *Microbiology, 156*(2), 400-407.

Andonova, M., & Urumova, V. (2013). Immune surveillance mechanisms of the skin against the stealth infection strategy of *Pseudomonas aeruginosa* review. *Comparative Immunology, Microbiology and Infectious Diseases, 36*(5), 433-448.

Anglen, J. O. (2001). Wound irrigation in musculoskeletal injury. *JAAOS-Journal of the American Academy of Orthopaedic Surgeons, 9*(4), 219-226.

Arakawa, H., Neault, J., & Tajmir-Riahi, H. (2001). Silver (I) complexes with DNA and RNA studied by fourier transform infrared spectroscopy and capillary electrophoresis. *Biophysical Journal, 81*(3), 1580-1587.

Armstrong, D. G., Lavery, L. A., & Boulton, A. J. (2007). Negative pressure wound therapy via vacuum-assisted closure following partial foot amputation: What is the role of wound chronicity? *International Wound Journal, 4*(1), 79-86.

Armstrong, D. G., Salas, P., Short, B., Martin, B. R., Kimbriel, H. R., Nixon, B. P., & Boulton, A. J. (2005). Maggot therapy in "lower-extremity hospice" wound care: Fewer amputations and more antibiotic-free days. *Journal of the American Podiatric Medical Association, 95*(3), 254-257.

Armstrong, D. G., Lavery, L. A., Quebedeaux, T. L., & Walker, S. C. (1997). Surgical morbidity and the risk of amputation due to infected puncture wounds in diabetic versus nondiabetic adults. *Journal of the American Podiatric Medical Association, 87*(7), 321-326.

Asselineau, D., Bernhard, B., Bailly, C., & Darmon, M. (1985). Epidermal morphogenesis and induction of the 67 kD keratin polypeptide by culture of human keratinocytes at the liquid-air interface. *Experimental Cell Research, 159*(2), 536-539.

Atiyeh, B. S., Costagliola, M., Hayek, S. N., & Dibo, S. A. (2007). Effect of silver on burn wound infection control and healing: Review of the literature. *Burns, 33*(2), 139-148.

Atrott, J., & Henle, T. (2009). Methylglyoxal in manuka honey correlation with antibacterial properties. *Czech Journal of Food Sciences, 27*(Spec.), S163-S165.

Ayan, I., Aslan, G., Comelekoglu, U., Yilmaz, N., & Colak, M. (2008). The effect of low-intensity pulsed sound waves delivered by the exogen device on *staphylococcus aureus* morphology and genetics. *Acta Orthopaedica Et Traumatologica Turcica, 42*(4), 272-277.

Baatout, S., De Boever, P., & Mergeay, M. (2006). Physiological changes induced in four bacterial strains following oxidative stress. *Applied Biochemistry and Microbiology, 42*(4), 369-377.

Baker, K. G., Robertson, V. J., & Duck, F. A. (2001). A review of therapeutic ultrasound: Biophysical effects. *Physical Therapy, 81*(7), 1351-1358.

Baldry, M. (1983). The bactericidal, fungicidal and sporicidal properties of hydrogen peroxide and peracetic acid. *Journal of Applied Bacteriology, 54*(3), 417-423.

Bardy, S. L., Ng, S. Y., & Jarrell, K. F. (2003). Prokaryotic motility structures. *Microbiology, 149*(2), 295-304.

Bauer, S. M., Bauer, R. J., & Velazquez, O. C. (2005). Angiogenesis, vasculogenesis, and induction of healing in chronic wounds. *Vascular and Endovascular Surgery, 39*(4), 293-306.

Baureder, M., Reimann, R., & Hederstedt, L. (2012). Contribution of catalase to hydrogen peroxide resistance in enterococcus faecalis. *FEMS Microbiology Letters, 331*(2), 160-164.

Bautista, L., Gaya, P., Medina, M., & Nunez, M. (1988). A quantitative study of enterotoxin production by sheep milk staphylococci. *Applied and Environmental Microbiology, 54*(2), 566-569.

Bavle, R.M., 2014. Eosinophilic nucleoli. J*ournal of oral and maxillofacial pathology*: JOMFP, 18(2), p.152.

Baxter, H. (2003). Management of surgical wounds. *Nursing Times, 99*(13), 66-68.

Beanes, S. R., Dang, C., Soo, C., & Ting, K. (2003). Skin repair and scar formation: The central role of TGF-β. *Expert Reviews in Molecular Medicine, 5*(8), 1-22.

Bechert, K., & Abraham, S. E. (2009). Pain management and wound care. *The Journal of the American College of Certified Wound Specialists, 1*(2), 65-71.

Belkaid, Y., & Segre, J. A. (2014). Dialogue between skin microbiota and immunity. *Science (New York, N.Y.), 346*(6212), 954-959.

Bellas, E., Seiberg, M., Garlick, J., & Kaplan, D. L. (2012). In vitro 3D full-thickness skin-equivalent tissue model using silk and collagen biomaterials. *Macromolecular Bioscience, 12*(12), 1627-1636.

Bennett, G., Dealey, C., & Posnett, J. (2004). The cost of pressure ulcers in the UK. *Age and Ageing, 33*(3), 230-235.

Beumer, R., Bloomfield, S., Exner, M., Fara, G., Nath, K., & Scott, E. (2000). (2000). Microbial resistance and biocides: A review by the international forum on home hygiene (IFH).

Bielecki, P., Glik, J., Kawecki, M., & dos Santos, Vítor AP Martins. (2008). Towards understanding *Pseudomonas aeruginosa* burn wound infections by profiling gene expression. *Biotechnology Letters, 30*(5), 777-790.

Bigelow, T. A., Northagen, T., Hill, T. M., & Sailer, F. C. (2009). The destruction of escherichia coli biofilms using high-intensity focused ultrasound. *Ultrasound in Medicine & Biology, 35*(6), 1026-1031.

Bir, S. C., Esaki, J., Marui, A., Yamahara, K., Tsubota, H., Ikeda, T., & Sakata, R. (2009). Angiogenic properties of sustained release platelet-rich plasma: Characterization in-vitro and in the ischemic hind limb of the mouse. *Journal of Vascular Surgery, 50*(4), 870-879. e2.

Bjarnsholt, T., Kirketerp-Møller, K., Jensen, P. Ø., Madsen, K. G., Phipps, R., Krogfelt, K., Givskov, M. (2008). Why chronic wounds will not heal: A novel hypothesis. *Wound Repair and Regeneration, 16*(1), 2-10.

Bjarnsholt, T., Kirketerp-Møller, K., Kristiansen, S., Phipps, R., Nielsen, A. K., Jensen, P. Ø., Givskov, M. (2007). Silver against *Pseudomonas aeruginosa* biofilms. *Apmis, 115*(8), 921-928.

Blackwood, L. L., Stone, R. M., Iglewski, B. H., & Pennington, J. E. (1983). Evaluation of *Pseudomonas aeruginosa* exotoxin A and elastase as virulence factors in acute lung infection. *Infection and Immunity, 39*(1), 198-201.

Block, S. S. (2001). *Disinfection, sterilization, and preservation* Lippincott Williams & Wilkins.

Boateng, J. S., Matthews, K. H., Stevens, H. N., & Eccleston, G. M. (2008). Wound healing dressings and drug delivery systems: A review. *Journal of Pharmaceutical Sciences, 97*(8), 2892-2923.

Boelsma, E., Verhoeven, M. C., & Ponec, M. (1999). Reconstruction of a human skin equivalent using a spontaneously transformed keratinocyte cell line (HaCaT). *Journal of Investigative Dermatology, 112*(4), 489-498.

Bohari, S. P., Grover, L. M., & Hukins, D. W. (2012). Pulsed-low intensity ultrasound enhances extracellular matrix production by fibroblasts encapsulated in alginate. *Journal of Tissue Engineering, 3*(1), 2041731412454672.

Bohari, S. P., Grover, L. M., & Hukins, D. W. (2015). Pulsed low-intensity ultrasound increases proliferation and extracelluar matrix production by human dermal fibroblasts in three-dimensional culture. *Journal of Tissue Engineering, 6*, 2041731415615777.

Bojar, R., & Holland, K. (2002). The human cutaneous microflora and factors controlling colonisation. *World Journal of Microbiology and Biotechnology, 18*(9), 889-903.

Boulton, A. J., Vileikyte, L., Ragnarson-Tennvall, G., & Apelqvist, J. (2005). The global burden of diabetic foot disease. *The Lancet, 366*(9498), 1719-1724.

Bousfield, C. B. (2002). *Burn trauma: Management and nursing care* Whurr London.

Bowden, M. G., Heuck, A. P., Ponnuraj, K., Kolosova, E., Choe, D., Gurusiddappa, S., Hook, M. (2008). Evidence for the "dock, lock, and latch" ligand binding mechanism of the staphylococcal microbial surface component recognizing adhesive matrix molecules (MSCRAMM) SdrG. *The Journal of Biological Chemistry, 283*(1), 638-647.

Bowler, P. G., Duerden, B. I., & Armstrong, D. G. (2001). Wound microbiology and associated approaches to wound management. *Clinical Microbiology Reviews, 14*(2), 244-269.

Bradford, P. A. (2001). Extended-spectrum beta-lactamases in the 21st century: Characterization, epidemiology, and detection of this important resistance threat. *Clinical Microbiology Reviews, 14*(4), 933-51, table of contents.

Brady, R. A., Leid, J. G., Calhoun, J. H., Costerton, J. W., & Shirtliff, M. E. (2008). Osteomyelitis and the role of biofilms in chronic infection. *FEMS Immunology & Medical Microbiology, 52*(1), 13-22.

Bragg, P., & Rainnie, D. (1974). The effect of silver ions on the respiratory chain of *Escherichia coli*. *Canadian Journal of Microbiology, 20*(6), 883-889.

Brandi, G., Salvaggio, L., Cattabeni, F., Cantoni, O., & Mortelmans, K. (1991). Cytocidal and filamentous response of escherichia coli cells exposed to low concentrations of hydrogen peroxide and hydroxyl radical scavengers. *Environmental and Molecular Mutagenesis, 18*(1), 22-27.

Bregnbak, D., Lundov, M. D., Zachariae, C., Menné, T., & Johansen, J. D. (2013). Five cases of severe chronic dermatitis caused by isothiazolinones. *Contact Dermatitis, 69*(1), 57-59.

Breitkreutz, D., Schoop, V. M., Mirancea, N., Baur, M., Stark, H., & Fusenig, N. E. (1998). Epidermal differentiation and basement membrane formation by

HaCaT cells in surface transplants. *European Journal of Cell Biology, 75*(3), 273-286.

Brinkman, F. S., Bains, M., & Hancock, R. E. (2000). The amino terminus of *Pseudomonas aeruginosa* outer membrane protein OprF forms channels in lipid bilayer membranes: Correlation with a three-dimensional model. *Journal of Bacteriology, 182*(18), 5251-5255.

Brodersen, D. E., Clemons Jr, W. M., Carter, A. P., Morgan-Warren, R. J., Wimberly, B. T., & Ramakrishnan, V. (2000). The structural basis for the action of the antibiotics tetracycline, pactamycin, and hygromycin B on the 30S ribosomal subunit. *Cell, 103*(7), 1143-1154.

Brohem, C. A., da Silva Cardeal, Laura B, Tiago, M., Soengas, M. S., de Moraes Barros, Silvia B, & Maria-Engler, S. S. (2011). Artificial skin in perspective: Concepts and applications. *Pigment Cell & Melanoma Research, 24*(1), 35-50.

Brownrigg, J., Apelqvist, J., Bakker, K., Schaper, N., & Hinchliffe, R. (2013). Evidence-based management of PAD & the diabetic foot. *European Journal of Vascular and Endovascular Surgery, 45*(6), 673-681.

Brozovich, F.V., Nicholson, C.J., Degen, C.V., Gao, Y.Z., Aggarwal, M. and Morgan, K.G., 2016. Mechanisms of vascular smooth muscle contraction and the basis for pharmacologic treatment of smooth muscle disorders. *Pharmacological reviews*, 68(2), pp.476-532.

Bu, S., Li, Y., Zhou, M., Azadin, P., Zeng, M., Fives-Taylor, P., & Wu, H. (2008). Interaction between two putative glycosyltransferases is required for glycosylation of a serine-rich streptococcal adhesin. *Journal of Bacteriology, 190*(4), 1256-1266.

Buchanan, E. P., Longaker, M. T., & Lorenz, H. P. (2009). Fetal skin wound healing. *Advances in Clinical Chemistry, 48*, 137-161.

Burrell, R. E. (2003). A scientific perspective on the use of topical silver preparations. *Ostomy Wound Management, 49*(5; SUPP), 19-24.

Byl, N. N., McKenzie, A., Wong, T., West, J., & Hunt, T. K. (1993). Incisional wound healing: A controlled study of low and high dose ultrasound. *Journal of Orthopaedic & Sports Physical Therapy, 18*(5), 619-628.

Caggiati, A. (2013). The venous valves of the lower limbs. *Phlebolymphology, 20*(2), 87-95.

Caldwell, C. C., Chen, Y., Goetzmann, H. S., Hao, Y., Borchers, M. T., Hassett, D. J., Lau, G. W. (2009). *Pseudomonas aeruginosa* exotoxin pyocyanin causes cystic fibrosis airway pathogenesis. *The American Journal of Pathology, 175*(6), 2473-2488.

Cannon, C., Neal, P., Southee, J., Kubilus, J., & Klausner, M. (1994). New epidermal model for dermal irritancy testing. *Toxicology in Vitro, 8*(4), 889-891. .

Canton, I., Cole, D., Kemp, E., Watson, P., Chunthapong, J., Ryan, A., Haycock, J. (2010). Development of a 3D human in vitro skin co-culture model for detecting irritants in real-time. *Biotechnology and Bioengineering, 106*(5), 794-803.

Capobianco, C. M., & Zgonis, T. (2009). An overview of negative pressure wound therapy for the lower extremity. *Clinics in Podiatric Medicine and Surgery, 26*(4), 619-631.

Carmen, J., Roeder, B., Nelson, J., Beckstead, B., Runyan, C., Schaalje, G., Pitt, W. (2004). Ultrasonically enhanced vancomycin activity against *Staphylococcus epidermidis* biofilms in vivo. *Journal of Biomaterials Applications, 18*(4), 237-245.

Carmen, J. C., Roeder, B. L., Nelson, J. L., Ogilvie, R. L. R., Robison, R. A., Schaalje, G. B., & Pitt, W. G. (2005). Treatment of biofilm infections on implants with low-frequency ultrasound and antibiotics. *American Journal of Infection Control, 33*(2), 78-82.

Carpentier, B., & Cerf, O. (1993). Biofilms and their consequences, with particular reference to hygiene in the food industry. *Journal of Applied Bacteriology, 75*(6), 499-511.

Carter, M. J., Tingley-Kelley, K., & Warriner III, R. A. (2010). Silver treatments and silver-impregnated dressings for the healing of leg wounds and ulcers: A systematic review and meta-analysis. *Journal of the American Academy of Dermatology, 63*(4), 668-679.

Castellano, J. J., Shafii, S. M., Ko, F., Donate, G., Wright, T. E., Mannari, R. J., Robson, M. C. (2007). Comparative evaluation of silver-containing antimicrobial dressings and drugs. *International Wound Journal, 4*(2), 114-122.

Cerca, N., Jefferson, K. K., Oliveira, R., Pier, G. B., & Azeredo, J. (2006). Comparative antibody-mediated phagocytosis of *Staphylococcus epidermidis* cells grown in a biofilm or in the planktonic state. *Infection and Immunity, 74*(8), 4849-4855.

Ceri, H., Olson, M. E., Stremick, C., Read, R. R., Morck, D., & Buret, A. (1999). The calgary biofilm device: New technology for rapid determination of antibiotic susceptibilities of bacterial biofilms. *Journal of Clinical Microbiology, 37*(6), 1771-1776.

Chakrabarty, K., Dawson, R., Harris, P., Layton, C., Babu, M., Gould, L., Freedlander, E. (1999). Development of autologous human dermal–epidermal composites based on sterilized human allodermis for clinical use. *British Journal of Dermatology, 141*(5), 811-823.

Chamberlain, N., & Brueggemann, S. (1997). Characterisation and expression of fatty acid modifying enzyme produced by *Staphylococcus epidermidis*. *Journal of Medical Microbiology, 46*(8), 693-697.

Chambers, H., Dumville, J. C., & Cullum, N. (2007). Silver treatments for leg ulcers: A systematic review. *Wound Repair and Regeneration, 15*(2), 165-173.

Chambers, H. F. (1997). Methicillin resistance in staphylococci: Molecular and biochemical basis and clinical implications. *Clinical Microbiology Reviews, 10*(4), 781-791.

Chan, D. C., Fong, D. H., Leung, J. Y., Patil, N., & Leung, G. K. (2007). Maggot debridement therapy in chronic wound care. *Hong Kong Medical Journal,*

Chang, S., Sievert, D. M., Hageman, J. C., Boulton, M. L., Tenover, F. C., Downes, F. P., Brown, W. J. (2003). Infection with vancomycin-resistant *Staphylococcus aureus* containing the vanA resistance gene. *New England Journal of Medicine, 348*(14), 1342-1347.

Chang, Y. R., Perry, J., & Cross, K. (2017). Low-frequency ultrasound debridement in chronic wound healing: A systematic review of current evidence. *Plastic Surgery, 25*(1), 21-26.

Chapman, J. S. (1998). Characterizing bacterial resistance to preservatives and disinfectants. *International Biodeterioration & Biodegradation, 41*(3-4), 241-245.

Chapman, J. S. (2003). Biocide resistance mechanisms. *International Biodeterioration & Biodegradation, 51*(2), 133-138.

Chapman, J., Diehl, M., & Fearnside, K. (1998). Preservative tolerance and resistance. *International Journal of Cosmetic Science, 20*(1), 31-39.

Chau, D. Y., Johnson, C., MacNeil, S., Haycock, J. W., & Ghaemmaghami, A. M. (2013). The development of a 3D immunocompetent model of human skin. *Biofabrication, 5*(3), 035011.

Chen, Z. J., Yang, J. P., Wu, B. M., & Tawil, B. (2014). A novel three-dimensional wound healing model. *Journal of Developmental Biology, 2*(4), 198-209.

Chomiczewska, D., Trznadel-Budzko, E., Kaczorowska, A., & Rotsztejn, H. (2009). The role of langerhans cells in the skin immune system. [Znaczenie komorek Langerhansa w ukladzie immunologicznym skory] *Polski Merkuriusz Lekarski: Organ Polskiego Towarzystwa Lekarskiego, 26*(153), 173-177.

Chopra, I. (2007). The increasing use of silver-based products as antimicrobial agents: A useful development or a cause for concern? *Journal of Antimicrobial Chemotherapy, 59*(4), 587-590.

Choy, H. A., Kelley, M. M., Chen, T. L., Moller, A. K., Matsunaga, J., & Haake, D. A. (2007). Physiological osmotic induction of leptospira interrogans adhesion: LigA and LigB bind extracellular matrix proteins and fibrinogen. *Infection and Immunity, 75*(5), 2441-2450.

Church, J., & Courtenay, M. (2002). Maggot debridement therapy for chronic wounds. *The International Journal of Lower Extremity Wounds, 1*(2), 129-134.

Church, D., Elsayed, S., Reid, O., Winston, B., & Lindsay, R. (2006). Burn wound infections. *Clinical Microbiology Reviews, 19*(2), 403-434.

Clement, J. L., & Jarrett, P. S. (1994). Antibacterial silver. *Metal-Based Drugs, 1*(5-6), 467-482.

Cloete, T. E. (2003). Resistance mechanisms of bacteria to antimicrobial compounds. *International Biodeterioration & Biodegradation, 51*(4), 277-282.

Cogen, A., Nizet, V., & Gallo, R. (2008). Skin microbiota: A source of disease or defence? *British Journal of Dermatology, 158*(3), 442-455.

Cole, W. E. (2016). Use of multiple adjunctive negative pressure wound therapy modalities to manage diabetic lower-extremity wounds. *Eplasty, 16*, e34.

Collier, P. J., Austin, P., & Gilbert, P. (1991). Isothiazolone biocides: Enzyme-inhibiting pro-drugs. *International Journal of Pharmaceutics, 74*(2-3), 195-201.

Collier, P. J., Austin, P., & Gilbert, P. (1991). Isothiazolone biocides: Enzyme-inhibiting pro-drugs. *International Journal of Pharmaceutics, 74*(2-3), 195-201.

Colobert, L., Montagnon, B., Nofre, C., & Cier, A. (1962). Bactericidal activity of chemical systems productive of free hydroxyl radicals on *Escherichia coli.* mechanism of the bactericidal activity of hydrogen peroxide and ascorbic acid. *Ann.Inst.Pasteur, 102*(3), 278-281.

Colombo, I., Sangiovanni, E., Maggio, R., Mattozzi, C., Zava, S., Corbett, Y., Fumagalli, M., Carlino, C., Corsetto, P.A., Scaccabarozzi, D. and Calvieri, S., (2017). HaCat cells as a reliable in vitro differentiation model to dissect the inflammatory/repair response of human keratinocytes. *Mediators of inflammation, 2017.*

Compton, C. C., Butler, C. E., Yannas, I. V., Warland, G., & Orgill, D. P. (1998). Organized skin structure is regenerated in vivo from collagen-GAG matrices seeded with autologous keratinocytes. *Journal of Investigative Dermatology, 110*(6), 908-916.

Conner-Kerr, T., Alston, G., Stovall, A., Vernon, T., Winter, D., Meixner, J., Kute, T. (2010). The effects of low-frequency ultrasound (35 kHz) on methicillin-resistant *Staphylococcus aureus* (MRSA) *in vitro. Ostomy Wound Manage, 56*(5), 32-42.

Cooper, R. A., Ameen, H., Price, P., McCulloch, D. A., & Harding, K. G. (2009). A clinical investigation into the microbiological status of 'locally infected'leg ulcers. *International Wound Journal, 6*(6), 453-462.

Cornejo, E., Schlaermann, P., & Mukherjee, S. (2017). How to rewire the host cell: A home improvement guide for intracellular bacteria. *The Journal of Cell Biology, 216*(12), 3931-3948.

Costerton, J. W. (1999). Introduction to biofilm. *International Journal of Antimicrobial Agents, 11*(3-4), 217-21; discussion 237-9.

Costerton, J. W. (1999). Introduction to biofilm. *International Journal of Antimicrobial Agents, 11*(3-4), 217-21; discussion 237-9. doi:S0924-8579(99)00018-7 [pii]

Costerton, J. W., Stewart, P. S., & Greenberg, E. P. (1999). Bacterial biofilms: A common cause of persistent infections. *Science (New York, N.Y.), 284*(5418), 1318-1322.

Coussens, L. M., & Werb, Z. (2002). Inflammation and cancer. *Nature, 420*(6917), 860.

Coward, J. E., Carr, H. S., & Rosenkranz, H. S. (1973). Silver sulfadiazine: Effect on the ultrastructure of *Pseudomonas aeruginosa*. *Antimicrobial Agents and Chemotherapy, 3*(5), 621-624.

Crailsheim, K. (1985). Distribution of haemolymph in the honeybee (apis mellifica) in relation to season, age and temperature. *Journal of Insect Physiology, 31*(9), 707-713.

Dalton, T., Dowd, S. E., Wolcott, R. D., Sun, Y., Watters, C., Griswold, J. A., & Rumbaugh, K. P. (2011). An in vivo polymicrobial biofilm wound infection model to study interspecies interactions. *PloS One, 6*(11), e27317.

Danihlík, J., Škrabišová, M., Lenobel, R., Šebela, M., Omar, E., Petřivalský, M., Brodschneider, R. (2018). Does the pollen diet influence the production and expression of antimicrobial peptides in individual honey bees? *Insects, 9*(3), 79.

Darby, I.A., Laverdet, B., Bonté, F. and Desmoulière, A., (2014). Fibroblasts and myofibroblasts in wound healing. *Clinical, cosmetic and investigational dermatology*, 7, p.301

Davies, S. C., Fowler, T., Watson, J., Livermore, D. M., & Walker, D. (2013). Annual report of the chief medical officer: Infection and the rise of antimicrobial resistance. *The Lancet, 381*(9878), 1606-1609.

Davies, J., & Davies, D. (2010). Origins and evolution of antibiotic resistance. *Microbiology and Molecular Biology Reviews : MMBR, 74*(3), 417-433.

Davis, M. H., Dunkley, P., Harden, R., Harding, K., Laidlaw, J., Morris, A., & Wood, R. (1992). The wound proGramme. *Dundee: Centre for Medical Education,*

Davis, S. C., Cazzaniga, A. L., Ricotti, C., Zalesky, P., Hsu, L., Creech, J., Mertz, P. M. (2007). Topical oxygen emulsion: A novel wound therapy. *Archives of Dermatology, 143*(10), 1252-1256.

Davis, S. C., Ricotti, C., Cazzaniga, A., Welsh, E., Eaglstein, W. H., & Mertz, P. M. (2008). Microscopic and physiologic evidence for biofilm-associated wound colonization in vivo. *Wound Repair and Regeneration, 16*(1), 23-29.

de Breij, A., Haisma, E. M., Rietveld, M., El Ghalbzouri, A., van den Broek, P. J., Dijkshoorn, L., & Nibbering, P. H. (2012). Three-dimensional human skin equivalent as a tool to study acinetobacter baumannii colonization. *Antimicrobial Agents and Chemotherapy, 56*(5), 2459-2464.

Dean, R. T., Fu, S., Stocker, R., & Davies, M. J. (1997). Biochemistry and pathology of radical-mediated protein oxidation. *The Biochemical Journal, 324 (Pt 1)*(Pt 1), 1-18.

Defloor, T. (1999). The risk of pressure sores: A conceptual scheme. *Journal of Clinical Nursing, 8*(2), 206-216.

DeLeon, S., Clinton, A., Fowler, H., Everett, J., Horswill, A. R., & Rumbaugh, K. P. (2014). Synergistic interactions of *Pseudomonas aeruginosa* and *Staphylococcus aureus* in an in vitro wound model. *Infection and Immunity, 82*(11), 4718-4728.

Demidova-Rice, T. N., Hamblin, M. R., & Herman, I. M. (2012). Acute and impaired wound healing: Pathophysiology and current methods for drug delivery, part 1: Normal and chronic wounds: Biology, causes, and approaches to care. *Advances in Skin & Wound Care, 25*(7), 304-314.

Denyer, S. P. (1995). Mechanisms of action of antibacterial biocides. *International Biodeterioration & Biodegradation, 36*(3-4), 227-245.

Deshpande, P., Ralston, D., & MacNeil, S. (2013). The use of allodermis prepared from euro skin bank to prepare autologous tissue engineered skin for clinical use. *Burns, 39*(6), 1170-1177.

Desprez, B., Barroso, J., Griesinger, C., Kandárová, H., Alépée, N., & Fuchs, H. W. (2015). Two novel prediction models improve predictions of skin corrosive sub-categories by test methods of OECD test guideline no. 431. *Toxicology in Vitro, 29*(8), 2055-2080.

Dibrov, P., Dzioba, J., Gosink, K. K., & Hase, C. C. (2002). Chemiosmotic mechanism of antimicrobial activity of ag(+) in vibrio cholerae. *Antimicrobial Agents and Chemotherapy, 46*(8), 2668-2670.

Diekema, D., Pfaller, M., Schmitz, F., Smayevsky, J., Bell, J., Jones, R., SENTRY Participants Group. (2001). Survey of infections due to *Staphylococcus* species: Frequency of occurrence and antimicrobial susceptibility of isolates collected in the united states, canada, latin america, europe, and the western pacific region for the SENTRY antimicrobial surveillance proGram, 1997–1999. *Clinical Infectious Diseases, 32*(Supplement_2), S114-S132.

Dlugosz, A. A., Cheng, C., Denning, M. F., Dempsey, P. J., Coffey Jr, R. J., & Yuspa, S. H. (1994). Keratinocyte growth factor receptor ligands induce transforming growth factor a expression and activate the epidermal growth factor receptor signaling pathway in cultured epidermal keratinocytes. *Cell Growth and Differentiation-Publication American Association for Cancer Research, 5*(12), 1283-1292.

Doan, N., Reher, P., Meghji, S., & Harris, M. (1999). In vitro effects of therapeutic ultrasound on cell proliferation, protein synthesis, and cytokine production by human fibroblasts, osteoblasts, and monocytes. *Journal of Oral and Maxillofacial Surgery : Official Journal of the American Association of Oral and Maxillofacial Surgeons, 57*(4), 409-19; discussion 420.

Domenici, F., Brasili, F., Giantulli, S., Cerroni, B., Bedini, A., Giliberti, C., Paradossi, G. (2017). Differential effects on membrane permeability and viability of human keratinocyte cells undergoing very low intensity megasonic fields. *Scientific Reports, 7*(1), 16536.

Domenici, F., Giliberti, C., Bedini, A., Palomba, R., Luongo, F., Sennato, S., Congiu Castellano, A. (2013). Ultrasound well below the intensity threshold of cavitation can promote efficient uptake of small drug model molecules in fibroblast cells. *Drug Delivery, 20*(7), 285-295.

Domenici, F., Giliberti, C., Bedini, A., Palomba, R., Udroiu, I., Di Giambattista, L., & Castellano, A. C. (2014). Structural and permeability sensitivity of cells to low intensity ultrasound: Infrared and fluorescence evidence in vitro. *Ultrasonics, 54*(4), 1020-1028.

Dong, Y., Chen, S., Wang, Z., Peng, N., & Yu, J. (2012). Synergy of ultrasound microbubbles and vancomycin against *Staphylococcus epidermidis* biofilm. *Journal of Antimicrobial Chemotherapy, 68*(4), 816-826.

Donlan, R. M., & Costerton, J. W. (2002). Biofilms: Survival mechanisms of clinically relevant microorganisms. *Clinical Microbiology Reviews, 15*(2), 167-193.

Dorobantu, L. S., Fallone, C., Noble, A. J., Veinot, J., Ma, G., Goss, G. G., & Burrell, R. E. (2015). Toxicity of silver nanoparticles against bacteria, yeast, and algae. *Journal of Nanoparticle Research, 17*(4), 172.

Dou, Y., Huan, J., Guo, F., Zhou, Z., & Shi, Y. (2017). *Pseudomonas aeruginosa* prevalence, antibiotic resistance and antimicrobial use in chinese

burn wards from 2007 to 2014. *Journal of International Medical Research, 45*(3), 1124-1137.

Dowd, S. E., Sun, Y., Secor, P. R., Rhoads, D. D., Wolcott, B. M., James, G. A., & Wolcott, R. D. (2008). Survey of bacterial diversity in chronic wounds using pyrosequencing, DGGE, and full ribosome shotgun sequencing. *BMC Microbiology, 8*(1), 43.

Dowd, S. E., Wolcott, R. D., Sun, Y., McKeehan, T., Smith, E., & Rhoads, D. (2008). Polymicrobial nature of chronic diabetic foot ulcer biofilm infections determined using bacterial tag encoded FLX amplicon pyrosequencing (bTEFAP). *PloS One, 3*(10), e3326.

Dowd, S., Sun, Y., Smith, E., Kennedy, J., Jones, C., & Wolcott, R. (2009). Effects of biofilm treatments on the multi-species lubbock chronic wound biofilm model. *Journal of Wound Care, 18*(12), 508-512.

Drewa, T., Szmytkowska, K., Czajkowski, R., Debski, R., Lysik, J., & Zegarska, B. (2008). The proapoptotic influence of AgNO3 on human keratinocytes and fibroblasts *in vitro*, the impact for burned patient management. *Acta Poloniae Pharmaceutica, 65*(5), 515-519.

Duan, X., Peng, D., Zhang, Y., Huang, Y., Liu, X., Li, R., Zhou, X. and Liu, J., (2018). Sub-cytotoxic concentrations of ionic silver promote the proliferation of human keratinocytes by inducing the production of reactive oxygen species. *Frontiers of medicine, 12(3), pp.289-300.*

Dubin, G., Chmiel, D., Mak, P., Rakwalska, M., Rzychon, M., & Dubin, A. (2001). Molecular cloning and biochemical characterisation of proteases from *Staphylococcus epidermidis. Biological Chemistry, 382*(11), 1575-1582.

Duvshani-Eshet, M., Haber, T., & Machluf, M. (2013). Insight concerning the mechanism of therapeutic ultrasound facilitating gene delivery: Increasing cell membrane permeability or interfering with intracellular pathways? *Human Gene Therapy, 25*(2), 156-164.

Duxbury, T. (1986). Microbes and heavy metals: An ecological overview. *Microbiological Sciences, 3*(11), 330-333.

Edwards-Jones, V. (2009). The benefits of silver in hygiene, personal care and healthcare. *Letters in Applied Microbiology, 49*(2), 147-152.

Efem, S. (1988). Clinical observations on the wound healing properties of honey. *British Journal of Surgery, 75*(7), 679-681.

El-Hady, F. K. A., & Hegazi, A. (2007). Influence of honey on the suppression of human low density lipoprotein (LDL) peroxidation (in-vitro). *Malaysian Journal of Medical Sciences, 14*(1)

Elkins, J. G., Hassett, D. J., Stewart, P. S., Schweizer, H. P., & McDermott, T. R. (1999). Protective role of catalase in *Pseudomonas aeruginosa* biofilm resistance to hydrogen peroxide. *Applied and Environmental Microbiology, 65*(10), 4594-4600.

Engel, J., & Balachandran, P. (2009). Role of *Pseudomonas aeruginosa* type III effectors in disease. *Current Opinion in Microbiology, 12*(1), 61-66.

Ensing, G. T., Neut, D., Horn, J. R. v., Mei, Henny C van der, & Busscher, H. J. (2006). The combination of ultrasound with antibiotics released from bone cement decreases the viability of planktonic and biofilm bacteria: An in vitro study with clinical strains. *Journal of Antimicrobial Chemotherapy, 58*(6), 1287-1290.

Ensing, G., Roeder, B., Nelson, J. L., Van Horn, J., Van der Mei, H., Busscher, H., & Pitt, W. (2005). Effect of pulsed ultrasound in combination with gentamycin on bacterial viability in biofilms on bone cements in vivo. *Journal of Applied Microbiology, 99*(3), 443-448.

Erriu, M., Blus, C., Szmukler-Moncler, S., Buogo, S., Levi, R., Barbato, G., Orrù, G. (2014). Microbial biofilm modulation by ultrasound: Current concepts and controversies. *Ultrasonics Sonochemistry, 21*(1), 15-22.

Estahbanati, H. K., Kashani, P. P., & Ghanaatpisheh, F. (2002). Frequency of *Pseudomonas aeruginosa* serotypes in burn wound infections and their resistance to antibiotics. *Burns, 28*(4), 340-348.

Ettorre, A., Neri, P., Di Stefano, A., Andreassi, M., Anselmi, C., & Andreassi, L. (2003). Involvement of oxidative stress in apoptosis induced by a mixture of isothiazolinones in normal human keratinocytes. *Journal of Investigative Dermatology, 121*(2), 328-336.

Etufugh, C. N., & Phillips, T. J. (2007). Venous ulcers. *Clinics in Dermatology, 25*(1), 121-130.

European Medicine Agency The bacterial challenge: time to react. A call to narrow the gap between multidrug-resistant bacteria in the EU and the development of new antibacterial agents. [Accessed: December 20, 2018]. Available at: http://www.ema.europa.eu/docs/en_GB/document_library/Report/2009/11/WC500008770.pdf.

European Union. (2008). 1976, council directive 1976/768/EEC of 27 july 1976 on the approximation of the laws of the member states relating to cosmetic products, as amended through commission directive 2008/42/EC.

Eves, P., Katerinaki, E., Simpson, C., Layton, C., Dawson, R., Evans, G., & Mac Neil, S. (2003). Melanoma invasion in reconstructed human skin is influenced by skin cells–investigation of the role of proteolytic enzymes. *Clinical & Experimental Metastasis, 20*(8), 685-700.

Exner, M., Tuschewitzki, G. J., & Scharnagel, J. (1987). Influence of biofilms by chemical disinfectants and mechanical cleaning. *Zentralblatt Fur Bakteriologie, Mikrobiologie Und Hygiene.Serie B, Umwelthygiene, Krankenhaushygiene, Arbeitshygiene, Praventive Medizin, 183*(5-6), 549-563.

Faglia, E., Clerici, G., Caminiti, M., Quarantiello, A., Gino, M., & Morabito, A. (2006). The role of early surgical debridement and revascularization in patients with diabetes and deep foot space abscess: Retrospective review of 106 patients with diabetes. *The Journal of Foot and Ankle Surgery, 45*(4), 220-226.

Fair, R. J., & Tor, Y. (2014). Antibiotics and bacterial resistance in the 21st century. *Perspectives in Medicinal Chemistry, 6*, PMC. S14459.

Fairbrother, R., & Taylor, G. (1961). Sodium methicillin in routine therapy. *Lancet,* 473-476.

Falanga, V. (2005). Wound healing and its impairment in the diabetic foot. *The Lancet, 366*(9498), 1736-1743.

Farooq Khan, Z., & Maqbool, T. (2008). Physical and spectroscopic characterization of pakistani honey. *Ciencia e Investigación Agraria, 35*(2), 199-204.

Fazli, M., Bjarnsholt, T., Kirketerp-Moller, K., Jorgensen, B., Andersen, A. S., Krogfelt, K. A.,Tolker-Nielsen, T. (2009). Nonrandom distribution of *Pseudomonas aeruginosa* and *Staphylococcus aureus* in chronic wounds. *Journal of Clinical Microbiology, 47*(12), 4084-4089.

Feng, Q. L., Wu, J., Chen, G., Cui, F., Kim, T., & Kim, J. (2000). A mechanistic study of the antibacterial effect of silver ions on *Escherichia coli* and *Staphylococcus aureus. Journal of Biomedical Materials Research, 52*(4), 662-668.

Fentem, J., Briggs, D., Chesné, C., Elliott, G., Harbell, J., Heylings, J., Botham, P. (2001). A prevalidation study on *in vitro* tests for acute skin irritation: Results and evaluation by the management team. *Toxicology in Vitro, 15*(1), 57-93.

Ferguson, M. W., & O'Kane, S. (2004). Scar-free healing: From embryonic mechanisms to adult therapeutic intervention. *Philosophical Transactions of the Royal Society of London.Series B, Biological Sciences, 359*(1445), 839-850.

Fernando, P., Kelly, J.F., Balazsi, K., Slack, R.S. and Megeney, L.A., (2002). Caspase 3 activity is required for skeletal muscle differentiation. *Proceedings of the National Academy of Sciences*, 99(17), pp.11025-11030.

Fernando, P., Brunette, S. and Megeney, L.A., (2005). Neural stem cell differentiation is dependent upon endogenous caspase 3 activity. *The FASEB journal*, 19(12), pp.1671-1673.

Fidaleo, M., Zuorro, A., & Lavecchia, R. (2011). Antimicrobial activity of some italian honeys against pathogenic bacteria. *Chemical Engineering, 24*, 1015.

Finnan, S., Morrissey, J. P., O'Gara, F., & Boyd, E. F. (2004). Genome diversity of *Pseudomonas aeruginosa* isolates from cystic fibrosis patients and the hospital environment. *Journal of Clinical Microbiology, 42*(12), 5783-5792.

Fleischmajer, R., Utani, A., MacDonald, E. D., Perlish, J. S., Pan, T. C., Chu, M. L., Yamada, Y. (1998). Initiation of skin basement membrane formation at the epidermo-dermal interface involves assembly of laminins through binding to cell membrane receptors. *Journal of Cell Science, 11*(Pt 14), 1929-1940.

Flock, J., Fröman, G., Jönsson, K., Guss, B., Signäs, C., Nilsson, B., Lindberg, M. (1987). Cloning and expression of the gene for a fibronectin-binding protein from *Staphylococcus aureus. The EMBO Journal, 6*(8), 2351-2357.

Forbes, S., McBain, A. J., Felton-Smith, S., Jowitt, T. A., Birchenough, H. L., & Dobson, C. B. (2013). Comparative surface antimicrobial properties of synthetic biocides and novel human apolipoprotein E derived antimicrobial peptides. *Biomaterials, 34*(22), 5453-5464.

Foss, O. A., Mjønes, P., Fismen, S., & Christensen, E. (2016). Is there a relationship between the stratum corneum thickness and that of the viable parts of tumour cells in basal cell carcinoma? *Journal of Skin Cancer, 2016*

Foster, T. J. (2005). Immune evasion by *Staphylococci. Nature Reviews Microbiology, 3*(12), 948.

Foster, T. J., Geoghegan, J. A., Ganesh, V. K., & Höök, M. (2014). Adhesion, invasion and evasion: The many functions of the surface proteins of *Staphylococcus aureus. Nature Reviews Microbiology, 12*(1), 49.

Frantz, S., Kelly, R. A., & Bourcier, T. (2001). Role of TLR-2 in the activation of nuclear factor kappaB by oxidative stress in cardiac myocytes. *The Journal of Biological Chemistry, 276*(7), 5197-5203.

French, V., Cooper, R. A., & Molan, P. C. (2005). The antibacterial activity of honey against coagulase-negative staphylococci. *Journal of Antimicrobial Chemotherapy, 56*(1), 228-231.

Frieder, S., Weisberg, J., Fleming, B., & Stanek, A. (1988). A pilot study: The therapeutic effect of ultrasound following partial rupture of achilles tendons in male rats. *Journal of Orthopaedic & Sports Physical Therapy, 10*(2), 39-46.

Frykberg, R. G., & Banks, J. (2015). Challenges in the treatment of chronic wounds. *Advances in Wound Care, 4*(9), 560-582.

Fujita, J., Crane, A.M., Souza, M.K., Dejosez, M., Kyba, M., Flavell, R.A., Thomson, J.A. and Zwaka, T.P., (2008). Caspase activity mediates the differentiation of embryonic stem cells. *Cell stem cell*, 2(6), pp.595-601.

Fuqua, C., & Greenberg, E. P. (2002). Signalling: Listening in on bacteria: Acyl-homoserine lactone signalling. *Nature Reviews Molecular Cell Biology, 3*(9), 685.

Fuqua, C. (2006). The QscR quorum-sensing regulon of *Pseudomonas aeruginosa*: An orphan claims its identity. *Journal of Bacteriology, 188*(9), 3169-3171.

Gadd, G. M. (1992). Metals and microorganisms: A problem of definition. *FEMS Microbiology Letters, 100*(1-3), 197-203.

Ganesan, B., Martini, S., Solorio, J., & Walsh, M. K. (2015). Determining the effects of high intensity ultrasound on the reduction of microbes in milk and orange juice using response surface methodology. *International Journal of Food Science, 2015*

Gantwerker, E. A., & Hom, D. B. (2012). Skin: Histology and physiology of wound healing. *Clinics in Plastic Surgery, 39*(1), 85-97.

Garcia, A. D., & Thomas, D. R. (2006). Assessment and management of chronic pressure ulcers in the elderly. *Medical Clinics, 90*(5), 925-944.

Garcia-Hidalgo, E., Sottas, V., Von Goetz, N., Hauri, U., Bogdal, C., & Hungerbühler, K. (2017). Occurrence and concentrations of isothiazolinones in detergents and cosmetics in switzerland. *Contact Dermatitis, 76*(2), 96-106.

Garrett, T.R., Bhakoo, M. and Zhang, Z., (2008). Bacterial adhesion and biofilms on surfaces. *Progress in Natural Science*, 18(9), pp.1049-1056.

Gauglitz, G. G., Shahrokhi, S., & Williams, F. N. (2017). Burn wound infection and sepsis. *Uptodate,*

Gawkrodger, D., & Ardern-Jones, M. R. (2016). *Dermatology E-book: An illustrated colour text* Elsevier Health Sciences.

Gee, J. B., Vassallo, C. L., Bell, P., Kaskin, J., Basford, R. E., & Field, J. B. (1970). Catalase-dependent peroxidative metabolism in the alveolar macrophage during phagocytosis. *The Journal of Clinical Investigation, 49*(6), 1280-1287.

Geer, D. J., Swartz, D. D., & Andreadis, S. T. (2004). In vivo model of wound healing based on transplanted tissue-engineered skin. Tissue Engineering, 10(7-8), 1006-1017.

Geer, D. J., Swartz, D. D., & Andreadis, S. T. (2002). Fibrin promotes migration in a three-dimensional in vitro model of wound regeneration. *Tissue Engineering, 8*(5), 787-798.

Geerlings, S. E., & Hoepelman, A. I. (1999). Immune dysfunction in patients with diabetes mellitus (DM). *FEMS Immunology & Medical Microbiology, 26*(3-4), 259-265.

Ghazali, F. C. (2009). Morphological characterization study of malaysian honey-A VPSEM, EDX randomised attempt. *Ann Microscopy, 9*, 93-102.

Gheldof, N., Wang, X., & Engeseth, N. J. (2002). Identification and quantification of antioxidant components of honeys from various floral sources. *Journal of Agricultural and Food Chemistry, 50*(21), 5870-5877.

Ghigo, J. (2001). Natural conjugative plasmids induce bacterial biofilm development. *Nature, 412*(6845), 442.

Ghosh, M. M., Boyce, S., Layton, C., Freedlander, E., & Mac Neil, S. (1997). A comparison of methodologies for the preparation of human epidermal-dermal composites. *Annals of Plastic Surgery, 39*(4), 390-404.

Ghuysen, J., & Strominger, J. L. (1963). Structure of the cell wall of *Staphylococcus aureus*, strain copenhagen. II. separation and structure of disaccharides. *Biochemistry, 2*(5), 1119-1125.

Gibbs, S., Corsini, E., Spiekstra, S. W., Galbiati, V., Fuchs, H. W., DeGeorge, G., Roggen, E. (2013). An epidermal equivalent assay for identification and ranking potency of contact sensitizers. *Toxicology and Applied Pharmacology, 272*(2), 529-541.

Glasser, J. S., Guymon, C. H., Mende, K., Wolf, S. E., Hospenthal, D. R., & Murray, C. K. (2010). Activity of topical antimicrobial agents against multidrug-resistant bacteria recovered from burn patients. *Burns, 36*(8), 1172-1184.

Goligorsky, M. S. (2005). Endothelial cell dysfunction: Can't live with it, how to live without it. *American Journal of Physiology-Renal Physiology, 288*(5), F871-F880.

Gottrup, F. (2004). Oxygen in wound healing and infection. *World Journal of Surgery, 28*(3), 312-315.

Gottrup, F., & Jorgensen, B. (2011). Maggot debridement: An alternative method for debridement. *Eplasty, 11*, e33.

Grecka, K., Kuś, P. M., Worobo, R. W., & Szweda, P. (2018). Study of the anti-staphylococcal potential of honeys produced in northern poland. *Molecules, 23*(2), 260.

Grey, J. E. (1998). Cellulitis associated with wounds. *Journal of Wound Care, 7*(7), 338-339.

Grey, J. E., Enoch, S., & Harding, K. G. (2006). Wound assessment. *BMJ (Clinical Research Ed.), 332*(7536), 285-288.

Grice, E. A., & Segre, J. A. (2011). The skin microbiome. *Nature Reviews Microbiology, 9*(4), 244.

Grimaldi, P., Di Giambattista, L., Giordani, S., Udroiu, I., Pozzi, D., Gaudenzi, S., Castellano, A. C. (2011). Ultrasound-mediated structural changes in cells revealed by FTIR spectroscopy: A contribution to the optimization of gene and drug delivery. *Spectrochimica Acta Part A: Molecular and Biomolecular Spectroscopy, 84*(1), 74-85.

Gristina, A. G., Hobgood, C. D., Webb, L. X., & Myrvik, Q. N. (1987). Adhesive colonization of biomaterials and antibiotic resistance. *Biomaterials, 8*(6), 423-426.

Groeber, F., Engelhardt, L., Lange, J., Kurdyn, S., Schmid, F.F., Rücker, C., Mielke, S., Walles, H. and Hansmann, J., 2016. A first vascularized skin equivalent as an alternative to animal experimentation. *ALTEX-Alternatives to animal experimentation*, 33(4), pp.415-422.

Gröne, A. (2002). Keratinocytes and cytokines. *Veterinary Immunology and Immunopathology, 88*(1-2), 1-12.

Grundling, A., & Schneewind, O. (2006). Cross-linked peptidoglycan mediates lysostaphin binding to the cell wall envelope of *Staphylococcus aureus. Journal of Bacteriology, 188*(7), 2463-2472.

Günther, F., Wabnitz, G. H., Stroh, P., Prior, B., Obst, U., Samstag, Y., Hänsch, G. M. (2009). Host defence against *Staphylococcus aureus* biofilms infection: Phagocytosis of biofilms by polymorphonuclear neutrophils (PMN). *Molecular Immunology, 46*(8-9), 1805-1813.

Guyton, A. C.Hall JE. (2006) textbook of medical physiology. *Philadelphia, PA: WB Saunders,*

Hall-Stoodley, L., Costerton, J. W., & Stoodley, P. (2004). Bacterial biofilms: From the natural environment to infectious diseases. *Nature Reviews Microbiology, 2*(2), 95.

Hamilton-Miller, J., & Shah, S. (1996). A microbiological assessment of silver fusidate, a novel topical antimicrobial agent. *International Journal of Antimicrobial Agents, 7*(2), 97-99.

Hamood, A. N., Griswold, J. A., & Duhan, C. M. (1996). Production of extracellular virulence factors by *Pseudomonas aeruginosaIsolates* obtained from tracheal, urinary tract, and wound infections. *Journal of Surgical Research, 61*(2), 425-432.

Hancock, R. E., Mutharia, L. M., Chan, L., Darveau, R. P., Speert, D. P., & Pier, G. B. (1983). *Pseudomonas aeruginosa* isolates from patients with cystic fibrosis: A class of serum-sensitive, nontypable strains deficient in lipopolysaccharide O side chains. *Infection and Immunity, 42*(1), 170-177.

Hansen-Wester, I., & Hensel, M. (2002). Genome-based identification of chromosomal regions specific for salmonella spp. *Infection and Immunity, 70*(5), 2351-2360.

Harrison, C. A., Gossiel, F., Layton, C. M., Bullock, A. J., Johnson, T., Blumsohn, A., & MacNeil, S. (2006). Use of an in vitro model of tissue-engineered skin to investigate the mechanism of skin graft contraction. *Tissue Engineering, 12*(11), 3119-3133.

Harrison-Balestra, C., Cazzaniga, A. L., Davis, S. C., & Mertz, P. M. (2003). A wound-isolated *Pseudomonas aeruginosa* grows a biofilm in vitro within 10 hours and is visualized by light microscopy. *Dermatologic Surgery, 29*(6), 631-635.

Hassett, D. J., Sutton, M. D., Schurr, M. J., Herr, A. B., Caldwell, C. C., & Matu, J. O. (2009). *Pseudomonas aeruginosa* hypoxic or anaerobic biofilm infections within cystic fibrosis airways. *Trends in Microbiology, 17*(3), 130-138.

Hauser, J., Ellisman, M., Steinau, H., Stefan, E., Dudda, M., & Hauser, M. (2009). Ultrasound enhanced endocytotic activity of human fibroblasts. *Ultrasound in Medicine & Biology, 35*(12), 2084-2092.

Heilmann, C., Hussain, M., Peters, G., & Götz, F. (1997). Evidence for autolysin-mediated primary attachment of *Staphylococcus epidermidis* to a polystyrene surface. *Molecular Microbiology, 24*(5), 1013-1024.

Heimbach, D., Engrav, L., Grube, B., & Marvin, J. (1992). Burn depth: A review. *World Journal of Surgery, 16*(1), 10-15.

Henle, E. S., & Linn, S. (1997). Formation, prevention, and repair of DNA damage by iron/hydrogen peroxide. *The Journal of Biological Chemistry, 272*(31), 19095-19098.

Henriques, A., Jenkins, R., Burton, N., & Cooper, R. (2010). The intracellular effects of manuka honey on *Staphylococcus aureus*. *European Journal of Clinical Microbiology & Infectious Diseases, 29*(1), 45.

Henriques, A., Jackson, S., Cooper, R., & Burton, N. (2006). Free radical production and quenching in honeys with wound healing potential. *Journal of Antimicrobial Chemotherapy, 58*(4), 773-777.

Hentzer, M., Teitzel, G. M., Balzer, G. J., Heydorn, A., Molin, S., Givskov, M., & Parsek, M. R. (2001). Alginate overproduction affects *Pseudomonas aeruginosa* biofilm structure and function. *Journal of Bacteriology, 183*(18), 5395-5401.

Hettiaratchy, S., Papini, R., & Dziewulskiedited, P. (2005). ABC of burns malden. *MA: BMJ Books,*

Hettiaratchy, S., & Dziewulski, P. (2004). ABC of burns: Pathophysiology and types of burns. *BMJ (Clinical Research Ed.), 328*(7453), 1427-1429.

Hidalgo, E., Bartolome, R., Barroso, C., Moreno, A., & Dominguez, C. (1998). Silver nitrate: Antimicrobial activity related to cytotoxicity in cultured human fibroblasts. *Skin Pharmacology and Applied Skin Physiology, 11*(3), 140-151.

Hill, D. S., Robinson, N. D., Caley, M. P., Chen, M., O'Toole, E. A., Armstrong, J. L., Lovat, P. E. (2015). A novel fully humanized 3D skin equivalent to model early melanoma invasion. *Molecular Cancer Therapeutics, 14*(11), 2665-2673.

Hirsch, T., Spielmann, M., Zuhaili, B., Koehler, T., Fossum, M., Steinau, H., Eriksson, E. (2008). Enhanced susceptibility to infections in a diabetic wound healing model. *BMC Surgery, 8*(1), 5.

Hobot, J., Walker, M., Newman, G., & Bowler, P. (2008). Effect of hydrofiber® wound dressings on bacterial ultrastructure. *Journal of Electron Microscopy, 57*(2), 67-75.

Hofman, D. (2007). The autolytic debridement of venous leg ulcers. *Wound Essentials, 2*, 68-73.

Hofmann, A. A., Goldberg, T. D., Tanner, A. M., & Cook, T. M. (2005). Ten-year experience using an articulating antibiotic cement hip spacer for the treatment of chronically infected total hip. *The Journal of Arthroplasty, 20*(7), 874-879.

Holland, D. B., Bojar, R. A., Farrar, M. D., & Holland, K. T. (2009). Differential innate immune responses of a living skin equivalent model colonized by *Staphylococcus epidermidis* or *Staphylococcus aureus*. *FEMS Microbiology Letters, 290*(2), 149-155.

Holland, D. B., Bojar, R. A., Jeremy, A. H., Ingham, E., & Holland, K. T. (2008). Microbial colonization of an in vitro model of a tissue engineered human skin equivalent–a novel approach. *FEMS Microbiology Letters, 279*(1), 110-115.

Holt, K. B., & Bard, A. J. (2005). Interaction of silver (I) ions with the respiratory chain of *Escherichia coli*: An electrochemical and scanning electrochemical microscopy study of the antimicrobial mechanism of micromolar ag. *Biochemistry, 44*(39), 13214-13223.

Hopf, H. W., Hunt, T. K., West, J. M., Blomquist, P., Goodson, W. H., Jensen, J. A., Upton, R. A. (1997). Wound tissue oxygen tension predicts the risk of wound infection in surgical patients. *Archives of Surgery, 132*(9), 997-1004.

Hornemann, J. A., Lysova, A. A., Codd, S. L., Seymour, J. D., Busse, S. C., Stewart, P. S., & Brown, J. R. (2008). Biopolymer and water dynamics in microbial biofilm extracellular polymeric substance. *Biomacromolecules, 9*(9), 2322-2328.

Housecroft, C. E., & Constable, E. C. (2010). *Chemistry: An introduction to organic, inorganic and physical chemistry* Pearson education.

Howell-Jones, R., Wilson, M., Hill, K., Howard, A., Price, P., & Thomas, D. (2005). A review of the microbiology, antibiotic usage and resistance in chronic skin wounds. *Journal of Antimicrobial Chemotherapy, 55*(2), 143-149.

Howell-Jones, R. S., Wilson, M. J., Hill, K. E., Howard, A. J., Price, P. E., & Thomas, D. W. (2005). A review of the microbiology, antibiotic usage and resistance in chronic skin wounds. *The Journal of Antimicrobial Chemotherapy, 55*(2), 143-149.

Hsiao, Y. H., Kuo, S. J., Tsai, H. D., Chou, M. C., & Yeh, G. P. (2016). Clinical application of high-intensity focused ultrasound in cancer therapy. *Journal of Cancer, 7*(3), 225-231.

Hugo, W. (1991). A brief history of heat and chemical preservation and disinfection. *Journal of Applied Bacteriology, 71*(1), 9-18.

Hutchinson, D., Ho, V., Dodd, M., Dawson, H. N., Zumwalt, A. C., Schmitt, D., & Colton, C. A. (2007). Quantitative measurement of postural sway in mouse models of human neurodegenerative disease. *Neuroscience, 148*(4), 825-832.

Ibrahim, D., Froberg, B., Wolf, A., & Rusyniak, D. E. (2006). Heavy metal poisoning: Clinical presentations and pathophysiology. *Clinics in Laboratory Medicine, 26*(1), 67-97, viii.

Ilkovitch, D. (2011). Role of immune-regulatory cells in skin pathology. *Journal of Leukocyte Biology, 89*(1), 41-49.

Imlay, J. A. (2013). The molecular mechanisms and physiological consequences of oxidative stress: Lessons from a model bacterium. *Nature Reviews Microbiology, 11*(7), 443.

Inohara, N., Koseki, T., del Peso, L., Hu, Y., Yee, C., Chen, S., Nunez, G. (1999). Nod1, an apaf-1-like activator of caspase-9 and nuclear factor-kappaB. *The Journal of Biological Chemistry, 274*(21), 14560-14567.

Ioannou, I., Dimitriadis, N., Papadimitriou, K., Sakellari, D., Vouros, I., & Konstantinidis, A. (2009). Hand instrumentation versus ultrasonic debridement in the treatment of chronic periodontitis: A randomized clinical and microbiological trial. *Journal of Clinical Periodontology, 36*(2), 132-141.

Ip, M., Lui, S. L., Poon, V. K., Lung, I., & Burd, A. (2006). Antimicrobial activities of silver dressings: An in vitro comparison. *Journal of Medical Microbiology, 55*(1), 59-63.

Izadifar, Z., Babyn, P. and Chapman, D., (2019). Ultrasound cavitation/ microbubble detection and medical applications. *Journal of Medical and Biological Engineering*, 39(3), pp.259-276.

Jackson, D. M. (1953). The diagnosis of the depth of burning. *British Journal of Surgery, 40*(164), 588-596.

Jackson, D. W., Suzuki, K., Oakford, L., Simecka, J. W., Hart, M. E., & Romeo, T. (2002). Biofilm formation and dispersal under the influence of the global regulator CsrA of escherichia coli. *Journal of Bacteriology, 184*(1), 290-301.

Jacquin, J., Cheng, J., Odobel, C., CONAN, P., Pujo-pay, M. and Jean-Francois, G., (2019). Microbial ecotoxicology of marine plastic debris: a review on colonization and biodegradation by the 'plastisphere'. *Frontiers in microbiology,* 10, p.865.

James, G. A., Swogger, E., Wolcott, R., deLancey Pulcini, E., Secor, P., Sestrich, J., Stewart, P. S. (2008). Biofilms in chronic wounds. *Wound Repair and Regeneration, 16*(1), 37-44.

Janzen, V., Fleming, H.E., Riedt, T., Karlsson, G., Riese, M.J., Celso, C.L., Reynolds, G., Milne, C.D., Paige, C.J., Karlsson, S. and Woo, M., 2008. Hematopoietic stem cell responsiveness to exogenous signals is limited by caspase-3. *Cell stem cell*, 2(6), pp.584-594.

Jeffcoate, W. J., & Harding, K. G. (2003). Diabetic foot ulcers. *The Lancet, 361*(9368), 1545-1551.

Jensen, P. Ø., Bjarnsholt, T., Phipps, R., Rasmussen, T. B., Calum, H., Christoffersen, L., Givskov, M. (2007). Rapid necrotic killing of polymorphonuclear leukocytes is caused by quorum-sensing-controlled production of rhamnolipid by *Pseudomonas aeruginosa*. *Microbiology, 153*(5), 1329-1338.

Jia, J., Wang, Y., Zhou, L., & Jin, S. (2006). Expression of *Pseudomonas aeruginosa* toxin ExoS effectively induces apoptosis in host cells. *Infection and Immunity, 74*(12), 6557-6570.

Jiménez, M., Mateo, J. J., Huerta, T., & Mateo, R. (1994). Influence of the storage conditions on some physicochemical and mycological parameters of honey. *Journal of the Science of Food and Agriculture, 64*(1), 67-74.

Johnson, A. P., & Woodford, N. (2013). Global spread of antibiotic resistance: The example of new delhi metallo-β-lactamase (NDM)-mediated carbapenem resistance. *Journal of Medical Microbiology, 62*(4), 499-513.

Johnson, L. L., Vaughn Peterson, R., & Pitt, W. G. (1998). Treatment of bacterial biofilms on polymeric biomaterials using antibiotics and ultrasound. *Journal of Biomaterials Science, Polymer Edition, 9*(11), 1177-1185.

Jover, J., Bosque, R., & Sales, J. (2008). A comparison of the binding affinity of the common amino acids with different metal cations. *Dalton Transactions,* (45), 6441-6453.

Joyce, E., Al-Hashimi, A., & Mason, T. (2011). Assessing the effect of different ultrasonic frequencies on bacterial viability using flow cytometry. *Journal of Applied Microbiology, 110*(4), 862-870.

Joyce, E., Phull, S., Lorimer, J., & Mason, T. (2003). The development and evaluation of ultrasound for the treatment of bacterial suspensions. A study of frequency, power and sonication time on cultured bacillus species. *Ultrasonics Sonochemistry, 10*(6), 315-318.

Jung, M. H., Jung, S., & Shin, H. S. (2016). Co-stimulation of HaCaT keratinization with mechanical stress and air-exposure using a novel 3D culture device. *Scientific Reports, 6*, 33889.

Kadioglu, A., Weiser, J. N., Paton, J. C., & Andrew, P. W. (2008). The role of streptococcus pneumoniae virulence factors in host respiratory colonization and disease. *Nature Reviews Microbiology, 6*(4), 288.

Kalani, M., Jörneskog, G., Naderi, N., Lind, F., & Brismar, K. (2002). Hyperbaric oxygen (HBO) therapy in treatment of diabetic foot ulcers: Long-term follow-up. *Journal of Diabetes and its Complications, 16*(2), 153-158.

Kamal, A., Raza, S., Rashid, N., Hameed, T., Gilani, M., Qureshi, M. A., & Nasim, K. (2002). Comparative study of honey collected from different flora of pakistan. *Online JB Sci, 2*, 626-627.

Kanta, J. (2015). Collagen matrix as a tool in studying fibroblastic cell behavior. *Cell Adhesion & Migration, 9*(4), 308-316.

Kanuka, H., Kuranaga, E., Takemoto, K., Hiratou, T., Okano, H. and Miura, M., (2005). Drosophila caspase transduces Shaggy/GSK-3β kinase activity in neural precursor development. *The EMBO journal*, 24(21), pp.3793-3806.

Karatan, E., & Watnick, P. (2009). Signals, regulatory networks, and materials that build and break bacterial biofilms. *Microbiology and Molecular Biology Reviews: MMBR, 73*(2), 310-347.

Kaufman, H., Gurevich, M., Tamir, E., Keren, E., Alexander, L., & Hayes, P. (2018). Topical oxygen therapy stimulates healing in difficult, chronic wounds: A tertiary centre experience. *Journal of Wound Care, 27*(7), 426-433.

Keren, I., Kaldalu, N., Spoering, A., Wang, Y., & Lewis, K. (2004). Persister cells and tolerance to antimicrobials. *FEMS Microbiology Letters, 230*(1), 13-18.

Khalil, H., Peltzer, N., Walicki, J., Yang, J.Y., Dubuis, G., Gardiol, N., Held, W., Bigliardi, P., Marsland, B., Liaudet, L. and Widmann, C., (2012). Caspase-3 protects stressed organs against cell death. *Molecular and cellular biology, 32(22)*, pp.4523-4533.

Khavari, P. A. (2006). Modelling cancer in human skin tissue. *Nature Reviews Cancer, 6*(4), 270.

Kim, J., Hegde, M., & Jayaraman, A. (2010). Co-culture of epithelial cells and bacteria for investigating host–pathogen interactions. *Lab on a Chip, 10*(1), 43-50.

Kim, M., Liu, W., Borjesson, D. L., Curry, F. E., Miller, L. S., Cheung, A. L., Simon, S. I. (2008). Dynamics of neutrophil infiltration during cutaneous wound healing and infection using fluorescence imaging. *Journal of Investigative Dermatology, 128*(7), 1812-1820.

Kirketerp-Moller, K., Jensen, P. O., Fazli, M., Madsen, K. G., Pedersen, J., Moser, C., Bjarnsholt, T. (2008). Distribution, organization, and ecology of bacteria in chronic wounds. *Journal of Clinical Microbiology, 46*(8), 2717-2722.

Kirzhner, F., Zimmels, Y., Malkovskaja, A., & Starosvetsky, J. (2009). Removal of microbial biofilm on water hyacinth plants roots by ultrasonic treatment. *Ultrasonics, 49*(2), 153-158.

Klasen, H. (2000). A historical review of the use of silver in the treatment of burns. II. renewed interest for silver. *Burns, 26*(2), 131-138.

Klueh, U., Wagner, V., Kelly, S., Johnson, A., & Bryers, J. (2000). Efficacy of silver-coated fabric to prevent bacterial colonization and subsequent device-based biofilm formation. *Journal of Biomedical Materials Research, 53*(6), 621-631.

Kluytmans, J., van Belkum, A., & Verbrugh, H. (1997). Nasal carriage of *Staphylococcus aureus*: Epidemiology, underlying mechanisms, and associated risks. *Clinical Microbiology Reviews, 10*(3), 505-520.

Knight, G. M., McIntyre, J. M., Craig, G. G., Zilm, P. S., & Gully, N. J. (2009). Inability to form a biofilm of *Streptococcus mutans* on silver fluoride-and potassium iodide-treated demineralized dentin. *Quintessence International, 40*(2).

Kobayashi, H., Aiba, S., Yoshino, Y., & Tagami, H. (2003). Acute cutaneous barrier disruption activates epidermal p44/42 and p38 mitogen-activated protein kinases in human and hairless guinea pig skin. *Experimental Dermatology, 12*(6), 734-746.

Kodama, T., Tomita, Y., Koshiyama, K., & Blomley, M. J. (2006). Transfection effect of microbubbles on cells in superposed ultrasound waves and behavior of cavitation bubble. *Ultrasound in Medicine & Biology, 32*(6), 905-914.

Koh, T.J. and DiPietro, L.A., 2011. Inflammation and wound healing: the role of the macrophage. *Expert reviews in molecular medicine*, 13.

Kohanski, M. A., Dwyer, D. J., Hayete, B., Lawrence, C. A., & Collins, J. J. (2007). A common mechanism of cellular death induced by bactericidal antibiotics. *Cell, 130*(5), 797-810.

Kolarsick, P. A., Kolarsick, M. A., & Goodwin, C. (2011). Anatomy and physiology of the skin. *Journal of the Dermatology Nurses' Association, 3*(4), 203-213.

Kolluru, G. K., Bir, S. C., & Kevil, C. G. (2012). Endothelial dysfunction and diabetes: Effects on angiogenesis, vascular remodeling, and wound healing. *International Journal of Vascular Medicine, 2012*

Komori, Y., Nonogaki, T., & Nikai, T. (2001). Hemorrhagic activity and muscle damaging effect of *Pseudomonas aeruginosa* metalloproteinase (elastase). *Toxicon, 39*(9), 1327-1332.

König, M., Vanscheidt, W., Augustin, M., & Kapp, H. (2005). Enzymatic versus autolytic debridement of chronic leg ulcers: A prospective randomised trial. *Journal of Wound Care, 14*(7), 320-323.

Kruger, T. E., Miller, A. H., & Wang, J. (2013). Collagen scaffolds in bone sialoprotein-mediated bone regeneration. *Thescientificworldjournal, 2013*, 812718.

Krystel-Whittemore, M., Dileepan, K.N. and Wood, J.G., 2016. Mast cell: a multi-functional master cell. *Frontiers in immunology*, 6, p.620.

Kuehnert, M. J., Kruszon-Moran, D., Hill, H. A., McQuillan, G., McAllister, S. K., Fosheim, G., Fridkin, S. K. (2006). Prevalence of *Staphylococcus aureus* nasal colonization in the United States, 2001–2002. *Journal of Infectious Diseases, 193*(2), 172-179.

Kumar, S., & Leaper, D. J. (2005). Classification and management of acute wounds. *Surgery-Oxford International Edition, 23*(2), 47-51.

Kwakman, P. H., te Velde, A. A., de Boer, L., Speijer, D., Vandenbroucke-Grauls, C. M., & Zaat, S. A. (2010). How honey kills bacteria. *The FASEB Journal, 24*(7), 2576-2582.

Lai, J., & Pittelkow, M. R. (2007). Physiological effects of ultrasound mist on fibroblasts. *International Journal of Dermatology, 46*(6), 587-593.

Lai, Y., Villaruz, A. E., Li, M., Cha, D. J., Sturdevant, D. E., & Otto, M. (2007). The human anionic antimicrobial peptide dermcidin induces proteolytic defence mechanisms in staphylococci. *Molecular Microbiology, 63*(2), 497-506.

Lansdown, A. (2007). Critical observations on the neurotoxicity of silver. *Critical Reviews in Toxicology, 37*(3), 237-250.

Lansdown, A. B., Mirastschijski, U., Stubbs, N., Scanlon, E., & Ågren, M. S. (2007). Zinc in wound healing: Theoretical, experimental, and clinical aspects. *Wound Repair and Regeneration, 15*(1), 2-16.

Lautenbach, E., Weiner, M. G., Nachamkin, I., Bilker, W. B., Sheridan, A., & Fishman, N. O. (2006). Imipenem resistance among *Pseudomonas aeruginosa* isolates risk factors for infection and impact of resistance on clinical and economic outcomes. *Infection Control & Hospital Epidemiology, 27*(9), 893-900.

Le Maitre, C. L., Freemont, A. J., & Hoyland, J. A. (2005). The role of interleukin-1 in the pathogenesis of human intervertebral disc degeneration. *Arthritis Research & Therapy, 7*(4), R732.

Le, K. Y., Park, M. D., & Otto, M. (2018). Immune evasion mechanisms of *Staphylococcus epidermidis* biofilm infection. *Frontiers in Microbiology, 9*, 359.

Leaper, D. (2002). Sharp technique for wound debridement. *World Wide Wounds.*

Lee, C., Kim, M., Chung, B. M., Leahy, D. J., & Coulombe, P. A. (2012). Structural basis for heteromeric assembly and perinuclear organization of keratin filaments. *Nature Structural & Molecular Biology, 19*(7), 707.

Leid, J. G., Shirtliff, M. E., Costerton, J. W., & Stoodley, P. (2002). Human leukocytes adhere to, penetrate, and respond to *Staphylococcus aureus* biofilms. *Infection and Immunity, 70*(11), 6339-6345.

Leid, J. G., Willson, C. J., Shirtliff, M. E., Hassett, D. J., Parsek, M. R., & Jeffers, A. K. (2005). The exopolysaccharide alginate protects *Pseudomonas aeruginosa* biofilm bacteria from IFN-gamma-mediated macrophage killing. *Journal of Immunology (Baltimore, Md.: 1950), 175*(11), 7512-7518.

Leiding, J.W., 2017. Neutrophil evolution and their diseases in humans. *Frontiers in immunology*, 8, p.1009.

Leng, X., Shang, J., Gao, D., & Wu, J. (2018). Low-intensity pulsed ultrasound promotes proliferation and migration of HaCaT keratinocytes through the PI3K/AKT and JNK pathways. *Brazilian Journal of Medical and Biological Research, 51*(12)

Lewin, P.A., Samuels, J.A., Weingarten, M.S., Zubkov, L.A., Sunny, Y., Bawiec, C.R., Margolis, D.J.,(2013). 20—100 kHz, ultrasound assisted treatment of chronic wounds. *J. Acoust. Soc. Am.* (134), 4121-4121.

Li, L., Fukunag*a-Kalabi*s, M., Yu, H., Xu, X., Kong, J., Lee, J.T. and Herlyn, M., (2010). Human dermal stem cells differentiate into functional epidermal melanocytes. *J Cell Sci*, 123(6), pp.853-860.

Li, L., Fukunaga-Kalabis, M. and Herlyn, M., 2011. The three-dimensional human skin reconstruct model: a tool to study normal skin and melanoma progression. *JoVE (Journal of Visualized Experiments)*, (54), p.e2937.

Li, S., Zhu, C., Fang, S., Zhang, W., He, N., Xu, W., Shang, X. (2015). Ultrasound microbubbles enhance human β-defensin 3 against biofilms. *Journal of Surgical Research, 199*(2), 458-469.

Li, W., Fei, J., Yang, Q., Li, B., Lin, C., Yue, Q., & Meng, Q. (2015). Acute toxic effects of sonodynamic therapy on hypertrophic scar fibroblasts of rabbit ears. *Genetics and Molecular Research, 14*(2), 4203-4214.

Li, J., Ahn, J., Liu, D., Chen, S., Ye, X., & Ding, T. (2016). Evaluation of ultrasound-induced damage to *Escherichia coli* and *Staphylococcus aureus* by flow cytometry and transmission electron microscopy. *Applied and Environmental Microbiology, 82*(6), 1828-1837.

Li, X., Song, J. L., Culotti, A., Zhang, W., Chopp, D. L., Lu, N., & Packman, A. I. (2015). Methods for characterizing the co-development of biofilm and habitat heterogeneity. *Journal of Visualized Experiments : JoVE, (97). doi*(97), 10.3791/52602.

Liao, X., Li, J., Suo, Y., Chen, S., Ye, X., Liu, D., & Ding, T. (2018). Multiple action sites of ultrasound on *Escherichia coli* and *Staphylococcus aureus. Food Science and Human Wellness, 7*(1), 102-109.

Liau, S., Read, D., Pugh, W., Furr, J., & Russell, A. (1997). Interaction of silver nitrate with readily identifiable groups: Relationship to the antibacterialaction of silver ions. *Letters in Applied Microbiology, 25*(4), 279-283.

Liguori, G. R., Jeronimus, B. F., de Aquinas Liguori, Tácia T, Moreira, L. F. P., & Harmsen, M. C. (2017). Ethical issues in the use of animal models for tissue engineering: Reflections on legal aspects, moral theory, three rs strategies, and Harm–Benefit analysis. *Tissue Engineering Part C: Methods, 23*(12), 850-862.

Liu, B., Wang, D., Liu, B., Wang, X., He, L., Wang, J., & Xu, S. (2011). The influence of ultrasound on the fluoroquinolones antibacterial activity. *Ultrasonics Sonochemistry, 18*(5), 1052-1056.

Livermore, D. M. (2001). Of pseudomonas, porins, pumps and carbapenems. *Journal of Antimicrobial Chemotherapy, 47*(3), 247-250.

Lok, C., Ho, C., Chen, R., He, Q., Yu, W., Sun, H., Che, C. (2006). Proteomic analysis of the mode of antibacterial action of silver nanoparticles. *Journal of Proteome Research, 5*(4), 916-924.

Loo, A. E. K., & Halliwell, B. (2012). Effects of hydrogen peroxide in a keratinocyte-fibroblast co-culture model of wound healing. *Biochemical and Biophysical Research Communications, 423*(2), 253-258.

Lorenz, H. P., Whitby, D. J., Longaker, M. T., & Adzick, N. S. (1993). Fetal wound healing. the ontogeny of scar formation in the non-human primate. *Annals of Surgery, 217*(4), 391-396.

Lundov, M. D., Zachariae, C., Menne, T., & Johansen, J. D. (2012). Airborne exposure to preservative methylisothiazolinone causes severe allergic reactions. *BMJ (Clinical Research Ed.), 345*, e8221.

Luoma, S.Silver nanotechnologies and the environment; woodrow wilson international center for scholars: Washington, DC, USA, 2008, p 72. *There is no Corresponding Record for this Reference,*

Lusby, P. E., Coombes, A. L., & Wilkinson, J. M. (2005). Bactericidal activity of different honeys against pathogenic bacteria. *Archives of Medical Research, 36*(5), 464-467.

Lyczak, J. B., Cannon, C. L., & Pier, G. B. (2000). Establishment of *Pseudomonas aeruginosa* infection: Lessons from a versatile opportunist. *Microbes and Infection, 2*(9), 1051-1060.

Maas-Szabowski, N., Stark, H., & Fusenig, N. E. (2000). Keratinocyte growth regulation in defined organotypic cultures through IL-1-induced keratinocyte growth factor expression in resting fibroblasts. *Journal of Investigative Dermatology, 114*(6), 1075-1084.

Maas-Szabowski, N., Starker, A., & Fusenig, N. E. (2003). Epidermal tissue regeneration and stromal interaction in HaCaT cells is initiated by TGF-alpha. *Journal of Cell Science, 116*(Pt 14), 2937-2948.

Macfarlane, M., Jones, P., Goebel, C., Dufour, E., Rowland, J., Araki, D., Kirst, A. (2009). A tiered approach to the use of alternatives to animal testing for the safety assessment of cosmetics: Skin irritation. *Regulatory Toxicology and Pharmacology, 54*(2), 188-196.

McLaughlin, B., Hartnett, K.A., Erhardt, J.A., Legos, J.J., White, R.F., Barone, F.C. and Aizenman, E., 2003. Caspase 3 activation is essential for neuroprotection in preconditioning. *Proceedings of the National Academy of Sciences*, 100(2), pp.715-720.

MacLeod, A. S., & Mansbridge, J. N. (2016). The innate immune system in acute and chronic wounds. *Advances in Wound Care, 5*(2), 65-78.

MacNeil, S. (2007). Progress and opportunities for tissue-engineered skin. *Nature, 445*(7130), 874.

Madhok, B. M., Vowden, K., & Vowden, P. (2013). New techniques for wound debridement. *International Wound Journal, 10*(3), 247-251.

Madhusoodanan, J., Seo, K. S., Remortel, B., Park, J. Y., Hwang, S. Y., Fox, L. K., Gill, S. R. (2011). An enterotoxin-bearing pathogenicity island in *Staphylococcus epidermidis. Journal of Bacteriology, 193*(8), 1854-1862.

Magnusson, B. (1969). The identification of contact allergens by animal assay. the guinea pig maximization test. *J.Invest.Dermatol., 52*, 268-276.

Mahvi, A.H., (2009). Application of ultrasonic technology for water and waste water treatment. Iranian Journal of Public Health, pp.1-17.

Maillard, J. (2002). Bacterial target sites for biocide action. *Journal of Applied Microbiology, 92*, 16S-27S.

Malachowa, N., Kobayashi, S. D., Braughton, K. R., & DeLeo, F. R. (2013). Mouse model of *Staphylococcus aureus* skin infection. *Mouse models of innate immunity* (pp. 109-116) Springer.

Malic, S., Hill, K. E., Hayes, A., Percival, S. L., Thomas, D. W., & Williams, D. W. (2009). Detection and identification of specific bacteria in wound biofilms using peptide nucleic acid fluorescent in situ hybridization (PNA FISH). *Microbiology, 155*(8), 2603-2611.

Malloy, J. L., Veldhuizen, R. A., Thibodeaux, B. A., O'Callaghan, R. J., & Wright, J. R. (2005). *Pseudomonas aeruginosa* protease IV degrades surfactant proteins and inhibits surfactant host defense and biophysical functions. *American Journal of Physiology.Lung Cellular and Molecular Physiology, 288*(2), L409-18.

Mann, E. R., Smith, K. M., Bernardo, D., Al-Hassi, H. O., Knight, S. C., & Hart, A. L. (2012). Review: Skin and the immune system. *Journal of Clinical & Experimental Dermatology Research, 2012*

Marazzi, M., Stefani, A., Chiaratti, A., Ordanini, M., Falcone, L., & Rapisarda, V. (2006). Effect of enzymatic debridement with collagenase on acute and chronic hard-to-heal wounds. *Journal of Wound Care, 15*(5), 222-227.

Margraf, H. W., & Covey, T. H. (1977). A trial of silver-zinc-allantoinate in the treatment of leg ulcers. *Archives of Surgery, 112*(6), 699-704.

Marin, M. E., de la Rosa, M. C., & Cornejo, I. (1992). Enterotoxigenicity of *Staphylococcus* strains isolated from spanish dry-cured hams. *Applied and Environmental Microbiology, 58*(3), 1067-1069.

Marinkovich, M. P., Keene, D. R., Rimberg, C. S., & Burgeson, R. E. (1993). Cellular origin of the dermal-epidermal basement membrane. *Developmental Dynamics, 197*(4), 255-267.

Marraffini, L. A., & Sontheimer, E. J. (2008). CRISPR interference limits horizontal gene transfer in staphylococci by targeting DNA. *Science (New York, N.Y.), 322*(5909), 1843-1845.

Martin, R. G. (1963). The first enzyme in histidine biosynthesis: The nature of feedback inhibition by histidine. *Journal of Biological Chemistry, 238*(1), 257-268.

Martinez, J. L., & Baquero, F. (2000). Mutation frequencies and antibiotic resistance. *Antimicrobial Agents and Chemotherapy, 44*(7), 1771-1777.

Martinotti, S., Calabrese, G., & Ranzato, E. (2017). Honeydew honey: Biological effects on skin cells. *Molecular and Cellular Biochemistry, 435*(1-2), 185-192.

Mathee, K., Ciofu, O., Sternberg, C., Lindum, P. W., Campbell, J. I., Jensen, P., Søren, M. (1999). Mucoid conversion of pseudomonas aeruginos by hydrogen peroxide: A mechanism for virulence activation in the cystic fibrosis lung. *Microbiology, 145*(6), 1349-1357.

Mavric, E., Wittmann, S., Barth, G., & Henle, T. (2008). Identification and quantification of methylglyoxal as the dominant antibacterial constituent of manuka (leptospermum scoparium) honeys from new zealand. *Molecular Nutrition & Food Research, 52*(4), 483-489.

Mboto, C., Eja, M., Adegoke, A., Iwatt, G., Asikong, B., Takon, I., Akeh, M. (2009). Phytochemical properties and antimicrobial activities of combined effect of extracts of the leaves of garcinia kola, vernonia amygdalina and honey on some medically important microorganisms. *African Journal of Microbiology Research, 3*(9), 557-559.

McDonnell, G., & Russell, A. D. (1999). Antiseptics and disinfectants: Activity, action, and resistance. *Clinical Microbiology Reviews, 12*(1), 147-179.

McNaught, A. D., & McNaught, A. D. (1997). *Compendium of chemical terminology* Blackwell Science Oxford.

Mears, A., White, A., Cookson, B., Devine, M., Sedgwick, J., Phillips, E., Bardsley, M. (2009). Healthcare-associated infection in acute hospitals: Which interventions are effective? *Journal of Hospital Infection, 71*(4), 307-313.

Medawar, P. (1941). Sheets of pure epidermal epithelium from human skin. *Nature, 148*(3765), 783.

Mertz, P. M., Patti, J. M., Marcin, J. J., & Marshall, D. A. (1987). Model for studying bacterial adherence to skin wounds. *Journal of Clinical Microbiology, 25*(9), 1601-1604.

Mestas, J., & Hughes, C. C. (2004). Of mice and not men: Differences between mouse and human immunology. *Journal of Immunology (Baltimore, Md.: 1950), 172*(5), 2731-2738.

Micallef, L., Belaubre, F., Pinon, A., Jayat-Vignoles, C., Delage, C., Charveron, M., & Simon, A. (2009). Effects of extracellular calcium on the growth-differentiation switch in immortalized keratinocyte HaCaT cells compared with normal human keratinocytes. *Experimental Dermatology, 18*(2), 143-151.

Mirsattari, S. M., Hammond, R. R., Sharpe, M. D., Leung, F. Y., & Young, G. B. (2004). Myoclonic status epilepticus following repeated oral ingestion of colloidal silver. *Neurology, 62*(8), 1408-1410.

Mishriki, S., Law, D., & Jeffery, P. J. (1990). Factors affecting the incidence of postoperative wound infection. *Journal of Hospital Infection, 16*(3), 223-230.

Mitchell, J. G., & Kogure, K. (2006). Bacterial motility: Links to the environment and a driving force for microbial physics. *FEMS Microbiology Ecology, 55*(1), 3-16.

Mitchell, B. G., Digney, W., Locket, P., & Dancer, S. J. (2014). Controlling methicillin-resistant *Staphylococcus aureus* (MRSA) in a hospital and the role of hydrogen peroxide decontamination: An interrupted time series analysis. *BMJ Open, 4*(4), e004522-2013-004522.

Molan, P. C. (2006). The evidence supporting the use of honey as a wound dressing. *The International Journal of Lower Extremity Wounds, 5*(1), 40-54.

Monstrey, S., Hoeksema, H., Verbelen, J., Pirayesh, A., & Blondeel, P. (2008). Assessment of burn depth and burn wound healing potential. *Burns, 34*(6), 761-769.

Moolenaar, R. L., Crutcher, J. M., San Joaquin, V. H., Sewell, L. V., Hutwagner, L. C., Carson, L. A., . . . Jarvis, W. R. (2000). A prolonged outbreak of *Pseudomonas aeruginosa* in a neonatal intensive care unit did staff fingernails play a role in disease transmission? *Infection Control & Hospital Epidemiology, 21*(2), 80-85.

Moore, J., & Jensen, P. (2004). Assessing the role and impact of enzymatic debridement. *Podiatry Today, 17*(7), 54-61.

Morton, L., Greenway, D., Gaylarde, C., & Surman, S. (1998). Consideration of some implications of the resistance of biofilms to biocides. *International Biodeterioration & Biodegradation, 41*(3-4), 247-259.

Mosser, D. M., & Edwards, J. P. (2008). Exploring the full spectrum of macrophage activation. *Nature Reviews Immunology, 8*(12), 958.

Mostafa, N. Z., Uludağ, H., Dederich, D. N., Doschak, M. R., & El-Bialy, T. H. (2009). Anabolic effects of low-intensity pulsed ultrasound on human gingival fibroblasts. *Archives of Oral Biology, 54*(8), 743-748.

Moyer, C. A., BRENTANO, L., GRAVENS, D. L., MARGRAF, H. W., & MONAFO, W. W. (1965). Treatment of large human burns with 0.5% silver nitrate solution. *Archives of Surgery, 90*(6), 812-867.

Mulet, X., Macia, M. D., Mena, A., Juan, C., Perez, J. L., & Oliver, A. (2009). Azithromycin in *Pseudomonas aeruginosa* biofilms: Bactericidal activity and

selection of nfxB mutants. *Antimicrobial Agents and Chemotherapy, 53*(4), 1552-1560.

Müller, G., & Kramer, A. (2008). Biocompatibility index of antiseptic agents by parallel assessment of antimicrobial activity and cellular cytotoxicity. *Journal of Antimicrobial Chemotherapy, 61*(6), 1281-1287.

Mullick, S., Watson-Jones, D., Beksinska, M., & Mabey, D. (2005). Sexually transmitted infections in pregnancy: Prevalence, impact on pregnancy outcomes, and approach to treatment in developing countries. *Sexually Transmitted Infections, 81*(4), 294-302.

Naglik, J. R., Challacombe, S. J., & Hube, B. (2003). Candida albicans secreted aspartyl proteinases in virulence and pathogenesis. *Microbiology and Molecular Biology Reviews : MMBR, 67*(3), 400-28, table of contents.

Naguib, K., & Hussin, L. (1972). Effect of hydrogen peroxide treatments on the bacteriological quality and nutritive value of milk. *Milchwissenschaft,*

Nakamura, K., Kanno, T., Mokudai, T., Iwasawa, A., Niwano, Y., & Kohno, M. (2010). A novel analytical method to evaluate directly catalase activity of microorganisms and mammalian cells by ESR oximetry. *Free Radical Research, 44*(9), 1036-1043.

Makarenkova, H.P. and Dartt, D.A., (2015). Myoepithelial cells: their origin and function in lacrimal gland morphogenesis, homeostasis, and repair. *Current molecular biology reports*, 1(3), pp.115-123.

National Prescribing Centre. (2010). Evidence-based prescribing of advanced wound dressings for chronic wounds in primary care. *MeReC Bulletin, 21*(1), 1-7.

National Pressure Ulcer Advisory Panel. (2016). National pressure ulcer advisory panel (NPUAP) announces a change in terminology from pressure ulcer to pressure injury and updates the stages of pressure injury.

Netzaff, F., Lehr, C., Wertz, P. W., & Schaefer, U. F. (2005). The human epidermis models EpiSkin (R), SkinEthic (R) and EpiDerm (R): An evaluation of morphology and their suitability for testing phototoxicity, irritancy, corrosivity, and substance transport. *European Journal of Pharmaceutics and Biopharmaceutics, 60*(2), 167-178.

Ng, K. H., Siar, C. H., & Ganesapillai, T. (1997). Sarcoid-like foreign body reaction in body piercing: A report of two cases. *Oral Surgery, Oral Medicine, Oral Pathology, Oral Radiology and Endodontics, 84*(1), 28-31.

Ngo, b. Q., Vickery, K., & Deva, A. (2007). Pr21 role of bacterial biofilms in chronic wounds. *ANZ Journal of Surgery, 77*, A66-A66.

Nicasio, A. M., Kuti, J. L., & Nicolau, D. P. (2008). The current state of Multidrug-Resistant Gram-Negative bacilli in north america: Insights from the society of infectious diseases pharmacists. *Pharmacotherapy: The Journal of Human Pharmacology and Drug Therapy, 28*(2), 235-249.

Nicholls, S. C. (2005). Sequelae of untreated venous insufficiency. *Seminars in Interventional Radiology, 22*(3), 162-168.

Nicoletti, G., Boghossian, V., Gurevitch, F., Borland, R., & Morgenroth, P. (1993). The antimicrobial activity in vitro of chlorhexidine, a mixture of isothiazolinones ('kathon' CG) and cetyl trimethyl ammonium bromide (CTAB). *The Journal of Hospital Infection, 23*(2), 87-111.

Nies, D. H. (1999). Microbial heavy-metal resistance. *Applied Microbiology and Biotechnology, 51*(6), 730-750.

Nunan, R., Harding, K. G., & Martin, P. (2014). Clinical challenges of chronic wounds: Searching for an optimal animal model to recapitulate their complexity. *Disease Models & Mechanisms, 7*(11), 1205-1213.

O'Brien Jr, W. D. (2007). Ultrasound–biophysics mechanisms. *Progress in Biophysics and Molecular Biology, 93*(1-3), 212-255.

Oda, S., Nitta, H., Setoguchi, T., Izumi, Y., & Ishikawa, I. (2004). Current concepts and advances in manual and power-driven instrumentation. *Periodontology 2000, 36*(1), 45-58.

Oddo, L. P., Heard, T. A., Rodríguez-Malaver, A., Pérez, R. A., Fernández-Muiño, M., Sancho, M. T., Vit, P. (2008). Composition and antioxidant activity of trigona carbonaria honey from australia. *Journal of Medicinal Food, 11*(4), 789-794.

O'Dell, M. L. (1998). Skin and wound infections: An overview. *American Family Physician, 57*(10), 2424-2432.

Okhiria, O. A. (2010). *The Role of Biofilm in Wounds,*

O'Leary, R., Sved, A., Davies, E., Leighton, T., Wilson, M., & Kieser, J. (1997). The bactericidal effects of dental ultrasound on actinobacillus actinomycetemcomitans and porphyromonas gingivalis: An in vitro investigation. *Journal of Clinical Periodontology, 24*(6), 432-439.

Oliveira, P. D. d., Oliveira, D. A., Martinago, C. C., Frederico, R. C. P., Soares, C. P., & Oliveira, R. F. d. (2015). Effect of low-intensity pulsed ultrasound therapy on a fibroblasts cell culture. *Fisioterapia e Pesquisa, 22*(2), 112-118.

Oliveira, R. F. D., Oliveira, D. A. P., Monteiro, W., Zangaro, R. A., Magini, M., & Soares, C. P. (2008). Comparison between the effect of low-level laser therapy and low-intensity pulsed ultrasonic irradiation in vitro. *Photomedicine and Laser Surgery, 26*(1), 6-9.

Olson, M. E., Ceri, H., Morck, D. W., Buret, A. G., & Read, R. R. (2002). Biofilm bacteria: Formation and comparative susceptibility to antibiotics. *Canadian Journal of Veterinary Research Revue Canadienne De Recherche Veterinaire, 66*(2), 86-92.

O'Meara, S., Al-Kurdi, D., Ologun, Y., Ovington, L. G., Martyn-St James, M., & Richardson, R. (2014). Antibiotics and antiseptics for venous leg ulcers. *Cochrane Database of Systematic Reviews,* (1)

Onguru, P., Erbay, A., Bodur, H., Baran, G., Akinci, E., Balaban, N., & Cevik, M. A. (2008). Imipenem-resistant *Pseudomonas aeruginosa*: Risk factors for nosocomial infections. *Journal of Korean Medical Science, 23*(6), 982-987.

Osseiran, S., Cruz, J. D., Jeong, S., Wang, H., Fthenakis, C., & Evans, C. L. (2018). Characterizing stratum corneum structure, barrier function, and chemical content of human skin with coherent raman scattering imaging. *Biomedical Optics Express, 9*(12), 6425-6443.

Otto, M. (2008). Staphylococcal biofilms. *Bacterial biofilms* (pp. 207-228) Springer.

Otto, M. (2009). *Staphylococcus epidermidis*—the'accidental'pathogen. *Nature Reviews Microbiology, 7*(8), 555.

Otto, M. (2012). Molecular basis of *Staphylococcus epidermidis* infections. Paper presented at the *Seminars in Immunopathology, 34*(2) 201-214.

Otto, M. (2013). Staphylococcal infections: Mechanisms of biofilm maturation and detachment as critical determinants of pathogenicity. *Annual Review of Medicine, 64*, 175-188.

Otto, M. (2014). *Staphylococcus epidermidis* pathogenesis. *Staphylococcus epidermidis* (pp. 17-31) Springer.

Oulahal-Lagsir, N., Martial-Gros, A., Boistier, E., Blum, L., & Bonneau, M. (2000). The development of an ultrasonic apparatus for the non-invasive and repeatable removal of fouling in food processing equipment. *Letters in Applied Microbiology, 30*(1), 47-52.

Pacak, C. A., Powers, J. M., & Cowan, D. B. (2011). Ultrarapid purification of collagen type I for tissue engineering applications. *Tissue Engineering Part C: Methods, 17*(9), 879-885.

Painter, K. L., Strange, E., Parkhill, J., Bamford, K. B., Armstrong-James, D., & Edwards, A. M. (2015). *Staphylococcus aureus* adapts to oxidative stress by producing H2O2-resistant small-colony variants via the SOS response. *Infection and Immunity, 83*(5), 1830-1844.

Palavutitotai, N., Jitmuang, A., Tongsai, S., Kiratisin, P., & Angkasekwinai, N. (2018). Epidemiology and risk factors of extensively drug-resistant *Pseudomonas aeruginosa* infections. *PloS One, 13*(2), e0193431.

Palmer, K. L., Aye, L. M., & Whiteley, M. (2007). Nutritional cues control *Pseudomonas aeruginosa* multicellular behavior in cystic fibrosis sputum. *Journal of Bacteriology, 189*(22), 8079-8087.

Palmer, K. L., Mashburn, L. M., Singh, P. K., & Whiteley, M. (2005). Cystic fibrosis sputum supports growth and cues key aspects of *Pseudomonas aeruginosa* physiology. *Journal of Bacteriology, 187*(15), 5267-5277.

Panayi, A. C., Leavitt, T., & Orgill, D. P. (2017). Evidence based review of negative pressure wound therapy. *World Journal of Dermatology, 6*(1), 1-16.

Park, P. W., Rosenbloom, J., Abrams, W. R., Rosenbloom, J., & Mecham, R. P. (1996). Molecular cloning and expression of the gene for elastin-binding protein (ebpS) in *Staphylococcus aureus*. *The Journal of Biological Chemistry, 271*(26), 15803-15809.

Parsek, M. R., & Singh, P. K. (2003). Bacterial biofilms: An emerging link to disease pathogenesis. *Annual Reviews in Microbiology, 57*(1), 677-701.

Parsons, D., Bowler, P. G., Myles, V., & Jones, S. (2005). Silver antimicrobial dressings in wound management: A comparison of antibacterial, physical, and chemical characteristics. *Wounds-A Compendium of Clinical Research and Practice, 17*(8), 222-232.

Parvizi, J., Pawasarat, I. M., Azzam, K. A., Joshi, A., Hansen, E. N., & Bozic, K. J. (2010). Periprosthetic joint infection: The economic impact of methicillin-resistant infections. *The Journal of Arthroplasty, 25*(6), 103-107.

Pastar, I., Stojadinovic, O., Yin, N. C., Ramirez, H., Nusbaum, A. G., Sawaya, A., Tomic-Canic, M. (2014). Epithelialization in wound healing: A comprehensive review. *Advances in Wound Care, 3*(7), 445-464.

Patel, R. (2005). Biofilms and antimicrobial resistance. *Clinical Orthopaedics and Related Research®, 437*, 41-47.

Patti, J. M., Jonsson, H., Guss, B., Switalski, L. M., Wiberg, K., Lindberg, M., & Hook, M. (1992). Molecular characterization and expression of a gene encoding a *Staphylococcus aureus* collagen adhesin. *The Journal of Biological Chemistry, 267*(7), 4766-4772.

Paul, B. B., Strauss, R. R., Selvaraj, R. J., & Sbarra, A. J. (1973). Peroxidase mediated antimicrobial activities of alveolar macrophage granules. *Science (New York, N.Y.), 181*(4102), 849-850.

Paulsson, M. (1992). Basement membrane proteins: Structure, assembly, and cellular interactions. *Critical Reviews in Biochemistry and Molecular Biology, 27*(1-2), 93-127.

Pearse, A. D., Gaskell, S. A., & Marks, R. (1987). Epidermal changes in human skin following irradiation with either UVB or UVA. *Journal of Investigative Dermatology, 88*(1), 83-87.

Peleg, A. Y., Weerarathna, T., McCarthy, J. S., & Davis, T. M. (2007). Common infections in diabetes: Pathogenesis, management and relationship to glycaemic control. *Diabetes/metabolism Research and Reviews, 23*(1), 3-13.

Peng, Z., Wu, H., Ruiz, T., Chen, Q., Zhou, M., Sun, B., & Fives-Taylor, P. (2008). Role of gap3 in Fap1 glycosylation, stability, in vitro adhesion, and fimbrial and biofilm formation of streptococcus parasanguinis. *Oral Microbiology and Immunology, 23*(1), 70-78. .

Percival, S. L., Emanuel, C., Cutting, K. F., & Williams, D. W. (2012). Microbiology of the skin and the role of biofilms in infection. *International Wound Journal, 9*(1), 14-32.

Pereira, R. F., Barrias, C. C., Granja, P. L., & Bartolo, P. J. (2013). Advanced biofabrication strategies for skin regeneration and repair. *Nanomedicine, 8*(4), 603-621.

Peterson, H. G., Hrudey, S. E., Cantin, I. A., Perley, T. R., & Kenefick, S. L. (1995). Physiological toxicity, cell membrane damage and the release of dissolved organic carbon and geosmin by aphanizomenon flos-aquae after exposure to water treatment chemicals. *Water Research, 29*(6), 1515-1523.

Peterson, R. V., & Pitt, W. G. (2000). The effect of frequency and power density on the ultrasonically-enhanced killing of biofilm-sequestered escherichia coli. *Colloids and Surfaces B: Biointerfaces, 17*(4), 219-227.

Phull, S., Newman, A., Lorimer, J., Pollet, B., & Mason, T. (1997). The development and evaluation of ultrasound in the biocidal treatment of water. *Ultrasonics Sonochemistry, 4*(2), 157-164.

Pitt, W. G., & Ross, S. A. (2003). Ultrasound increases the rate of bacterial cell growth. *Biotechnology Progress, 19*(3), 1038-1044.

Pitt, W. G., McBride, M. O., Lunceford, J. K., Roper, R. J., & Sagers, R. D. (1994). Ultrasonic enhancement of antibiotic action on Gram-negative bacteria. *Antimicrobial Agents and Chemotherapy, 38*(11), 2577-2582.

Piyasena, P., Mohareb, E., & McKellar, R. (2003). Inactivation of microbes using ultrasound: A review. *International Journal of Food Microbiology, 87*(3), 207-216.

Ponec, M., Weerheim, A., Kempenaar, J., Mulder, A., Gooris, G. S., Bouwstra, J., & Mommaas, A. M. (1997). The formation of competent barrier lipids in reconstructed human epidermis requires the presence of vitamin C. *Journal of Investigative Dermatology, 109*(3), 348-355.

Ponec, M., Boelsma, E., Gibbs, S., & Mommaas, M. (2002). Characterization of reconstructed skin models. *Skin Pharmacology and Applied Skin Physiology, 15 Suppl 1*, 4-17.

Potvin, E., Lehoux, D. E., Kukavica-Ibrulj, I., Richard, K. L., Sanschagrin, F., Lau, G. W., & Levesque, R. C. (2003). In vivo functional genomics of *Pseudomonas aeruginosa* for high-throughput screening of new virulence factors and antibacterial targets. *Environmental Microbiology, 5*(12), 1294-1308.

Pritt, B., O'brien, L., & Winn, W. (2007). Mucoid pseudomonas in cystic fibrosis. *American Journal of Clinical Pathology, 128*(1), 32-34.

Prompers, L., Schaper, N., Apelqvist, J., Edmonds, M., Jude, E., Mauricio, D., Holstein, P. (2008). Prediction of outcome in individuals with diabetic foot ulcers: Focus on the differences between individuals with and without peripheral arterial disease. The EURODIALE study. *Diabetologia, 51*(5), 747-755.

Prunieras, M., Regnier, M., & Woodley, D. (1983). Methods for cultivation of keratinocytes with an air-liquid interface. *Journal of Investigative Dermatology, 81*(1), S28-S33.

Qian, B., & Pollard, J. W. (2010). Macrophage diversity enhances tumor progression and metastasis. *Cell, 141*(1), 39-51.

Qian, Z., Sagers, R. D., & Pitt, W. G. (1997). The effect of ultrasonic frequency upon enhanced killing ofP. aeruginosa biofilms. *Annals of Biomedical Engineering, 25*(1), 69-76.

Qian, Z., Sagers, R. D., & Pitt, W. G. (1999). Investigation of the mechanism of the bioacoustic effect. *Journal of Biomedical Materials Research, 44*(2), 198-205.

Qian, Z., Stoodley, P., & Pitt, W. G. (1996). Effect of low-intensity ultrasound upon biofilm structure from confocal scanning laser microscopy observation. *Biomaterials, 17*(20), 1975-1980.

Raad, I., Alrahwan, A., & Rolston, K. (1998). *Staphylococcus epidermidis*: Emerging resistance and need for alternative agents. *Reviews of Infectious Diseases, 26*(5), 1182-1187.

Rai, M., Yadav, A., & Gade, A. (2009). Silver nanoparticles as a new generation of antimicrobials. *Biotechnology Advances, 27*(1), 76-83.

Ramsey, S. D., Newton, K., Blough, D., McCulloch, D. K., Sandhu, N., Reiber, G. E., & Wagner, E. H. (1999). Incidence, outcomes, and cost of foot ulcers in patients with diabetes. *Diabetes Care, 22*(3), 382-387.

Randall, C. P., Oyama, L. B., Bostock, J. M., Chopra, I., & O'neill, A. J. (2012). The silver cation (ag): Antistaphylococcal activity, mode of action and resistance studies. *Journal of Antimicrobial Chemotherapy, 68*(1), 131-138.

Rapoport, N., Smirnov, A. I., Timoshin, A., Pratt, A. M., & Pitt, W. G. (1997). Factors affecting the permeability of *Pseudomonas aeruginosa* Cell walls toward lipophilic compounds: Effects of ultrasound and cell age. *Archives of Biochemistry and Biophysics, 344*(1), 114-124.

Recsei, P., Kreiswirth, B., O'reilly, M., Schlievert, P., Gruss, A., & Novick, R. (1986). Regulation of exoprotein gene expression in *Staphylococcus aureus* by agr. *Molecular and General Genetics MGG, 202*(1), 58-61.

Reddy, M., Gill, S. S., & Rochon, P. A. (2006). Preventing pressure ulcers: A systematic review. *Jama, 296*(8), 974-984.

Rediske, A., Rapoport, N., & Pitt, W. (1999). Reducing bacterial resistance to antibiotics with ultrasound. *Letters in Applied Microbiology, 28*(1), 81-84.

Rediske, A. M., Hymas, W. C., Wilkinson, R., & Pitt, W. G. (1998). Ultrasonic enhancement of antibiotic action on several species of bacteria. *The Journal of General and Applied Microbiology, 44*(4), 283-288.

Rediske, A. M., Roeder, B. L., Nelson, J. L., Robison, R. L., Schaalje, G. B., Robison, R. A., & Pitt, W. G. (2000). Pulsed ultrasound enhances the killing of escherichia coli biofilms by aminoglycoside antibiotics in vivo. *Antimicrobial Agents and Chemotherapy, 44*(3), 771-772.

Reiber, G. E. (1992). Diabetic foot care. financial implications and practice guidelines. *Diabetes Care, 15 Suppl 1*, 29-31.

Reijnders, C. M., van Lier, A., Roffel, S., Kramer, D., Scheper, R. J., & Gibbs, S. (2015). Development of a full-thickness human skin equivalent in vitro model derived from TERT-immortalized keratinocytes and fibroblasts. *Tissue Engineering Part A, 21*(17-18), 2448-2459.

Renzoni, A., Kelley, W. L., Vaudaux, P., Cheung, A. L., & Lew, D. P. (2010). Exploring innate glycopeptide resistance mechanisms in *Staphylococcus aureus. Trends in Microbiology, 18*(2), 55-56.

Rheinwatd, J. G., & Green, H. (1975). Seria cultivation of strains of human epidemal keratinocytes: The formation keratinizin colonies from single cell is. *Cell, 6*(3), 331-343.

Rhoads, D. D., Wolcott, R. D., & Percival, S. L. (2008). Biofilms in wounds: Management strategies. *Journal of Wound Care, 17*(11), 502-508.

Richmond, N. A., Maderal, A. D., & Vivas, A. C. (2013). Evidence-based management of common chronic lower extremity ulcers. *Dermatologic Therapy, 26*(3), 187-196.

Riedel, K., & Eberl, L. (2007). Social behavior of members of the genus burkholderia: Quorum sensing and biofilms. *Burkholderia: Molecular Microbiology and Genomics,* 251-282.

Riesbeck, K., Bredberg, A., & Forsgren, A. (1990). Ciprofloxacin does not inhibit mitochondrial functions but other antibiotics do. *Antimicrobial Agents and Chemotherapy, 34*(1), 167-169.

Ríos-Castillo, A. G., González-Rivas, F., & Rodríguez-Jerez, J. J. (2017). Bactericidal efficacy of hydrogen Peroxide-Based disinfectants against Gram-Positive and Gram-Negative bacteria on stainless steel surfaces. *Journal of Food Science, 82*(10), 2351-2356.

Rivalland, P., Vié, K., Coiffard, L., & De Roeck-Holtzhauer, Y. (1994). Cytotoxicity tests of antibacterial agents on human fibroblasts cultures. *Pharmaceutica Acta Helvetiae, 69*(3), 159-162.

Riyat, M. S., & Quinton, D. N. (1997). Tap water as a wound cleansing agent in accident and emergency. *Journal of Accident & Emergency Medicine, 14*(3), 165-166.

Rnjak, J., Wise, S. G., Mithieux, S. M., & Weiss, A. S. (2011). Severe burn injuries and the role of elastin in the design of dermal substitutes. *Tissue Engineering Part B: Reviews, 17*(2), 81-91.

Roberts, A. E., Maddocks, S. E., & Cooper, R. A. (2014). Manuka honey reduces the motility of pseudomonas aeruginosa by suppression of flagella-associated genes. *Journal of Antimicrobial Chemotherapy, 70*(3), 716-725.

Robertson, K., & Rees, J. L. (2010). Variation in epidermal morphology in human skin at different body sites as measured by reflectance confocal microscopy. *Acta Dermato-Venereologica, 90*(4), 368-373.

Roe, A. L. (1915). Collosol argentum and its ophthalmic uses. *British Medical Journal, 1*(2820), 104.

Roeckl-Wiedmann, I., Bennett, M., & Kranke, P. (2005). Systematic review of hyperbaric oxygen in the management of chronic wounds. *British Journal of Surgery, 92*(1), 24-32.

Rogers, K. L., Fey, P. D., & Rupp, M. E. (2009). Coagulase-negative staphylococcal infections. *Infectious Disease Clinics of North America, 23*(1), 73-98.

Romanovsky, A. A. (2014). Skin temperature: Its role in thermoregulation. *Acta Physiologica, 210*(3), 498-507.

Roper, J., Harrison, A., & Bass, M. D. (2012). Induction of adhesion-dependent signals using low-intensity ultrasound. *Journal of Visualized Experiments: JoVE, (63):e4024. doi*(63), e4024.

Rosenkranz, H. S., & Carr, H. S. (1972). Silver sulfadiazine: Effect on the growth and metabolism of bacteria. *Antimicrobial Agents and Chemotherapy, 2*(5), 367-372.

Ross, M., Pawlina, W., & Histology, A. (1989). A text and atlas. *Williams and Wilkins.*

Rowan, M. P., Cancio, L. C., Elster, E. A., Burmeister, D. M., Rose, L. F., Natesan, S., Chung, K. K. (2015). Burn wound healing and treatment: Review and advancements. *Critical Care, 19*(1), 243.

Runyan, C. M., Carmen, J. C., Beckstead, B. L., Nelson, J. L., Robison, R. A., & Pitt, W. G. (2006). Low-frequency ultrasound increases outer membrane permeability of *Pseudomonas aeruginosa*. *The Journal of General and Applied Microbiology, 52*(5), 295-301.

Ruparelia, J. P., Chatterjee, A. K., Duttagupta, S. P., & Mukherji, S. (2008). Strain specificity in antimicrobial activity of silver and copper nanoparticles. *Acta Biomaterialia, 4*(3), 707-716.

Russell, A. D. (2004). Factors influencing the efficacy of antimicrobial agents. *Russell, Hugo and Ayliffe's Principles and Practice of Disinfection, Preservation and Sterilization,* 98-127.

Russell, A. (2003). Biocide use and antibiotic resistance: The relevance of laboratory findings to clinical and environmental situations. *The Lancet Infectious Diseases, 3*(12), 794-803.

Russell, A. D., & Chopra, I. (1990). *Understanding antibacterial action and resistance* E. Horwood.

Russell, H. (2003). Ayliffe's principles and practice of disinfection. *Preservation & Sterilization,*

Russell, W. M. S., Burch, R. L., & Hume, C. W. (1959). The principles of humane experimental technique.

Rutala, W. A., & Weber, D. J. (1999). Disinfection of endoscopes: Review of new chemical sterilants used for high-level disinfection. *Infection Control & Hospital Epidemiology, 20*(1), 69-76.

Rybak-Chmielewska, H., & Szczęsna, T. (1995). Composition and properties of polish buckwheat honey. *Current Advances in Buckwheat Research.Institute of Pomology and Floriculture, Puławy,*

Saager, R. B., Kondru, C., Au, K., Sry, K., Ayers, F., & Durkin, A. J. (2010). (2010). Multilayer silicone phantoms for the evaluation of quantitative optical techniques in skin imaging. Paper presented at the *Design and Performance Validation of Phantoms used in Conjunction with Optical Measurement of Tissue II, 7567* 756706.

Safferling, K., Sutterlin, T., Westphal, K., Ernst, C., Breuhahn, K., James, M., Grabe, N. (2013). Wound healing revised: A novel reepithelialization mechanism revealed by in vitro and in silico models. *The Journal of Cell Biology, 203*(4), 691-709.

Saga, T., & Yamaguchi, K. (2009). History of antimicrobial agents and resistant bacteria.

Said-Salim, B., Dunman, P. M., McAleese, F. M., Macapagal, D., Murphy, E., McNamara, P. J., Kreiswirth, B. N. (2003). Global regulation of *Staphylococcus aureus* genes by rot. *Journal of Bacteriology, 185*(2), 610-619.

Salmon, J. K., Armstrong, C. A., & Ansel, J. C. (1994). The skin as an immune organ. *The Western Journal of Medicine, 160*(2), 146-152.

Samuels, J. A., Weingarten, M. S., Margolis, D. J., Zubkov, L., Sunny, Y., Bawiec, C. R., Lewin, P. A. (2013). Low-frequency (<100 kHz), low-intensity (< 100 mW/cm^2) ultrasound to treat venous ulcers: A human study and in vitro experiments. *The Journal of the Acoustical Society of America, 134*(2), 1541-1547.

Sanderson-Wells, T. (1918). a case of puerperal septicæmia successfully treated with intravenous injections of collosol argentum. *The Lancet, 191*(4929), 258-259.

Sanford, B., De Feijter, A., Wade, M., & Thomas, V. (1996). A dual fluorescence technique for visualization of *Staphylococcus epidermidis* biofilm using scanning confocal laser microscopy. *Journal of Industrial Microbiology, 16*(1), 48-56.

Santucci, S., Gobara, S., Santos, C., Fontana, C., & Levin, A. (2003). Infections in a burn intensive care unit: Experience of seven years. *Journal of Hospital Infection, 53*(1), 6-13.

Santucci, S. G., Gobara, S., Santos, C. R., Fontana, C., & Levin, A. S. (2003). Infections in a burn intensive care unit: Experience of seven years. *The Journal of Hospital Infection, 53*(1), 6-13.

Saukko, P., & Knight, B. (2015). *Knight's forensic pathology fourth edition* CRC press.

Scarponi, C., Nasorri, F., Pavani, F., Madonna, S., Sestito, R., Simonacci, M.,. Albanesi, C. (2009). Low-frequency low-intensity ultrasounds do not influence the survival and immune functions of cultured keratinocytes and dendritic cells. *Journal of Biomedicine & Biotechnology, 2009*, 193260.

SCENIHR (Scientific Committee on Emerging and Newly Identified Health Risks). (2009). Assessment of the antibiotic resistance effects of biocides. *European Commission, Health & Consumer Protection.*

Schäfer, M., & Werner, S. (2008). Cancer as an overhealing wound: An old hypothesis revisited. *Nature Reviews Molecular Cell Biology, 9*(8), 628.

Scherba, G., Weigel, R. M., & O'Brien, W. D.,Jr. (1991). Quantitative assessment of the germicidal efficacy of ultrasonic energy. *Applied and Environmental Microbiology, 57*(7), 2079-2084.

Scherr, T. D., Heim, C. E., Morrison, J. M., & Kielian, T. (2014). Hiding in plain sight: Interplay between staphylococcal biofilms and host immunity. *Frontiers in Immunology, 5*, 37.

Schierholz, J. M., Beuth, J., Pulverer, G., & Konig, D. P. (1999). Silver-containing polymers. *Antimicrobial Agents and Chemotherapy, 43*(11), 2819-20; author reply 2820-1.

Schittny, J., & Yurchenco, P. (1989). Basement membranes: Molecular organization and function in development and disease. *Current Opinion in Cell Biology, 1*(5), 983-988.

Schmidt, H., & Hensel, M. (2004). Pathogenicity islands in bacterial pathogenesis. *Clinical Microbiology Reviews, 17*(1), 14-56.

Schneider, G. (1984). Silver nitrate prophylaxis. *Canadian Medical Association Journal, 131*(3), 193-196.

Schönfelder, U., Abel, M., Wiegand, C., Klemm, D., Elsner, P., & Hipler, U. (2005). Influence of selected wound dressings on PMN elastase in chronic wound fluid and their antioxidative potential in vitro. *Biomaterials, 26*(33), 6664-6673.

Schoop, V. M., Fusenig, N. E., & Mirancea, N. (1999). Epidermal organization and differentiation of HaCaT keratinocytes in organotypic coculture with human dermal fibroblasts. *Journal of Investigative Dermatology, 112*(3), 343-353.

Schultz, G. S., Ladwig, G., & Wysocki, A. (2005). Extracellular matrix: Review of its roles in acute and chronic wounds. *World Wide Wounds, 2005*, 1-18.

Semeykina, A. L., & Skulachev, V. P. (1990). Submicromolar ag increases passive na permeability and inhibits the respiration-supported formation of na gradient in bacillus FTU vesicles. *FEBS Letters, 269*(1), 69-72.

Sen, C. K., Gordillo, G. M., Roy, S., Kirsner, R., Lambert, L., Hunt, T. K., Longaker, M. T. (2009). Human skin wounds: A major and snowballing threat to public health and the economy. *Wound Repair and Regeneration, 17*(6), 763-771.

Seyhan, T. (2011). Split-thickness skin grafts. *Skin grafts-indications, applications and current research* () Intech.

Sharma, B. K., Saha, A., Rahaman, L., Bhattacharjee, S., & Tribedi, P. (2015). Silver inhibits the biofilm formation of *Pseudomonas aeruginosa. Advances in Microbiology, 5*(10), 677.

Shepherd, J., Douglas, I., Rimmer, S., Swanson, L., & MacNeil, S. (2009). Development of three-dimensional tissue-engineered models of bacterial infected human skin wounds. *Tissue Engineering Part C: Methods, 15*(3), 475-484.

Shepherd, J., Sarker, P., Rimmer, S., Swanson, L., MacNeil, S., & Douglas, I. (2011). Hyperbranched poly (NIPAM) polymers modified with antibiotics for the reduction of bacterial burden in infected human tissue engineered skin. *Biomaterials, 32*(1), 258-267.

Sherlock, D. J., Ward, A., & Holl-Allen, R. T. (1984). Combined preoperative antibiotic therapy and intraoperative topical povidone-iodine: Reduction of wound sepsis following emergency appendectomy. *Archives of Surgery, 119*(8), 909-911.

Shevchenko, R. V., James, S. L., & James, S. E. (2010). A review of tissue-engineered skin bioconstructs available for skin reconstruction. *Journal of the Royal Society, Interface, 7*(43), 229-258.

Sibbald, R. G., Orsted, H., Schultz, G. S., Coutts, P., & Keast, D. (2003). Preparing the wound bed 2003: Focus on infection and inflammation. *Ostomy Wound Management, 49*(11), 24-51.

Sieggreen, M. Y., & Kline, R. A. (2004). Arterial insufficiency and ulceration: Diagnosis and treatment options. *Advances in Skin & Wound Care, 17*(5), 242-251.

Sievert, D. M., Ricks, P., Edwards, J. R., Schneider, A., Patel, J., Srinivasan, A., Fridkin, S. (2013). Antimicrobial-resistant pathogens associated with healthcare-associated infections summary of data reported to the national healthcare safety network at the centers for disease control and prevention, 2009–2010. *Infection Control & Hospital Epidemiology, 34*(1), 1-14.

Silver, S. (2003). Bacterial silver resistance: Molecular biology and uses and misuses of silver compounds. *FEMS Microbiology Reviews, 27*(2-3), 341-353.

Silver, S., Phung, L. T., & Silver, G. (2006). Silver as biocides in burn and wound dressings and bacterial resistance to silver compounds. *Journal of Industrial Microbiology and Biotechnology, 33*(7), 627-634.

Simm, R., Morr, M., Kader, A., Nimtz, M., & Römling, U. (2004). GGDEF and EAL domains inversely regulate cyclic di-GMP levels and transition from sessility to motility. *Molecular Microbiology, 53*(4), 1123-1134.

Simon, D., Fischer, S., Grossman, A., Downer, C., Hota, B., Heroux, A., & Trenholme, G. (2005). Left ventricular assist Device Related infection: Treatment and outcome. *Clinical Infectious Diseases, 40*(8), 1108-1115.

Singer, A. J., Coby, C. T., Singer, A. H., Thode Jr, H. C., & Tortora, G. T. (1999). The effects of low-frequency ultrasound on *Staphylococcus epidermidis. Current Microbiology, 38*(3), 194-196.

Sinno, H., & Prakash, S. (2013). Complements and the wound healing cascade: An updated review. *Plastic Surgery International, 2013*, 146764. doi:10.1155/2013/146764 [doi]

Smeltzer, M. S., Hart, M. E., & Iandolo, J. J. (1993). Phenotypic characterization of xpr, a global regulator of extracellular virulence factors in *Staphylococcus aureus. Infection and Immunity, 61*(3), 919-925.

Smits, J. P., Niehues, H., Rikken, G., van Vlijmen-Willems, I. M., van de Zande, Guillaume WHJF, Zeeuwen, P. L., van den Bogaard, Ellen H. (2017). Immortalized N/TERT keratinocytes as an alternative cell source in 3D human epidermal models. *Scientific Reports, 7*(1), 11838.

Snyder, R. J., & Sigal, B. (2005). The physiology of wound healing. *Podiatry Management, 24*(9), 187.

Sondi, I., & Salopek-Sondi, B. (2004). Silver nanoparticles as antimicrobial agent: A case study on E. coli as a model for Gram-negative bacteria. *Journal of Colloid and Interface Science, 275*(1), 177-182.

Song, K. Y., Lee, S., Suh, D. H., Kim, M. K., Min, H. J., & Chi, J. G. (2001). Expression of cytokeratin 1, 10 and 14 in fetal skin. *The Korean Journal of Pathology, 35*(3), 226-231.

Sorg, H., Tilkorn, D. J., Hager, S., Hauser, J., & Mirastschijski, U. (2017). Skin wound healing: An update on the current knowledge and concepts. *European Surgical Research. Europaische Chirurgische Forschung.Recherches Chirurgicales Europeennes, 58*(1-2), 81-94.

 Sorokin, L. (2010). The impact of the extracellular matrix on inflammation. *Nature Reviews Immunology, 10*(10), 712.

Srinivasan, A., Wolfenden, L. L., Song, X., Mackie, K., Hartsell, T. L., Jones, H. D., Ross, T. L. (2003). An outbreak of *Pseudomonas aeruginosa* infections associated with flexible bronchoscopes. *New England Journal of Medicine, 348*(3), 221-227.

Stadelmann, W. K., Digenis, A. G., & Tobin, G. R. (1998). Impediments to wound healing. *The American Journal of Surgery, 176*(2), 39S-47S.

Stark, H., Baur, M., Breitkreutz, D., Mirancea, N., & Fusenig, N. E. (1999). Organotypic keratinocyte cocultures in defined medium with regular epidermal

morphogenesis and differentiation. *Journal of Investigative Dermatology, 112*(5), 681-691.

Steenvoorde, P., & Oskam, J. (2006). Modern wound treatment of infected transtibial amputation. *JPO: Journal of Prosthetics and Orthotics, 18*(1), 17-20.

Sterry, W., Paus, R., Burgdorf, W., & Holtermann, H. (2006). Dermatology thieme clinical companions.

Stewart, P. S., Grab, L., & Diemer, J. (1998). Analysis of biocide transport limitation in an artificial biofilm system. *Journal of Applied Microbiology, 85*(3), 495-500.

Stewart, P. S., Roe, F., Rayner, J., Elkins, J. G., Lewandowski, Z., Ochsner, U. A., & Hassett, D. J. (2000). Effect of catalase on hydrogen peroxide penetration into *Pseudomonas aeruginosa* biofilms. *Applied and Environmental Microbiology, 66*(2), 836-838.

Stoodley, P., Sauer, K., Davies, D. G., & Costerton, J. W. (2002). Biofilms as complex differentiated communities. *Annual Reviews in Microbiology, 56*(1), 187-209.

Stuelten, C. H., Barbul, A., Busch, J. I., Sutton, E., Katz, R., Sato, M., Niederhuber, J. E. (2008). Acute wounds accelerate tumorigenesis by a T cell-dependent mechanism. *Cancer Research, 68*(18), 7278-7282.

Sukumaran, V., & Senanayake, S. (2016). Bacterial skin and soft tissue infections. *Australian Prescriber, 39*(5), 159-163.

Sullivan, T. P., Eaglstein, W. H., Davis, S. C., & Mertz, P. (2001). The pig as a model for human wound healing. *Wound Repair and Regeneration, 9*(2), 66-76.

Sun, Y., Smith, E., Wolcott, R., & Dowd, S. (2009). Propagation of anaerobic bacteria within an aerobic multi-species chronic wound biofilm model. *Journal of Wound Care, 18*(10), 426-431.

Sun, Y., Dowd, S. E., Smith, E., Rhoads, D. D., & Wolcott, R. D. (2008). In vitro multispecies lubbock chronic wound biofilm model. *Wound Repair and Regeneration, 16*(6), 805-813.

Sutherland, I. W. (2001). Biofilm exopolysaccharides: A strong and sticky framework. *Microbiology, 147*(1), 3-9.

SütteriinN, S., Tano, E., Begsten, A., Taiiberg, A., & Meihus, Å. (2012). Effects of silver-based wound dressings on the bacterial flora in chronic leg ulcers and its susceptibility in vitro to silver. *Acta Dermato-Venereologica, 92*(1), 34-39.

Svedman, P., Ljungh, A., Rausing, A., Banck, G., Sanden, G., Miedzobrodzki, J., & Wadstrom, T. (1989). Staphylococcal wound infection in the pig: Part I. course. *Annals of Plastic Surgery, 23*(3), 212-218.

Tang, H. B., DiMango, E., Bryan, R., Gambello, M., Iglewski, B. H., Goldberg, J. B., & Prince, A. (1996). Contribution of specific *Pseudomonas aeruginosa* virulence factors to pathogenesis of pneumonia in a neonatal mouse model of infection. *Infection and Immunity, 64*(1), 37-43.

Ter Haar, G. (1999). Therapeutic ultrasound. *European Journal of Ultrasound, 9*(1), 3-9.

Texter, J., Ziemer, P., Rhoades, S., & Clemans, D. (2007). Bactericidal silver ion delivery into hydrophobic coatings with surfactants. *Journal of Industrial Microbiology & Biotechnology, 34*(8), 571-575.

Thénard, L. J. (1818). Observations sur des nouvelles combinaisons entre l'oxigène et divers acides. *Ann Chim Phys, 8*, 306-312.

Thiruvoipati, T., Kielhorn, C. E., & Armstrong, E. J. (2015). Peripheral artery disease in patients with diabetes: Epidemiology, mechanisms, and outcomes. *World Journal of Diabetes, 6*(7), 961-969.

Thomas, L., Maillard, J., Lambert, R., & Russell, A. (2000). Development of resistance to chlorhexidine diacetate in *Pseudomonas aeruginosa* and the effect of a'residual'concentration. *Journal of Hospital Infection, 46*(4), 297-303.

Timpl, R., Rohde, H., Robey, P. G., Rennard, S. I., Foidart, J. M., & Martin, G. R. (1979). Laminin--a glycoprotein from basement membranes. *The Journal of Biological Chemistry, 254*(19), 9933-9937.

Tomankova, K., Kolarova, H., Kolar, P., Kejlova, K., & Jirova, D. (2009). Study of cytotoxic effect of photodynamically and sonodynamically activated sensitizers in vitro. *Toxicology in Vitro, 23*(8), 1465-1471.

Tong, G., Pan, Y., Dong, H., Pryor, R., Wilson, G. E., & Schaefer, J. (1997). Structure and dynamics of pentaglycyl bridges in the cell walls of *Staphylococcus aureus* by 13C− 15N REDOR NMR. *Biochemistry, 36*(32), 9859-9866.

Tote, K., Horemans, T., Vanden Berghe, D., Maes, L., & Cos, P. (2010). Inhibitory effect of biocides on the viable masses and matrices of *Staphylococcus aureus* and *Pseudomonas aeruginosa* biofilms. *Applied and Environmental Microbiology, 76*(10), 3135-3142. Trautner, C., Haastert, B., Giani, G., & Berger, M. (1996). Incidence of lower limb amputations and diabetes. *Diabetes Care, 19*(9), 1006-1009.

Tredget, E. E., Shankowsky, H. A., Groeneveld, A., & Burrell, R. (1998). A matched-pair, randomized study evaluating the efficacy and safety of acticoat silver-coated dressing for the treatment of burn wounds. *Journal of Burn Care & Rehabilitation, 19*(6), 531-537.

Tsukamoto, A., Higashiyama, S., Yoshida, K., Watanabe, Y., Furukawa, K. S., & Ushida, T. (2011). Stable cavitation induces increased cytoplasmic calcium in

L929 fibroblasts exposed to 1-MHz pulsed ultrasound. *Ultrasonics, 51*(8), 982-990.

Tumah, H. (2009). Bacterial biocide resistance. *Journal of Chemotherapy, 21*(1), 5-15.

Udroiu, I., Domenici, F., Giliberti, C., Bedini, A., Palomba, R., Luongo, F., Castellano, A. C. (2014). Potential genotoxic effects of low-intensity ultrasound on fibroblasts, evaluated with the cytokinesis-block micronucleus assay. *Mutation Research/Genetic Toxicology and Environmental Mutagenesis, 772*, 20-24.

Ug, A., & Ceylan, Ö. (2003). Occurrence of resistance to antibiotics, metals, and plasmids in clinical strains of *Staphylococcus* spp. *Archives of Medical Research, 34*(2), 130-136.

Vacheethasanee, K., Temenoff, J. S., Higashi, J. M., Gary, A., Anderson, J. M., Bayston, R., & Marchant, R. E. (1998). Bacterial surface properties of clinically isolated *Staphylococcus epidermidis* strains determine adhesion on polyethylene. *Journal of Biomedical Materials Research: An Official Journal of the Society for Biomaterials, the Japanese Society for Biomaterials, and the Australian Society for Biomaterials, 42*(3), 425-432.

Valente, J. H., Forti, R. J., Freundlich, L. F., Zandieh, S. O., & Crain, E. F. (2003). Wound irrigation in children: Saline solution or tap water? *Annals of Emergency Medicine, 41*(5), 609-616.

Van Delden, C., & Iglewski, B. H. (1998). Cell-to-cell signaling and *Pseudomonas aeruginosa* infections. *Emerging Infectious Diseases, 4*(4), 551-560.

Van Gestel, J., Vlamakis, H. and Kolter, R., (2015). Division of labor in biofilms: the ecology of cell differentiation. Microbiol. Spectr. 3. MB-0002–2014. http://dx. doi. org/10.1128/microbiolspec. MB-0002-2014.

Varkey, M., Ding, J., & Tredget, E. E. (2013). Superficial dermal fibroblasts enhance basement membrane and epidermal barrier formation in tissue-engineered skin: Implications for treatment of skin basement membrane disorders. *Tissue Engineering Part A, 20*(3-4), 540-552.

Veenstra, D. L., Saint, S., Saha, S., Lumley, T., & Sullivan, S. D. (1999). Efficacy of antiseptic-impregnated central venous catheters in preventing catheter-related bloodstream infection: A meta-analysis. *Jama, 281*(3), 261-267.

Veerachamy, S., Yarlagadda, T., Manivasagam, G., & Yarlagadda, P. K. (2014). Bacterial adherence and biofilm formation on medical implants: A review. *Proceedings of the Institution of Mechanical Engineers, Part H: Journal of Engineering in Medicine, 228*(10), 1083-1099.

Vik, H., Andersen, K., Julshamn, K., & Todnem, K. (1985). Neuropathy caused by silver absorption from arthroplasty cement. *The Lancet, 325*(8433), 872.

Vincent, S. H. (1989). Oxidative effects of heme and porphyrins on proteins and lipids. *Seminars in Hematology, 26*(2), 105-113.

Vitkauskiene, A., Scheuss, S., Sakalauskas, R., Dudzevicius, V., & Sahly, H. (2005). *Pseudomonas aeruginosa* strains from nosocomial pneumonia are more serum resistant than *P. aeruginosa* strains from noninfectious respiratory colonization processes. *Infection, 33*(5-6), 356-361.

Wahdan, H. (1998). Causes of the antimicrobial activity of honey. *Infection, 26*(1), 26-31.

Walmsley, A., Laird, W., & Williams, A. (1984). A model system to demonstrate the role of cavitational activity in ultrasonic scaling. *Journal of Dental Research, 63*(9), 1162-1165.

Walmsley, A. D. (1988). Potential hazards of the dental ultrasonic descaler. *Ultrasound in Medicine & Biology, 14*(1), 15-20.

Walraven, M., Gouverneur, M., Middelkoop, E., Beelen, R. H., & Ulrich, M. M. (2014). Altered TGF-β signaling in fetal fibroblasts: What is known about the underlying mechanisms? *Wound Repair and Regeneration, 22*(1), 3-13.

Wang, Y., Ikawa, A., Okaue, S., Taniguchi, S., Osaka, I., Yoshimoto, A., Enomoto, K. (2008). Quorum sensing signaling molecules involved in the production of violacein by pseudoalteromonas. *Bioscience, Biotechnology, and Biochemistry, 72*(7), 1958-1961.

Wang, Y., Beekman, J., Hew, J., Jackson, S., Issler-Fisher, A. C., Parungao, R., Maitz, P. K. (2018). Burn injury: Challenges and advances in burn wound healing, infection, pain and scarring. *Advanced Drug Delivery Reviews, 123*, 3-17.

Ward, K. ed., (2015). Routledge handbook of sports therapy, injury assessment and rehabilitation. Routledge.

Wardle, M. D., & Renninger, G. M. (1975). Bactericidal effect of hydrogen peroxide on spacecraft isolates. *Applied Microbiology, 30*(4), 710-711.

Warriner, R., & Burrell, R. (2005). Infection and the chronic wound: A focus on silver. *Advances in Skin & Wound Care, 18*(8), 2-12.

Weber, D. J., & Rutala, W. A. (2001). Use of metals as microbicides in preventing. *Disinfection, Sterilization, and Preservation,* 415.

Webster, D., Harvey, W., Dyson, M., & Pond, J. (1980). The role of ultrasound-induced cavitation in the 'in vitro'stimulation of collagen synthesis in human fibroblasts. *Ultrasonics, 18*(1), 33-37.

Werner, S., & Smola, H. (2001). Paracrine regulation of keratinocyte proliferation and differentiation. *Trends in Cell Biology, 11*(4), 143-146.

Werner, S., Smola, H., Liao, X., Longaker, M. T., Krieg, T., Hofschneider, P. H., & Williams, L. T. (1994). The function of KGF in morphogenesis of epithelium and reepithelialization of wounds. *Science (New York, N.Y.), 266*(5186), 819-822.

White Jr, J. W., Subers, M. H., & Schepartz, A. I. (1963). The identification of inhibine, the antibacterial factor in honey, as hydrogen peroxide and its origin in a honey glucose-oxidase system. *Biochimica Et Biophysica Acta (BBA)-Specialized Section on Enzymological Subjects, 73*(1), 57-70.

White, J., & Doner, L. W. (1980). Honey composition and properties. *Beekeeping in the United States Agriculture Handbook, 335*, 82-91.

White, R. J., Cooper, R., & Kingsley, A. (2001). Wound colonization and infection: The role of topical antimicrobials. *British Journal of Nursing, 10*(9), 563-578.

Whiteley, M., Bangera, M. G., Bumgarner, R. E., Parsek, M. R., Teitzel, G. M., Lory, S., & Greenberg, E. (2001). Gene expression in *Pseudomonas aeruginosa* biofilms. *Nature, 413*(6858), 860.

Wilkinson, J. M., & Cavanagh, H. M. (2005). Antibacterial activity of 13 honeys against escherichia coli and *Pseudomonas aeruginosa*. *Journal of Medicinal Food, 8*(1), 100-103.

Williams, R. G., & Pitt, W. G. (1997). In vitro response of escherichia coli to antibiotics and ultrasound at various insonation intensities. *Journal of Biomaterials Applications, 12*(1), 20-30.

Williams, P., Camara, M., Hardman, A., Swift, S., Milton, D., Hope, V. J., Bycroft, B. W. (2000). Quorum sensing and the population-dependent control of virulence. *Philosophical Transactions of the Royal Society of London.Series B, Biological Sciences, 355*(1397), 667-680.

Wilson, L. A., Sawant, A. D., Simmons, R. B., & Ahearn, D. G. (1990). Microbial contamination of contact lens storage cases and solutions. *American Journal of Ophthalmology, 110*(2), 193-198.

Winterbourn, C. C. (2013). The biological chemistry of hydrogen peroxide. *Methods in enzymology* (pp. 3-25) Elsevier.

Wisplinghoff, H., Bischoff, T., Tallent, S. M., Seifert, H., Wenzel, R. P., & Edmond, M. B. (2004). Nosocomial bloodstream infections in US hospitals: Analysis of 24,179 cases from a prospective nationwide surveillance study. *Clinical Infectious Diseases, 39*(3), 309-317.

Wollina, U., Heinig, B., Naumann, G., Scheibe, A., Schmidt, W. D., & Neugebauer, R. (2011). Effects of low-frequency ultrasound on microcirculation in venous leg ulcers. *Indian Journal of Dermatology, 56*(2), 174-179.

Wood, A. K., & Sehgal, C. M. (2015). A review of low-intensity ultrasound for cancer therapy. *Ultrasound in Medicine & Biology, 41*(4), 905-928.

Woods, D., Lam, J., Paranchych, W., Speert, D., Campbell, M., & Godfrey, A. (1997). Correlation of *Pseudomonas aeruginosa* virulence factors from clinical and environmental isolates with pathogenicity in the neutropenic mouse. *Canadian Journal of Microbiology, 43*(6), 541-551.

Wright, E., Neethirajan, S., & Weng, X. (2015). Microfluidic wound model for studying the behaviors of *Pseudomonas aeruginosa* in polymicrobial biofilms. *Biotechnology and Bioengineering, 112*(11), 2351-2359.

Wright, S. D., Ramos, R. A., Tobias, P. S., Ulevitch, R. J., & Mathison, J. C. (1990). CD14, a receptor for complexes of lipopolysaccharide (LPS) and LPS binding protein. *Science (New York, N.Y.), 249*(4975), 1431-1433.

Xie, Y., Rizzi, S. C., Dawson, R., Lynam, E., Richards, S., Leavesley, D. I., & Upton, Z. (2010). Development of a three-dimensional human skin equivalent wound model for investigating novel wound healing therapies. *Tissue Engineering Part C: Methods, 16*(5), 1111-1123.

Xin, Z., Lin, G., Lei, H., Lue, T. F., & Guo, Y. (2016). Clinical applications of low-intensity pulsed ultrasound and its potential role in urology. *Translational Andrology and Urology, 5*(2), 255-266.

Xu, K. D., McFeters, G. A., & Stewart, P. S. (2000). Biofilm resistance to antimicrobial agents. *Microbiology, 146*(3), 547-549.

Xu, F. F., & Imlay, J. A. (2012). Silver(I), mercury(II), cadmium(II), and zinc(II) target exposed enzymic iron-sulfur clusters when they toxify escherichia coli. *Applied and Environmental Microbiology, 78*(10), 3614-3621.

Xue, M., & Jackson, C. J. (2015). Extracellular matrix reorganization during wound healing and its impact on abnormal scarring. *Advances in Wound Care, 4*(3), 119-136.

Yamanaka, M., Hara, K., & Kudo, J. (2005). Bactericidal actions of a silver ion solution on escherichia coli, studied by energy-filtering transmission electron microscopy and proteomic analysis. *Applied and Environmental Microbiology, 71*(11), 7589-7593.

Yanagihara, K., Tomono, K., Kaneko, Y., Miyazaki, Y., Tsukamoto, K., Hirakata, Y., Kohno, S. (2003). Role of elastase in a mouse model of chronic respiratory *Pseudomonas aeruginosa* infection that mimics diffuse panbronchiolitis. *Journal of Medical Microbiology, 52*(6), 531-535.

Yao, Y., Sturdevant, D. E., & Otto, M. (2005). Genomewide analysis of gene expression in *Staphylococcus epidermidis* biofilms: Insights into the pathophysiology of S. epidermidis biofilms and the role of phenol-soluble modulins in formation of biofilms. *Journal of Infectious Diseases, 191*(2), 289-298.

Yin, H., Langford, R., & Burrell, R. (1999). Comparative evaluation of the antimicrobial activity of ACTICOAT antimicrobial barrier dressing. *The Journal of Burn Care & Rehabilitation, 20*(3), 195-200.

Yoshpe-Purer, Y., & Eylan, E. (1968). Disinfection of water by hydrogen peroxide. *Health Laboratory Science, 5*(4), 233-238.

Yua, H., Chen, S. and Cao, P. (2011) Synergistic bactericidal effects and mechanisms of low intensity ultrasound and antibiotics against bacteria: A review. Elsevier B.V.

Yu, H., Chen, S., & Cao, P. (2012). Synergistic bactericidal effects and mechanisms of low intensity ultrasound and antibiotics against bacteria: A review. *Ultrasonics Sonochemistry, 19*(3), 377-382.

Zanelli, G., Sansoni, A., Zanchi, A., Cresti, S., Pollini, S., Rossolini, G., & Cellesi, C. (2002). *Staphylococcus aureus* nasal carriage in the community: A survey from central italy. *Epidemiology & Infection, 129*(2), 417-420.

Zhang, Y., Tachibana, R., Okamoto, A., Azuma, T., Sasaki, A., Yoshinaka, K., Matsumoto, Y. (2012). Ultrasound-mediated gene transfection in vitro: Effect of ultrasonic parameters on efficiency and cell viability. *International Journal of Hyperthermia, 28*(4), 290-299.

Zheng, B. J. (2017). Analyzing the effect of silver nitrate on *Pseudomonas aeruginosa.*

Zhou, S., Schmelz, A., Seufferlein, T., Li, Y., Zhao, J., & Bachem, M. G. (2004). Molecular mechanisms of low intensity pulsed ultrasound in human skin fibroblasts. *The Journal of Biological Chemistry, 279*(52), 54463-54469.

Zhu, H. X., Cai, X. Z., Shi, Z. L., Hu, B., & Yan, S. G. (2014). Microbubble-mediated ultrasound enhances the lethal effect of gentamycin on planktonic escherichia coli. *BioMed Research International, 2014*, 142168.

Zucchelli, G., Mounssif, I., Stefanini, M., Mele, M., Montebugnoli, L., & Sforza, N. (2009). Hand and ultrasonic instrumentation in combination with root-coverage surgery: A comparative controlled randomized clinical trial. *Journal of Periodontology, 80*(4), 577-585.

9. Appendix
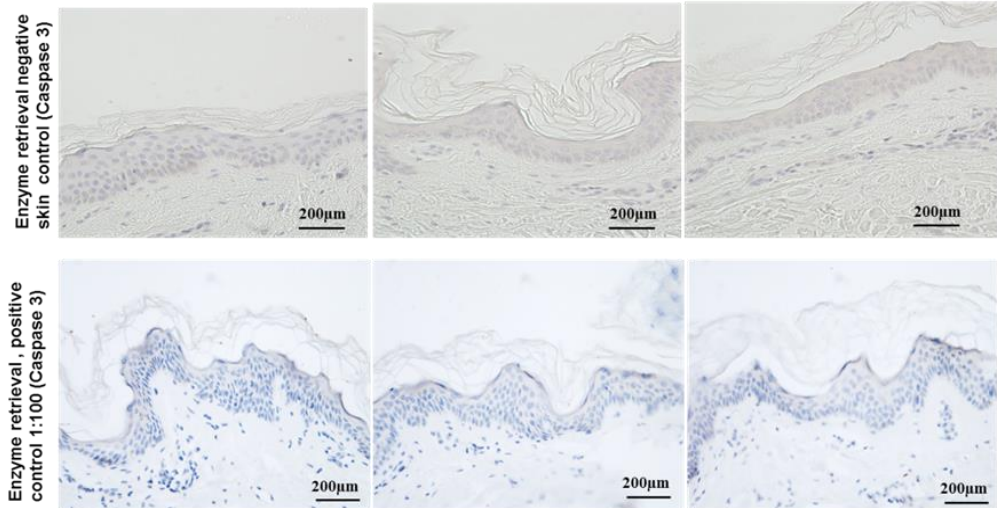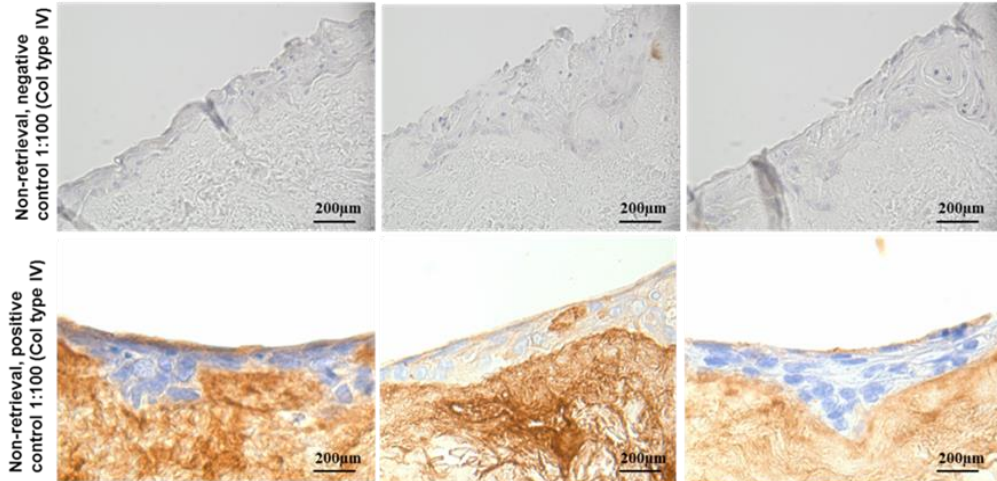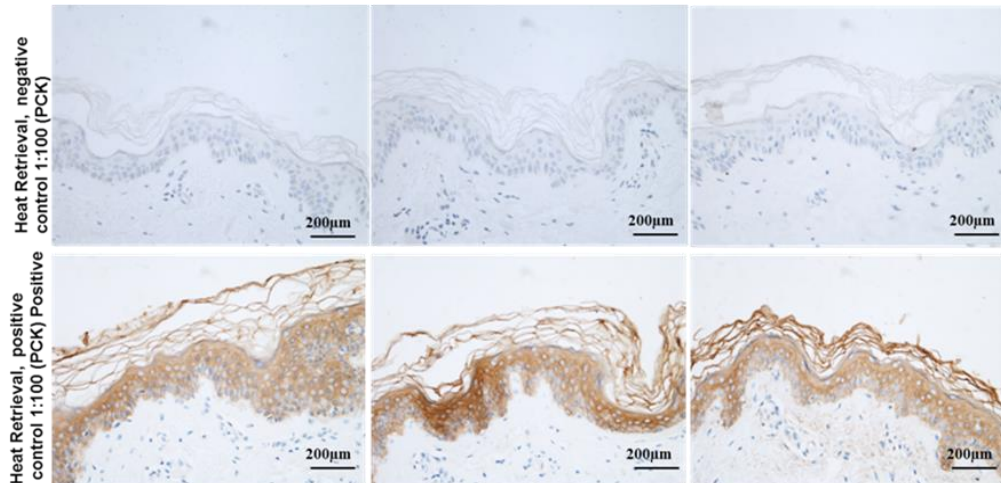
Figure 9.1: Antibody bodies negative and postive control for all the immunohistochemistry skin section. Caspase 3, collagen IV, Panacytokeratine, Scale Bar = 200µm.
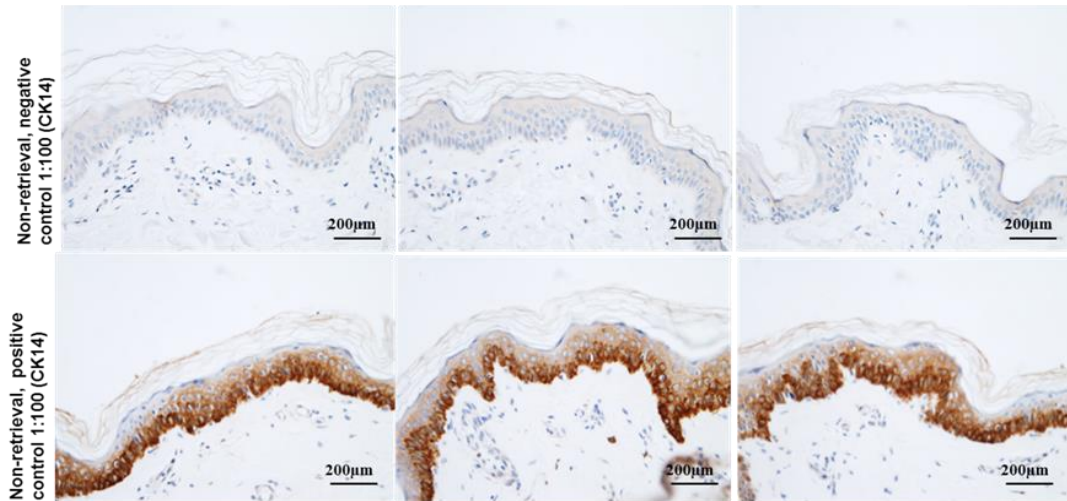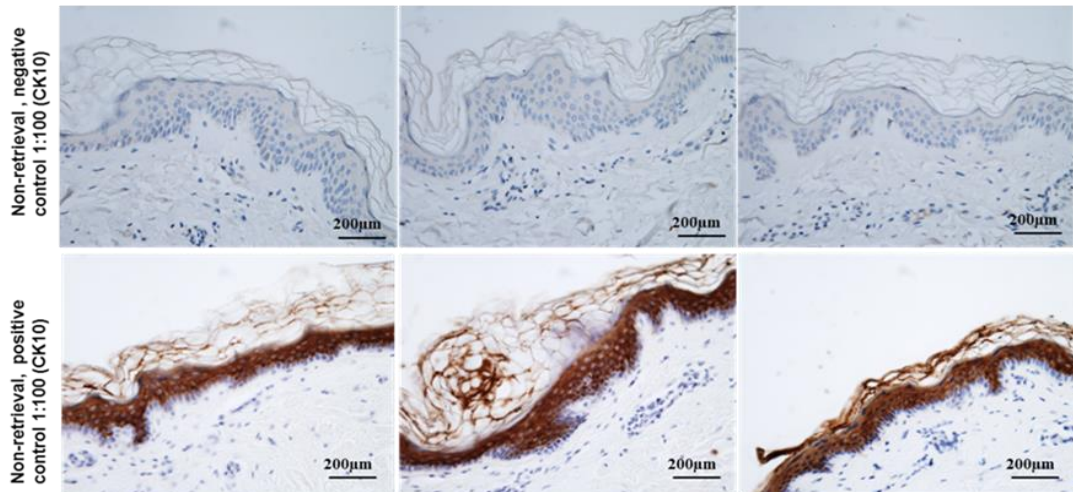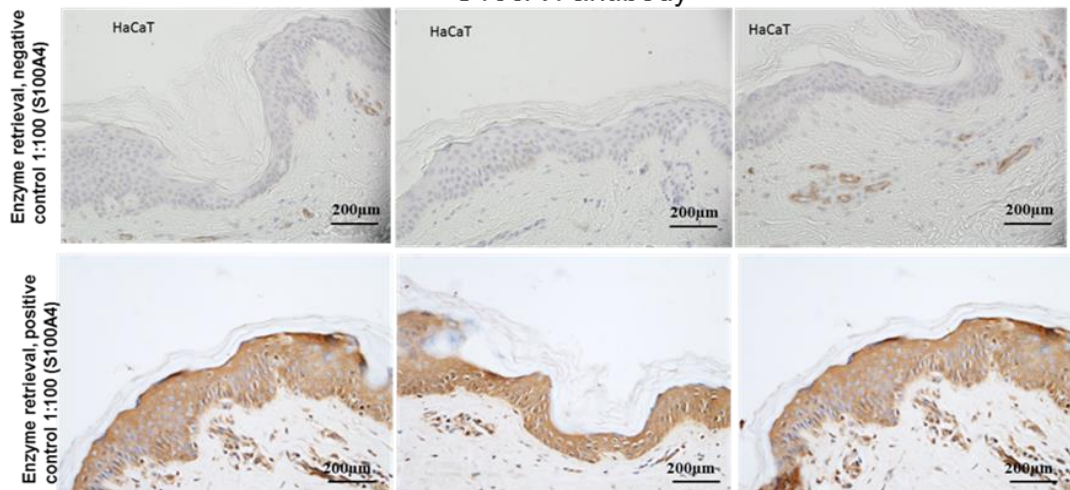
Figure 9.2: Antibody bodies negative and postive control for all the immunohistochemistry skin section, CK14, CK10 and S100A4.   Scale Bar = 200μm.